IN TWO SECTIONS—SECTION ONE

Transactions of the ASME

TRANSACTIONS OF THE AMERICAN SOCIETY OF MECHANICAL ENGINEERS

VOLUME 76 JANUARY 1954 NUMBER 1

Transactions

of The American Society of Mechanical Engineers

Published on the tenth of every month, except March, June, September, and December

Published monthly by The American Society of Mechanical Engineers. Publication office at 20th and Northampton Streets, Easton, Pa. The editorial department is located at the headquarters of the Society, 29 West Thirty-Ninth Street, New York 18, N. Y. Cable address, "Dynamic," New York. Price $1.50 a copy, $12.00 a year for Transactions and the *Journal of Applied Mechanics*; to members and affiliates, $1.00 a copy, $6.00 a year. Changes of address must be received at Society headquarters four weeks before they are to be effective on the mailing list. Please send old as well as new address. . . . By-Law: The Society shall not be responsible for statements or opinions advanced in papers or . . . printed in its publications (B13, Par. 4). . . . Entered as second-class matter March 2, 1928, at the Post Office at Easton, Pa., under the Act of August 24, 1912. . . .

Performance of Free-Piston Gas Generators

By J. J. McMULLEN[1] and W. G. PAYNE[2]

The rapid development now under way of the free-piston gas generator-turbine power plant is outlined. The original Pescara unit in France, and the Cooper-Bessemer and Baldwin-Lima-Hamilton generators being perfected in the United States, are described, and possible applications are mentioned.

THE free-piston gas generator-turbine power plant combines the high thermal efficiency of the diesel-engine combustion cycle with the simplicity and flexibility of the turbine-power take-off. It consists of a gas generator producing high-temperature and pressure gas which is used to drive a turbine. The gas generator has two opposing pistons in a single power cylinder. These pistons compress their own air for scavenging and charging the power cylinder. They also store the energy required to halt their outward movement and return them for the next compression stroke. Combustion proceeds on the two-stroke diesel cycle and power is produced by the exhaust gas which drives the turbine. The crankshaft, connecting rods, and bearings of the diesel engine are eliminated.

In comparison to a gas-turbine power plant, the free-piston gas generator supplants the compressor, compressor turbine, combustion chamber, and heat exchanger. Ducting is much less.

The use of a free-piston gas generator-turbine combination for producing power has long ago passed the theoretical stage. Test data are available on two designs of free-piston units which have been developed to an operating condition and which provide factual information for their evaluation. A third unit is now in the test phase and information will be available at a later date.

These successful designs cover units intended for varying types of application and with considerable differences in concept:

1 The SIGMA Model GS-34, based on the original patents of Pescara and manufactured by Société Industrielle Générale de Mécanique Appliquée in France, is intended for operation with low-temperature and pressure gas to the turbine. It is designed primarily for economy of construction and low maintenance cost for both gas producer and turbine. It is an inward-compression unit and is essentially a "hot" running compressor. It is unquestionably the most highly developed gas generator built to date and has been applied successfully to electric power station generation (1),[3] locomotive drive (2), and ship propulsion (3).

2 The Cooper-Bessemer Model R is in the intermediate class and is an outward-compression unit equipped with internal water cooling. Its exhaust-gas output is increased from the 50 psig of the SIGMA design to 72.5 psig. The exhaust temperature is increased from 945 F to 1000 F. It is designed to compete favorably with other types of commercial power units on the basis of initial cost, operating cost, and reliability. This model is primarily a heavy-duty unit designed for application to natural gas-pipe-line pumping units, electric power-station generation, and marine applications such as auxiliaries, transports, and cargo vessels where the weight and space are not prime considerations. This unit has been developed by the Cooper-Bessemer Corporation, Mount Vernon, Ohio (4).

3 The Baldwin-Lima-Hamilton Model B is an outward-compression internally cooled unit intended for lightweight applications. Its exhaust-gas output at 90 psig and 1300 F makes cylinder operating conditions higher than those normally attained by internal-combustion engines. Owing to these higher operating conditions, this unit has a higher specific power than either the SIGMA or the Cooper-Bessemer models. The BLH unit has been developed, built, and tested by the Baldwin-Lima-Hamilton Corporation, Hamilton, Ohio, under the cognizance of the Bureau of Ships, Navy Department (5). Its development represents the most difficult approach because of the extreme operating conditions but, at the same time, has the best possibility for naval combatant-vessel application where low weight and space and high specific power output are required. Development is continuing on a later model having still higher specific output. This later development indicates the possibility of greatly exceeding the performance of the BLH Model B Unit.

This paper will present a brief description of the possibilities inherent in free-piston gas generator-turbine power plants and their applications. Primarily, it will present comparative data from test results of the French SIGMA GS-34 and the BLH Model B Units. Reference (4) describes the C-B Model R Unit and presents available data.

Effect of Type of Operation

The present free-piston gas generator, or gasifier, is supercharged in the sense that the scavenging and charging air are at pressures up to 90 psig. The cylinder charge at the beginning of each compression stroke is therefore much greater than atmospheric. With the full circle of ports at both scavenge and exhaust ends of the opposed-piston power cylinder, the 3 to 8-lb differential of the scavenge air over the exhaust pressure should provide adequate scavenging and charge the power cylinder with fresh air slightly above the exhaust pressure. The scavenge differential is not effective in charging because the intake ports close considerably before the exhaust ports.

There are varying approaches to the design concept for free-piston gas generators. Possible methods of increasing the specific output of any free-piston gas generator include the following:

Supercharging of Power Cylinder. The possible supercharging effect of the high pressure is lost in present designs. The cylinder is charged at high pressure but the air is at high temperature. The density is only 55 per cent of that which could be obtained if the present scavenging pressure were maintained and the air temperature were reduced from its present peak of about 550 F to 100 F, readily attained by cooling the air after the supercharger. This increases the density of the cylinder charge.

Improvement of Port Timing. The free-piston gas generator varies, in so far as the highest possible power is concerned, from the normal diesel in two respects: (*a*) Best power is obtained when a long compression stroke gives the greatest density of charge with the lowest scavenge pressure; (*b*) best power also is obtained when the expansion stroke is the shortest which will

[1] Commander, USN, Bureau of Ships, Department of the Navy, Washington, D. C.

U. S. Naval Engineering Experiment Station, Annapolis, Md.

[3] Numbers in parentheses refer to the Bibliography at the end of the paper.

Contributed by the Gas Turbine Power Division and presented at the Spring Meeting, Columbus, Ohio, April 28–30, 1953, of The American Society of Mechanical Engineers.

Note: Statements and opinions advanced in papers are to be understood as individual expressions of their authors and not those of the Society. Manuscript received at ASME Headquarters, February 13, 1953. Paper No. 53—S-18.

produce the same gas quantity. The exhaust gases should be released at the highest level of pressure and temperature in order to make maximum energy available to the turbine. Variable port timing is required to give this relationship of compression and expansion strokes. The full extent of the power which could be produced cannot be realized until gas-generator and turbine materials are available which will withstand the higher temperatures.

Higher Operating Pressure. Another method of realizing higher than the present specific outputs from the gas generator is to increase the maximum cylinder pressure and temperature. They are already higher than those for a normal diesel engine. The peak pressures in a gas generator reach a maximum of 2200 psig. Higher operating conditions are troublesome because piston rings are not ordinarily built to take the high shock pressures. Also, cylinders must be specially designed to sustain high pressures at these higher temperatures. Moderate success has been obtained with piston rings and cylinder liners under present operating conditions. These operating conditions will be made even more severe as improved materials become available. Present prospects for such materials are good.

Analyses have been made to show the improvement which could be realized with operating conditions surpassing those now used. These are more than theoretical analyses as they are based on, and confirmed by, actual operation of gas generators. One such analysis (6) shows the value of operating at higher exhaust pressures to the turbine. There is a limit to the pressure ratio across the gas generator, depending upon adequate scavenging of the power cylinder which is a function of the port size and arrangement and piston timing.

The value of operating at high-pressure outputs is evident in Fig. 1. Adiabatic efficiency, i.e., the total energy available in the exhaust gas as compared to that in the fuel burned, is 41.5 per cent at the 50 psig used by SIGMA as compared to a possible 46 per cent at the 90 psig used by Baldwin-Lima-Hamilton. These data are for simple operation of the gas generator with no supercharging and no air cooling. This is shown by the maximum scavenging-air temperature of 575 F. Exhaust temperature of 1265 F at the highest pressure of 90 psig is still well within the allowable limits for turbine operation. The temperature could be raised to 1350 F on the turbine, but flattening of the efficiency curve indicates little additional increase of thermal efficiency at the higher working pressure for the SIGMA Model GS-34 on which the analysis was based.

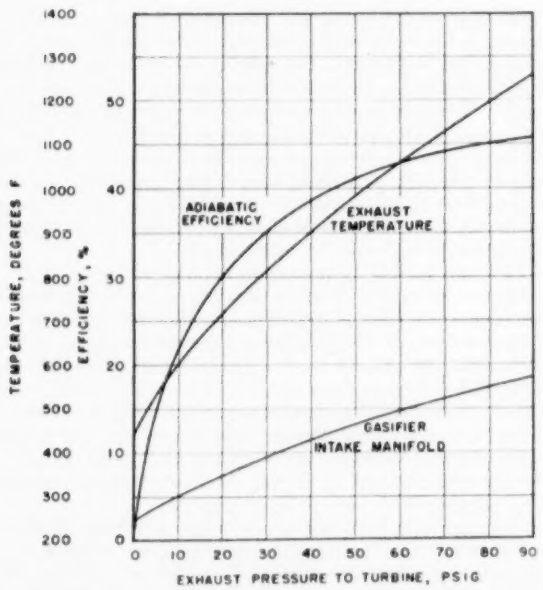

Fig. 1 Theoretical Study Showing Variation of Efficiency and Temperature With Working Pressure of Free-Piston Gas Generators

The same analysis (6) indicates similar improvement can be obtained by increasing power-cylinder compression pressure, Fig. 2. This effect could be obtained with a longer compression

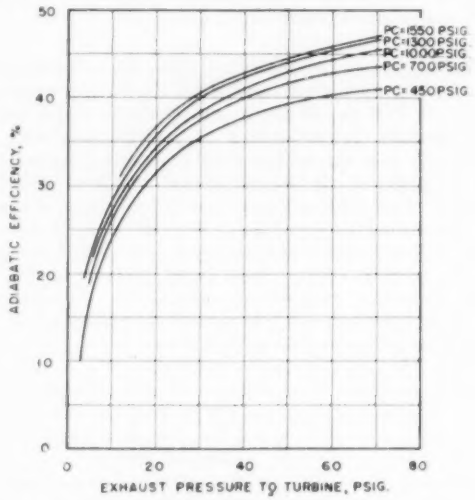

Fig. 2 Theoretical Study Showing Variation of Efficiency With Working Pressure for Various Compression Pressures of Free-Piston Gas Generators

stroke or with a higher charging-air pressure. But, in either case, in so far as combustion is concerned, it could represent supercharging the cylinder with additional oxygen for combustion while maintaining the same piston-clearance volume. The exact level or shape of the curves shown would vary with the mechanical details of the free-piston unit being investigated. The relative level of the curves is representative of the variation. At higher working pressures, an improvement of 15 per cent in efficiency could be obtained by increasing the firing pressure from the minimum of 450 psig to the maximum of 1550 psig. It was for these reasons that the developments at BLH were directed toward a unit operating under extreme pressure and temperature conditions.

Exact application of supercharging to any given gasifier requires an extensive investigation. Preliminary investigations are not entirely consistent. It appears, however, that increases in output up to 100 per cent over the nonsupercharged versions are possible, but with a slight decrease in thermal efficiency.

SIGMA Model GS-34 Gas Generator

The SIGMA Model GS-34 gas generator-turbine power plant is the only one presently in commercial production. It is an inward-compression type; i.e., the power-cylinder charging-and-scavenging air is compressed during the inward movement of the pistons. It is now being used in stationary power-plant, locomotive, and marine services.

The design of the GS-34 is shown in Fig. 3. Its principal specifications are given in Table 1.

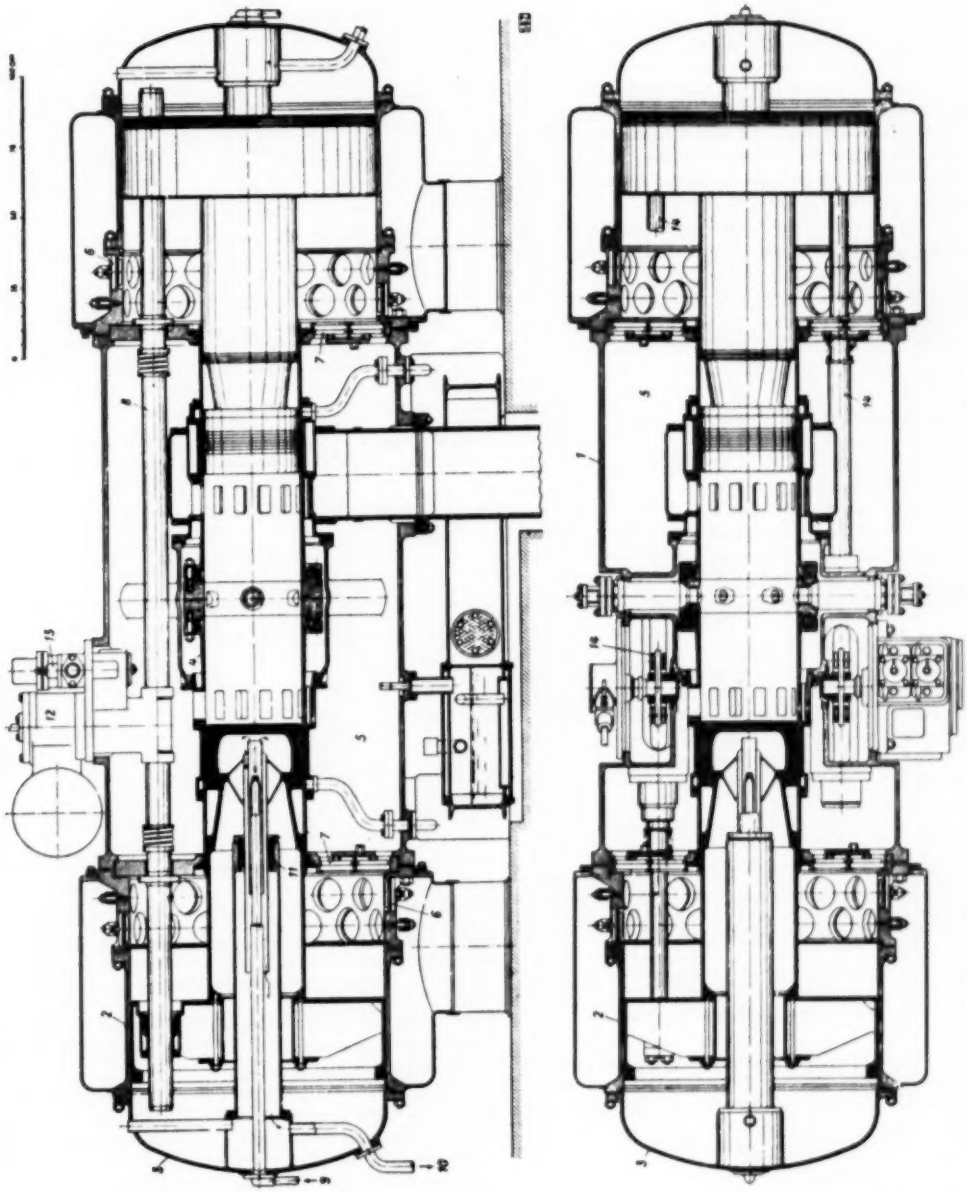

Free-piston power gas generator, GS-34. Vertical longitudinal section.

Free-piston power gas generator, GS-34. — Horizontal longitudinal section.

1 Engine case, 2 Compressor cylinder, 3 Dashed rods, 4 Motor cylinder, 5 Scavenge air receiver, 6 Suction valve, 7 Delivery valve, 8 Balance pipe, 9 Cooling inlet, 10 Coolant outlet, 11 Guard rail, 12 Starter, 13 Stabilizer, 14 Synchronizing rod.

FIG. 3 CROSS SECTION OF SIGMA MODEL GS-34 FREE-PISTON GAS GENERATOR

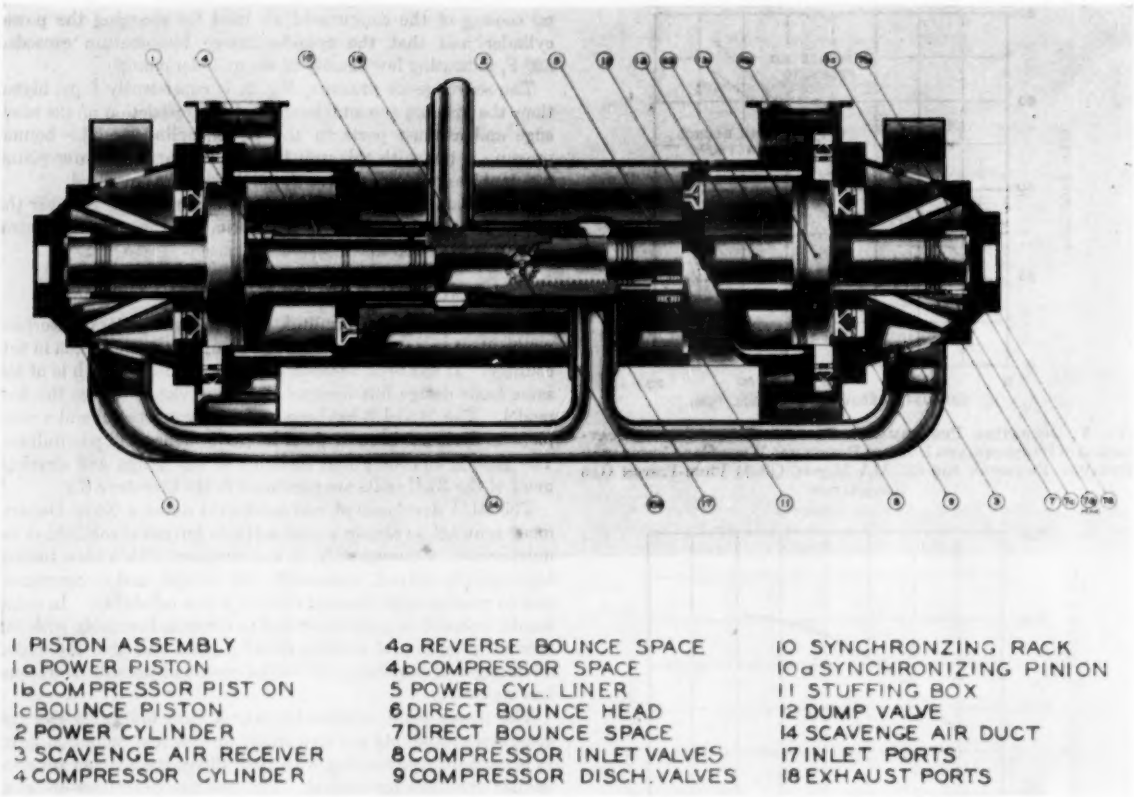

FIG. 10 CROSS SECTION OF BALDWIN-LIMA-HAMILTON MODEL B FREE-PISTON GAS GENERATOR

horsepower curve in Fig. 11 shows that the output is increasing without any decrease in rate up to the limiting exhaust temperature and pressure set by this particular turbine design.

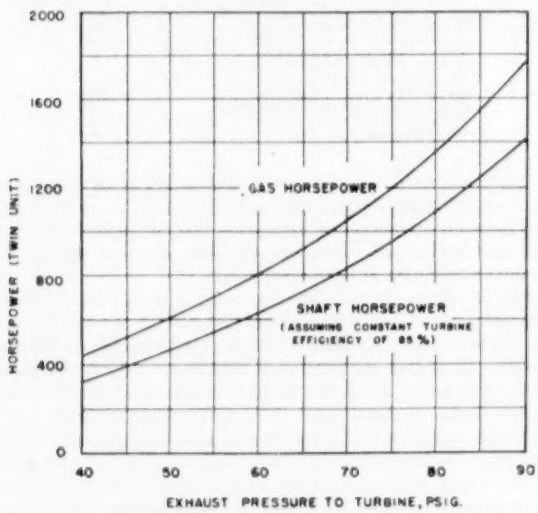

FIG. 11 VARIATION OF HORSEPOWER WITH GAS-GENERATOR EXHAUST PRESSURE FOR BALDWIN-LIMA-HAMILTON MODEL B FREE-PISTON GAS GENERATOR

The shaft-horsepower curve in Fig. 11 is based on the desired 85 per cent efficiency for turbine and reduction gear, as it was in the SIGMA data. That efficiency was not reached with the turbine used on the actual tests. However, turbines are available with peak efficiency of 85 per cent or higher. The shaft-horsepower curve is corrected for the power requirement of the auxiliary equipment which cannot be driven directly from the turbine. Thus about 1420 shp is available from an installation with a weight and space no greater than that of current diesel installations and less than that of other types of power plants having comparable thermal efficiency. The model now under development at BLH is much smaller and lighter.

Figs. 12 and 13 show the measured fuel consumption and thermal efficiencies on a gas-horsepower basis and those calculated for a possible turbine efficiency of 85 per cent. The maximum thermal efficiency of 40.3 per cent at the gasifier discharge is very satisfactory and compares favorably with the SIGMA maximum of 38.2 per cent. This increase in thermal efficiency is to be expected in view of higher operating conditions. The correction to a shaft-horsepower basis shows a greater reduction than was made for the SIGMA design because exact information was available on the BLH power plant and deduction was made for all losses, including supply of auxiliary control air, cooling-water pumping, and similar power expenditures. The only deduction made for the SIGMA unit was based on turbine efficiency of 85 per cent. It is not known if the previously published data include corrections for power to auxiliary equipment. After making these corrections to a minimum shaft-horsepower basis, the thermal efficiency is still 32 3 per cent.

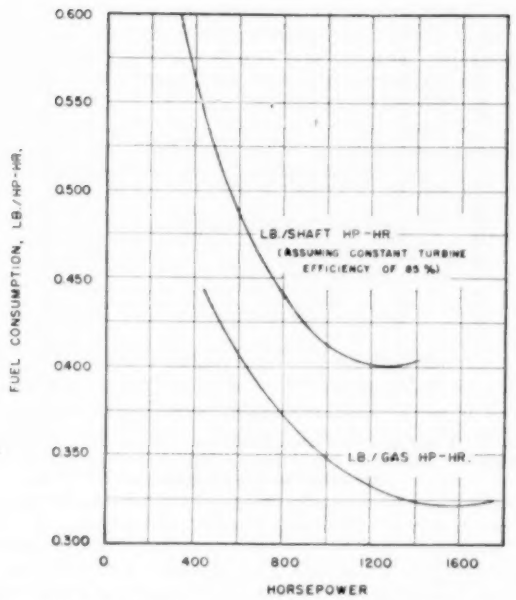

FIG. 12 VARIATION OF SPECIFIC FUEL CONSUMPTION WITH HORSEPOWER FOR BALDWIN-LIMA-HAMILTON MODEL B FREE-PISTON GAS GENERATOR

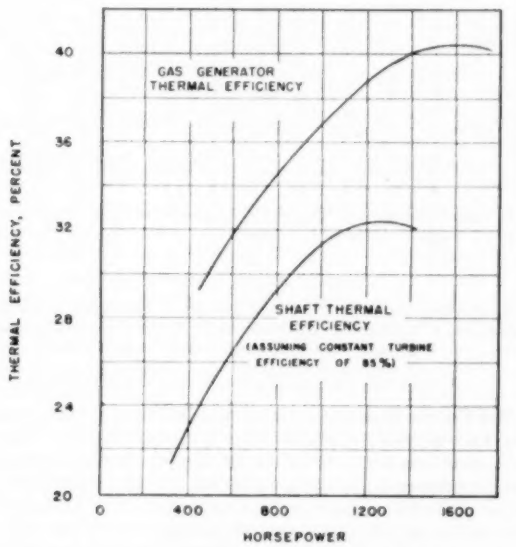

FIG. 13 VARIATION OF THERMAL EFFICIENCY WITH HORSEPOWER FOR BALDWIN-LIMA-HAMILTON MODEL B FREE-PISTON GAS GENERATOR

The maximum exhaust temperature shown in Fig. 14 was intended to be the limiting factor for operation. The turbine was rated at a maximum inlet temperature of 1350 F. However, the peak pressure of 90 psig was reached with less than 1300 F. As stated before, without the turbine and with a variation in the gas pressure-to-orifice relationship, the same temperature gave as much load with only 70 psig exhaust-gas pressure.

Fig. 15 shows the effect of output on the temperature rise

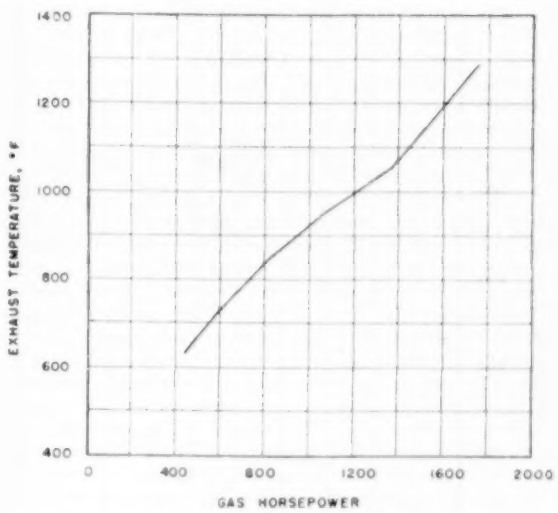

FIG. 14 VARIATION OF EXHAUST TEMPERATURE WITH GAS HORSEPOWER FOR BALDWIN-LIMA-HAMILTON MODEL B FREE-PISTON GAS GENERATOR

through the gas generator. Again, it may be noted that there was no cooling of the compressed air used for scavenging. Consequently, the cylinder was charged with air at temperatures up to 500 F. As mentioned previously, cooling of this air is a very important future step for increasing the output from this or similar units. No attempt at intercooling has yet been made. A mathematical analysis has shown that the output would be increased substantially.

The main pressures are plotted in Fig. 16. The scavenge-air pressure must be slightly above the exhaust pressure, the difference of 3 to 7 psi being an indication of the restriction of the scavenge and exhaust ports. Reverse-bounce and direct-bounce pressures are a function of the control system and the load carried. These pressures would vary with the design of the unit and the type of control. Direct-bounce pressure is much higher with this unit than with the SIGMA unit because the Model B has a small-area bounce piston whereas the Model GS-34 has a large-area bounce piston. Thus less pressure is necessary in order to obtain the required force.

Fig. 17 shows another important difference from the SIGMA and BLH designs. In addition to the higher exhaust-gas pressure, the BLH unit has a much higher cyclic frequency. The maximum frequency was 1035 cpm as compared to 613 cpm on the Model GS-34. The comparative piston speeds vary much less, being approximately the same at 1790 fpm for the GS-34 and 1890 fpm for the Model B.

The free-piston gas generator has high efficiency because of its low friction losses and because the balanced arrangement of pistons and the absence of bearings makes operation possible at higher than normal diesel-cylinder pressures. The maximum cylinder pressures measured with the BLH gas generator are plotted in Fig. 18. The peak pressure varied with load, reaching 2200 psig at the highest output. This high pressure and the rapid rate of pressure rise present a problem in top compression-ring and cylinder-liner life. The problem is being overcome and reasonably satisfactory life has been obtained already. The high efficiency attainable with high pressure has made the development worth-while. Still higher pressures should be used when ring and cylinder materials permit.

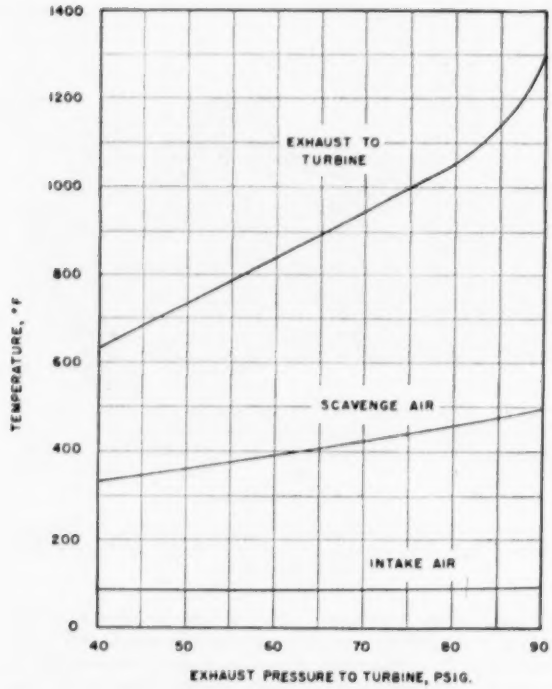

FIG. 15 VARIATION OF INTAKE AIR, SCAVENGE AIR, AND EXHAUST TEMPERATURES WITH GAS-GENERATOR EXHAUST PRESSURE FOR BALDWIN-LIMA-HAMILTON MODEL B FREE-PISTON GAS GENERATOR

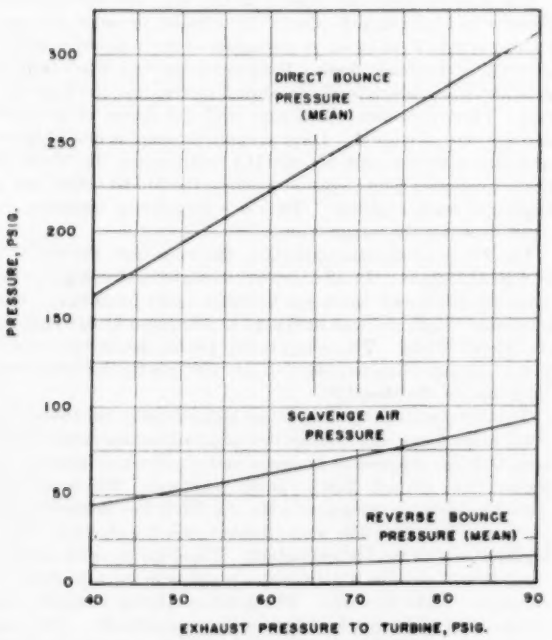

FIG. 16 VARIATION OF SCAVENGE AIR, REVERSE-BOUNCE, AND DIRECT-BOUNCE PRESSURE WITH GAS-GENERATOR EXHAUST PRESSURE FOR BALDWIN-LIMA-HAMILTON MODEL B FREE-PISTON GAS GENERATOR

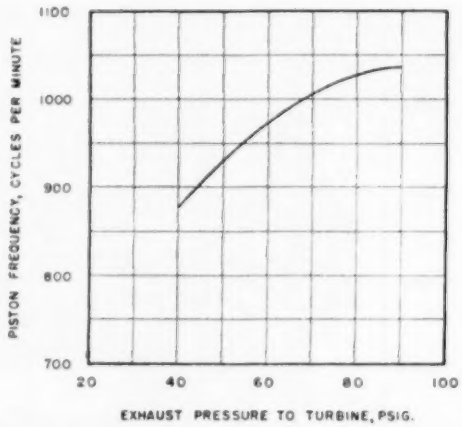

FIG. 17 VARIATION OF PISTON FREQUENCY WITH GAS-GENERATOR EXHAUST PRESSURE FOR BALDWIN-LIMA-HAMILTON MODEL B FREE-PISTON GAS GENERATOR

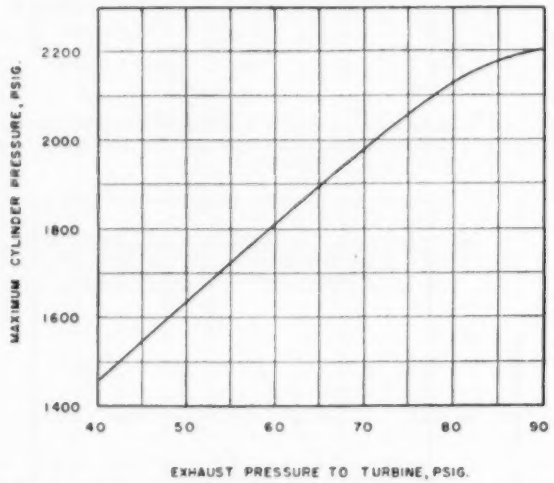

FIG. 18 VARIATION OF MAXIMUM CYLINDER PRESSURE WITH GAS-GENERATOR EXHAUST PRESSURE FOR BALDWIN-LIMA-HAMILTON MODEL B FREE-PISTON GAS GENERATOR

COOPER-BESSEMER MODEL R GAS GENERATOR

The Cooper-Bessemer gas generator-turbine plant is an example of a heavy-duty approach to the free-piston engine. The development has been carried on by Cooper-Bessemer primarily for the purpose of producing a pipe-line pumping unit which will be more reliable, cheaper, easier to manufacture, and will require less maintenance than the present gas-engine pipe-line pumping units and, at the same time, have a high-speed drive more suitable to centrifugal-compressor requirements. The C-B Model R is a multipurpose unit having several applications. The principal applications are described in the literature (4). The test program on this unit is not yet completed and comparative test data are not available at the time of preparation of this paper.

AIR COMPRESSORS

Before mentioning the applications of the free-piston gas generator-turbine combination, it should be pointed out that the free-piston principle is also most advantageously applied to air compressors (9). In fact, the first successes were made in this field, and Pescara's original concept was to produce high-pressure

air to be discharged from the ends of a helicopter rotor. The present success of the SIGMA GS-34 is based largely on the extensive design, construction, and operating experience obtained with the P-13 air compressor; 1500 units of which have been built since about 1946. The free-piston air compressor has definitely proved itself to be reliable and efficient under all conditions of service. Table 3 lists some of the various models of free-piston air compressors which have been built.

TABLE 3 FREE-PISTON AIR COMPRESSORS

Junkers Model FK: 5 capacities ranging from 70 cfm at 2845 psig to 425 cfm at 57 psig
BLH Model 210-100: 210 cfm at 100 psig
Pescara-Muntz: (no particulars)
SIGMA P-13: 194.5 cfm at 85.3 psig

Free-Piston-Engine Applications

An outstanding advantage of the free-piston gas generator is its multiplicity of application. One basic model can be used in a variety of installations. Since the crux of the free-piston gas generator-turbine combination is the gas generator itself, the advantages of this flexibility of application are obvious. In France, the SIGMA Model GS-34 is now actually installed in a power plant, in a locomotive, and in a number of French naval vessels, where it is used for main propulsion. Similarly, the C-B Model R has outstanding advantages in its application to power plants, pipe lines, and auxiliary vessels where a heavy-duty, reliable, highly efficient unit is desirable. The BLH Models of free-piston engines exemplify the lightweight approach and are well suited to applications such as portable electric generation stations, locomotives, truck drive, and special marine uses where weight and space are of an essence. Since the main purpose of this paper is to present comparative test data, reference is made to the literature as much as possible for details of various applications.

Power Plants. The application of the free-piston engine to electric power-generation stations has been discussed extensively in the literature (1, 4, 9). Reference (4) lists the outstanding advantages which, in general, apply to all free-piston power stations. Reference (9) describes the SIGMA Model GS-34 gas generator-turbine combination in the power station at Rheims. Reference (4) also contains a general but complete description of a proposed power plant equipped with a C-B Model R free-piston engine. The BLH Corporation has been working primarily to develop a lightweight marine unit for the Bureau of Ships, Navy Department, but as previously mentioned it, too, will be applicable to electric-generation power stations. Its light weight and low space requirements are well suited to a portable-type plant.

Natural-Gas-Pipe-Line Pumping Stations. It is possible that the free-piston engine will attain its greatest immediate success in the United States in its application to natural-gas-pipe-line pumping stations. As pointed out in the literature (4), it combines the advantages of a high-speed drive for centrifugal compressors and the good performance characteristics of a gas engine with low costs.

Locomotives. The literature (2) describes the first free piston-engine locomotive installation. It appears that a successful free-piston engine will have all the advantages and, at the same time, eliminate some disadvantages of the diesel engine in its application to locomotives. In addition to lower initial cost, it can be expected that the maintenance costs will be less. The free-piston engine eliminates many of the moving parts of a diesel engine, all of which require maintenance. As mentioned, the French locomotive installation is very well described in the literature(1, 2). As pointed out (1), the reduced weight and space, as well as the perfect balance of moving masses, favors the application of free-piston engines to locomotives. The transmission of power between the turbine shaft and the trucks can be effected either mechanically or electrically. The former solution, namely, mechanical transmission, is simple and inexpensive. The high torque of the turbine at low speeds permits a simplification of the gear drive. In fact, it may be sufficient to have only a single-speed reduction between the turbine shafts and the truck axles. The important point is that a turbine can be selected which will have a starting torque about 2 to 4 times greater than the full-load torque. Furthermore, this torque can be increased instantaneously during the starting period by a momentary increase in gas horsepower from the gas generator.

The BLH Corporation has given extensive thought to the application of free-piston engines to locomotives. Its Model D gas generator has been designed, constructed, and partially developed for locomotive application. Owing to limited test facilities, however, and to the priority of the Navy work, the testing of this unit necessarily must be delayed for a short time. It is now obvious that the model for locomotive application will be greatly improved both in design and construction, as the result of development of the newest lightweight free-piston engine for the Bureau of Ships, Navy Department. Fig. 19 is an artist's conception of how a 3200-hp free-piston gas generator-turbine installation would appear in a locomotive. It appears that the application of a successful free-piston gas generator-turbine power plant to locomotives should be one of the next steps in the modernization of railroads in the United States, a modernization which is already under-way as evidenced by the replacement of steam locomotives with diesel locomotives.

Marine Installations. Marine installations must be divided into two separate and distinct groups: namely, those in combatant vessels where weight and space are of a premium, and those in cargo-carrying vessels where weight and space are of secondary importance. The latter case has been described in the literature (4).

The BLH approach to the free-piston engine (5) is directed toward naval applications where light weight and space, combined with good thermal efficiency and satisfactory part-load

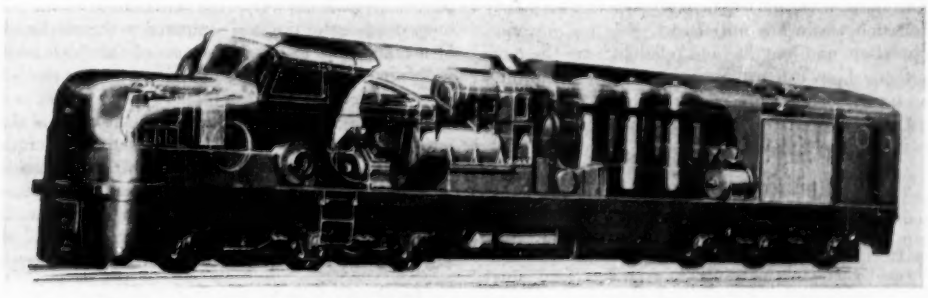

Fig. 19 Locomotive With 3200-Hp Free-Piston Gas Generator-Turbine Power Plant

characteristics, are of an essence. The Model B unit built by BLH has a specific weight of about 30 lb/shp. The unit now under development will be much lighter and smaller than the Model B, about 14 lb/shp inclusive.

The most important progress in the application of free-piston engines to marine use also has been made in France. The French Navy is actually installing SIGMA Model GS-34 power plants in fifteen minesweepers and two frigates (3).

Truck Engines. The literature (8) mentions that one of the most interesting investigations being conducted by SIGMA is the application of the free-piston engine to truck drive. A proposed method of installation in a heavy truck is very well described. Many of the same advantages of a free-piston locomotive installation also apply to heavy-truck drives. Furthermore, in addition to lowering the cost of maintenance and operation of the engine itself, a free-piston truck drive should permit a greater pay load and provide a better transmission system.

Future Possibilities

The free-piston gas generator-turbine power plant already has shown its commercial suitability and acceptability by the variety of installations made with the SIGMA units in France. The developments of the BLH and the C-B Corporations in this country have shown that several concepts of the same principle of operation can be perfected. Operational data have shown that the thermal efficiency of modern diesel engines can be surpassed with a power plant of no greater bulk or weight, fewer working parts, and reduced cost and time of construction. The free-piston engine has shown that it has many peculiar advantages, such as absence of mechanical vibration. It provides an independent high-speed drive well suited to various types of applications (4).

The free-piston unit as presently available in this country is the result of comparatively little development. A total of only seven gas generators has been constructed. Two models now appear ready for commercial exploitation. These models have not reached the stage of perfection which will be possible with continued development but they are commercially competitive.

One line of development certain to be continued, especially for uses where low specific weight and mass are required, is supercharging of the power cylinder. Outputs approaching twice the present output with little increase in severity of operation will be obtained. The weight of the power plant will be decreased accordingly.

Another line of development is afterburning. This possibility is attractive because the exhaust gases from the gas generator contain approximately 75 per cent of the original oxygen, and by afterburning, the power output can be increased about 30 per cent with only an approximate 10 per cent increase in specific fuel consumption. When one considers that this increase in power is obtained by the addition of a comparatively simple combustion chamber of low weight, yet maintaining the same operating conditions in the gas generator, the possibilities are apparent.

A parallel line of development will be perfection of heavy-duty units for installation where low initial cost, easy maintenance, economy of operation, and long life and reliability are the more important factors. Low exhaust pressures and temperatures will reduce cost and increase life of the turbine. The power plants will still have a specific weight and mass superior to that of comparable diesel power plants.

BIBLIOGRAPHY

1 "Les Groupes Générateurs à Pistons Libres-Turbines à Gaz et Leur Regulation," by R. Huber, International Congress of Engines, Paris, May, 1951.

2 "L'emploi des Générateurs à Pistons Libres en Traction Ferroviaire," by F. Picard and R. Huber, Extrait du Bulletin No. 3, December, 1951. De La S.F.M. (Editions Science et Industrie.)

3 "Application aux Navires d'un Appareil Propulsif Constitué par des Générateurs de Gaz à Pistons Libres et des Turbines à Gaz," by A. Augustin-Normand—Association Technique Maritime et Aéronautique, Session, 1950.

4 "The Free-Piston Type of Gas Turbine Plant and Applications," by J. J. McMullen and Robert Ramsey, published in this issue, pp. 15–29.

5 "The Development of High-Output Free-Piston Gas Generators," by F. M. Lewis and Robert Lasley, presented at the Spring Meeting, Columbus, Ohio, April 28–30, 1953, of The American Society of Mechanical Engineers.

6 "The Efficiency of Free Piston Gasifiers. Theoretical Considerations and Experimental Results—Future Prospects," by L. Peillon, presented at Association Technique Maritime et Aéronautique, 1949 Meeting, Paris, France.

7 "Free Piston Generators," by Professor G. Eichelberg, Eidgenossische Technische Hochschule, Zurich, Switzerland, *Schweizerische Bauzeitung*, 1948, Nos. 48 and 49.

8 "French Gas Turbine Truck Has Two Free-Piston Engines," by W. F. Bradley, *Automotive Industries*, vol. 106, February 15, 1952, pp. 52, 106.

9 "The Free-Piston Engine Development—Present Status and Design Aspects," by A. L. London and A. K. Oppenheim, Trans. ASME, vol. 74, 1952, pp. 1349–1361.

Discussion

R. Huber.[4] This paper gives evidence that the free-piston gas turbine has passed the theoretical stage and that this type of industrial gas turbine has numerous and diversified applications, particularly in France.

The engineer not specially acquainted with the free-piston technique may be surprised to learn that in spite of the additional losses in the compressor and the turbine, the efficiency of a free-piston gas turbine set is as good as the efficiency of a diesel engine. The two ways in which these additional losses are compensated are as follows:

Primarily, the relative heat losses through the diesel cylinder walls during combustion are much lower than the corresponding losses in a conventional diesel engine.

Also, the blowdown losses during exhaust are partially regained by reheating the gas feeding the turbine.

In the SIGMA GS-34 gas generator, the heat losses to the cooling water of the diesel cylinder and the piston cooling oil are only 18 per cent of the heat of combustion of the fuel, compared to 25 per cent in the conventional diesel engine.

The reduction of the heat losses through the walls is obtained principally by the small extent of the wall surface exposed to the hot gases during combustion. If we compare, for example, the total wall surface of the combustion chamber of a six-cylinder conventional diesel engine to the corresponding wall surface of a free-piston gas generator cylinder, we find that, for the same mean piston speed, the six-cylinder diesel engine will have 3 times the combustion-chamber wall surface exposed to high temperature.

Another reason why the heat losses are so low in the free-piston engine is the very high acceleration of the pistons in their inner dead-center position compared to the acceleration of pistons of a crankshaft engine. Because of this high acceleration, the walls are exposed to hot combustion gases for much less time in a free-piston engine.

There may be another question in the mind of the nonspecialized engineer, "Why does the free-piston technique develop so slowly in spite of the numerous and very interesting features which have been exposed by the authors of this paper?"

It is true that many attempts by big firms have been made to solve the free-piston problem, without success. We think the answer to this question is that the free-piston generator, in spite

[4] Le Directeur Technique, Société d'Études Mécaniques et Énergétique, Bellevue, France.

of its simplicity, is a very complex engine with an intricate mixture of thermodynamic and constructional problems which can only be solved by a long evolution.

The paper contains numerous data of the two most highly developed free-piston generators, the SIGMA GS-34 and the Baldwin-Lima-Hamilton model B.

The test figures presented for the SIGMA GS-34 refer to the prototype and were published some time ago; meanwhile 30 new gas generators have been tested and delivered. The efficiency of the recently delivered generators shows an appreciable increase, compared to the prototype. Based on the same higher heating value of 19,600 Btu/lb, referred to by the authors, the efficiency of the SIGMA GS-34 has now reached 41.6 per cent. This improvement was obtained mainly by a better design of the intake valves.

As a consequence of the improved efficiency, the exhaust-gas temperature before the turbine dropped from 945 F to 870 F at full load. Such a low gas temperature leaves an important margin for increase of power output by afterburning. If we consider 1300 F to be the gas temperature limit for the turbine blades, afterburning will increase the gas power output of the GS-34 from 1310 hp to 1730 hp. The efficiency at maximum load with afterburning would be only 9.5 per cent or 4 points lower than without afterburning. The maximum efficiency would then occur at about 80 per cent of maximum load.

The efficiency of a complete free-piston gas turbine set without afterburning is as follows:

	Per cent
Thermal efficiency based on adiabatic expansion (heating value 19,600 Btu/lb)	41.6
Percentage of adiabatic expansion work lost, due to pressure and temperature losses in ducting	1.3
Efficiency of turbine (measured on a 6-stage impulse turbine of 1000 hp)	86
Auxiliary drive	1.2
Total efficiency	34.8

The multiplicity of uses of the free-piston gasifier, as pointed out by the authors, is best illustrated by the actual program for the application of the SEME designed GS-34 by SIGMA. A summary of the applications of 70 GS-34 gasifiers which are delivered or on order is as follows:

Propulsion sets for naval vessels	44
Propulsion sets for coastal vessels	4
Prime mover for Renault locomotive	1
Electric power-generating sets (600 kw to 6000 kw)	21

W. A. Morain.[5] The paper is of interest and particularly so in that the first free-piston plant submitted to the Naval Experiment Station has given a good account of itself. Efficiencies and specific outputs are certainly acceptable on a competitive basis with other prime movers, and there is every reason to expect substantial improvement through refinements in design.

We are all interested in improving specific output, and there are quite a few methods available. The scheme of supercharging the compressor intake should receive first consideration. The authors do not feature this prominently, and the writer does not feel that one of the methods proposed is as desirable as it first appears.

Cooling of the scavenge air, mentioned as method 1 in the schemes for increasing specific output, has certain merits but also entails several undesirable features. It introduces a loss in thermal efficiency. Working back from the gas horsepower and exhaust conditions given for the Model B design, the air flow appears to run about 199 lb per min for one unit. Cooling this quantity of air from 550 F to 100 F entails a heat rejection from the system of 22,000 Btu per min. At rated load, the total heat supplied in the fuel is only about 93,000 Btu per min. Of course this aftercooling will increase the air for combustion considerably and we can burn more fuel without exceeding permissible temperature limits. However, even with the higher heat input, the loss in thermal efficiency could still be excessive.

Another drawback is that the compressor will not aspirate any more intake air since the conditions ahead of the scavenging header are unchanged. And yet, all the extra power available from the power cylinder will have to be absorbed in the air compressor owing to the nature of the gas-generator design. This means then that the pressure ratio across the compressor will have to go up considerably. The writer does not believe we are ready to go much higher than the present 7 to 1 ratio in a one-stage compressor. If we do, we again may lose out on decreased efficiencies in this portion of the cycle.

External supercharging of the compressor intake is a much more logical solution. Even a mild boost in intake pressure will produce sizable net gains in power. Intercooling at this level will reject considerably less heat, if such a step is deemed advisable.

Another step worthy of serious consideration is that of wet compression in the compressor portion. Also, there is the possibility of water injection into the scavenging header or power cylinder. This, of course, cannot be haphazard but must be worked out accurately as to quantity, particle size, and manner and timing of injection. Theoretical calculations show efficiency as well as power gains for this method.

With regard to item 3 under the same heading, it is believed we should not regard the free-piston power cylinder as anything very far out of line with present high-output engine practice. The air-fuel ratios used in the power cylinder of most gas generators with which the writer is familiar exceeds that of highly rated diesel engines. The higher air-fuel ratio means lower combustion-chamber temperature rise. Calculations made of representative cycles show that the free-piston gas generator maximum combustion temperature may reach 3000-3500 R, whereas the writer has seen similar analyses on diesel cylinders showing maxima of 4000 R. The pressures employed are usually higher in free-piston machinery, since we want to take full advantage of the elimination of the crank and associated bearings. The higher pressures are usually not sustained as long. The rate of pressure rise should be controlled as carefully as possible. The pressure alone does not seem to be harmful, but an excessive rate of rise can cause plenty of trouble in any type of engine.

J. K. Salisbury.[6] Although this discussion is not directed specifically at the excellent paper which the authors have presented, its substance is intended to approve enthusiastically the basic thought that has motivated the authors, namely, that the hot-gas generator deserves indeed the attention that is being given to it. It deserves, in fact, far more attention, as the writer shall attempt to prove.

The power portion of the engineering world has found itself in a dilemma for a good many years. Certain of its problems have been resolved to the complete satisfaction of all concerned. Certain other problems remain to be resolved by early application of new types of power machinery and observation of the economics in service of these new types. Present efforts and expenditures are completely out of balance with respect to the intensity of our activity in the respective fields.

The entire power-plant field may be readily subdivided into

[5] Project Engineer, Cooper-Bessemer Corporation, Mt. Vernon, Ohio. Mem. ASME.

[6] Department of Mechanical Engineering, Stanford University, Stanford, Calif. Mem. ASME.

two distinct broad categories. One of these involves indirect heat transfer. It is characterized by its application in situations where large blocks of power are required such as central stations and industrial power plants. In this classification fall the conventional steam plant, already used in large numbers, the mercury-steam plant, and several other types such as the closed-cycle gas turbine and variations thereof, as well as combination cycles.

The other general category of power plants includes all plants in which the transfer of heat from fuel to working fluid is by direct contact of the fuel used in the combustion process with the working fluid. This category is characterized by the use of little or no heat-transfer surface, and its application in the lower power ranges and where portability is a prime requirement, such as the transportation industry and construction projects. Two primary types, differing vastly in their basic characteristics, make up this category. They are the combustion-gas turbine, a rotating machine, and the engine, a reciprocating machine. Within the engine subdivision falls the reciprocating hot-gas generator, a thermal engine, the function of which is to supply hot pressurized gas to a gas turbine.

Considering in more detail the economic status of these plants, we note that the steam plant has attained a state of development and economic value that makes it acceptable in all large power installations without the slightest question on the part of the user. The elements of power cost (both initial and operating cost) are entirely consistent with the thermal efficiencies obtainable. In addition, units of tremendous capacity may be built. No other type of power plant offers this feature.

Over the past 25 years several mercury-steam plants have been built, all successful from the standpoint of reliability, thermal performance, and other similar considerations. In general, the cost of such plants is somewhat higher than steam plants of the same capacity, but so is the efficiency. The difference in thermal efficiency justifies the cost differential whenever fuel costs are high enough. Its position in the economic complex is widely known and well understood through years of operation of such plants.

The world is not yet well enough acquainted with the closed-cycle power plant, sometimes known as the aerodynamic turbine plant, to judge its economics accurately. Unquestionably, this type of plant has certain advantages with respect to some of its immediate competitors. It is amenable to construction in large sizes, and its light-load efficiency is quite acceptable. Although it requires an appreciable amount of heat-transfer surface when designed for high efficiency, the elevated pressure of the working fluid is tremendously effective in reducing the investment required. Occasionally the criticism of complexity is leveled at the closed-cycle plant, but this criticism may be the result of unfamiliarity rather than an objective appraisal of the plant, since so few are in operation.

Each of these plants, then, has been evaluated or is in the process. No appreciable doubt exists as to their applicability in any given power situation. The economic importance of each has led to its exploitation in proportion to this importance.

Among power plants which do not use heat-transfer surface the economic place of each is not nearly as well defined. The newest of these, at least from the standpoint of public notice, is the combustion-gas turbine. It has potentialities for applications where space and weight are at a premium, or portability is important. The absence of a requirement for water makes it unique. For the past 15 years technical journals have been deluged with articles on the future possibilities of the gas turbine, many of them predicated on the use of much higher temperatures than experience to date has proved to be feasible, the use of extensive regeneration surface, reheat, intercooling, and special devices such as comprex. It is obvious from the number of units built that a tremendous amount of manpower, money, and talent has been devoted to exploitation of the combustion-gas turbine. Many manufacturers are engaged in their construction, and most of those who are not are planning to be in the near future. Many units are currently in operation, and most of them operate satisfactorily.

The second subdivision within this category is the engine or hot-gas-generator subdivision. The writer holds no brief for any particular type of hot-gas generator, either free-piston or crank-connected. The eternal controversy over which type is better can be settled only by experience with both types in service. Thus the present discussion concerns itself only with the hot-gas generator as a principle rather than with any specific variety thereof.

Foreign manufacturers have carried on developments of the free-piston unit for many years, and not less than three domestic manufacturers have actively interested themselves in this type of power plant. Despite these facts, however, the magnitude of the development expenditures to date is completely insignificant with respect to development expenditures on the combustion-gas turbine.

The reasons are not at all clear. Perhaps the fact that hot-gas generators reciprocate instead of rotate has been a serious deterrent. However, the almost universal use of reciprocating machinery on all the railroads of the nation, in thousands of ships of the wartime Navy, and in all commercial aircraft testifies to the value of the reciprocating machine. In all of these applications the prime mover is required to be reliable and in many cases to be economically sound. It obviously has met these challenges.

The chief virtue of the hot-gas generator lies in the fact that it can readily attain the economy of the highly efficient diesel engine and simultaneously the smooth high-speed output power characteristic of the gas turbine. It is essentially a reciprocating combustion chamber capable of operation at the highest temperature that has yet been proposed by even the most ardent exponents of the rotating gas turbine. The diesel engine has demonstrated this capability during 50 years of its existence. The reciprocating combustion chamber is alternately heated by combustion and cooled by scavenging air so that its average temperature is considerably lower than the maximum temperature of the cycle. Despite this fact, the very nature of its operation is such that only hot gas is utilized for production of power in the gas turbine. Thus the hot-gas generator, in effect, constitutes a cooled combustion chamber, operating at about 3000 F, and capable of compressing gas for use in a turbine at exceptionally high efficiency, all in one package.

Since the hot-gas generator is essentially a diesel engine it must use diesel fuel. This might be a serious economic disadvantage if it had a competitor that could successfully and reliably utilize a lower grade of fuel. Although this happy circumstance may eventually come to pass, and considerable progress has been made in this direction, nevertheless today it is not a reality.

In the long run the economics of power production determine the acceptability of the prime mover. The economics become entirely favorable where either the first cost is extremely low for a reasonable efficiency or where, as in the case of the mercury-steam plant, an extremely high efficiency justifies a higher first cost. Modern gas-turbine efficiencies range from 17 or 18 per cent thermal efficiency for the simplest type to about 30 per cent for more complex units. First costs, in general, increase with efficiency. To date no gas turbine has demonstrated a marked economic superiority over other types of power plant despite the tremendous world-wide effort devoted to its development, with the single exception of the aircraft gas turbine, where military necessity for high speed makes it an obvious and nautral

selection. Similar fields exist in naval propulsion, but for the most part they are as yet unexploited.

In summary, the engineering world has available to it in the hot-gas generator a gas-turbine plant that excels the rotating gas turbine by as much as 2:1 in fuel consumption with comparable simplicity in the plants, but with some disadvantage in size and weight. Most of the elements of this type of plant are well known through experience with similar types of equipment. Certain components of the free-piston hot-gas generator were not well understood originally, but experience over the past 10 years has yielded much knowledge, so that today there is no longer a mystery with respect to the feasibility of a resonant type of machine for the production of hot gas. It is, therefore, the writer's belief that the engineering world will do well to invest an appreciable fraction of its attention in the development and evaluation of the hot-gas generator in its several forms, particularly since this may be accomplished at the expense of an extremely small fraction of its effort on other types of prime mover.

Authors' Closure

The authors appreciate the comments of Mr. Huber, who is recognized throughout the world as the guiding genius behind the French development of their free-piston gas generators.

The authors feel that the free-piston gas generator will enjoy the same numerous and diversified applications in the United States as it does in France. As a matter of fact, the applications may be even more numerous and diversified in this country. For example, the application of the Cooper-Bessemer Model R free-piston gas generator to gas-pipe-line pumping is one which, for the present, is unique in the United States. Also, the extensive trucking industry of the United States is another ripe field for further development of free-piston gas generators for this application.

Mr. Huber states that because of the intricate mixture of thermal dynamic and constructional problems, the free-piston gas generator can only be developed by a long evolution. This is, in general, true of any new prime mover. The development of the free-piston gas-generator turbine plant in the United States may seem slow but in reality this slowness has been a result of low effort. When one considers that the development was started in the United States less than 10 years ago, and that the effort in this field has been very limited, the progress appears much greater. As a matter of fact, in view of the results already attained, the progress has been rather swift in comparison with other developed prime movers such as the gas turbine, diesel engine, and steam plant.

Although this paper presents the performance data of the Baldwin-Lima-Hamilton Model B unit, the authors wish to point out that Baldwin-Lima-Hamilton is continuing development on a more advanced model.

The higher efficiencies now being attained by the SIGMA GS-34 gas generator are excellent. SIGMA is to be congratulated on their efforts and results. The authors feel that these improvements in design and performance will continue as more effort and more time is given to the free-piston gas-turbine development.

The paper has mentioned the desirable characteristics of afterburning. This method of obtaining maximum power is most interesting for plants which require peak load, especially for naval applications where full power is utilized a very small percentage of the underway time.

The multiplicity of uses which Mr. Huber has listed in his discussion definitely prove that the free-piston gas generator is now a practical power plant and not just a theoretical concept. The production and mobilization possibilities of such a prime mover are quite apparent. The identical design and size can be used in many varying applications.

It is hoped that the U. S. manufacturers will soon attain the comparable success which Mr. Huber's firm has developed in France.

In conclusion the authors wish to sincerely thank Mr. Huber for his discussion. It adds greatly to the interest of the paper and offers concrete evidence that the free-piston gas-generator turbine power plant is now an actuality.

In regard to Mr. Morain's comments, we agree entirely with his statements on the desirability of supercharging as the best method to get greater output efficiently.

The methods of increasing output stated in the paper were not intended to be all-inclusive. They were mentioned briefly and, apparently, the first one was too brief to give Mr. Morain our entire thought.

We had in mind supercharging of the cylinder, as we headed the section, and not merely cooling of the intake air, which was one factor noted specifically. Cooling of the pressure air only would not be sufficient unless the pressure of the compressed air was increased to give it the necessary differential over the exhaust pressure. We prefer exhaust pressure higher than current practice, not lower.

Our comments were general and not applied specifically to any of the current models. It was realized that a two-stage compressor would be required to give the desired air volume and pressure. So, to repeat, we agree.

We did not mention wet compression because of the lack of test data or even a full theoretical analysis to back up the expected results. Theoretically it sounds promising; but practically, very little has been proved.

We wish we could agree that the free-piston power-cylinder conditions were not out of line with present diesel practice. Reliability is improving, but even the best of which we have knowledge have not met the compression-ring life standards of our diesels because of the more severe combustion conditions. We hope that the continued improvement now in progress, however, will meet those life standards and permit us to go to even more severe operating conditions.

The authors wish to thank Professor Salisbury for his fine discussion of the paper. We wish to re-emphasize the point regarding expenditure of funds. As stated, very little has been spent on the free-piston development, but the results in proportion to these expenditures have been good. Therefore the authors agree with Professor Salisbury's conclusion that the engineering world will do well to invest in the development and application of the free-piston gas generator.

The Free-Piston Type of Gas-Turbine Plant and Applications

By J. J. McMULLEN[1] and R. P. RAMSEY[2]

This paper is intended to set forth the latent possibilities in heavy-duty free-piston machinery. The cycle promises diesel efficiency from a simple low-temperature gas turbine having low first costs. Many features are described in the paper. Cooper-Bessemer has built a test plant and is now investigating its operating characteristics. No conclusions have been announced. Economic evaluations are being made requiring additional field work which includes an examination of the general acceptance by engineering and operating people who ultimately will decide the actual utility. Detailed cost studies of complete plants, including careful estimates of the machinery, have been made for electric power generation, pipe-line pumping, and marine installations. Some of these have been made available for use in this paper with the belief that such an evaluation of this prime mover will be of general interest to the Society.

THE Bureau of Ships, Navy Department, has been actively interested in the development of free-piston gas generators since 1942.[3] This active participation has been directed primarily toward gas generators of high specific outputs and low weight for application to combatant vessels. However, the desirability of a heavy-duty unit for auxiliary-type vessels and for other uses has always been recognized. Consequently, the Cooper-Bessemer investigation of a heavy-duty free-piston-turbine power plant has been followed with interest by the Bureau of Ships because of its possible future application to all types of auxiliary vessels such as cargo ships, troop transports, tankers, and the others.

Free-piston machinery may be applied to wide ranges of weights and outputs, some of which only recently have been undertaken; however, these findings indicate a very definite suitability to many heavy-duty applications.

In this case the free-piston machine weighs about 30 lb per hp normally aspirated and will weigh less than 20 lb per hp when supercharged, yet it is designed structurally as heavy as a 100-lb per hp motorship diesel.

This paper has three objectives:

1 To describe the potential effectiveness of heavy-duty free-piston machinery.

2 To discuss an investigation of heavy-duty free-piston-turbine prime mover.

3 To make a realistic appraisal of free-piston-turbine power in three heavy-duty-service applications—an electric-power-generating station, a pipe-line pumping station, and a cargo vessel.

Background

The Cooper-Bessemer Corporation is conducting both a full-scale free-piston investigation and a study of various prime movers. The actual findings are of a confidential nature and have not been released for publication, but the company is now presenting some of the general information along with the substance of some of the more important studies, in the belief that it has general value.

Economic studies of prime movers are always complex. The analysis of thermal cycles is one matter, but the costs of manufacturing, the problems of facility, and the field requirements have to be integrated carefully with the matters of fuel competition and market costs, the installation expense of the equipment, labor of operation, costs of maintenance, and the character of the driven equipment.

The need is growing in nearly all fields for a prime mover of high efficiency and relatively low cost to drive such high-speed machinery as centrifugal pumps, compressors, and electric alternators. Then, too, the American preference for turbine drives in cargo ships and tankers is well known.

The basic feature of the free-piston-gas-turbine prime mover is the combination of the high-thermal-efficiency qualities of the reciprocating internal-combustion engine and the high-speed rotating power take-off provided by the turbine.

Present-day turbocharged engines of large sizes are equipped with gas turbosuperchargers aggregating many thousands of horsepower now in daily continuous operation in large plants. Thus, gas turbines operating on the pulsating flow of exhaust gas have been proved over the past 15 years.

The single power bore of a free-piston generator merges the many cylinders of a large multicylinder engine and, since the direct thrust of the power pistons compresses the generator's own scavenge air, the concept of this design then sheds the crankshaft, bearings, rods, pistons, and cylinder heads common to the usual crank engine.

The free-piston design and cycle make for great simplicity. Low maintenance expense and lower costs are synonymous with the low number of operating parts. The net result is a turbine power take-off shaft having the pneumatic flexibility of torque comparable to that of the steam turbine or the hydraulic drive of an automobile.

Thermodynamic Reason for Free-Piston Cycle

Since the preceding evolution is all directed toward simplicity and high efficiency, this paper must make some mention of certain differences between the continuous-combustion gas turbine and the free-piston gas generator-turbine combination. The basic Brayton cycle provides the means for comparison

$$\text{Limiting thermal efficiency} = 1 - \left(\frac{P_1}{P_2}\right)^{\frac{k-1}{k}}$$

for any heat engine where P_1 is the initial pressure before compression and P_2 is the pressure at which combustion takes place.

Supercharged diesel engines operate at a P_2/P_1 of 40 : 1 to 65 : 1.

---

[1] Commander, USN, Bureau of Ships, Navy Department, Washington, D. C. Mem. ASME.

[2] Consulting Engineer, The Cooper-Bessemer Corporation, Mount Vernon, Ohio.

[3] "Performance of Free-Piston Gas Generators," by Commander J. J. McMullen, USN, and Warren G. Payne, published in this issue, pp. 1–14.

Contributed by the Gas Turbine Power Division and presented at the Spring Meeting, Columbus, Ohio, April 28–30, 1953, of The American Society of Mechanical Engineers.

Note: Statements and opinions advanced in papers are to be understood as individual expressions of their authors and not those of the Society. Manuscript received at ASME Headquarters, February 9, 1953. Paper 53—S-13.

The free-piston engine is a form of highly charged diesel or gas-engine cylinder, without the limiting physical compression ratio of a fixed-crank engine. It may operate with combustion taking place at any point throughout a wide range of selectivity, adjusted by the pneumatic pressure-regulating valve. This combustion level may be as high as 100:1 over the atmospheric-pressure line.

Thus, the free-piston engine may attain a pressure ratio over atmospheric at the end of compression as high as 100:1 with an ideal Brayton-cycle efficiency of 69.7 per cent. The single-shaft nonregenerative gas turbine on an open cycle burns its fuel at a pressure ratio of about 6 times atmospheric and therefore has an ideal Brayton-cycle efficiency of 37.2 per cent.

It would be necessary to increase the compression ratio of the simple type of gas turbine from 6:1 to 100:1 and the top temperature to 3900 F abs in order to equal the ideal efficiency of the free-piston cycle operating at a conservative 1000 F inlet temperature and about 40 per cent over-all thermal efficiency. Actually the free-piston turbine amounts to a low-temperature gas turbine provided with high-pressure combustors and a reciprocating scavenge compressor.

Popular belief has it that a mere increase of temperature of operation of the simple open-cycle gas turbine immediately will raise the efficiency to the high brackets. This is a complete misconception. For example, an increase from 1350 to 1800 F would raise the actual efficiency from about 17 per cent up to about 18½ per cent at a compression ratio of 6:1.

It is necessary to clear up that general misunderstanding; but at the same time point out that the more complex turbine plants with axial compressors, intercooling, regeneration, reheat, and with HP and LP turbines, when 1800 F materials become commercial, may be expected to approach the efficiency of the 1000 F simple free-piston plant. It is also necessary to point out that the free-piston plant designed as a compact, self-contained unit requiring no intercooling, regeneration, reheat, or multiple turbines may be expected to show decided improvement in efficiency and output when its turbine is constructed for temperatures above 1000 F. The 1000 F temperature of operation was selected for this investigation. Of greatest importance, however, is the fact that the free-piston generator lends itself ideally to supercharging, and the design investigated herewith, when operated at 1200 F supercharged, will show double the horsepower output, thereby reducing present conservative cost estimates so drastically that it would seem that the free-piston unit stands in a very sound position in the foreseeable evolution of prime movers. That, concisely, is the free-piston's basic case as we look ahead.

It is not the purpose of this paper to set forth the free-piston unit as the "omega" of all types of prime movers. They all have certain good qualities which recommend them for specific purposes. These good possibilities of the free-piston design are naturally set forth for further consideration.

Any view of the free-piston unit must encompass the whole development of the modern engine and must be broad enough to take in all of the achievements of the gas turbine. Actually the free piston stands between these two with, potentially, the virtues of each—high efficiency and simplicity—and without the principal faults of either; that is, the weight, complication, crankshafts, pistons, rods, and heads of the engine, and without the fuel and efficiency problems of the turbine and its physical requirement for high-temperature materials.

So much for background comment. We wish only to add that our investigations have been made with conservatism and the pressures and temperatures are well below actual test achievements. We hope the material offered here will provide a basis for further examination.

Objectives

The major objectives in undertaking the investigation were to prove the following:

1 That it is possible to drive a variable-speed gas turbine at conservative inlet conditions, especially as regards temperature, but with much higher thermal efficiency than comparable steam or gas-turbine plants. Low temperature permits the wide use of noncritical materials throughout the gas generator-gas turbine combination. For example, the gas-turbine inlet chamber is a nodular-iron casting and the major parts of the gas generator are cast iron. Where required for shock purposes, nodular-iron castings would be used.

2 That a reduction results in foundation weight and space requirements because of complete freedom from vibration. The over-all center of gravity of the gas generator-gas turbine combination is very low.

3 That great flexibility of installation is the result of the gas turbine being independently located.

4 That a method is possible for obtaining a high variable shaft speed suitable for electric drives, centrifugal compressors and pumps, and turbine ship propulsion, but at diesel-engine efficiency. The gas generator shows the same insensitivity to ambient conditions as the diesel engine and steam plants.

5 That because of the high specific output of the prime mover, the space and weight requirements are favorably low. In larger applications which require a multiplicity of units, still greater reductions in cost, weight, and space can be effected by grouping multiple gas generators about a common turbine.

6 That it is possible to build a unit of simple construction and good accessibility, low initial cost, low operating cost, and low maintenance cost.

7 That flexibility may be attained in the gas-generator power-cylinder compression ratio to suit various fuel requirements and to facilitate cold starting, and so on. Also for this reason, gas generators will be very adaptable to supercharging.

8 That an instant, nondestructive shutdown protection is possible in the event of any mechanical difficulties in the gas generator, since there are no stored up inertia forces.

9 That the gas generator-gas turbine combination has ideal torque characteristics over a wide speed range. The torque characteristics are similar to a steam turbine, but at much higher efficiency.

10 That starting is easier in cold weather because of absence of large quantities of lube oil in crankcase and elimination of crankshafts and connecting rods. This elimination of crankcase should result in a lower lube-oil consumption.

11 That air mass flow is comparable to steam and diesel installations; ducting problems are simplified as compared to those of the constant-pressure type of gas turbine.

Description of Test Unit

Laboratory test investigation at Cooper-Bessemer began in January, 1952, when the test unit first operated on diesel fuel.

As a basis for investigation, the following figures have been used in Cooper-Bessemer tests. The gas-generator power-cylinder bore is about 14 in. with a compressor-cylinder bore of 37 in. Scavenging-air compression is outward, single acting, with a net stroke at full load of approximately 18½ in. at a cyclic frequency of 555 cpm. A gas-generator rating approximately 1750 ghp at 72 psig, discharging at 1000 F, is taken as the basis of tests. Thermal efficiency is 45 per cent (on ghp basis). This is a design figure which has been confirmed. The direct-bounce piston is outboard of the compressor piston.

There is no necessity for governing the reverse bounce since the pressure in the bounce and compressor rear spaces are controlled

automatically. Bounce air supply is to be taken from the scavenge air. A single pair of racks connects the two piston assemblies. Three fuel injectors are used in the power cylinder and the fuel-injection system is of the high-pressure storage type with suitable modifications to adapt it to the specific requirements for free-piston machinery.

This test system was developed at Cooper-Bessemer as a result of detailed studies and exhaustive bench analysis. The gas generator is expected to be adapted to operate as a dual-fuel or spark-ignited gas engine or on heavy oils. This requires complete laboratory investigation.

Starting (in this design) is extremely simple. It is accomplished by a cycle which automatically places the machine in normal running equilibrium on the first stroke. There are no abnormal starting conditions requiring the use of a governor. Since starting is accomplished in one cycle, a minimum amount of air is used, and transition from the starting to the running condition is effected instantly and automatically. A simple push-button starter is furnished and there are no critically timed valves in the system.

Low Maintenance

The power cylinder is built in three sections, consisting of an exhaust section, central combustion chamber, and inlet section. The entire cylinder is easily accessible from the top and may be removed as one unit for servicing. This is an important factor from a maintenance standpoint. The power-piston rings may be serviced by sliding back the bounce and compressor cylinders as complete assemblies. The pistons and liners are internally cooled, and metered lubrication is used. The reed-type compressor valves are arranged in cages which can be removed readily from the outside for inspection. The controls, which are reliable and simple, consist of commercial-type pneumatic and hydraulic devices. Complete control of the gas generator is accomplished by a single lever which governs fuel quantity and timing, and bounce effect. This lever is actuated directly by the turbine governor. Safety protection is furnished in the event of piston overstroke, turbine overspeed, excessive temperatures, and inadequate lube-oil pressure.

The gas generator-gas turbine combination is capable of operating at any rate from full load down to the turbine idling condition without any complicated or additional control devices, such as intake throttles and exhaust-waste gates. Good part-load efficiency is a result.

Fig. 1 shows the clean simple lines of the unit being used for the investigation. There is very little external piping. The auxiliaries are all independently driven and can be arranged so that one set is capable of providing for a group of gas generators in multiple applications.

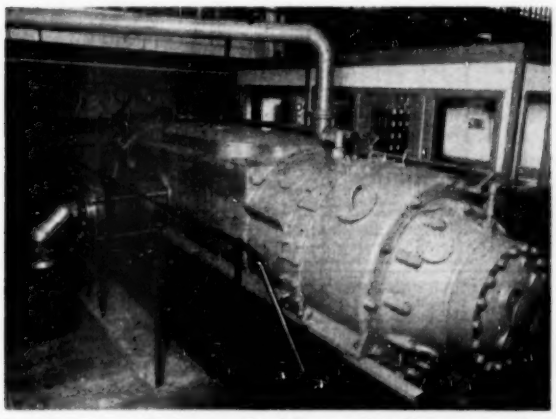

Fig. 1 Cooper-Bessemer Free-Piston Gas-Generator Test Unit

In addition to the gas generator, it was also necessary to build a gas turbine. The gas turbine is essentially a simple power turbine embodying techniques perfected by the company over the past years during which large turbosuperchargers have been manufactured. It was designed to operate at 1000 F and 72 psig in order to match the gas generator and to provide maximum

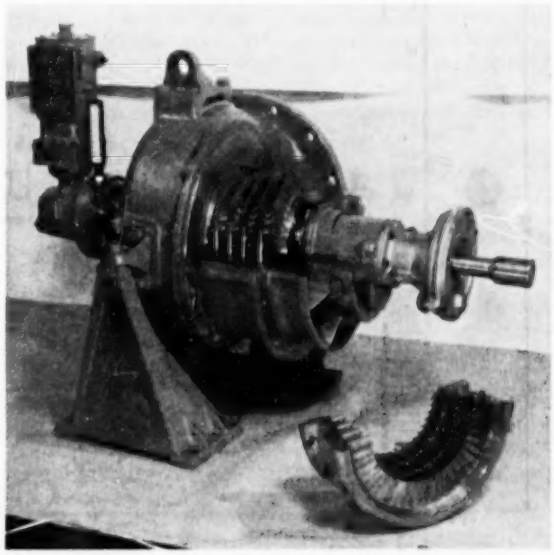

Fig. 2 Cooper-Bessemer Free-Piston Gas-Turbine Test Unit

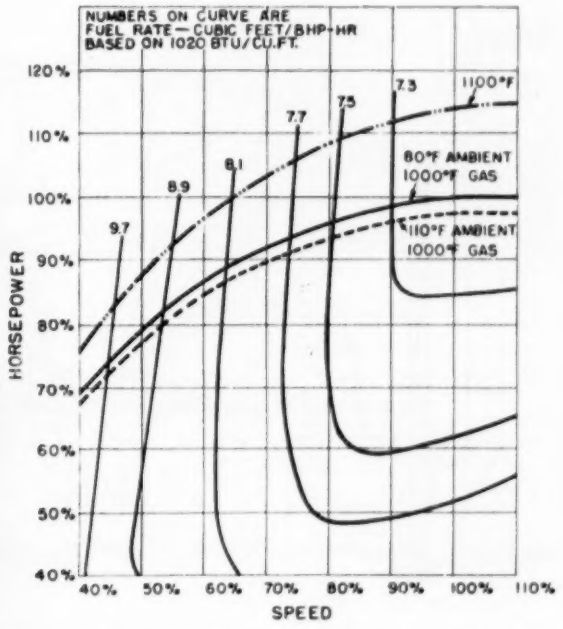

Fig. 3 Typical Part-Load Performance Free-Piston-Type Gas-Turbine Power Plant

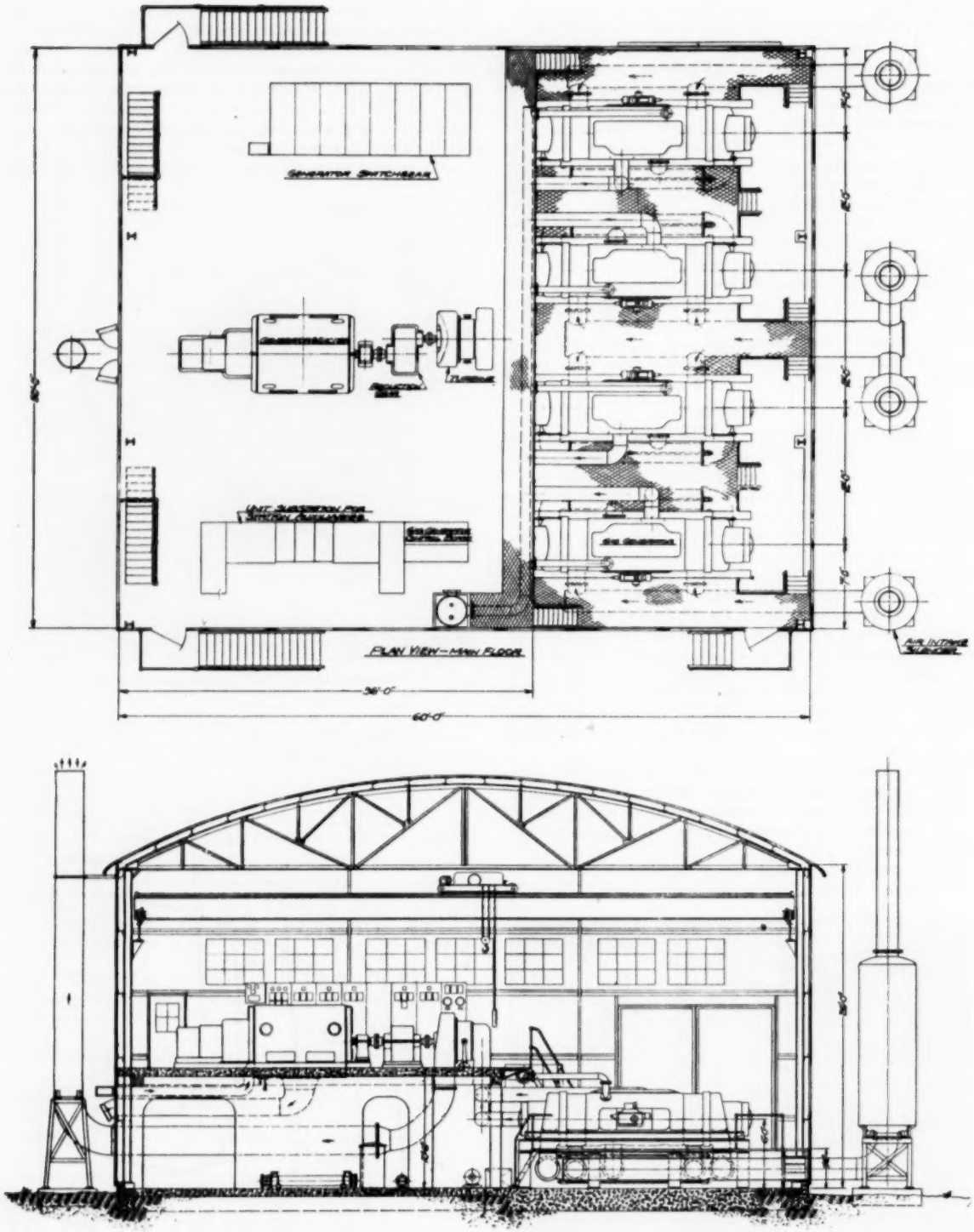

Fig. 4 5000-Kw Free-Piston Gas-Turboelectric Station

durability using noncritical materials. As a result of careful design investigation, the turbine is a small, efficient, high-speed unit. It has five reaction stages, and its speed rating is 14,400 rpm. The rated output is 1500 shp at 85 per cent efficiency and the gas flow rate is 32,000 lb per hr.

Fig. 2 shows the gas turbine with the upper half of the casing removed. The major casing members are cast from nodular iron. The rotor, illustrated in Fig. 2, is a solid forged-steel spindle. The blades are precision castings with maximum usage of interchangeability of basic blades. The two shaft bearings and the thrust bearing are of the conventional type.

TABLE 1 FREE-PISTON TURBOPOWER-UNIT SPECIFICATION

F.P. Gas Generator

Type - Two Stroke, Horizontal, Opposed Free Piston

Exhaust Gas HP, Nat. Aspir.	1750
Exhaust Gas HP, Supercharged	3000
Exhaust Pressure, Full Load, psig.	72.5
Exhaust Temperature, Full Load, °F.	1000
Power Cylinder Diameter	14
Nominal Stroke, Inches	18½
Cycles per Minute	555
Thermal Efficiency on Gas HP Basis, %	45

Gas Turbine

Type	Reaction
No. of Stages	5
Shaft HP at 85% Efficiency	1500
Inlet Pressure, Full Load, psig.	72.5
Inlet Temperature, Full Load, °F.	1000
Gas Flow, Lbs. per Hour	32,000
Turbine Speed, RPM	14,400
Weight, Lbs.	6000

The turbine overspeed protective device is unique in that, in the event of excess speed, a by-pass valve is tripped open and the residual gases in the exhaust system are by-passed directly to atmosphere. This is in addition to the fuel cutoff and permits the fastest possible unloading of the plant.

The gas generator - gas turbine test unit was designed conservatively to study the usefulness of such machinery for heavy-duty continuous operation.

The free-piston power gas cycle is certainly not confined in its usefulness to the heavy-duty application. It would seem to have a great deal to offer in every class of service. This investigation, however, necessarily has been concerned with continuous operating service, with particular reference to the fields in which turbines are frequently used.

The specifications of the gas-generator design used in this investigation are shown in Table 1. Typical part-load operation is shown in Fig. 3.

In examining any relatively new prime mover, it is essential that a multiplicity of applications be considered, especially to insure sufficient broadness of fields. We believe that the heavy-duty free-piston gas generator - gas turbine combination will be competitive in the general base power field, as well as useful for stand-by, semiportable, and other applications where foundations are a problem. In all uses for these prime movers, the weight and space saving, together with improved plant layout, simplicity, reduced costs, and high thermal efficiency, is notable. For example, compared to heavy-duty engines, weight and space savings of 30 to 60 per cent are expected, depending on type of drive and application. The same holds true in comparison with steam-turbine plants, and, of course, the high thermal efficiency of the gas generator-turbine unit excels that of both steam and continuous-combustion gas turbines.

In order to discuss specific cases, we have selected three of the basic applications—electric-power generation, pipe-line pumping, and ship propulsion.

Electric-Power-Generation Station

The development of the free-piston gas generator-gas turbine combination for electric-power generation is aimed initially toward installations of moderate power. Considerable thinking today is directed toward a 5000-kw unit consisting of one alternator, one gear, and one turbine, with three or four gas generators, all considered as one assembly, Fig. 4. There will be a lesser number of units when supercharging is applied. These unitized 5000-kw prime movers may be used efficiently in multiples. The ultimate limiting size of gas turbogenerator-electric power plants will be determined only by practical experience and the economics of specific applications. Multiunit gas-engine plants of 150,000 hp are now a reality and even larger plants are practical.

The outstanding advantages of this application include the following:

1 High thermal efficiency even at low powers.

2 A high-speed drive which permits the use of compact low-cost electrical equipment.

3 The possibility of several gas generators discharging into a common gas turbine, making for a more compact inexpensive installation.

4 Low initial maintenance and operating costs for equipment and housing.

5 Rapid control of output, permitting instantaneous response to load changes.

6 Ideal adaptation to either stand-by or peak-load service because of simplicity, low initial operating and maintenance costs, and instant availability for service. The simple foundation requirements are suited to plants which have to be moved from time to time.

A small 1000-kw electric-power-generation installation is shown in Fig. 5. A concrete mat is set in at ground level. The

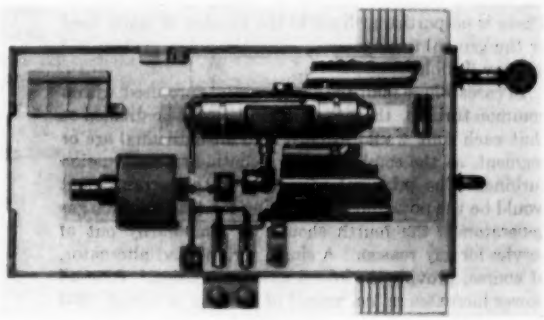

Fig. 5 Prototype Electric Test Plant

gas generator - gas turbine, reduction gear, and electric generator are supported on runners or columns at a height sufficient to allow all piping to be placed conveniently in the space between floor level and the mat. The floor level is about 4 ft above the concrete mat. Accessories may be mounted at either level as desired and are driven independently. This arrangement has known advantages in that coolants and lubricants may be circulated before starting up and after shutting down to insure proper lubrication and an adequate cooling-down process, without the necessity of keeping the prime mover in operation during these periods. This general construction may be expanded to multiple units in plants desiring the turbines and power gas generators on one floor level.

The reducer is of conventional type, with a speed reduction of about 4:1. The even torque of the gas turbine permits simple,

light construction. The electric generator is of the high-speed, compact type operating at 3600 rpm rated speed. It is a complete unit with self-contained accessory equipment.

The light foundation and the compactness of equipment permit a relatively cheap and simple building construction. Clearance of approximately 7 ft above the floor level is ample for the removal of the major gas-generator parts.

The turbine is shown closely coupled to the gas-generator exhaust. While there is some evidence that the use of an exhaust surge chamber at this location would be beneficial, it is not entirely necessary. In the event one is added, it can be arranged under the floor in such a manner as to make little, if any, change in the present general arrangement.

The installation shown is one of the smaller ones which would be most applicable to booster, stand-by, or peak-load plants. Larger plants would employ a multiplicity of gas generators feeding into a common turbine of much greater output. There is no particular limit to the number of units used or the general arrangement, since the entire system will be very flexible.

In cases where multiple gas generators are used with a common turbine, the nozzle casing would be divided so that each unit would exhaust into an individual arc or segment, as the combustors of a continuous combustion turbine. The principal advantage of this arrangement would be the possibility of carrying the load on three gas generators if the fourth should be temporarily out of service for any reason. A single turbine and alternator, of course, provide the lowest-cost installation. Over-all power increases in increments of 1500 hp or about 1000 kw would be available with a 6000-kw unit, available in multiples, using standard gas generators with turbines of the required designs. High thermal efficiency would be maintained in all plants from the smallest to the largest. The efficiency at part loads would be maintained at a relatively high level.

The governing of the plant is straightforward and simple and makes use of the various devices noted in the general description of the gas generator-gas turbine plant given earlier. The single control system for the gas generator is actuated from the turbine governor shown at the input end of the turbine. The generator itself can be any of the conventional types furnished for electric-power-generation equipment. All of the safety devices which we have previously described are applicable.

Listed in Table 2 are the general characteristics for a 5000-kw free-piston electric generation-station installation.

TABLE 2 GENERAL INFORMATION AND COST ESTIMATE FOR 10,000-KW FREE-PISTON TURBOELECTRIC POWER PLANT

Estimates made from manufacturing detail drawings and design drawings of installation with land, structures, installation cost, facilities, handling, wiring and piping, engineering, and contingencies as summarized in Tables 2A and 2B.

Rating	10000 KW
Number of Turbo Alternators	2
Number of Gas Generators per Unit	4 (Battery of 4 unitized with each turbo alternator)
Fuel Rate at Generator Terminals	9500 BTU/KW Hr. Bunker Oil or Gas
Gear 98% Eff.	
Turbine 85% Eff.	
Alternator 96% Eff.	
Overload Capacity	125% at ambients up to 105°
Machinery Cubage Overall	19,300 Cu. ft./5000 KW Unit
Total Weight not Including Generator or Gear	195,000 lb./5000 KW Unit
Air Requirement at 80° at 1000 ft. alt.	43.7 lbs./sec./5000 KW Unit

Operating Expense

The free-piston generator is expected to have low operating and maintenance expense. Comparable engine powers will run into many cylinder multiples. The fact that the free-piston generator is essentially a single-cylinder internal-combustion engine and does not include multiple pistons, rods, bearings, crankshaft, or heads, certainly reduces the actual labor of handling. The next factor is the design attention given to direct accessibility. Valve cages are exterior and easily removable. The end cylinders may be slid back exposing the piston rings, with little effort or time

TABLE 2A ESTIMATE OF CAPITAL INVESTMENT FOR 10,000-KW GAS-TURBOELECTRIC GENERATING STATION

I.	Land & Improvements	$ 32,500
II.	Structures	146,500
	A. Main Generating Building	
	B. Shop & Warehouse Building	
	C. Office Building	
	D. Water Well Building & Equipment	
III.	Equipment	$1,380,000
	A. Main Engines, Turbines & Generators	
	B. Electrical Install. & Standby Gener.	
	C. Fan Cooled Radiator Equip.	
	D. Mech. Install., Piping & Instru.	
	Total Direct Cost	$1,559,000
Add 7% for contingencies, omissions & contractrs. Equip.		109,100
	Sub. Total	$1,668,100
Add 9% for Engrg., Overhead & Interest		150,100
	Total Capital Investment	$1,818,200
	Avg. Cost = $182/KW	

TABLE 2B BREAKDOWN FOR ESTIMATE OF CAPITAL INVESTMENT FOR 10,000-KW GENERATING STATION

I.	Land & Improvements	
	25 Acre Site	$ 7,500
	Grading, Fencing, Walkways & Drivemats	25,000
	Area Lighting & Waste Disposal Plant	
II.	Structures	
	A. Main Generator Building	$ 93,400
	Steel Frame Building 50' x 108' x 14' on R.C. Footings, and 2' R.C. mat under entire area, 5 Ton Crane	
	B. Shop and Warehouse Building	$ 22,100
	Steel Frame Building 28' x 48' x 12' on R.C. Footings, with 8" R.C. Slab Floors, Plumbing & Millwork Incl. Tools & Test Instruments, 3 Ton Crane	
	C. Office Building	$ 9,700
	Steel Frame Building 12' x 36' x 10' on R.C. Footings, Millwork and Office Furniture	
	D. Water Well	$ 21,300
	Well Contract	
	Well House and Pump	
	Treating Plant	
III.	Equipment	
	A. 2 - 5000 Turbo Generator Units	$ 919,600
	Each Unit 4 - Gas Generators	
	1 - Gas Turbine	
	1 - Speed Reducer Drive	
	1 - 13.8 KV, 3 Ph., 60 Cycle alternator	
	Incl. Accessories, Freight and Handling	
	B. Electrical Installation & Standby Generator	$ 234,100
	Unitized Auxiliary Sub-Station	
	100 KW 1200 RPM Engine-Generator Set	
	Switch Gear Panels & Feeders	
	Electrical Installation Labor	
	10,000 KVA Transformer 13.8/69 KV	
	69 KV Oil Circuit Breaker, 500,000 KVA	
	Distribution Structure	
	C. Fan Cooled Radiator Equipment	$ 74,200
	D. Mechanical Installation, Piping & Instrumentation	$ 152,100
	Total Direct Cost	$1,559,000

consumed. The power cylinder may be removed by a sling from a hand hoist directly from the top of the generator. This is believed to represent the maximum of accessibility. A single gas generator may be shut down, automatically valving off the turbine, while the load is still on the line, and any ring, nozzle, or plug attention given with least loss of time or effort.

Ring and liner wear may be minimized by using the best possible cooling inside and outside the piston head and in the liner. Since only one cylinder is involved, highest-quality materials can be afforded and greater attention given to detailed cooling than is ordinarily considered economical in a crank engine of multicylinder type.

Careful attention to ring design and cooling can be made to dry up the lube-oil consumption to lowest limits, especially with cooled walls and metered oil. The low-temperature turbine consumes little lube oil. The alternator or any centrifugal machine will have characteristic maintenance and lube-oil consumption.

Operating labor is minimized with this type of equipment. Automatic controls may be applied to whatever extent may be found cheaper than the use of manpower. Actual control of the free-piston gas turbine is extremely simple because all functions of the fuel feed and load are tied to a single central point. This one control may be operated manually by lever or push button, which may be remote if so required.

It is doubtful that any expensive installation will ever be let run with a complete absence of attendance; however, if this is desired, the apparatus may be applied with a minimum of complication as compared with other prime movers. Protective devices for overspeed, overheating, and component failures are of usual types. The cooling is done with a closed-cycle radiator arrangement requiring practically no make-up even in the hottest climates, Fig. 3. In the usual case of the constant-pressure gas turbine, evaporative cooling is used when ambient temperatures exceed 80 F, otherwise there is loss of power and efficiency. In engines the compression ratio is fixed by the crank; this brings about the necessity, in hot climates, for cooling the intake air to maintain power output as well as control of the detonating point in some fuels. The free-piston generator having a variable compression ratio can be adjusted to fuels and can be overstroked to maintain rated power in hot ambients.

The ability to handle wide ranges of gas and liquid fuels is a matter requiring broad investigation (now under way), but in general it is known that the free piston with a large excess of combustion air is ideally suited to handle these ranges of fuel. This is a subject for a technical report in itself.

Pipe-Line Pumping Unit

The application of the free-piston generator to pipe-line pumping was significant in Cooper-Bessemer's decision to undertake a free-piston investigation. As one of the nation's foremost suppliers of pipe-line pumping power, the company recognized a growing interest on the part of pipe-line companies, refinery and chemical-processing companies in centrifugal machinery.

A reliable and highly efficient turbotype prime mover is desirable in some installations, but such a unit will have to embody high efficiency. The wastage of any natural resource as a fuel is certainly to be avoided. Rapidly rising costs of some fuels in the field also will dictate the use of an efficient prime mover.

For booster-station applications, power sizes as small as 1500 hp may be installed inexpensively and with high efficiency. The free-piston turboengine lends itself to parallel-connected high-speed centrifugal wheels, since it has ideal flexibility for parallel operation in contrast to fixed-speed electric motors. The advantages of paralleling are smaller cheaper centrifugals and smaller piping.

The usefulness of the small 1500-hp type of free-piston unit is notable for the foregoing reasons. However, the use of free-piston machinery in groups or batteries of gas generators driving a single turbine provides a most flexible and inexpensive arrangement. This latter type of plant has a great advantage over other large, single, prime-mover installations in that one of the gas generators can be taken out of service and the other units in the battery can continue to carry the load.

To sum up, the outstanding advantages of free-piston gas generator-gas turbine combinations for pipe-line pumping installations include the following:

1 Good adaptation to centrifugal machinery. The unit has a high-speed drive and flexibility in speed control.

2 Low installation, maintenance, and operating costs. Low fixed charges which are a large factor in pipe-line operating costs.

3 Reliability with simplicity and durability with low temperatures and high thermal efficiency. Pipe-line pumping machinery must be capable of continuous operation at maximum loads over long periods of time.

A complete pipe-line pumping unit is shown in Fig. 6. (The gas turbine and gas generator have been described already.) A standard centrifugal compressor of company make is shown. The general design, shown in Fig. 7, is based on that of a typical compressor station of this type.

A 1500-hp turbocompressor pumping unit, installed in a typical building, is shown in Fig. 8. The concrete flat mat may be at ground level. Runners or columns support the gas generator, turbine, reduction gear, and centrifugal unit at a height sufficient to allow all piping to be placed conveniently in the space, about 4 ft high, between the floor level and the concrete mat. This represents lowest-cost construction and permits the main-line piping to cross above grade in the building. Valve heights are at a convenient level.

The operating floor is smooth, unobstructed, and with convenient working space, room for controls, and easy observation of all elements. Low building height is permissible because the highest part of the machinery is only about 4 ft above floor level. Removal of any major elements could be accomplished within 3 ft above the machinery, making for a total required dismantling height of 11 ft above the concrete mat. The simplicity of the entire installation is evident from the drawing.

This 1500-hp station is typical of a smaller pumping or booster station.

In Fig. 7, the accessories are all unitized on the basis of three gas generators grouped in this manner. An independent radiator serves the 5000-hp group. Similarly all accessories such as water and oil pumps are manifolded and piped to serve this group.

Stations of 5000 hp, 10,000 hp, 15,000 hp or larger multiples may be installed on this inexpensive basis in 5000-hp units.

Fig. 9 shows parallel arrangements of an oil-line station.

The foregoing examples represent several possibilities. There is a wide choice of arrangements and powers available and a single standardized design and size of gas generator may be used over a wide range of powers.

Listed in Table 3 are the general characteristics and estimated installed cost of typical 10,000-hp and 15,000-hp gas-turbocentrifugal pipe-line pumping stations.

The Free-Piston Turbomotorship

In discussing the marine field, we must distinguish between the requirements for ships of the combatant type and ships of the auxiliary or cargo-carrying type. Combatant ships usually require propulsion machinery having the lowest weight and space characteristics. In the auxiliary or cargo-carrying class, however, other factors are more prominent. It has been mentioned

TABLE 3 GENERAL INFORMATION AND COST ESTIMATE FOR 10,000-HP AND 15,000-HP PIPE-LINE PUMPING STATIONS

Estimates made from manufacturing detail drawings and design drawings of installation with land, structures, installation cost, facilities, handling, wiring and piping, engineering, and contingencies as summarized in Tables 3A and 3B.

Rating	10000 HP	15000 HP
No. of 5000 HP Units	2	3
No. of F.P. Gas Gens. for Unit	3	3
No. of Centrifugal Pumps or Compressors	2	3
Plant Fuel Rate at Turbine Coupling	7000 BTU	7000 BTU with Nat. Gas or Bunker Oil
Overload Capacity	125%	125% at any ambient up to 105°F. without evap. cooling
Machinery Cubage Overall	10,660 cu. ft. per 5000 HP Unit	10,660 cu. ft. per 5000 HP Unit
Total Weight not Including Centrifugal Pump or Compressor	350,000 lbs.	525,000 lbs.
Air Required 80° at 1000° F.	58.5 lb./sec.	87.5 lb./sec.

TABLE 3A ESTIMATE OF CAPITAL INVESTMENT FOR 10,000-HP AND 15,000-HP GAS-TURBOCENTRIFUGAL COMPRESSOR STATIONS

Rating	10,000 HP	15,000 HP
I. Land & Improvements	$ 32,500	32,500
II. Structures	118,000	146,500
A. Main Compressor Building B. Shop & Warehouse Bldg. C. Office & Comm. Bldg. D. Water Well Bldg. & Equip.		
III. Equipment	$1,119,800	$1,598,900
A. Main Engines, Turbine & Compressor B. Elec. Install. & Standby Gener. C. Fan Cooled Radiator Equip. D. Mech. Equip. Install. & Piping & Instr. E. Main Gas Piping		
Total Direct Cost	$1,270,300	$1,777,900
Add 7% for Contingencies, Omissions & Equipment	88,900	124,500
Sub. Total	$1,359,200	$1,902,400
Add 9% for Engineering, Overhead & Interest	122,300	171,200
Total Capital Invest.	$1,481,500	$2,073,600
Station Cost	148/BHP	138/BHP
With Operators Housing	155/BHP	143/BHP

TABLE 3B BREAKDOWN FOR ESTIMATE OF CAPITAL INVESTMENT FOR 15,000-BHP COMPRESSOR STATION

I.	Land & Improvements	
	25 Acre Site	7,500
	Grading, Fencing, Walkways & Drivemats	25,000
	Area Lighting & Waste Disposal Plant	
II.	Structures	
	A. Main Compressor Building Steel Frame Building 60' x 120' x 14' on R.C. Footings and 2' R.C. Mat under entire area, 3 Ton Crane	93,400
	B. Shop and Warehouse Building Steel Frame Building 28' x 48' x 12' on R.C. Footings with 8" R.C. Slab Floors, Plumbing & Millwork incl. power & hand tools, 3 Ton Crane	22,100
	C. Office & Communication Building Steel Frame Building 12' x 36' x 10' on R.C. Footings Millwork and Office Furniture	9,700
	D. Water Well Well contract, well house, pump & treating system	21,300
III.	Equipment	
	A. 3 - 5000 BHP compressor units Each unit 3 - Gas Generators 1 - Gas Turbine 1 - Speed Reducer Drive 1 - Centrifugal Compressor Incl. Accessories and freight, handling	1,035,000
	B. Electrical Installation & Standby Generator Light & Power Wiring 300 KW 1200 RPM Engine Generator Set Utility Sub-Station Complete Panels for Motor Starters and Lights	70,500
	C. Fan Cooled Radiator Equipment	90,300
	D. Mechanical Equipment Install., Piping & Instruments Setting, Grouting, Painting, Insulating, Service Piping for engines, Turbines and Compressors, Instruments, Heating Plant, L.O. Storage & Handling, Starting Air System, Equipment Builders, Serviceman's Expense, Building Service Piping	186,300
	E. Main Gas Piping Main Gas Piping, Station Emergency Shutdown System, Fuel Gas Regulators & Piping, Misc. Yard Piping	216,800
	Total Direct Cost	1,777,900

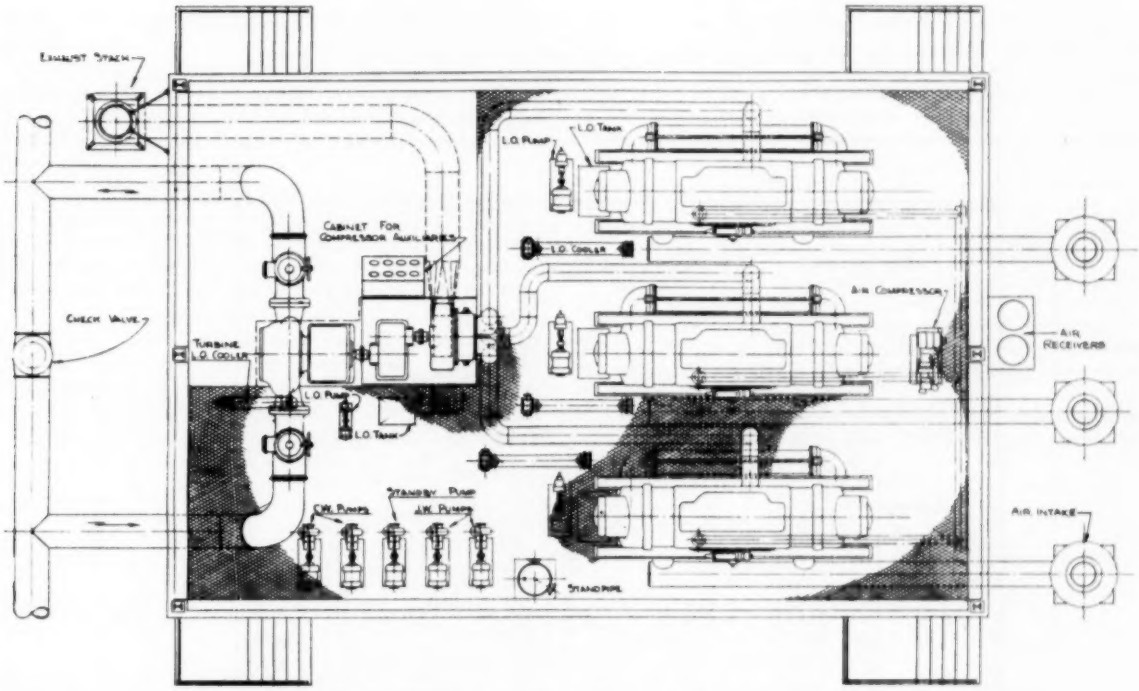

FIG. 6 5000-HP FREE PISTON - GAS TURBOCENTRIFUGAL PUMPING STATION

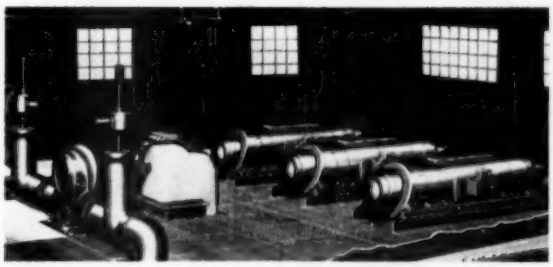

FIG. 7 PERSPECTIVE 5000-HP FREE PISTON - GAS TURBOCENTRIFUGAL PUMPING STATION

in the literature[4] that space requirements are not too important in ships of the merchant type because of the effects of the tonnage laws. The need for lower costs, however, is foremost in the merchant-ship class, and the need for low fuel consumption is also of great importance in Navy logistics.

The free-piston turboengine used in this investigation is well suited to marine use in vessels of the merchant class. This propulsion plant combines all of the desirable characteristics of the steam turbine with the economy of the diesel engine and avoids most of the undesirable elements. To illustrate, we have considered the application of the free-piston turbo drive to a C-3 cargo vessel.

[4] "A Gas-Turbine Plant With Reference to a Cargo Vessel," by Commander J. J. McMullen, USN, and Warren Payne, Trans. The Society of Naval Architects and Marine Engineers, vol. 59, 1951, pp. 502–535.

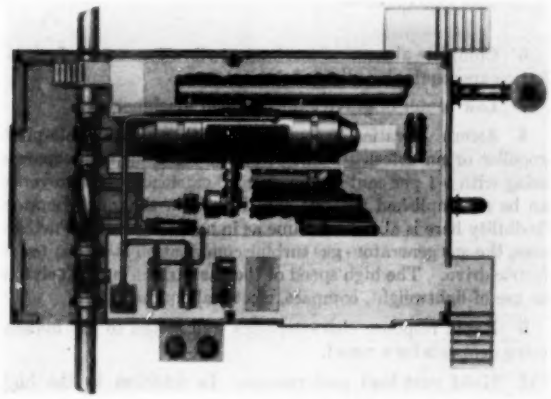

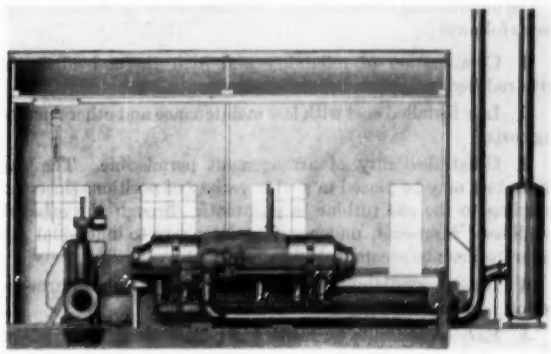

FIG. 8 SINGLE UNIT FREE-PISTON TURBOCENTRIFUGAL INSTALLATION

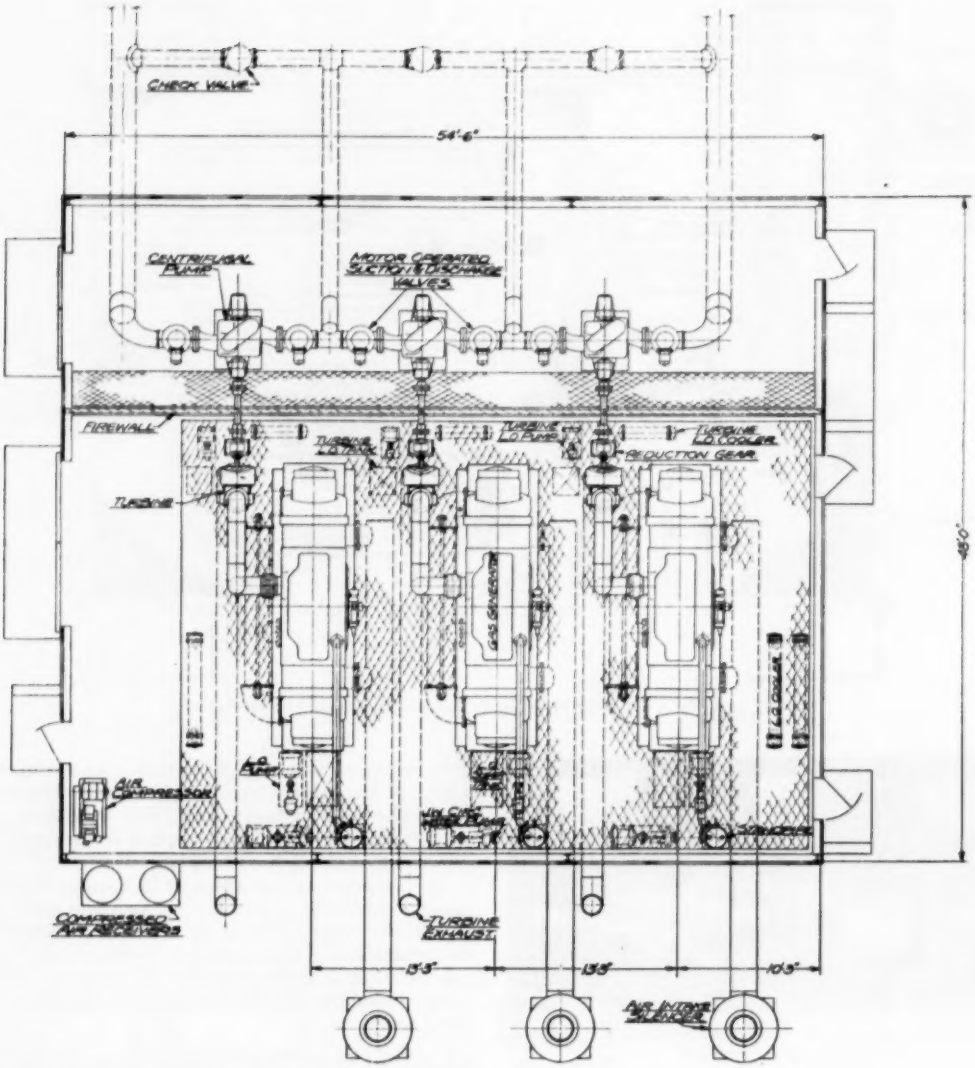

FIG. 9 TYPICAL 5000-HP OIL PIPE-LINE INSTALLATION

The outstanding advantages of the free-piston turbomotorship are as follows:

1 Combination of reliability and high thermal efficiency with reduced weight and space requirements.

2 Low installed cost with low maintenance and other operating costs.

3 Great flexibility of arrangement permissible. The gas generators may be placed in a wide variety of positions since the coupling to the gas turbine is pneumatic through the exhaust gas lines. Moreover, under-way maintenance to individual gas generators can be accomplished.

4 Instant availability of power. No particular warm-up period is required to get the plant under-way.

5 Easy accessibility for repair and maintenance. Headroom of only 7 ft above floor level is required to remove major components. Low number of moving parts, all easy to reach.

6 Complete absence of mechanical vibration. Such foundations as are required are light and simple.

7 Low center of gravity for installed machinery.

8 Astern operation accomplished with a controllable-pitch propeller or an astern turbine either in the same or a separate casing with a 1 per cent loss in over-all efficiency. The reversal can be accomplished without shutting down the gas generator. Flexibility here is about the same as in a steam plant. Furthermore, the gas generator - gas turbine combination is well suited to electric drive. The high speed of the gas turbine is conducive to the use of lightweight, compact, electrical equipment.

9 Rapid response characteristics well suited to the maneuvering demands for a vessel.

10 Good part-load performance. In addition to the high part-load efficiency of the individual gas generators, it is necessary to operate only the number required to meet load require-

ments. The shutdown units can be started immediately as required.

11 Combination of all the outstanding features of motorships, and, at the same time, elimination of many of the complications of diesel engines. The free-piston unit has good economy, with simple equipment designed for a low-temperature turbine and low maintenance expense.

12 Relative freedom from smoke under all normal conditions.

13 Good adaptability to various types of ships. Because of the anticipated lower costs and the high thermal efficiency at all loads, there are excellent opportunities for application in such ships as auxiliaries, transports, tankers, cargo vessels, and tugs.

14 Reserve torque overload capacity comparable to a steam-turbine plant. The gas generator, for instance, can be made to deliver great overloads in mass flow almost instantly and without the thermal inertia of a steam boiler. This can develop high torques at reduced turbine speeds.

15 Low-cost construction and the elimination of all critical materials. An established standard size of gas generator may be used for a large range of powers by multiunit application to selected turbine sizes of relatively simple construction and design. The mass-production possibilities of such a program, in the event of a national emergency, are obvious.

A preliminary layout of the free-piston gas-turbine installation in a C-3 cargo vessel is shown in Fig. 10. It should be remembered that the ideal method of applying any prime mover to a vessel would be to design the ship for the specific power plant. Fig. 10 is a layout of a conversion. It includes many compromises which would not be necessary in an original design. For example, in a vessel designed for free-piston turbomotors, the engine-room height could be much less than that for steam turbines with their boilers and diesel-engine installations. Also, the ship's service generators might be coupled up with a spare gas generator, and the donkey boiler could be "fired" by the exhaust gases of the gas turbines.

Fig. 11 shows the six gas generators grouped around the turbine and reduction gear. Table 4 lists the general characteristics of

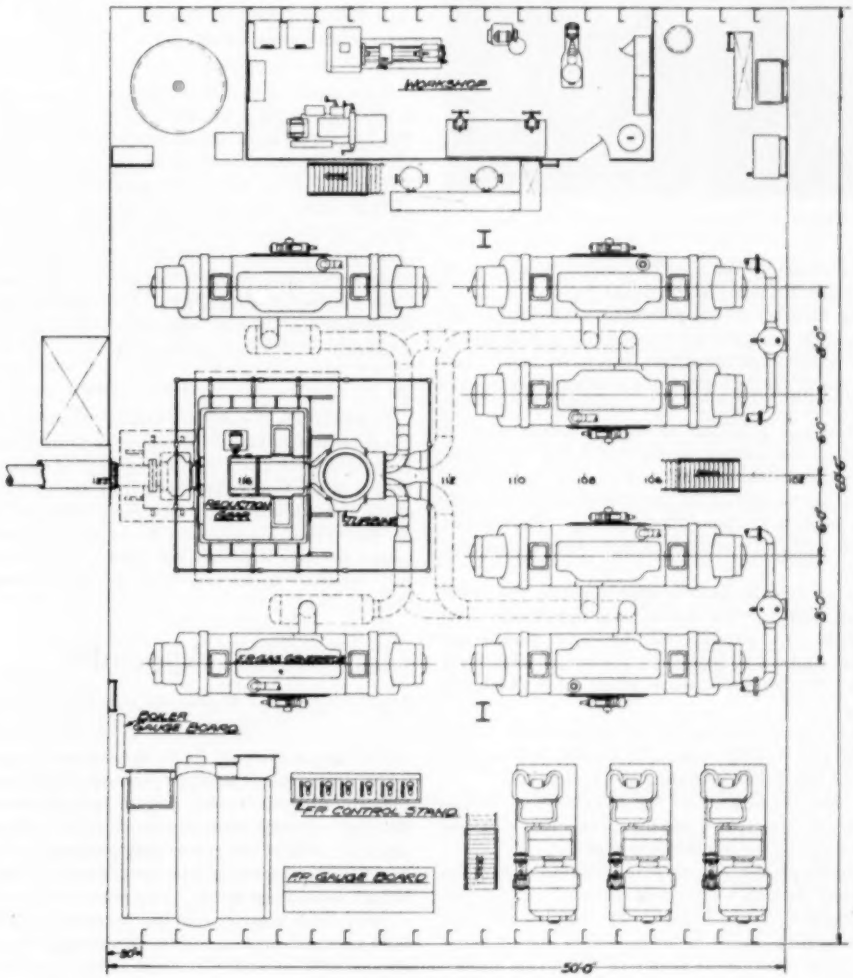

Plan view and machinery flat

FIG. 10 FREE-PISTON TURBOMOTORSHIP—C-3 CARGO VESSEL

TABLE 4 ESTIMATED INSTALLED COSTS OF 9000-HP FREE PISTON-GAS TURBINE PROPELLING MACHINERY IN A C-3 CARGO VESSEL

Main Turbines and Gears	720,000
Shafting, Bearings, and Propellers	97,000
Pumping Machinery, Incl. Coolers & Filters	75,000
Piping for Propulsion Plant Only	171,000
Auxiliary Boiler	164,000
Uptakes, Gratings, Compressors, Purifiers, Water Heater, Fans, Evaporators, & Misc.	200,000
Total	$1,427,000
Installed Cost in $ per HP (including labor)	$158
Total Installed Weight	664 Tons

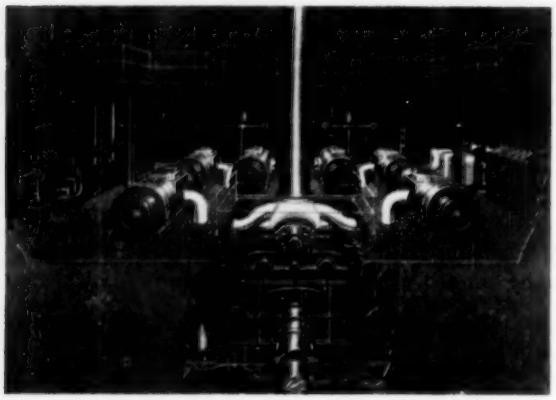

FIG. 11 FREE-PISTON MACHINERY DECK—C-3 CARGO VESSEL

the free-piston-engine installation in a C-3 vessel. An analysis of the estimates in Table 4 is given in the Appendix.

As shown in Fig. 11, all of the gas generators are located at one level. Ample space is provided for disassembly and servicing. The exhausts are run through individual lines to a common turbine and the free-piston motors rest on rails so situated that operation and adjustment are easy at the operating level. The scavenging headers, gas generator to turbine interconnecting piping, and most of the cooling piping run below this level, where they are easily accessible from below. The gas turbine and reduction gear are located at the lower level, so that suitable connection can be made to the propulsion shafting. The turbine-nozzle arc is divided into six sections, one connecting to each gas-generator exhaust.

The volume in all exhaust lines is approximately the same; surge chambers are added to the shorter ones to balance. The gas-generator intakes are grouped for minimum interference without excess size, and a 4-ft-diam stack connection suffices for this arrangement. The turbine exhaust requires a 3.25-ft-diam or equivalent area.

On the machinery level are also located the auxiliary boiler, the turbogenerator sets with the usual switchboard and controls, and other standard auxiliaries, including the workshop.

On the lower level are located all the required engine-room auxiliaries for the C-3 cargo vessel, and the accessories for the gas generators, in addition to the propulsive equipment.

The operation of the plant is remotely controlled from a station which can be located centrally wherever convenient. A pushbutton starter is furnished for each unit. The turbine governor will have a speed-setting device under control of the operator. The governor in turn controls the output of the gas generators. When all units are running, they are controlled simultaneously, as practice has proved this to be the most efficient generation with a common turbine. In the event one gas generator must be shut down for any reason, it is isolated automatically from the turbine by a swinging gate check. As previously stated in this paper, all necessary safety protective devices are furnished.

An alternative arrangement, not shown, would make use of two gas turbines on individual pinions, each supplied with gas from three gas generators. This plant would be more flexible and would make possible half-load operation in case of failure of one of the gas turbines. Also, with this arrangement, the part-load efficiency could be maintained at a slightly higher level.

The general characteristics of the C-3 cargo vessel, for which the proposed installation was developed, are shown in Table 5.

TABLE 5 GENERAL CHARACTERISTICS OF A C-3 CARGO VESSEL

Type of Vessel	C-3 Cargo Carrier
Gross, Tons	7,800
Displacement, Tons	17,615
Cargo Deadweight, Tons	10,000
Bale, Cubic	700,000
Rated Shaft Horsepower	8,500
Rated Shaft RPM	85
Design Speed, Knots	16.5
Normal Cruising Radius, Mi.	14,500
Schedule - Days at Sea	160
Days in Port	190
Repairs & Drydocking	15

It is interesting to note that the percentage of motorships under foreign construction greatly exceeds that of the United States. The ratio of steam to diesel tonnage of all foreign construction is about 1:1; in the United States, however, this ratio is about 30:1. This is due principally to the greater importance of fuel cost to over-all labor and operating expense in European shipping. Since the free-piston installation combines the over-all advantages of both steam and diesel installations, and at the same time promises to have reduced maintenance expense because of the fewer number of moving parts, it is possible that the free-piston turbo combination may bring about the wide application of such a power plant in American shipping.

CONCLUSION

In conclusion, the authors wish to point out that the free-piston gas generator is rapidly becoming a proved unit of machinery. Extensive testing of the Navy-sponsored units, the preliminary testing of the Cooper-Bessemer unit, and the actual performance of the Pescara units of France, have indicated great possibilities for free-piston machinery. As in all new developments, difficulties are to be expected, but these troubles will all be mechanical. In other words, the basic theoretical design aspects have been proved.

Appendix

ANALYSIS OF COST ESTIMATES FOR FREE-PISTON GAS-TURBINE MACHINERY FOR C-3 CARGO VESSEL

The figures given in Table 4 have been compiled with great care. Installations made 10 years ago do not lend themselves to 1953 comparisons because design, performance, and prices have changed. Recent estimates on ships of other types cannot be applied. Rather than presenting comparative figures that might prove to be misleading, accurate estimates of the free-piston machinery for this specific C-3 ship conversion are shown.

As of 1952, there is a widely accepted installed cost figure of $180 per hp for steam-turbine-driven ships, having power plants up to 13,000 hp, with 600 psi pressures at 850 F. It is generally found that diesel installed costs up until this time have been above $200 per hp; however, there are staunch arguments supporting the use of these somewhat higher-priced diesel installations where bunker fuels are used.

Supercharged diesel engines, available in 1953, are substantially better in outputs and costs than the product of 10 years ago.

It is not the purpose of this paper to point out any particular advantages of steam or diesel, but since the most accurate estimates possible at this time indicate lower-cost installation for unsupercharged free-piston machinery, it seems clear that the operating economics of the free-piston turbomotorship will be superior to either steam or diesel. The 13,000-hp crossover point, which is not necessarily accepted in this paper, but which is mentioned because of its wide use for comparative purposes, would be raised to a much higher value in comparing steam with the free piston. It is believed that there may be no crossover point whatever.

A low supercharging pressure of $2^1/_2$ psi will raise the free-piston turboplant from 9000 to 13,000 hp, with a decrease of $10 per installed hp, and very much higher supercharging seems practicable.

Discussion

T. S. Bacon.[5] It has been extremely gratifying to read this paper. As a practical engineer, engaged in the natural-gas industry, the implications of this paper seem almost without limit.

The practical advantages of the free-piston type of gas-turbine plant are excellently presented in the paper. The significant reduction in weight, installed cost, and estimated operating and maintenance costs of the free-piston type of gas-turbine plant as compared with the conventional reciprocating-piston type of gas-fueled prime mover seems to be reasonable of attainment within the near future. Yet all this is done without imposing new unknowns into the picture. The reciprocating piston has adequately demonstrated its rugged reliability through millions of horsepower-years of operation. It has, as does any mechanical device, its peculiar disadvantages. But certainly, in this case, these disadvantages have been defined completely, are understood, and are capable of evaluation. With present perfection of mechanical design and execution, with clean air and clean fuel supplied to the combustion zone, and with clean oil supplied by positive metering, the piston can be economically and reliably maintained for a very nominal cost per horsepower-year. The elimination of unbalanced forces inherent in the free-piston design is also significant in adding to the operating satisfaction that may be anticipated from this type of equipment.

Our experiences with small steam turbines operating at very moderate temperatures and pressures have convinced us of the reliability and economy of equipment of this type also. We certainly prefer to remain within the limits of temperature and pressure of the fluid supplied to the turbine that are known to insure satisfactory operation rather than to hope that the metallurgists have now, or will soon develop, alloys that will permit reliable operation at higher temperature ranges. Therefore the combination of the high-pressure high-temperature combustion of natural gas in the free-piston device with the conservative design of the turbine is extremely appealing.

The paper is silent on the details of the starting mechanism and the details of the control mechanism. It is obvious from the paper that these devices have been engineered satisfactorily and the great ingenuity that must have gone into this engineering is very commendable. It is my impression that previous German attempts toward development of the free-piston gas-turbine machine became so involved in complexities of starting and control equipment that realistic progress was impossible. It appears that straightforward Yankee ingenuity has been able to overcome and eliminate these complexities and provide adequate devices that are simple but effective.

In view of the fact that the conventional reciprocating-piston gas engine is already competitive with the steam turbine for generation of electric power, particularly under circumstances such as prevail in the production of aluminum, it seems reasonable to speculate on the possibility that all power in the natural-gas-rich Southwest will be generated by the installation of free-piston gas-turbine plants in the future. These plants are independent of large supplies of cooling water, and therefore will offer much more latitude in selection of sites for installation in the Southwest. There seems to be no upper limit to the economic size of the free-piston type of installation. The lower limit will of course be largely determined by the cost of starting and control equipment. The writer personally hopes that someday he may have the pleasure of driving an automobile powered with a free-piston type of gas-turbine power plant.

H. W. Egger.[6] Ever since the Texas Eastern Transmission Company so effectively proved a few years ago the advantages of using centrifugal compressors for the movement of large volumes of natural gas through pipe lines the natural-gas industry has awaited anxiously for the development of a suitable and economical driving unit for these compressors. The gas turbine was the obvious answer but until higher efficiencies became possible it could not be acceptable.

As Texas Eastern proved the advantages of centrifugal compressors, so is El Paso Natural now proving the advantages of the gas turbine for a driving unit. With twenty-eight General Electric units being installed they now have about half of this number in operation. The writer has visited several of these installations and has found everyone very enthusiastic over their performance and their possibilities. They are coming up to all expectations.

The writer does not presume to speak for the compressor operators in the natural-gas industry but believes his opinions are shared by a large majority of them when stating that even though the two-shaft turbine with regenerator is proving to be a very satisfactory and popular unit, the industry is still looking for a unit which will be higher in efficiency and will be adaptable to a wider range of conditions.

It is not the purpose of this discussion to enter into any controversy on the feasibility of the free-piston turbine. This question should be left up to those engineers who are in the field of design and development. The Pescara engine has long been recognized as a highly efficient design of an internal-combustion machine. Feasibility, after all, will be determined not by opinions pro and con but by performance of this machine in actual service. If successful it should find a wide field of application in the natural-gas industry.

The authors have done an excellent job of presenting the case for the free-piston turbine. They have presented it in terms that are readily understandable to the operator of internal-combustion equipment, with emphasis on those features which mean most to him as follows:

High Efficiency. This is extremely important, for although we operators in the natural-gas pipe-line industry handle hundreds of millions, even billions, of cubic feet of gas daily, we are highly cognizant of our fuel consumption and what it means in terms of dollars and cents. We cannot accept lower efficiencies in any phase of our operations, particularly in fuel consumption, for several reasons, chief of which is the rapidly rising cost of gas at the well head.

[5] Chief Engineer, Transmission Division, Lone Star Gas Company, Dallas, Texas.

[6] General Superintendent, Compressor Stations, United Gas Pipe Line Company, Shreveport, La.

Wide Range of Selection in Size of Units. This too is very important to the operator particularly those who engage in the gathering of gas for ultimate delivery into the large main lines. We cannot hope for gas-turbine units on very small horsepower installations but there is a definite need for a unit much smaller and simpler than the 5000-hp turbine. Many high-pressure fields are declining now to the point where field compressors are necessary. These compressors must be dispersed throughout the gathering system at strategic points in order to produce the wells economically and maintain the necessary pressures in the gathering system. Major pipe lines are fed by numerous smaller lines from various fields which necessitates a wide dispersal of horsepower. Even on some main-line stations a few small units would be preferable to one or two large units from the standpoint of flexibility and continuity of operation.

Simplicity. This feature is very attractive from an operator's viewpoint for it will enable him to take care of practically all maintenance of the unit without outside help and will thus reduce his down time and expense.

Low Weight and Low Installation Costs. The absence of massive regenerators, long air and exhaust ducts, extensive lagging, and complicated air-cooled foundations will hold these costs to a minimum and simplify design of the installation a great deal.

Total weight of the 10,000-hp free-piston turbine installation as given in the paper is 350,000 lb exclusive of the centrifugal compressor. Comparable weight of a 10,000-hp continuous-combustion turbine with regenerator installation is 650,000 lb as disclosed by the manufacturer. This difference in weight will require piling under foundations in many installations as we have discovered in our proposed installation at Napoleonville, La.

An increasing amount of the nation's gas production is coming from coastal areas of Louisiana and Texas. Much of this area is composed of swamps or lowlands with poor soil-loading characteristics. Several compressor installations already have been constructed on barges and no doubt many more will become necessary as time goes on. When full development of the tidelands gets under way it is safe to assume that more offshore pipe lines will be built and offshore compressor installations will no doubt be needed in time. The free-piston-type gas turbine will lend itself admirably to barge and offshore platform installations as well as to areas where soil conditions are poor.

Assuming that minor mechanical difficulties will be overcome, if found, when this unit is field-tested, the writer believes it will be quickly accepted by the natural-gas industry. Its wide field of application along with its many advantages should make it a very popular compressor unit, and the writer, for one, awaits its coming with considerable interest.

FREDERICK NETTEL.[7] From this interesting paper it may be concluded that the free-piston gas-turbine plant is a serious competitor of the straight gas turbine.

However, the place of the latter in the not-too-distant future seems by no means as insecure as may be inferred.

On the basis of efficiency alone it appears at this moment difficult to match the free-piston gas-turbine plant, but prospects to approach its fuel consumption with a rather simple straight gas turbine exist, resulting from the possible use of valveless, pistonless pulsating combustion chambers along the lines of Esnault-Pelterie's idea, perhaps in a form similar to that under test by Reynst.

Furthermore, good, compact, and cheap heat exchangers are under development, which when used together with pulsating combustion chambers will improve further the chances of the straight gas turbine.

It still has to be proved that the free-piston gas-turbine plant can operate consistently on lowest-grade fuels and the authors' reservations on this point are well taken. Straight gas-turbine plants, provided the top temperature does not exceed 1200 F, seem better suited to burn such fuels.

One advantage that cannot easily be obtained on straight gas-turbine plants is good part-load efficiency, but this is not too important for cargo vessels or stand-by plants.

Intercoolers and regenerators, being located at the low-temperature end of the cycle, are thoroughly proved reliable elements and preferable to the free-piston gas generators, especially when used in multiples.

In marine plants controllable-pitch propellers continue to be objectionable to most owners. It would be interesting to know how an astern turbine can be accommodated in the casing of the main turbine without overheating.

It must remain the ultimate aim for medium-size and especially large plants for every application, to get away from engine cylinders, pistons, piston compressors, and timed fuel injection so as to arrive at a purely rotating plant which will show many of the advantages claimed for the free-piston gas-turbine plants.

AUTHORS' CLOSURE

Mr. Bacon's remarks are very much appreciated. It seems apparent that free-piston machinery will appear in the field in the not-too-distant future and practical operating experience will confirm the expectations. No data are available on the combustion of natural gas, but it is hoped that they will be forthcoming shortly.

The starting of a gas generator is accomplished by compressed air and numerous methods have been applied successfully. The principal concern of the designer is to apply the air under normally available pressures and in such a way that sufficient compression is produced on the first stroke to insure combustion. It is also necessary that the amount of air used is so proportioned that the machine is in general running equilibrium at the end of the first stroke or that means are regulated to control the energy balance during the first several strokes to let out any excess air that may have been applied during the starting period. The free-piston machinery undoubtedly will find applications in various high-output, lightweight designs; and in heavy automotive duty there is no reason why it cannot serve a very useful purpose. The general idea of hydraulic turbines in automotive transmissions is not very far from the application of pneumatic torque converters which are in essence gas turbines and they may be combined successfully with small, high-output gas generators with a high degree of thermal efficiency.

The discussion by Mr. Egger is extremely practical and interesting. The advent of the gas turbine in any of its forms is particularly suitable to driving high-speed machinery. Centrifugal compressors, centrifugal pumps, and high-speed electric machinery are examples of the types of applications which seem to be finding rapid development in this period. Free-piston machinery is also applicable to direct-displacement compression; and through the usage of the gas turbine and the centrifugal air compressor, designs are developed which will make the usage of either the high-speed-drive rotary compressor or the direct-reciprocating compressor equally possible of attainment, depending upon ratios of compression that may be required. The centrifugal compressor is essentially a high-flow low-ratio unit, whereas the reciprocating compressor is particularly adaptable to high-ratio compression and may be used in paralleling low flowing streams. The need for highest possible efficiency is certainly apparent in studying the trends in fuel costs, and the piston-type combustor operating at high levels of combustion pressures will provide thermal efficiencies that always will be theoretically higher than the low-pressure combustors.

[7] Consulting Engineer, Manhasset, N. Y. Mem. ASME.

Referring to Mr. Nettel's comments, the burning of low-grade fuel is considered to be particularly interesting in the free-piston engine because the nozzle requirements indicate coarse injection-spray characteristics. The low temperature of the gas from the free-piston engine to the turbine is satisfactory from a standpoint of materials and the metallurgical effects of vanadium pentoxide and other formations, some of which cause abrasion at the higher temperatures.

Altogether the free-piston engine is inherently suitable to low-grade-fuel combustion. The use of controllable reversible-pitch propellers seems to be indicated clearly through the late work which has been put into practical service. The combination of the free-piston-engine, gas turbine, and CRP propeller provides a combination of torque and speed characteristics which is ideally suited to marine work.

Generally speaking, the apparatus required for heat salvage in continuous-combustion turbine plants is rather large and expensive and the over-all possibilities of high thermal efficiency and high outputs in the free piston-turbine combination are certainly parallel to the advancement which can be made in continuous-combustion turbines; therefore, the relative position in thermal efficiencies may be expected to continue.

The Application of Additives to Fuel Oil and Their Use in Steam-Generating Units

By J. B. McILROY,[1] E. J. HOLLER, JR.,[2] AND R. B. LEE[3]

Ash deposits in steam-generating units have been becoming more troublesome and have presented a design and operating problem. It is recognized that troublesome deposits are characterized by a high content of low-temperature-melting constituents. This paper is concerned with the addition of high-temperature melting-point compounds to the fuel oil to elevate generally the melting point of the aggregate above the troublesome temperature level. Fusing temperatures of intimate mixtures of oil ash with many additive compounds were determined. Alumina was found to be the best material, with magnesium and calcium oxides showing promise. The fusing-temperature tests were substantiated by pilot-furnace-firing tests and these results in turn were applied to further experimentation on a full-sized unit. Alumina was the first additive used in a steam-generating unit of the Florida Power Corporation. Alumina was later replaced by dolomite. Both materials raised the fusing temperature of the ash to the extent that the work of removal was considerably decreased, but dolomite proved to be the most desirable from an operating as well as an economic standpoint. Other benefits, such as decreasing the acidity of the ash in the unit, were apparent when using dolomite. The use of the process is now being extended to other units. An arrangement of necessary equipment with detailed description of the components is appended.

Introduction

FOR some time it has been more and more apparent that some of the advantages of fuel-oil over coal firing are being lost with particular reference to cleanliness factors of the high-temperature convection surface. The problems of ash removal throughout the unit have become more acute. This seems to have accelerated to the point where, with some types of oil fuels, ash removal is a serious problem. It is difficult to say just what has caused the problem to become serious in recent years, but various reasons have been advanced such as the advent of catalytic cracking with resulting greater concentrations of residual, the increase in pressure and temperature levels of steam-generating units, and other reasons.

When it became evident that operating units were experiencing excessive slagging difficulties, The Babcock & Wilcox Company engineers were confronted with a twofold problem: (*a*) To assist in relieving the cleaning difficulties of units in operation, and (*b*) to modify the design to produce a unit capable of operating indefinitely with normal cleaning schedules. Fig. 1 shows an FH integral-furnace-type unit of the company with furnace screen and superheater spacing designed to handle the so-called difficult ash oils. A unit as shown is in operation at the Bayboro Station of the Florida Power Corporation. It was placed in initial operation in December, 1949, and has been in service since that date at a high load factor with regularly scheduled outages at about yearly intervals. A similar FH unit but of an earlier design, Fig. 2, which experienced slagging difficulties, is in operation at the Inglis Station of the Florida Power Corporation.

Both units are basically of the same construction and arrangement with the exception of the superheater. The unit in Fig. 2 has an inverted-loop superheater with a generally closer pitched tubing arrangement than that of the revised design. In the later design the superheater is of the pendant type and the back pitch of the boiler screen as well as the transverse pitch of the close-spaced section of the superheater has been increased. This unit operates indefinitely without any cleaning other than the normal use of soot blowers. Both units burn the same fuel with the same type of burners.

1 Survey of Problem and Laboratory Phase of Investigation[4]

The Problem

It is with the solution of the slagging problem that this paper is concerned. Unfortunately, its solution was not as straightforward as that of modifying the design for future units.

A survey of the analyses of heavy residual fuel oils and fuel-oil ash extending back over some 20 years in the company's records discloses the same ash constituents to be present today, but with a definite trend toward higher sulphur, vanadium, and alkali content. There is also a definite increase in the amount of ash.

In the analyses survey, the ash content of the fuel oil was found to vary from approximately 0.004 per cent to 0.25 per cent by weight. Present-day fuels seldom show less than 0.07 per cent ash and are usually in the range of 0.10 to 0.15 per cent.

A wide variety of metals have been reported present in fuel-oil ash, originating in part from metals inherent in the crude oils processed, entrainment of solids, as from salt water, pipe lines, and so on, and contamination during refinery operations. The survey showed a wide variation in the amount of certain constituents, with a definite trend from the relatively low alkali, sulphur, and vanadium content of the earlier fuels to the high alkali, sulphur, and/or vanadium content generally found in the ash from currently available residual fuel oils.

The averaged values in Table 1 and Fig. 3 are typical of the analyses of ash from bunker-C type fuels showing the change that has taken place in the ash concurrently with the change from oils that were largely trouble-free in practice to oils that have produced troublesome fireside deposits.

This change in the oil ash is the result of changes in the nature of the crude oils processed and in refinery practices. Poorer-quality crude oils and more extensive cracking and refining to

[1] Group Leader of Fuels Section of Chemical Laboratory, The Babcock & Wilcox Company, Alliance, Ohio.

[2] Associate Chemist, Research Development Division, The Babcock & Wilcox Company, Alliance, Ohio.

[3] Assistant Superintendent of Power Production, Florida Power Corporation, St. Petersburg, Fla.

Contributed by the Power and Fuels Divisions and presented at the Annual Meeting, New York, N. Y., November 30–December 5, 1952; re-presented at the Semi-Annual Meeting, Los Angeles, Calif., June 28–July 2, 1953, of THE AMERICAN SOCIETY OF MECHANICAL ENGINEERS.

NOTE: Statements and opinions advanced in papers are to be understood as individual expressions of their authors and not those of the Society. Manuscript received at ASME Headquarters, November 21, 1952. Paper No. 52—A-160.

[4] Part 1 of the paper is by J. B. McIlroy[1] and E. J. Holler, Jr.[2]

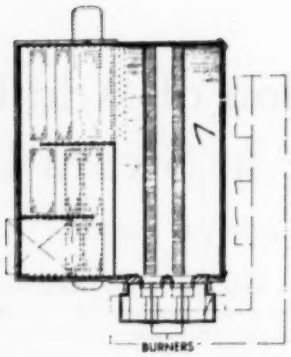

FIG. 1 (*right*) INTEGRAL-FURNACE-TYPE BOILER AT BAYBORO STATION OF FLORIDA POWER CORPORATION

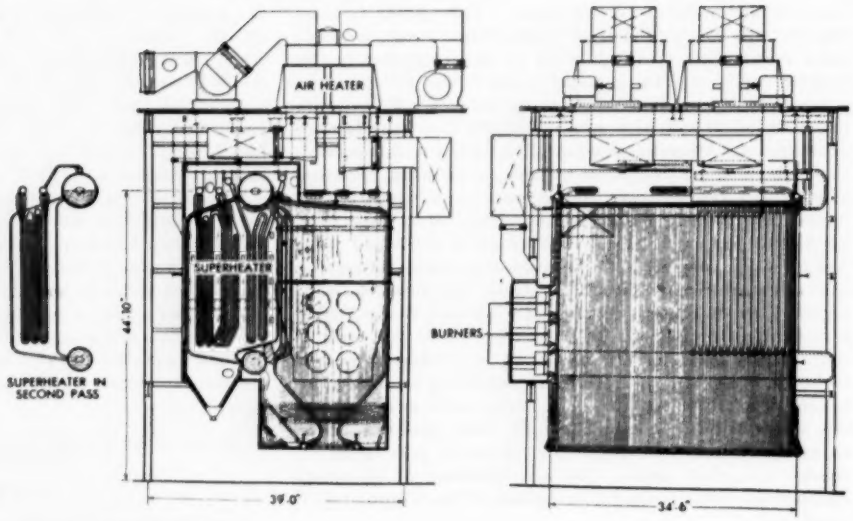

FIG. 2 (*below*) TYPE OF BOILER AT INGLIS STATION

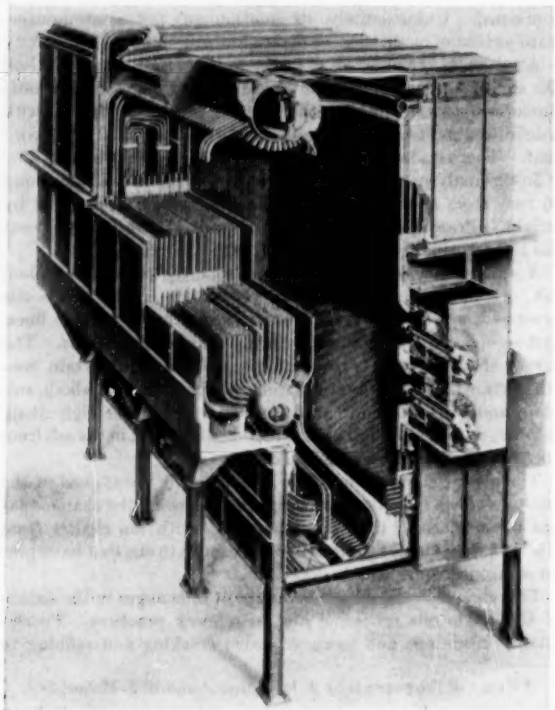

TABLE 1 AVERAGE VALUES OF FUEL-OIL-ASH ANALYSES

		Trouble-free oil, per cent	Troublesome oil, per cent
Silica	SiO_2	22	7
Alumina	Al_2O_3	6	2
Iron oxide	Fe_2O_3	47	7
Calcium oxide	CaO	4	5
Magnesium oxide	MgO	7	3
Nickel oxide	NiO	5	3
Vanadium oxide	V_2O_5	Trace	18
Alkalies as sodium oxide	Na_2O	2	25
Sulphur as sulphate	SO_3	3	32
Ash		0.06	0.12

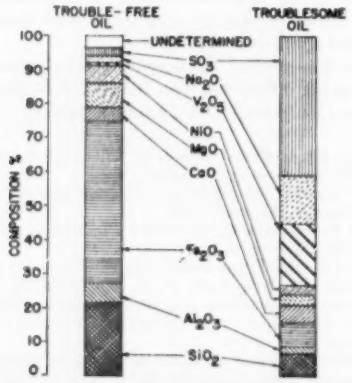

FIG. 3 FUEL-OIL-ASH ANALYSES—AVERAGE VALUES

obtain greater yields of the more valuable oil fractions tend toward concentration of the undesirable inorganic-ash constituents in the residues. These residues, generally dispersed in a heavy distillate oil to control the viscosity, comprise the heavy or residual fuel oils of today. The objectionable ash constituents are present in such small amounts and in such chemical combinations in the crude and fuel oils that methods for their removal are difficult to apply on an economically commercial scale. Mechanical methods have been tried and found to be only partially effective, and it is questionable if any satisfactory economic process is likely to be developed. Deeper cracking and further refining of crude oils to meet the increasing demand for distillate products is likely to result in a higher content of inorganic material in the residues and thus the problem of deposits from the combustion of these fuels is likely to become even more acute.

Superheater Deposits

Analysis of the ash from a fuel oil, typical of the oil available on the eastern seaboard and producing troublesome deposits, and the analysis of a superheater deposit, formed from the combustion of a similar fuel oil in a large stationary unit, are shown in Table 2 and Fig. 4. The latter illustration brings out the similarity of the two materials in the high content of alkali and sulphate.

In Table 2 the elements are reported as oxides but they do not necessarily occur as such in the ash or deposit. X-ray diffraction examination of superheater deposits has shown the presence of sodium and calcium sulphates, and, in a few cases, some vanadium pentoxide has been noted, but as a rule the actual vanadium compounds have not been identified.

TABLE 2 ANALYSIS OF ASH AND SUPERHEATER DEPOSIT FROM TROUBLESOME FUEL OILS

		Oil ash, per cent	Superheater deposit, per cent
Silica	SiO_2	1.7	7.0
Alumina	Al_2O_3	0.3	4.1
Iron oxide	Fe_2O_3	3.8	5.8
Calcium oxide	CaO	1.7	4.5
Magnesium oxide	MgO	1.1	2.5
Nickel oxide	NiO	1.9	1.1
Vanadium oxide	V_2O_5	7.9	0.9
Alkalies as sodium oxide	Na_2O	31.8	23.7
Sulphur as sulphate	SO_3	42.3	46.4
Calculated sodium sulphate	Na_2SO_4	73.0	54.0
Ash in oil, per cent by weight	...	0.16	...

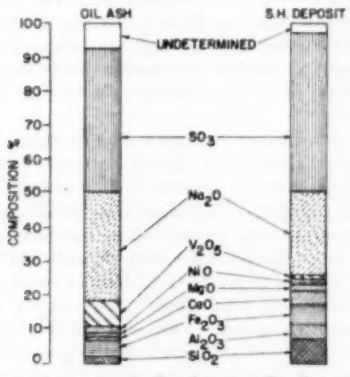

Fig. 4 Typical Analyses of Oil-Ash and Superheater Deposit From Troublesome Oils

Visual examination of superheater deposits has shown them to vary in their physical characteristics from a hard, glassy, fused condition through a sintered state to a powdery nature, frequently with stratification of the deposit. On stationary units nearest to the superheater-tube metal a layer is often noted that is higher in alkalies and sulphates than the general average analysis of the deposit.

Sodium sulphate usually constitutes a large percentage of these troublesome deposits, the balance being composed of oxides, vanadates and/or sulphates of the other metals. Consideration of the reported melting points of some of the possible principal constituents of the oil ash and of the deposit, as shown in Table 3, indicates a probable cause of the selective deposition and the formation of a dense, fused, or semifused mass not readily removable from an operating boiler. Melting points as low as 1000 F have been reported for synthetic mixtures of sodium sulphate and vanadium pentoxide, with even lower temperatures of 800 to 900 F for potassium sulphate-vanadium pentoxide mixtures.

TABLE 3 MELTING POINT OF POSSIBLE DEPOSIT CONSTITUENTS

Compound		Melting point, deg F
Sodium pyrovanadate	$Na_4V_2O_7$	1170–1207
Vanadium pentoxide	V_2O_5	1274
Sodium sulphate	Na_2SO_4	1624
Magnesium sulphate	$MgSO_4$	2055
Calcium sulphate	$CaSO_4$	2642

Troublesome superheater deposits, in general, all show relatively low fusing temperatures as indicated in the typical examples in Table 4 and Fig. 5.

TABLE 4 FUSING TEMPERATURES OF TYPICAL TROUBLESOME SUPERHEATER DEPOSITS

Atmosphere	Sample A		Sample B	
	Reducing temp, deg F	Oxidising temp, deg F	Reducing temp, deg F	Oxidising temp, deg F
(Cone support, Standard ASTM — kaolin + alumina)				
Initial deformation	1590	1590	1910	2090
Softening temperature	1640	1620	2020	2550
Fluid temperature	1690	1650	2250	2610

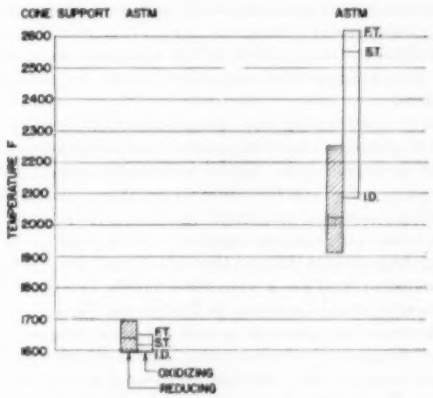

Fig. 5 Fusing Temperatures of Typical Troublesome Superheater Deposits

While there is considerable controversy as to the mechanism of the deposit formation, the low-fusing sodium and vanadium compounds seem to play an important part in the start of the formation and its subsequent build-up.

Laboratory Investigations

Early in 1949, a study was begun at The Babcock & Wilcox Research Center to determine some means of preventing the superheater-deposit formation or of altering its nature to make it more readily removable with a minimum of expense and labor.

It has been mentioned already that the most desirable remedy would be the removal of the objectionable constituents from the

oil, particularly the sodium, sulphur, and vanadium ions, before combustion. Little encouragement along such lines was found.

The alternative of modifying the oil and ash constituents to minimize the deposit formation and amend the characteristics of the deposit was therefore studied.

Since the ash-slag deposits from jobs having superheater-slag troubles had relatively low fusing temperatures, it was suggested that it might be possible to change the characteristics of the deposit favorably by adding some material to the oil which would raise the fusing temperature of the ash. Experiments were conducted on various materials considered promising.

The first step in the laboratory study was the decision that the fusing temperatures of an intimate mixture of the ash and additives would serve as a satisfactory method for preliminary evaluation of the various possible additive materials.

Fusing-Temperature Studies. The preparation of an adequate supply of oil ash to cover all the proposed tests was considered impractical, because this would require the burning down of a very considerable quantity of fuel oil. A synthetic ash therefore was compounded to simulate the ash shown in Table 2 and reproduce its fusing temperatures as closely as possible.

With the exception of omitting the oxidation of the ash prior to forming it into a cone and the cone-support material used, all fusing temperatures were determined in accordance with the ASTM Standard Method D-271, "Fusibility of Coal Ash." The experimental variables involved in making these fusing-temperature determinations proved to be very troublesome. It was found necessary to iron out these difficulties before consistent data could be obtained. Natural oil ash and the synthetic ash were found to be very reactive with the cone-support materials specified in the ASTM method, kaolin-alumina, kaolin-alundum, cement mixtures, and refractory brick. Of the many materials tried, the kaolin-alumina mixture, preformed and fired to 2900 F, and fused silica sheet proved to be the best cone-support materials in the investigation.

In addition to the standard ASTM reducing-atmosphere test, fusing temperatures also were determined in an oxidizing atmosphere.

In many cases during the fusing-temperature studies, it was difficult to state the exact temperature, as customarily observed, when the three points, the "initial deformation point," the "softening temperature," and the "fluid temperature," occurred. The averaged temperatures reported for these points represent the operator's best judgment on duplicate runs in most cases.

Fusing-temperature data of the oil ash and the synthetic ash compounded to simulate it were taken on the two types of cone-support material and are shown in Table 5 and Fig. 6.

The fusing-temperature data with the same support material showed fair agreement between the natural oil-ash and the synthetic-ash temperatures and were considered satisfactory for the purpose. The initial deformation and softening temperatures were considered the significant points in this study and, by using both cone-support materials, a better measure of the effect of any additive tried was obtained.

Additives Used in Fusing-Temperature Studies. The materials tried as additives are given in Table 6.

Since the ash content of most fuel oils lies in the range of 0.1 to 0.2 per cent by weight, it was decided that the addition of the additive material equal in quantity to the ash content would be practical. One hundred per cent addition of the additive to oil ash therefore was used as a basis for testing the effect of the additive on the deposit characteristics. In many cases, varying proportions of ash and additive were tried to determine the optimum proportion.

Weighed amounts of the synthetic oil ash and additive were dry-mixed, pulverized to pass a U. S. No. 200 sieve, made into cones, and fusing temperatures obtained by the standard procedure.

TABLE 5 COMPARISON OF FUSING TEMPERATURES OF NATURAL AND SYNTHETIC OIL ASH

Atmosphere	Oil ash		Synthetic ash	
	Reducing	Oxidizing	Reducing	Oxidizing
(Cone support—prefired, 50% kaolin + 50% alumina mixture)				
Initial deformation, deg F	1590	1640	1630	1620
Softening temp, deg F	2080	2680	2000	2780
Fluid temp, deg F	2500	above 2900	2430	above 2900
Cone support—fused silica sheet				
Initial deformation, deg F	1460	1610	1560	1630
Softening temp, deg F	1500	1640	1600	1660
Fluid temp, deg F	1700	1820	1880	1970

TABLE 6 ADDITIVES TESTED FOR EFFECT ON FUSING TEMPERATURE OF OIL ASH

Silica	SiO_2
Aluminum oxide	Al_2O_3
Calcium oxide	CaO
Magnesium oxide	MgO
Barium oxide	BaO
Kaolin	Al_2O_3, $2SiO_2$, $2H_2O$
Sodium chloride	NaCl

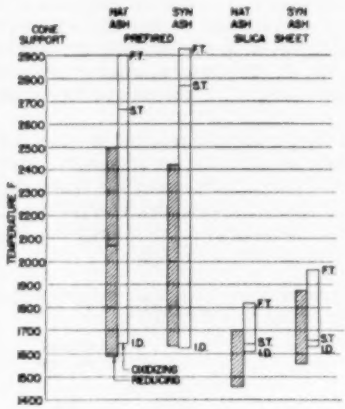

FIG. 6 COMPARISON OF FUSING TEMPERATURES OF NATURAL AND SYNTHETIC OIL ASH

The effect of a few of the additives tried on the fusing temperature of the ash is shown in Table 7 and Fig. 7. Silica was not considered satisfactory since too large a quantity was indicated as being necessary to produce the desired rise in fusing temperatures in contrast to the effect obtained by the use of alumina or calcium oxide.

The effect of several of the additives on the fusing temperature of superheater deposits from oil-fired stationary jobs was determined with typical results as shown in Table 8 and Fig. 8.

In many of the fusing-temperature runs, shrinkage and separation of components from the test cones were noted and definite conclusions as to the ultimate effect of such additives on the superheater deposits in practical application could not be based on fusing-temperature work alone. However, the tests showed that of the additive materials tried, only the oxides of aluminum, calcium, and magnesium required relatively small amounts to produce a marked elevation of the fusing temperature of the oil ash or deposit. Actual burning trials, on a small scale, seemed warranted on the use of these oxides and their compounds which produce the oxide on combustion. These trials were conducted to establish definitely whether sufficient reaction would take place between the additive and the oil ash, during the short period of combustion, to form the high-fusing end product obtained in the cone tests.

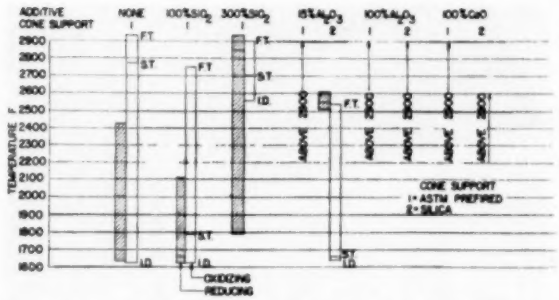

FIG. 7 FUSING TEMPERATURES OF SYNTHETIC ASH PLUS ADDITIVES

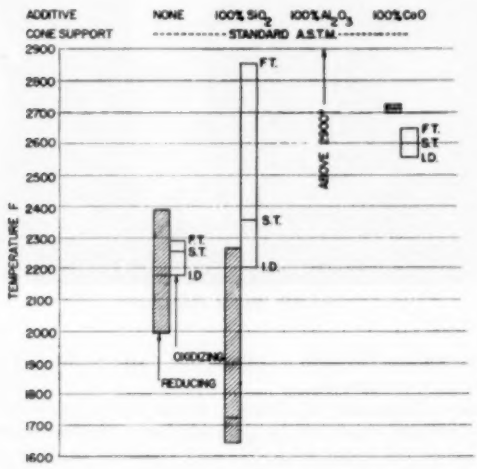

FIG. 8 FUSING TEMPERATURES OF SUPERHEATER DEPOSIT PLUS ADDITIVES

TABLE 7 FUSING TEMPERATURES OF SYNTHETIC ASH PLUS ADDITIVES

Mixture	Atmos[a]	Temperature, deg F—ID	ST	FT	Cone support
None	Red	1630	2000	2430	Prefired
(synthetic ash)	Oxid	1620	2780	2900[b]	Prefired
1 part ash +	Red	1620	1660	2110	Prefired
1 part SiO_2	Oxid	1620	1790	2750	Prefired
1 part ash +	Red	1790	2860	2900[b]	Prefired
3 parts SiO_2	Oxid	2580	2700	2900[b]	Prefired
1 part ash +	Red		Above 2900		Prefired
0.15 part Al_2O_3	Oxid		Above 2900		Prefired
	Red	2510	2550	2610	Silica sheet
	Oxid	1640	1660	2530	Silica sheet
1 part ash +	Red		Above 2900		Prefired
1 part Al_2O_3	Oxid		Above 2900		Prefired
	Red		Above 2900		Silica sheet
	Oxid		Above 2900		Silica sheet
1 part ash +	Red		Above 2900		Prefired
1 part CaO	Oxid		Above 2900		Prefired
	Red		Above 2600		Silica sheet
	Oxid		Above 2600		Silica sheet

[a] Atmosphere surrounding cones.
[b] above 2900 F.
ABBREVIATIONS:
Red, reducing atmosphere ASTM D-271.
Oxid, oxidizing atmosphere.
ID, initial deformation temperature.
ST, softening temperature.
FT, fluid temperature.
Prefired, 50% kaolin + 50% alumina mixture, prefired at 2900 F.

TABLE 8 FUSING TEMPERATURES OF SUPERHEATER DEPOSIT PLUS ADDITIVES

Mixture	Atmos[a]	Temperature, deg F—ID	ST	FT	
Deposit	Red	1990	2180	2390	Standard ASTM
(no additive)	Oxid	2180	2260	2290	(kaolin and alumina)
1 part deposit +	Red	1640	1720	2270	Standard ASTM
1 part SiO_2	Oxid	2200	2360	2860	Standard ASTM
1 part deposit +	Red	2700	2720	2730	Standard ASTM
1 part CaO	Oxid	2560	2600	2650	Standard ASTM
1 part deposit +	Red		Above 2900		Standard ASTM
1 part Al_2O_3	Oxid		Above 2900		Standard ASTM

[a] Abbreviations are as given in Table 7.

PILOT-FURNACE TESTS

In the burning tests it was necessary that the additive material be mixed with the fuel prior to combustion because this was the most effective means of insuring thorough mixing with the oil-ash solids to perform the following possible functions: The finely divided additive particles would be readily available (*a*) to serve as nuclei for the deposition of oil-ash vapors or solids at the earliest opportunity and (*b*) to allow the maximum amount of time for high-temperature chemical reactions to take place and for ash-additive solutions to form while passing through the high-temperature combustion zone. The brief time in which the oil ash and additive materials would be present in the higher-temperature zones was not considered to be sufficient for such chemical reactions or high-temperature solutions to reach equilibrium, but it was considered possible that sufficient action might occur to alter the physical and chemical characteristics of the ash deposited on the superheater tubes.

Accordingly, a small furnace was constructed with deposit-collecting coils located in the combustion-gas stream. Figs. 9 and 10 show the general arrangement of the test equipment.

The combustion section of the pilot furnace consisted of 6-in-ID Carbofrax-tile cylinders, backed with K-28 insulating firebrick, with an over-all length of 6 ft. The stainless-steel stack, 10 ft over-all length and 7-in-square cross section, carried three stainless-steel cooling coils for collecting the deposit. The coils were installed in a manner to permit ease of removal so that the deposit collected in a test could be weighed and sampled. The coils were made from $^3/_8$-in-OD stainless tubing in eight turns of $6^1/_2$ in. OD to present as large a deposit-collecting surface as possible and were placed at different levels in the stack to permit exposure to different flue-gas-temperature zones. Compressed air was used to cool the collecting coils. Coil-metal temperatures were obtained by thermocouples brazed to the center turn of each coil. The air flow through the coils was regulated to produce coil-metal temperatures from about 750 to 1350 F, covering the range occurring in superheaters in operating boilers.

A special low-capacity single-hole jet air-atomizing burner was designed to burn ordinary bunker-C grade fuel oil at a rate of 1 to 2 gph. Using oil with an average ash content of about 0.1 per cent by weight, a deposit on the coils was obtained, but the time required for sufficient deposit to collect was prohibitive. Therefore it was decided to accelerate the rate of deposit formation by loading the fuel with several times the amount of ash solids usually contained in commerical fuels.

It soon became apparent, however, that bunker-C oil with such quantities of solids could not be burned in the extremely small burner used for the pilot furnace. Since the oil in the tests could be considered mainly as a carrier and a means of providing the combustion reaction and atmosphere it was deemed legitimate in this instance to go to the expedient of using a lighter fuel. Diesel fuel oil was substituted for the heavy fuel oil and, with up to 3 per cent by weight of synthetic ash and additive solids, was burned successfully in the pilot furnace. The diesel oil with approximately 1 per cent by weight of synthetic oil ash was used throughout as the basic fuel for the tests of the various additive materials.

The same synthetic ash used in the fusing-temperature work was used in these tests. The dry solids were mixed, ball-milled, and screened to pass a No. 100 sieve before addition to the oil.

Additives Used in Pilot-Furnace Studies. Some of the addi-

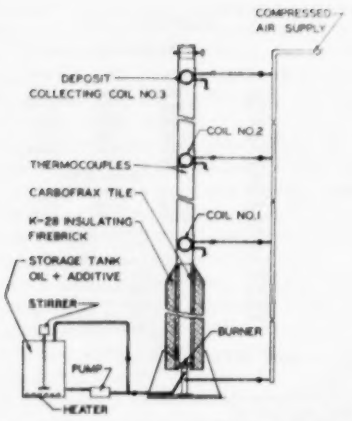

FIG. 9 ARRANGEMENT OF TEST EQUIPMENT

tives tried are listed in Table 9 with an approximate comparison of the market price of each and general rating of their behavior in the tests.

TABLE 9 ADDITIVES USED IN PILOT-FURNACE TESTS

Additive	Approximate price per lb in bulk	Rating of test results
Alumina (extra fine)	$0.04–0.06	Good
Kaolin	0.005	Bad
Silica	0.01	Bad
Calcium oxide	0.005	Fair
Calcium carbonate	...	Fair
Magnesium oxide	0.08	Fair
Magnesium carbonate	0.10	Fair
Sodium aluminate	...	Bad
Calcium aluminate	0.20	Bad
Iron oxide (Fe_2O_3)	...	Bad
Alumina—magnesia mixture	...	Fair
Aluminum, metallic flake	0.30	Fair
Aluminum oxide–hydrated	0.07	Good
Aluminum stearate, technical	0.30–0.40	Good
Ethyl silicate	0.65	Bad

Metal-organic compounds other than aluminum stearate were not tested extensively owing to the cost of such compounds and the apparent quantity required to produce satisfactory deposits.

Test Procedure. Calculated weights of the synthetic ash and the additive to be tested were ball-milled for several hours with a small quantity of diesel oil and the slurry produced added to the bulk of the diesel oil to be used for the test in a storage tank provided with a heater and stirrer. This fuel, as required during the test, was measured into a smaller supply tank, continuously stirred, and fed to the burner by a small centrifugal pump. The amount of fuel to the burner was controlled by valves on the burner line and return line to the supply tank. With the stirring and recirculation provided, no appreciable settling out of the ash and additive solids was noted. A composite sample taken over the duration of each test agreed well in total solids content with the value calculated from the weighed solids added.

To avoid deposition of carbon on the coils, the furnace was preheated with a gas burner before combustion of the loaded test fuel was started. Test runs were from 6 to 8 hr in duration with a total fuel consumption per test of 7 to 10 gal. Temperatures of the coil metal and the flue gas in the vicinity of the face of each coil were taken at intervals throughout the test. Runs with the basic fuel without additives were made in the same manner to provide deposits for comparison.

After each run the coils were dismounted, photographed, and examined visually for the physical characteristics of the deposit. The ease of removal was evaluated by brushing with a camel-hair brush. Chemical analyses were made for the main constituents of

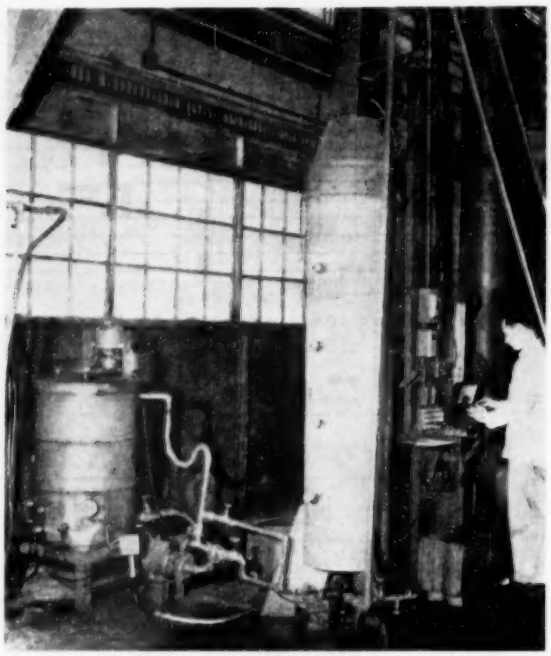

FIG. 10 PILOT FURNACE

the ash and additive used and the fusing temperatures of the deposits were determined.

General Discussion of Results. In all of the tests the deposits collected chiefly on the upstream face of the coils and were thickest on the center turns. In every test the quantity of deposit was much greater on coil No. 1, the coil in the hottest flue-gas zone, than on the other two coils. The quantity of deposit collected on the coils was variable even in duplicate runs. There was evidence, in some tests, that some of the deposit had fallen off, or had been shaken off in removing the coil. This demonstrated the looseness of the deposit formation.

Without additive, the deposit on coil No. 1 was invariably in a fused state, on coil No. 2 powdery but slightly sintered in some tests, while on coil No. 3 the deposit was a powder. With additives, coil No. 1 deposit was powdery with certain additives and fused with others; coil No. 2 deposit also varied from a powder to sintered condition dependent on the additive and its amount. Coil No. 3 deposit was powdery in all cases.

In many of the tests some gradation in the physical nature of the deposit on coil No. 1 was observed. At the cold-air-inlet end the deposit was powdery on the first two turns. In some of the tests this changed to a sintered or definitely fused condition across the remaining turns of the upstream face toward the hot-air-outlet end. The bulk of the deposit on coil No. 1, however, was strikingly different with and without additive.

Table 10 gives a summary of the test data for a few selected tests covering the additive-ash weight ratio used, general range of metal and gas temperatures, and so on.

Table 11 gives the analyses and fusing-temperature data of the deposits from coils Nos. 1 and 3 of the same tests as tabulated in Table 10. Fusing-temperature data on the deposits covered in Table 11 are illustrated in Fig. 11.

Figs. 12 and 13 show the nature of the deposits collected on coil No. 1 during a test run without additive and with additive. The hard glassy appearance of the deposit without additive in Fig. 12

TABLE 10 SUMMARY OF TEST DATA

(Fuel: Diesel oil loaded with synthetic oil ash)

Test no.	Additive	Ratio of additive to ash by weight	Test duration, hr	Fuel burned, gal	Coil metal temp range, deg F—Coil 1	Coil 2	Coil 3	Flue-gas temp range, deg F—Coil 1	Coil 2	Coil 3
47	None	..	7.3	9.5	1230–1350	970–1070	840–920	1440–1610	1020–1170	900–990
23	Alumina	1 to 1	6.5	7.4	1080–1310	840–1000	740–900	1230–1580	970–1170	770–920
45	Aluminum stearate	1 to 1	8.3	10.0	1130–1340	830–1000	740–880	1330–1530	970–1140	800–920
26	Calcium oxide	1 to 1	5.8	6.9	1000–1360	840–1040	740–900	1250–1620	940–1140	760–920
61	Dolomite	1 to 1	7.5	10.3	1240–1320	980–1070	850–910	1450–1650	1000–1180	920–970

Table 10 (*Continued*)

Test no.	Deposit collected—Coil 1—Grams	Nature	Coil 2—Grams	Nature	Coil 3—Grams	Nature
47	18	Fused	7	Powdery	5	Powder
23	12	Powdery	5	Powder	4	Powder
45	7	Powdery	2	Powder	1	Powder
26	28	Partly sintered	6	Powder	5	Powder
61	28	Hard packed	9	Powder	5	Powder

TABLE 11 ANALYSIS OF DEPOSITS FROM COILS

(Fuel: Diesel oil loaded with synthetic oil ash)

Test	47		23		45	26	61
Additive	None		Alumina Al_2O_3		Aluminum stearate (technical grade)	Calcium oxide CaO	Dolomite $CaCO_3$ $MgCO_3$
Additive: Ash ratio	..		1:1		1:1	1:1	1:1
Coil no.	1	3	1	3	1	1	1
	Fusing temperatures, deg F						
Reducing atmosphere:							
Initial deformation	1940[a]	1780[a]	2900[b]	2900[b]	2510	2440	2570
Softening temperature	2100	2050	2900[b]	2900[b]	2590	2630	2730
Fluid temperature	2230	2330	2900[b]	2900[b]	2680	2670	2780
Oxidizing atmosphere:							
Initial deformation	1630	1630	2900[b]	2900[b]	2590	1740[a]	2380
Softening temperature	1870	2340	2900[b]	2900[b]	2680	2550	2700
Fluid temperature	2630	2520	2900[b]	2900[b]	2710	2680	2760
	Chemical Analysis, Per Cent						
Silica as SiO_2	2.6	..	..	..	..	..	..
Alumina as Al_2O_3	3.1	..	48.6	57.2	9.3	..	..
Iron oxide as Fe_2O_3	9.5	..	..	..	..	..	..
Calcium oxide as CaO	1.3	..	..	..	..	38.1	17.0
Magnesium oxide as MgO	1.3	..	..	..	..	..	9.9
Vanadium as V_2O_5	8.2	9.6	4.3	3.9	7.8	3.4	6.1
Alkalies as Na_2O	27.5	31.1	13.6	13.6	25.9	9.2	19.0
Sulphur as SO_3	45.8	42.5	20.4	17.7	40.1	34.5	38.9

[a] Some drainage noted before initial deformation point.
[b] Above 2900 F.

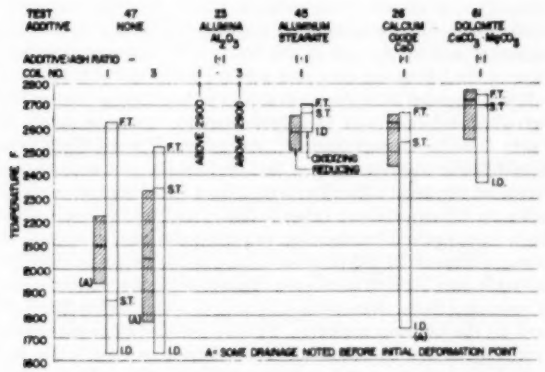

Fig. 11 Fusing Temperatures of Deposits From Coils

(Fuel, diesel oil loaded with synthetic oil ash.)

is in marked contrast to the powdery friable deposit with additive in Fig. 13 where the deposit has been removed from the lower half of the coil by means of a camel-hair brush.

Oxides of aluminum, magnesium, and calcium, in that order, with little difference in the last two, were the additives found to give the best results from the point of view of producing loose powdery deposits, readily removable, and showing high fusing temperatures.

Other additives tried produced no improvement in the deposit characteristics when used in amounts considered to be practical and within economic limits.

The use of a technical grade of aluminum stearate, partially soluble and readily miscible with the oil, containing about 15 per cent equivalent aluminum oxide, appeared to be the most effective additive for producing aluminum oxide. Its use in the ratio of 1 lb of aluminum stearate (0.15 lb aluminum oxide) to 1 lb of oil-ash solids gave as good results as a 1 to 1 ratio of alumina. The price of the aluminum stearate, about 34 cents per lb in bulk at the present time, however, makes its use economically doubtful.

Various ratios of alumina to oil-ash solids were tried and it was found that its use in amounts equal to the weight of the oil ash would give a safe working margin for the formation of a friable deposit; greater amounts produced no proportionate benefit.

The total weight of deposit collected during the test with alumina was about the same as that collected from the same weight of oil-ash solids alone. Magnesium-oxide and calcium-oxide additive tests showed a slight increase in the weight of deposit collected, with calcium oxide showing the greater amount.

In an examination of the chemical analyses of the deposits formed with additives it is interesting to note that the additive was depositing in approximately the same proportion as added to the oil.

The deposits were apparently largely amorphous materials and did not give good x-ray diffraction patterns. No extensive chemical combination of the additive and ash constituents was observed. Some indication of the formation of calcium sulphate with calcium oxide and of complex aluminum sulphate with the

FIG. 12 COIL NO. 1—NO ADDITIVE
(Basic fuel, diesel oil, and synthetic ash.)

FIG. 13 COIL NO. 1—WITH ADDITIVE
(Basic fuel, diesel oil, and synthetic ash.)

aluminum-oxide additive was found. This suggested the possibility that the use of additives would result in a decrease of the sulphur-trioxide content of the flue gases passing to the cooler sections of an operating unit and thereby have an effect on the acid corrosion sometimes occurring in such locations.

A check on the viscosity of a bunker-C fuel oil to which the preferred additives had been added in the amount indicated to be necessary to improve the ash deposit showed no real change from that of the straight fuel oil. Therefore it appeared reasonable to assume that no real difficulty would be experienced in the addition of such materials to fuel oil of a central-station unit, in so far as burner performance is concerned.

The next step in the investigation into the problem of remedying the accumulations of deposits on the heating surfaces of oil-fired boilers was to apply the pilot-plant results to a full-scale unit. A survey was made of operating units that had been experiencing particular difficulties because of such accumulations, and the Florida Power Corporation was approached with regard to the possibility of conducting field tests with additives on the boiler at the Inglis Station of its system. Part 2 of this paper will be concerned with the field application.

2 EXPERIENCE WITH ADDITIVES ON A COMMERCIAL UNIT[4]

On the basis of previous experience, engineers of the Florida Power Corporation had tried to purchase and install two trouble-free boilers in 1947. All types of operation with soot blowers for removing slag had been tried, including water-washing, and gas passages could not be kept open.

In 1950 Mr. M. W. Peterson, District Service Engineer for The Babcock & Wilcox Company, proposed a trial installaton using aluminum oxide based on laboratory tests and results obtained in a mercury boiler. Two other additives had been tried without success, and it seemed that the only solution of this slagging problem was to redesign the boilers. It was agreed to try this program.

The installation chosen at Inglis consists of a 30,000-kw single-boiler single-turbine unit. The station is located about 75 miles north of St. Petersburg on the Gulf side of the peninsula and it is a vital link in the Florida Power system.

The unit at Inglis is a Babcock & Wilcox Type FH integral-furnace boiler, having a capacity of 300,000 lb per hr of steam at 900 psi and 910 F total steam temperature. It is equipped with an inverted-loop superheater, a hopper-bottom tube-to-tube furnace, fired with six circular-type, steam-atomizing Y-jet oil burners. The general arrangement is shown in Fig. 2. This unit originally was placed in operation in 1947. The fuel burned is residual fuel oil. Samples of oil were taken over a period at the beginning and at the end of the tests. Oil analyses, including those of the laboratory-prepared ash, are given in Table 12.

It will be noted from these ash analyses that there is present the high-alkali-sulphate and vanadium content that was shown in Table 1 to be characteristic of the ashes of troublesome oils. Actually, this was borne out in fact because the unit at Inglis experienced the usual difficulties with a hard fused deposit accumulating on the superheater tubes to the extent that periodic shutdown was required for cleaning to permit the unit to operate at rating. Because of the physical nature of the deposits, three retractable soot blowers in the superheater sections were ineffective in removing them, even when mixtures of water and steam were used as the blowing medium. It was established maintenance procedure at this installation to water-lance the superheater frequently and air-lance and water-wash the tubular air heater after each superheater cleaning.

In spite of this the unit had to be removed from service every 6 months for thorough cleaning. This involved soaking the superheater tubes with water for a period of time to remove the soluble portion of the deposits and considerable work to loosen the hard clinging portions. Each outage meant a loss in availability of the unit amounting to 4 or 5 days.

TESTS WITH ALUMINA

In accordance with the laboratory findings, a system was installed at Inglis for the purpose of testing the use of alumina when mixed with the fuel oil prior to combustion as an effective

[4] Part 2 of this paper is by R. B. Lee.[3]

TABLE 12 FUEL-OIL AND LABORATORY OIL-ASH ANALYSES

	Sample no. 1	Sample no. 2
Oil analyses:		
API at 80 F	10.6	11.2
API at 60 F	9.6	10.1
Specific gravity at 60 F	1.003	0.9993
Sediment, per cent	1.0	0.7
Btu per lb	18,090	18,470
Ash (ASTM), per cent	0.2	0.10
Ultimate analysis, per cent:		
Carbon	85.5	86.0
Hydrogen	10.2	10.2
Sulphur	3.0	2.4
Oxygen and nitrogen (by difference)	1.3	1.4
Ash analyses, per cent:		
Silica	1.8	7.4
Alumina	3.0	0.3
Iron oxide	3.9	5.1
Titanium oxide	0.2	.....
Calcium oxide	6.0	1.2
Magnesium oxide	1.2	2.6
Sodium oxide	19.5	26.4
Potassium oxide	1.0	...
Vanadium as V_2O_5	13.0	15.0
Nickel as NiO	2.1	3.2
Sulphur as SO_3	45.7	40.3
Ignition loss at 900 F	1.0	.....
Undetermined	1.6	.....
Sodium and potassium sulphates calculated on basis of alkali content	46.6	60.5

means of changing deposit characteristics. A line diagram of the additive system is given in Fig. 14 and machinery specifications are included in the Appendix.

At this point it may be well to call attention to some of the important features of the additive system as installed at Inglis. The mixing tank had a capacity of 250 gal, sufficient to contain a batch of oil-additive mixture for an 8-hr operating period on the basis of a normal oil consumption of approximately 20,000 lb per hr at the 275,000 lb per hr steaming rate. It was insulated and fitted with a hopper and agitator. The additive was mixed with heated oil from the regular oil system to form an oil slurry consisting of approximately 1 lb of additive per gal of oil. The slurry was pumped by means of a variable-stroke plunger pump into the oil supply line and thence to the burners at a pressure of about 175 psi. It was found that a simple mixing tee was all that was required to mix the slurry with the main oil stream. The succession of meters, valves, and fittings in the system before the individual burner lines was sufficient to take care of any additional mixing that might be necessary. The slurry feed rate was regulated manually to keep the quantity of alumina added to the main oil stream substantially equal to the amount of ash in the oil. The additive system has not required more frequent maintenance than that which normally is given to other components of the station system. Nor has it required additional manpower to operate. Normal station personnel have been able to do this.

Prior to starting the test with alumina, the boiler was removed from service and cleaned down to the bare tube metal in the usual manner. The use of alumina was begun in November, 1950, and continued until April, 1951. The effectiveness of the procedure could not be gaged until approximately 6 weeks of operation had passed, owing to the cleanliness of the heating surfaces. It then became more and more apparent that the use of alumina as an additive to the fuel oil was producing results in conformity with those anticipated from the laboratory testing.

A rather heavy granular sintered layer of deposit formed on the boiler screen and on the front wide-spaced sections of the superheater. The rear sections of the superheater had a dusty type of deposit with little or no evidence of sintering. The consistency of the ash became more powdery from front to back of the tube bank. These deposits were readily removable by use of the retractable soot blowers from the tube rows adjacent to the blowers, but supplementary hand-lancing was required for the rows in the middle bank.

It has been determined that the superheater sections and the tubes of the boiler screen can be kept operably clean indefinitely by normal use of soot blowers and by a weekly period of hand-lancing with air at 200 psi. It also has been found necessary to air-lance the air heater following air-lancing of the superheater so that the loose deposits which carried over from the superheater could be removed from the air-heater tube sheet. Outages for periodic water-washing have been eliminated.

From an economic standpoint, the use of alumina as an addi-

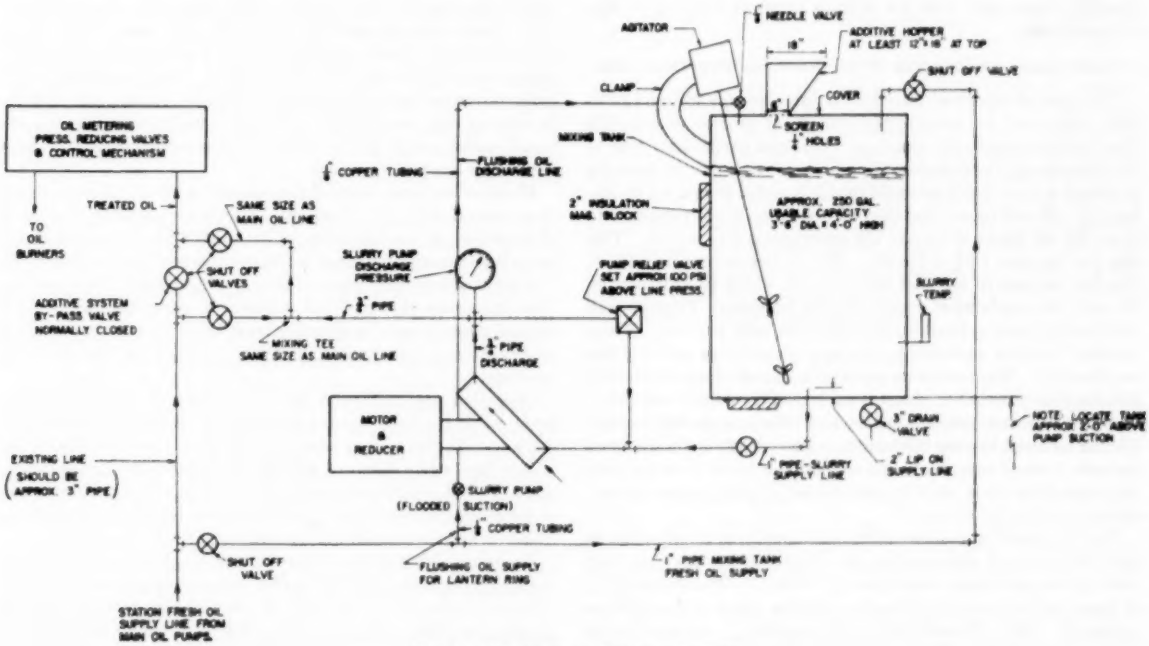

FIG. 14 DIAGRAM OF ADDITIVE SYSTEM

tive on the Inglis installation where approximately 20,000 lb of oil per hr is required for the 275,000 lb per hr load, costs about $1 per hr or $750 per month. In addition, alumina in the oil increased burner-atomizer wear to the point where it was necessary to renew standard sprayer plates every 30 days. The use of special plates of hardened steel alleviated this wear problem to a certain extent, but it still was excessive.

Tests With Dolomite

During the course of the alumina-additive tests it was suggested by operating personnel at the Inglis Station that possibly dolomite might prove to be an effective additive for use in this manner. Dolomite is a natural 60-40 per cent mixture of calcium and magnesium carbonates. It is available locally and the material suggested for use consisted of the fines from the dolomite roasting-kiln gases which have a fineness of 95-100 per cent through 325-mesh screen. A sample was sent to the laboratory for analysis and it was determined that a deposit similar to that obtained when using alumina could be anticipated. The effect of dolomite with regard to raising the fusing temperature of the constituents in the ash, although not as pronounced as that of alumina, was sufficient to indicate that the ash would not form a dense, fused, rocklike slag. It was decided, therefore, to try this material in place of alumina in the additive system at Inglis.

Dolomite was mixed with oil to form a slurry in the same manner as was the alumina. It was added in an amount to obtain a ratio of one part of additive to one part of ash in the oil supplied to the burners. The initial tests with dolomite were made without removing the unit from service for cleaning. The tubes were merely blown clean and hand-lanced. This test period lasted for approximately 2 months. Frequent inspections showed that the deposits were similar to those obtained with alumina. At the regular scheduled boiler outage in May, 1951, the boiler was cleaned thoroughly to the bare tube metal so that a satisfactory comparison between the two additive materials could be obtained. Operation with dolomite was resumed in June, 1951. Since that time to the present it has been possible to maintain an operably clean unit with no outages required because of slag accumulations.

Comparison of Results With Alumina and Dolomite

The type of deposit obtained with dolomite was soft and powdery, very easy to remove, but somewhat greater in quantity than that obtained with alumina. This was particularly true of the furnace and the first-pass superheater. Apparently dolomite produced a more fluffy material that was easier to remove by air-lancing. It will be recalled that with alumina it was necessary to clean the air heater whenever the superheater was lanced. This was not the case with dolomite. The air heater remained clean, possibly because of the fact that the ash which passed through the unit was made up of smaller lighter particles. Furnace-wall ash deposits were evident during operation with alumina. These resulted in some variation in the gas temperature entering the superheater. Measurements revealed a change of approximately 200 deg F in a period of about 3 weeks. Therefore it was found desirable to remove such deposits and this was readily accomplished by hand-lancing the furnace walls. With dolomite, these deposits formed but would fall off periodically so that furnace-wall heat absorption could be maintained at equilibrium without resorting to hand-lancing.

The comparative analyses of the ash deposits obtained when no additive was used with the fuel oil, when alumina was used, and with the use of dolomite are shown in Table 13. The examination of these ash analyses indicates the dilution effect of the additive materials. With alumina the analysis shows a composition of 53.7 per cent Al_2O_3. This means that the alumina is depositing with the ash in the same proportion in which it was added to the oil. Both additives caused a substantial reduction in the sodium and potassium content of the deposits. Dolomite was the more effective in reducing the vanadium content. Alumina caused a reduction in the sulphur content, whereas dolomite did not. This may have been due to the fact that dolomite is more reactive with sulphur compounds. The effect of additives in raising the fusing temperature of the deposits is clearly shown in Table 13.

TABLE 13 ANALYSES OF ASH DEPOSITS FROM UNIT AT INGLIS STATION

	Without additives, per cent	With alumina, per cent	With dolomite, per cent
SiO_2	2.8	1.1	2.0
Al_2O_3	2.1	53.7	1.7
TiO_2	0.1	0.1	...
Fe_2O_3	1.8	3.2	1.6
FeO	1.4	0.3	...
P_2O_5	0.037	0.06	0.1
MnO	Nil	Nil	...
CaO	7.8	2.4	22.6
MgO	1.8	1.0	15.2
SO_3	43.8	18.6	44.8
V_2O_5	8.6	6.6	4.9
NiO	2.9	1.3	2.0
K_2O	8.6	1.2	...
Na_2O	18.6	8.4	7.6
LOI-900 F	0.2	0.4	...
Undetermined	Nil	1.7	Nil

	Fusing temperature, deg F					
	With alumina		With dolomite		Without additives	
Atmosphere	Reducing	Oxidizing	Reducing	Oxidizing	Reducing	Oxidizing
Shrinkage	1750	2050	...	...	2280	2640
Initial deformation	2260	1640	2900+	2900+	2790	2800
Softening	2380	2660	2900+	2900+	...	..
Fluid	2460	2900+	2900+	2900+	...	..

In the installation at Inglis there are eight rows of closely spaced superheater tubes in the first bank. Results with dolomite and aluminum oxide indicated that no method of cleaning would extend through this section. An outage was arranged late in 1951 and three rows of tubes were removed. This was possible since the steam temperature had always exceeded the expected-performance data and it was not believed that this boiler would be operated much below the output giving 900 F steam temperature with 18 per cent excess air. It was found that steam from the soot blowers in the hot zone of the superheater tended to harden the slag. This was determined by operating the soot blowers with steam for 1 month, cleaning with boiler water, and using an air lance without any steam for 1 month. In view of this, the soot blowers are not used except for an occasional washing with boiler water. Normal cleaning is now done with an air lance twice a week.

Mention has been made of the original point of injection ahead of all shutoff and control valves. After approximately 6 months of operation, an accumulation in the control valves and oil meter made it necessary to operate on the by-pass to obtain sufficient oil. The point of injection was moved to the burner side of the valves. This introduces oil that is not metered or controlled by the combustion control, but the quantity is negligible in so far as control is concerned and this known quantity is added to the oil-meter readings.

Operation also indicated that the stroke of the oil-additive pump could not be reduced sufficiently to proportion the original mixture. It also was necessary to use steam on the coils in the mixing tank every 8 hr. A setting was determined on the pump, and sufficient mixture was made to last 4 hr. The concentration of dolomite was maintained by the amount added at each mixing based on expected boiler oil demand for the following hours.

Economically, the use of dolomite at the Florida Power Corporation's Inglis Station has resulted in real savings in boiler availability and efficiency. The cost of the material itself is approximately one fifth that of alumina, 0.6 cent per lb compared to 3.25 cents for alumina. The elimination of costly outages re-

sulting from slag accumulations and the comparative ease with which it has been possible to keep the unit clean have reduced considerably the costs chargeable to this type of maintenance. Table 14 is a comparative summary of the cost factors involved with and without the use of additives at Inglis Station. The cost of cleaning the unit and the additive operations are considered as increases to the cost of the fuel oil, since they would not have been required if the oil had been ash-free. The values given are based on cleaning costs and the costs of substitute power, the latter computed on the differential between high-pressure and low-pressure steam power generation. At installations where no low-pressure stand-by generating capacity is available the power must be purchased during outages and the cost of cleaning prior to the use of additives thereby would be at least twice that shown. It is interesting to note that the difference between no additives and additives, as shown in Table 14, is equivalent to a 3 per cent increase in generation efficiency.

TABLE 14 COMPARATIVE COST OF CLEANING UNIT AT INGLIS PER 42-GAL BARREL OF FUEL OIL; 0.15 PER CENT ASH

	Without additives, cents	With alumina, cents	With dolomite, cents
Cleaning in addition to normal soothblowing	7.3	0.5	0.46
Cost of alumina (3.25 cents/lb)	...	1.76	..
Cost of dolomite (0.6 cents/lb)	...	..	0.32
Total	7.3	2.26	0.78

It must be remembered that the comparative costs apply only to the unit at Inglis Station. Each boiler-unit installation of necessity will have its own evaluation of cleaning costs. However, it is believed that because of the low cost of the additive and the marked advantage to be derived from its use in so far as deposit characteristics are concerned, the use of dolomite in such an application is bound to result in economic advantages in boiler cleanliness and availability.

Additional Benefits From Use of Additives

The prime concern in the field-testing of additive materials at Inglis was to determine if alumina and dolomite would produce results in an operating unit comparable to those obtained during the laboratory phase of this investigation. Would the fusing temperature of the ash be raised sufficiently to make it possible for the ash constituents to accumulate on the heating surfaces in the form of a powdery, dry, easily removable deposit? In obtaining the answer to this question certain other benefits also were indicated. These are briefly described in the following.

During the testing of the unit at Inglis attention also was given to the effect of additives on over-all boiler efficiency. In this connection it has been shown already how the use of alumina and dolomite has permitted operation of the unit at optimum efficiency by enabling the operators to keep the heating surfaces free from excessive deposits. Another source of heat loss is the stack where it is necessary to maintain a minimum temperature to prevent condensation on the air-heater tubes and the consequent corrosion of the tubular materials. It was found, during the tests at Inglis, that the use of dolomite had a definite influence on the dew-point temperature of the flue gas. When burning a 2.75 per cent sulphur fuel, a dew-point temperature of 150 F was recorded when using the additive. Without additive, dew-point temperatures between 250 and 275 F were recorded. The consequent reduction in the minimum stack-temperature requirement can mean reduced air-heater corrosion with increased boiler efficiency, provided facilities are available to permit operation at lower stack temperatures.

The effect of dolomite on air-heater corrosion has not yet been determined fully. It is known, however, that the major non-metallic constituent in the dolomite ash is calcium sulphate and, therefore, it is reasonable to expect that the amount of free sulphur trioxide probably is reduced. This definitely would remove from the flue gas one of the highly corrosive substances that attack the tube metal. In addition, the lower flue gas dew point would mean that the corrosive gas would not condense on the air-heater surfaces.

During the periods before using aluminum oxide, considerable pluggage had occurred in the tubular air heater. This heater has two gas passes and one air pass. The tubes are 2 in. OD, 16 ft long. Steam soot blowers originally were installed at the outlet of the second gas-pass section. In an effort to eliminate the plugging, the soot blowers were first moved to the inlet or bottom of the second pass. Then superheated steam was used. Considerable corrosion of tubes and ductwork was noted and it was necessary to retube the second pass in 1949. The pattern of tube failures and tests indicated uneven gas and air distribution, also overcapacity. Several rows of tubes in the cold end were plugged. Corrosion continued to some extent, so air-puff soot blowers were installed in 1950. This did not eliminate corrosion but it was reduced materially, and very little tube pluggage occurred. During the period when aluminum oxide was used, no change was noted in air-heater condition except that it was necessary to hand-lance the top tube sheets with air. During the outage in May, 1951, just after the use of dolomite had been started, approximately 1500 tubes had to be replaced. Since that time, with continuous usage of dolomite, no cleaning other than that with the air-puff soot blowers has been required and there is very little evidence of corrosion.

Up until the time when dolomite was used, it was impossible to keep any outside painted surface in good appearance or condition. The particles from the stack ruined any paint including automobile finishes. Wet clothes could not be hung outside. This condition has been eliminated. Two water tanks outside the plant were painted light gray in February, 1952, and there is no evidence of discoloration.

The question of blowing the dolomite into the furnace was discussed several times. This would eliminate sprayer-plate wear, mixing additive in oil, and so on. A tank with air injection was designed and the same amount injected into the furnace in a dry form between the middle and bottom row of burners. At the end of a 2-week test, the slag in the top half of the superheater resembled that obtained with the dolomite mixed in the oil, but the bottom half was very hard and similar to the slag without any additive. The point of injection was changed to the back of the furnace, but then very little effect was noted on any of the slag deposit. This method does not appear too promising, because, even though it were possible to obtain an even distribution in the gases, it is believed that at least twice as much dolomite would be required and this would greatly increase the build-up in the superheater and hoppers.

Conclusion

To sum up the results obtained from the experience at Inglis Station with the use of fuel-oil additive materials in the operation of a steam-generating unit at this installation, we list the following:

1 It has been possible to change the usual hard rocklike deposit that tenaciously adhered to the heating surfaces, into a powdery easily removable substance that permits uninterrupted unit operation by lancing with air at 200 psi twice a week.

2 Not only has unit availability been increased but it has been possible to maintain unit efficiency at the level required for economical operation.

3 When using dolomite as the additive, in addition to the normal cost, the cost of maintaining an operably clean boiler has been decreased. It has been reduced from 7.3 cents per bbl of oil without additives to 0.78 cent with dolomite.

4 In addition to the effect of dolomite on the unit deposits, there are indications that its use tends to lower the dew point of the flue gases, reduce the corrosive quality of the fumes from the stack, and lessen the nuisance from fly-ash particles.

5 Because of the foregoing, the Florida Power Corporation has taken over the additive system at Inglis and is adding dolomite in an amount equal to the ash in the oil as regular operating procedure. A similar additive system has been installed and is in use at the Florida Power Corporation's Turner Station where there is a Type FH boiler similar to the one at Inglis.

In evaluating these results and in considering a possible extension of the use of additive materials to other applications, it must be remembered that the method described here is relatively new. It has proved to be effective with the type of oil used at Inglis and with the unit in operation there. Undoubtedly, problems will arise as its use is extended, but because of the experience at Inglis it is felt that the way has been prepared for a better understanding of the problem of deposit formation and a basic method provided by means of which the individual operators will be able to obtain increased boiler availability and higher average efficiency on high-duty high-steam-temperature power boilers burning troublesome oils.

Appendix

Comments on Design and Operation of Oil-Additive System Sized for 275,000 Lb Per Hr Steam Flow

Mixing Tank:

3 ft 6 in. diam × 4 ft length, 285 gal.

"Working capacity": volume actually pumped out before refill, 250 gal.

Insulate with 2-in. magnesia block on side and bottom.

Install right-angle thermometer in well in side of tank to give slurry temperature.

Let slurry supply pipe stick up above bottom of tank about 2 in.

Install screen in bottom of hopper with $^1/_4$-in-diam holes.

Agitator:

No. 115 portable gear mixer complete with clamp and $^1/_3$-hp explosion-proof, 440-volt a-c, 60-cycle, 3-phase motor—gear reduction of 1720 to 420 rpm—shaft and two propellers suitable for tanks 3 ft 6 in. diam and 4 ft high (approximate cost $250). Actual power consumption measured at 0.25 hp handling 12 per cent concentration of additive in fuel oil at 130 F.

Set lower blade as near bottom of mixing tank as possible to prevent settling of additive.

Run agitator continuously.

Additives:

Finely divided alumina
Selected collector fines
Screen size 98 per cent through 325
Price: lots 2000 to 19,999 lb ..... 4 50 cents/lb
20,000 to 39,999 ..... 3 5 cents/lb
over 40,000 ..... 3 25 cents/lb
Prices FOB East St. Louis
Dolomite—Red Level Mine, Inglis, Fla.
100 per cent through 325
Price: approx. $12.00 per ton at mine

Slurry Concentration:

Assume 20,000 lb oil per hr
Assume 0.15 per cent ash in oil
Assume additive-to-ash ratio 1:1
20,000 × 0.0015 = 30 lb ash per hr
30 lb additive per hr or 240 lb additive per 8-hr shift
Assume 8.136 lb oil per gal
Mixing tank will mix 240 lb additive with 250 gal of fresh fuel oil to make an 8-hr batch of slurry.
Therefore additive concentration will be

$$\frac{240 \times 100}{250 \times 8.136 + 240} = \frac{24{,}000}{2270} = 10.6 \text{ per cent additive by weight}$$

Slurry Pump:

Simplex pump with single coverplate to handle a maximum of 35 gph of specified fuel oil with 10 per cent additive suspension at specified temperature against a specified discharge pressure (oil-header pressure). Operation to be with a flooded suction. Unit will be equipped with variable screw adjustment of plunger-stroke length from 0 to 100 per cent.

Materials of construction: Cast-steel liquid end, stainless-steel ball checks, ball seats and plunger of 18-8 stainless steel hardened to 500 Bhn.

Pump to be provided with flush stream connection to lantern ring. Fresh fuel oil from main oil-supply line is run into lantern ring and discharge is run into mixing tank. A small needle valve on discharge side limits flushing oil flow to a trickle.

Actual power consumption measured at 2.44 hp handling 12 per cent concentration of additive in fuel oil at 130 F temperature.

Recommended spare parts:

1 plunger	1 set 4 ball seats	1 coverplate gasket
1 set 4 balls	2 sets packing	1 set of rod bushings

Mixing Tee:

A mixing tee is provided in the additive loop of the main oil stream under conditions of turbulence to provide a mixing action. In the piping arrangement fresh oil meets the slurry "head on" and both streams must make several 90-deg turns before reaching the oil burners, thus providing more turbulence or mixing.

Additive Distribution:

The distribution of additive to each burner position serves as a check on the quality of mixing accomplished. Individual treated-oil samples taken from each burner line can be analyzed for their additive content. Equal distribution indicates good mixing.

Precautions:

Additive has a tendency to settle out in mixing tanks. Keep agitator in use.

Sometimes sludge forms on the bottom of the mixing tank and it is carried over into the pump. Sludge can hold the ball check valves off their seats and prevent further pumping. Clean pump chamber.

Sludge in pump chamber sometimes can be melted by use of heat lamps beamed onto the pump casing.

Pump can become air-bound by sucking in air through the packing gland. Look for sludge in pump housing and tighten packing gland slightly.

Sludge can unseat the pump relief valve causing a reverse flow of oil from the header back into the mixing tank.

Keep the unit oil-return lines closed during addition of additive to prevent recirculation of treated oil back through the oil heater and main oil pumps.

Alumina-treated oil is very abrasive at high velocities. Wear has shown up in oil-burner sprayer plates and ball seats.

Because of its lower specific weight dolomite requires more care in mixing than alumina.

Discussion

O. F. CAMPBELL.[6] The authors are to be congratulated on assembling the interesting and worth-while information in this paper.

The writer's company has had some experience with the use of dolomitic lime on three 250,000 lb per hr 900-psig 900 F integral-type B&W boilers. These boilers were operated on unmerchantable fuel oil which was high in ash content and had an appreciable amount of difficulty with slag deposits on superheater tubes to the extent that frequent water washings were necessary to maintain operation. Subsequently, the fuel supply for the boilers was merchantable heavy fuel oil. Slag deposits on superheater tubes were troublesome and substantially in proportion to the ash contents of the merchantable and unmerchantable fuel oil.

To reduce the difficulties with merchantable fuel oils, the company elected to try out dolomitic lime on these boilers. A marked improvement in the nature of the deposits on the superheater tubes was noticed immediately. The superheater tubes continued to have some ash deposits, but this ash deposit was of such a nature that it could be removed readily with hand lances to the extent that these boilers could be operated on annual shutdown schedule. Retractable "IK" Diamond soot blowers were installed and as a result these boilers can be operated quite satisfactorily with no appreciable difficulties from deposits on superheater tubes.

For the quality of fuel oil burned on these boilers we consider that the use of dolomitic lime is very satisfactory and overcomes most of our operating difficulties.

In addition to the formation of easily removed slag deposits on superheater tubes, we have an indication that the corrosion of air heaters and ducts has been reduced materially. The use of dolomitic lime therefore serves two purposes; (1) it conditions the slag deposits on superheater tubes for easy removal, and (2) reduces the corrosion on air preheaters.

J. O. COLLINS.[7] The Babcock & Wilcox Company and the Florida Power Corporation are to be congratulated for the development and successful commercial demonstration of the use of additives to reduce the slagging tendency of heavy fuel oil. As has been pointed out in the paper and elsewhere, slagging of boiler superheaters is not new but has become more prevalent in recent years because of the trend toward higher steam temperatures and pressures which means higher metal temperatures. Furthermore, from the oil supplier's side, in general, there has been an increase in the concentration of ash constituents in the fuel. This has resulted from an increased demand for distillate products such as gasoline, domestic heating oil, and diesel fuel, and from the development of refining processes for maximizing the yield of these products from crude. This has been accomplished in many cases by reduction in heavy-fuel-oil yield, particularly from domestic crudes, resulting in the afore-mentioned increase in ash.

The relatively low price of residual fuel oil in relation to distillate fuel oils in the past has discouraged the refiner from developing or applying processes to reduce the amount of undesirable ash constituents. In the light of the more recent developments in power plants, however, oil suppliers are searching for means of improving the performance quality of their heavy-fuel products, in regard to slagging and high-temperature corrosion properties, as cheaply as possible. Considerable effort is being expended along these lines within our company. Therefore the development of a method whereby fuel-oil consumers having slag problems can immediately and economically improve the performance of the fuel in their equipment has considerable merit.

At the same time, the Standard Oil Company (N. J.) and its affiliates are also interested in taking advantage of new developments which will improve their own furnace and boiler operations. The reader may be interested, therefore, in a brief description of preliminary experiences with the use of dolomite to reduce the formation of hard fireside superheater deposits in two marine water-tube boilers installed in two tankers. As in the case of shore installations, the Esso Shipping Company also has experienced slagging of superheaters in its marine boilers. The promise shown by the work of the Florida Power Corporation on the use of dolomite suggested that similar benefits might be obtained in marine-boiler operation.

The Esso Shipping Company experiments to date have been concerned primarily with finding the most suitable method of introducing the additive into the boiler. Conditions aboard ship are quite different from those on shore, and it was felt that some modification of the "slurry-in-oil" injection technique was necessary. Because the boiler load may change widely and very rapidly, particularly when maneuvering, and complete control of firing rate is an absolute necessity, the possibility of the additive causing malfunctioning of the fuel valves must be eliminated. Furthermore, government regulations prohibit the storage or handling of fuel aboard ships in open tanks such as that used for making and storing the slurry at the Florida Power Corporation plant. Accordingly, two methods have been tried to date, namely, injecting the dry powder into the furnace by air and injecting a water slurry of dolomite directly into the furnace by means of a steam injector.

The initial trials with dry dolomite at a rate equivalent to about 0.25 weight per cent on fuel in one or two boilers on one tanker resulted in heavy deposits accumulating in 7 days with a loss of superheat. The deposits were very soft and friable and could be removed easily by either of two techniques. In one experiment the boiler was taken off the line and water-washed. In another case, the boiler was shut down temporarily, and the front plates removed to expose the superheater section and the deposits removed by hand-lancing with air or steam. Had soot-blowing equipment or lancing ports in the superheater section of this boiler been available, it was felt that the surfaces could have been kept clean by periodic blowing without the need for shutting down the boiler.

Disadvantages of handling an extremely fine powder in open hoppers in the ship's boiler room and the need for obtaining better distribution of the additive led to the use of the second technique namely, steam injection of an aqueous slurry. The water slurry (3 lb dolomite/45 gal water) was fed from a 55-gal drum by gravity to a steam injector where it was picked up and discharged into the furnace through an opening in the back casing and target wall that was originally intended for inspection purposes. A dolomite-fuel ratio of 1 lb per 1500 lb of fuel or roughly 0.07 weight per cent of fuel was used. Starting with two clean boilers in August, 1952, the port boiler using dolomite slurry has maintained normal superheat, and the expedient of temporarily shutting down and hand-lancing has been used only once during a $2^1/_2$-month period. The starboard boiler in which no dolomite was injected during the same period had to be removed from service for water-washing to remove the hard slag deposit.

Other experiments have been tried on another tanker wherein the dolomite injection rate has been varied and the point of injection changed to (1) a position in the center of the group of 4 burners, (2) in the forced-air system, and (3) at the back of the flame cone or diffuser of one burner.

Conclusive results from these various experiments probably

[6] Combustion Engineer, Sinclair Refining Company, East Chicago, Ind. Fellow ASME.

[7] Esso Laboratories, Research Division, Standard Oil Development Company, Linden, N. J.

will not be obtained until the opportunity arises to equip these ship's boilers with suitable soot-blowing or lancing equipment to service the superheater section. However, it is evident to date that (1) the amount of dolomite added for a given fuel must be sufficient to form the desired friable, easily removed slag, otherwise the slagging problems may be aggravated, (2) suitable soot-blowing equipment must be installed or openings provided so that hand-lancing can be done in order to remove periodically the soft deposits which do build up, and (3) as uniform distribution of the additive as possible is necessary for most efficient utilization. Sufficient promise is shown by these preliminary trials to justify continued work on Esso Shipping Company's part. It is hoped that others will become interested in modifications of the authors' method of alleviating slagging problems so that further experimental work will be initiated elsewhere.

M. Schreiner.[8] The work described by the authors represents a realistic approach to the solution of the problem of slag formation in and removal from the fireside surfaces within stationary steam-generating units.

Work at the Naval Boiler and Turbine Laboratory has pointed to the fact that fireside deposits in marine boilers may be attributed to the fuel ash plus other inorganic cations accidentally introduced to the fuel mixture.

It is certainly true that radical changes in design of the boiler units would permit the less troublesome use of higher-ash fuels, but we of the Navy are faced with the proper utilization of present installations. In addition, we recognize the important consideration such as unit efficiency, and space requirements most likely will have to be sacrificed if we are to seek those designs wherein less fireside fouling is to occur.

In giving attention to utilization of present installations, it was reasoned that we had two alternatives of action plus a combination of the two. We could place emphasis on the use of a low-ash fuel. Equally great emphasis should be given to the proper handling of such fuel oil to prevent its contamination by sea water which, in effect, would amount to increasing the ash content. In this connection we have calculated that the contamination of fuel oil by 0.26 per cent volume sea water has the equivalent effect of increasing the ash content of the fuel by 0.01 per cent weight.

The U. S. Navy is in a relatively good position with respect to the ash content of its Navy-grade special boiler fuel oil. One comprehensive survey has indicated that 44 per cent of our fuel has an ash content of less than 0.021 per cent; 90 per cent has less than 0.051 per cent; and 97.5 per cent less than 0.0617 per cent, the maximum allowable ash being 0.10 per cent. Therefore we are using a fuel which, on the average, contains about 1/5 the ash content of fuels consumed by the average stationary power plant.

We believe that we can control boiler slagging most effectively by the prevention of contamination of fuel by sea water through its proper handling.

On the other hand, we have tried to deal with the boiler-slag problem by looking at the possibility of changing the nature of the slag to make it less adherent to boiler heat-exchange surfaces. The Babcock & Wilcox Research and Development Division has worked closely with us in this matter.

In a limited test of the dolomite additive we were successful in obtaining a more friable, dry deposit, having a greatly increased fusion point. This characteristic was one of those sought since it was reasoned that a higher-fusing material would result in a lesser total of slag being deposited within the boiler furnace. It was believed that a higher-fusing material would be more readily carried out the stack in the stream of combustion gases. The result of our limited test of the dolomite was not exactly gratifying. It is believed that the shape, tube spacing, and configuration of Naval boilers are not so conducive to the use of dolomite additive as stationary plant equipment.

We have tested the use of aluminum-sulphate additive only in pilot-plant apparatus. Again, we were successful in obtaining a very friable high-fusing ash. We did not experience ease in its removal from heat-exchange surface by use of the air lance, with the result that an increasing quantity of material was deposited on heat-exchange surfaces over that resulting from the fuel ash without the additive.

Marine boilers are otherwise more restrictive than stationary steam-generating units in that the relatively large areas of refractories in marine boilers are affected adversely, particularly by the calcium ion. It likewise has been demonstrated that the carbonate and sulphate anions cause severe deterioration of brickwork. It is expected that use of aluminum oxide would present fewer difficulties to the refractory materials where present.

The introduction of any metal cation highly reactive with sulphur undoubtedly would tend to lower the dew point of the combustion gases. This is the most valuable feature in the introduction of the calcium carbonate of the dolomite. That compound has the dual advantage of increasing CO_2 content in stack gases, thus decreasing SO_3 and/or SO_2 concentrations therein; also through the reaction of the liberated calcium ion with sulphur to yield the sulphate of calcium. It is natural to expect a reduction in the dew point of stack gases by the introduction of the dolomite additive; however, it really is surprising that a reduction of from 100–125 deg F would result. The dew-point depression appears extremely significant where air heaters are employed, and where air pollution is a problem.

It is the writer's belief that possibly one of the greatest advantages of the dolomite additive has not been noted in its use at Inglis. It is to be expected that the presence of the calcium ion particularly in the furnace gases will tend to reduce the effect of vanadium in fuel ash which, by all indications, acts as a corrosion accelerator at the temperature prevailing in furnace structural members and even in heat-exchange-surface materials.

Surely the monetary saving in operating cost experienced at the Inglis Station is the best indication of the utility of the dolomite additive. The authors and those rendering assistance are complimented on the thorough and complete presentation of their efforts.

H. Weisberg.[9] Two additives have been tried in the mercury boiler at Kearny Station, Public Service Electric and Gas Company, New Jersey, using equipment furnished by The Babcock & Wilcox Company. The primary purpose of this installation is different from the Florida plant. It is to counteract corrosion of 1250 F mercury wall surface by high-vanadium-bearing fuel oil. Vanadium runs as high as 70 per cent of the fuel-oil ash which is probably considerably higher than that reported by the authors. The additives were introduced into the fuel oil prior to combustion, equipment and arrangement being similar to that installed at Inglis Station.

Aluminum oxide in the ratio of 1 lb of additive to 1 lb of oil ash was tried during two periods, August–September and November–December, 1951. Test probes, supplied by the Alliance Research Laboratory, installed in the furnace during these periods, indicated corrosion and pitting of the same nature and degree of attack as similar probes tested during a period when no additive

[8] Captain, USN, U. S. Naval Boiler and Turbine Laboratory, Philadelphia Navy Yard, Philadelphia, Pa.

[9] Mechanical Engineer, Electric Engineering Department, Public Service Electric and Gas Company, Newark, N. J. Mem. ASME.

was used. Slag appeared to be dry, friable, and could be readily broken off slag-screen tubes in flakes. Deposit on tube surfaces did not increase to any appreciable extent. Alumina did not appear to have any effect on old slag.

Dolomite was used in a 1:1 ratio from April 16 to May 26, 1952. The resulting slag was sticky, and the thickness of deposit on convection-tube surfaces increased, requiring more frequent use of soot blowers and hand-lancing.

From July 12 to the end of September dolomite was tried in the ratio of 2:1 and produced a drier slag which was removed by soot blowers but only on direct impingement of blowing air. The soot blowers in use on the boiler are not sufficiently effective to maintain normal draft loss through the fog bank, and continuous feed of this additive was stopped.

Examination of probes which had been in the furnace for 1-month periods while firing oil with 1:1 and 2:1 dolomite-ash ratio indicated that dolomite did not prevent or reduce metal corrosion significantly. None of the additives was used for a sufficiently long time to determine the effect on the furnace-wall surfaces themselves. Incidentally, dolomite in both 1:1 and 2:1 ratio changed the character of the old slag deposits so that they were readily removable by water-washing when the unit was shut down whereas previously these deposits were not soluble by water, cold or hot. Also, at the end of the service period when dolomite was used in 2:1 ratio, the Ljungström air preheater was found dry, clean, free of plugging, and in better condition than at any previous run with high-vanadium-content oil. Dew-point measurement of boiler exit gas varied from 340 to 350 F, no appreciable difference being noted with and without use of dolomite, despite the marked improvement of air-heater deposits. Either the dew-point determination is incorrect or the additive has some effect other than lowering the dew point of the gases.

At present dolomite is added to the fuel oil intermittently in a 2:1 ratio to obtain a light deposit on the convection-tube surfaces. Also, arrangements are under way to inject dry dolomite ahead of the air preheater further to observe its effectiveness for preventing deposits on the heating elements.

An experimental additive system is being installed at Sewaren Station on No. 1 boiler in which bunker-C fuel oil is fired and where corrosion attack has been found on superheater-tube surfaces and spacers. Here it is believed the soot-blower installation is adequate to remove the deposits formed by introduction of the dolomite additive.

Our limited experience up to this time with the high-vanadium-bearing fuel oil which is burned at Kearny is that when dolomite is added in a 2:1 ratio to ash content, it makes the slag friable and water-soluble but may not prevent hot-end corrosion. Also it is beneficial in reducing cold-end deposits although it may not lower the dew point of the gases.

G. B. Arnold.[10] The authors have capably presented the problem of increasingly troublesome ash deposits resulting from the continued lowering of fuel-oil quality. While ash analyses of local fuel oils may differ from those of oils available in the East, and as noted specifically in the subject paper, the trend is parallel.

The difficulty has been reduced locally, in many cases, by considering in the original design of units now installed the possibility of future coal firing. This resulted in larger units with wider superheater-tube spacing than necessary for the oils of a few years ago. Even with such provision, uneconomical hand-lancing has been required in some units where fixed-position rotary-type soot blowers were included with the original installation.

Units are now being designed for future coal-firing but with even wider superheater-tube spacing than heretofore, in addition to the use of more effective retractable mass-flow soot blowers.

When ash deposits increase to the point noted in the paper, the use of additives of the nature indicated certainly appears to provide an expedient for such existing units.

Since many units utilize the constant-differential oil-burner system rather than steam-atomizing burners, considerable constant-differential pump abrasion, as well as difficulties from additive accumulation in the system, can be expected. The required frequency of sprayer-plate renewal apparently is excessive and the difference in additive cost between the east and west coasts is an additional factor for consideration.

While presented as a secondary benefit from the use of additives, the apparent reduction of sulphur trioxide in the flue gas, as evidenced by reduced dew-point temperatures, may bear increased importance locally in view of smog conditions and certainly as affecting areas adjacent to the plant site.

Dust collectors which have been or are being installed in order to reduce local air pollution are underworked with the relatively small quantities of fly-ash resulting from oil firing. In such cases, effectively doubling the ash quantities by the addition of additives in a 1 to 1 ratio with ash in the oil could be expected to cause little difficulty. Unfortunately, some of the older units do not have dust collectors.

The authors are to be congratulated on a comprehensive report and the attempt at solution of a common and increasingly difficult problem.

C. L. Hathaway.[11] The authors are to be commended for their contribution to the conquest of slag deposition and its attendant evils. The information supplied in this paper will be of assistance to those who use fuel oil on a large scale.

The San Diego Gas & Electric Company has had its share of slag difficulties. These were most serious on the superheaters of B&W type-F integral-furnace boilers. Slagging was most pronounced in the first units of Silver Gate Station (1943), where the deposits were so heavy that actual bridging between the tubes resulted. This was reduced materially in later installations (1948), where the tube spacing was increased from 3 in. on centers (for 2-in. tubes) to 6 in. on centers. At that time it was feared that increasing the tube spacing might carry the slag farther into the bundle and cause heavy deposits there. This fear was unfounded. Although some slag was deposited farther in the bundle, the amounts were not excessive and a marked improvement over the close tube spacing was effected.

The slag deposit on the superheater is an extremely tough hard material. It cannot be blown off and is extremely difficult to remove mechanically. Fortunately, it is sufficiently soluble in water so that, in most cases, it may be washed off readily. All recent San Diego steam generators (1948 and subsequent) are designed so that superheater and economizer sections can be water-washed during outages.

During overhaul, on units where hosing was not deemed advisable, condensed moisture has been tried as a method of slag removal. This is effected by filling the superheater with water chilled by the addition of ice and blowing a small amount of steam into the furnace near the tube bundle to be cleaned. In other instances, the slag actually has been sprayed with water at regular intervals and softened in this manner. The theory of the chilled-water method is that the warm moisture, provided by the steam, penetrates the porous slag and the dew point is reached first at the cold tube surface rather than at the outer surface of the slag. This method has proved reasonably satisfactory.

[10] Steam Design Engineer, Los Angeles Department of Water & Power, Los Angeles, Calif. Jun. ASME.

[11] Superintendent of Electric Production, San Diego Gas & Electric Company, San Diego, Calif.

At San Diego, natural gas also is used as fuel. Large quantities are burned during the summer months when the domestic demand is low. It has been noted that during periods of burning gas, the slag deposits are reduced. It is not known whether or not a reaction takes place between the slag and the products of combustion. More likely there is a natural sloughing off of the slag under varying temperature conditions, which slag is not replaced with gas firing. If it were possible to utilize the two fuels alternately for short periods, the slag problem would be lessened somewhat. Unfortunately, the rate of build-up during oil firing is considerably greater than the reduction during gas firing. Further, no gas is available for a period of 5 or 6 months during the winter season.

An attempt was made to temper the slag action by the use of lime. The tubes were sprayed with a limewater solution prior to start-up following a thorough cleaning. Periodically, dry slaked lime was blown into the air stream at the burners. This treatment was not successful; the slag deposit was not reduced but was made hard and more difficult to remove. In addition, a heavy slag deposit formed on the furnace target wall.

From the foregoing, it is evident that a method of controlling slag deposition, such as the authors have provided, offers great possibility for improvement in oil firing. Apparently the method of application and the nature of the action produced by dolomite as compared with slaked lime spells the difference between the successful application at the Florida Power Corporation and the poor results at San Diego.

It is particularly interesting to note the authors' findings on the appearance of sulphur in the form of harmless salts and the attendant reduction of SO_3 and SO_2 in the gases. The resulting reduction in dew point is an important advance in itself.

During the war San Diego was supplied with a bunker-C fuel oil prepared in part at least from crudes from the Santa Maria field. Sulphur content was as high as $3^1/_2$ per cent. Following serious corrosion in the cold end of tubular air heaters, dew points were measured and found to be close to 400 F. Later tests on fuel oil with sulphur content around 1 per cent showed dew points below 150 F. All recent San Diego steam generators have been supplied with air-heater by-passes to control temperature during low-load operation. This extra expense and the loss in operating efficiency has been deemed necessary to meet the ever-present threat of higher-sulphur oil. Any method of controlling dew point is most welcome.

By pointing out a method of maintaining more nearly slag-free superheaters, together with a less corrosive flue gas of lower dew-point, the authors have made a contribution toward better efficiency, less troublesome operation, and longer periods between out-ages.

Authors' Closure

It is gratifying to learn that the use of additives has proved beneficial on a number of widely scattered installations burning fuel oil where the ash composition differs from that of the Florida Power Corporation oil. Mr. Campbell has indicated that the use of dolomite lime coupled with retractable "IK" soot blowers has very largely solved their operating difficulties from superheater slagging when burning available middle-western fuel oils. Hand-lancing is no longer necessary between annual shutdowns in his case.

Mr. Collins has reported on the application to marine units and indicates that the action of the dolomite is similar to that in stationary boilers but, due to marine boiler construction, it is more difficult to dispose of the somewhat larger volume of dry ash from the tube surfaces. The removal of the dry ash by hand-lancing represents a saving in cleaning time over that required for water washing for removal of hard fused deposits and indicates that properly located soot blowers would increase boiler availability in marine units.

Capt. Schreiner points out the production of a dry friable deposit but the problem of its removal still remains in the operating marine unit. Present day marine construction is not excessively troubled with air heater corrosion problems and his suggested use of a water solution of aluminum sulphate as the additive is not expected to materially affect the air-heater corrosion. The use of a water-soluble alumina additive can be expected to produce a finer additive particle size and should result in less additive being necessary to produce a friable deposit. The use of alumina as an additive would be less detrimental on the customary high alumina-silica type refractories on marine units than the dolomite type additive.

Mr. Weisberg indicates that a higher ratio of additive to ash is necessary to produce a dry, removable deposit when dealing with a high vanadium-content oil ash. Although the benefits hoped for in elimination of the high temperature corrosion were not realized in the probe tests, it is gratifying to note that the beneficial effects on the air-preheater deposits and corrosion were similar to those experienced at Florida Power and mentioned by Mr. Campbell. It will be interesting to follow the results of the Sewaren Station additive installation.

Mr. Arnold has suggested a further benefit in the use of dolomitic additive where air pollution and smog conditions are prevalent factors to be considered. The use of such additives coupled with dust precipitators and collectors can be expected to reduce the acid nature of the dust ultimately discharged and to minimize corrosion and pluggage on low temperature surfaces including the dust collector and duct work.

Mr. Hathaway's unsuccessful experience with the intermittent use of an additive is borne out by reports from other operators. Continuous addition of lime was the least effective of the better additives in the pilot scale trials; its intermittent use may result in the formation of higher proportions of calcium sulphate, bonding the deposit and rendering it difficult to remove even by water washing.

One of the benefits noted by the discussors and others using additives has been the improvement in conditions in the air-heater. Additional work is being carried out to determine the effect of additives on the formation of sulphur trioxide, the lowering of the acid dew point and low temperature end corrosion.

Reports from operators show that the use of dolomite along the lines outlined in the paper results in a slightly greater amount of deposit but in a dry and more easily removable condition. In most cases this enables the operator to keep the boiler in service for longer periods with a minimum of hand-lancing. The additional benefit of the improvement in air-heater conditions due to the use of dolomite has not yet been fully evaluated.

The authors wish to express their appreciation of the remarks by the discussers and feel that the information they have contributed has resulted in a valuable addition to the paper.

Chemical Cleaning in Central Stations

By P. H. CARDWELL,[1] TULSA, OKLA.

Chemical cleaning now has been applied to all equipment which contains scale and sludge deposits in central stations. A discussion is given of these various units along with a description of the different types of solvents employed. An explanation of certain types of corrosion is given. Improved acid corrosion inhibitors are now being used in order to give the necessary protection on stressed areas, on zones having dissimilar grain sizes, and on metals containing the Widmanst"tten structure. Information is given as to the ferric-iron corrosion problem.

Introduction

ACID cleaning has been used successfully to remove scale, oxide, and sludge deposits from central-station equipment for many years (1, 2, 3).[2] Initially only a few items were cleaned, mainly boilers, economizers, and surface condensers, whereas now it is possible to clean many different pieces of equipment. The introduction of cleaning to other units such as the turbine-oil system and the water-treating system has required the development of new cleaning solvents as well as new cleaning techniques and in addition to this, improvements have been made in the inhibitors used in the acid solvents. It is the purpose of this paper to discuss the units which can be cleaned chemically, the new solvents that can be used, the improved cleaning techniques, explain certain types of corrosion and the value of the recently developed new acid-corrosion inhibitors.

In the acid cleaning of equipment of central stations there are five possible techniques which can be used for removing deposits of scale, oxide, and sludge. The procedures are (*a*) soaking procedure; (*b*) jetting at high pressures; (*c*) spraying of thin and thick solvents; (*d*) circulating technique; (*e*) cleaning while in service.

The technique to use depends upon the shape and size of the unit being cleaned, and the amount, the hardness, and the chemical composition of the scale being removed. When equipment is of sufficient structural strength to support the weight of the solvent, and the surface area being cleaned is relatively large in relation to the liquid volume of the unit, it usually is advisable to fill the equipment with the solvent. Boilers, economizers, and surface condensers are treated in this manner. In such treatments the solvent is left within the unit until the deposit has been removed, either by dissolution or by disintegration.

The high-pressure jet is used normally when the scale is not sufficiently soluble in a chemical solvent for removal, or when the deposit is of such a quantity that it is not economical to remove by the soaking technique. Such a procedure is often used at the steam and water inlet to the lime-soda water-softening equipment. The spraying technique is used on large units where it is not possible to fill because of the structural strength or because the surface area of the unit is relatively small in relation to the liquid volume required to fill the unit. The water-softening unit and fuel-oil storage tanks are often cleaned this way.

Technique (*d*), that of circulation, is employed for cleaning rather small systems in which the solubility of the deposit is usually not very high but disintegration is satisfactory for removal, or where the amount of deposit present is of such a magnitude that one filling of solvent is not sufficient to remove it. Solvents normally used for circulation treatments are alkaline materials, organic solvents, or emulsions of organic liquids in aqueous-alkaline solvents.

The technique of cleaning a piece of equipment while that equipment is in service has not been used to any great extent for the chemical cleaning of central stations. It is a simple method to use in that the solvent is introduced into the water stream as it enters the unit and is returned from the unit in the exit water.

Soaking Procedure

The major portion of chemical cleaning in central stations is accomplished by the filling and soaking procedure. Figs. 1 and 2 are diagrammatic sketches of the various equipment within central stations which can be cleaned chemically. These sketches are not to be taken as an outline of a working system of a central station, but rather they are to illustrate the equipment which should be considered for chemical cleaning.

Boilers are always treated by the filling and soaking procedure. Many improvements have been made in recently constructed boilers, and chemical cleaning has been one of the important factors in making it possible to change their design. Controlled circulation boilers (4) and cyclone-furnace boilers (5) have been and are being built. Besides these different types of boilers, it is possible to make many structural changes, such as sharper bends in the tubes which heretofore have been held to a minimum radius of about 18 in. Considerably less hand-hole caps are now required. It is quite possible that in future boilers the majority, if not all of the hand-hole caps, can be omitted. In the future, the principal use of hand-hole caps will be to allow flushing the headers to remove sloughed and disintegrated deposits which have accumulated during chemical cleaning. The rolling of the tubes within the drums also may become unnecessary.

The deposits usually found in boilers consist of iron oxides, silicates, phosphate sludges, and metallic copper. The first three materials are soluble in inhibited hydrochloric-acid solutions and thus can be removed. The copper is not soluble but may be dissolved by ferric chloride which is formed by the reaction of the acid with the iron oxide. Whenever this happens the copper will deposit on the boiler metal surface in the form of sheets. In order to remove the copper from the boiler it is necessary to use an ammoniacal oxidizing solution (6, 7). Such a solution will oxidize the copper into a soluble form which in turn will be converted to a copper ammonia complex that prevents the deposition of copper onto the steel surface.

Economizers normally require more frequent cleaning than the boilers. Thus they are often cleaned by themselves. Since the economizers usually contain more sludge and scale than the boiler it is advisable to introduce the solvent through the economizer whenever the boiler is cleaned.

Superheaters and desuperheaters by their nature require less frequent cleaning normally than does the boiler. The deposits are due usually to the carryover from the boilers. The draina-

---

[1] Laboratory Director, Dowell Incorporated. Mem. ASME.

[2] Numbers in parentheses refer to the Bibliography at the end of the paper.

Contributed by the Power Division and presented at the Spring Meeting, April 28–30, 1953, of The American Society of Mechanical Engineers.

Note: Statements and opinions advanced in papers are to be understood as individual expressions of their authors and not those of the Society. Manuscript received at ASME Headquarters, May 26, 1953. Paper No. 53—S-19.

ble types of superheaters present no particular problem in regard to the cleaning technique, but the pendant-type (nondrainable) superheaters are difficult to fill and it is not possible to drain them. In the case of the pendant-type superheater the usual method is to introduce the acid solvent directly to each tube through hand-hole caps whenever they are available. This is accomplished by means of a flexible hose that has a fitting which seals the end of the tube. The solvent is displaced by the same procedure with water, then soda-ash solution, and finally with water again. Whenever hand-hole caps are not available then other means of filling and flushing have to be used. Sometimes it is possible to use an inlet header for introduction of the flushing fluids, having all of the tubes but one plugged in the steam drum. In other cases it is possible to enter an intermediate heater and there are still other designs in which a vacuum has to be used for filling and flushing. In regard to desuperheaters, both types can be cleaned; that is, the noncontact as well as the direct-contact types.

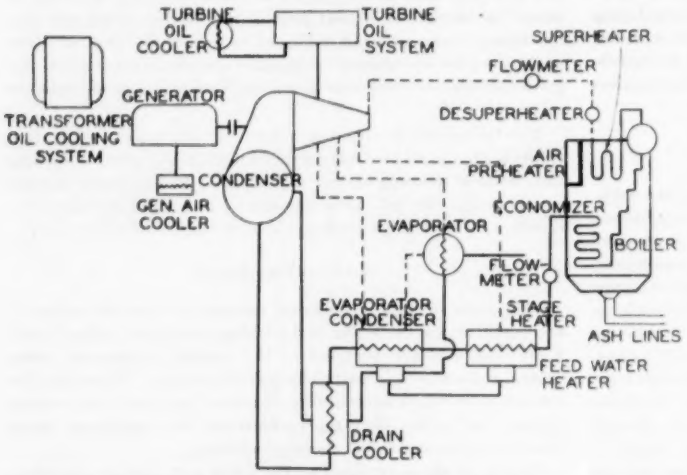

FIG. 1 SCHEMATIC DIAGRAM OF EQUIPMENT WHICH CAN BE CLEANED CHEMICALLY IN A STEAM-GENERATING SYSTEM

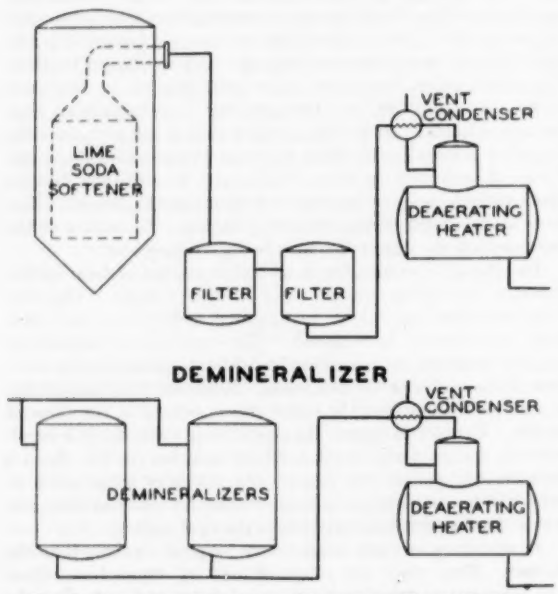

FIG. 2 SCHEMATIC DIAGRAM OF EQUIPMENT WHICH CAN BE CLEANED CHEMICALLY IN A WATER-TREATING SYSTEM

Surface condensers are more frequently cleaned on the water side than on the steam side. At times considerable quantities of acid are required for the water side, whereas normally only very weak acid solutions are consumed on the steam side. In cleaning the water side it is sometimes necessary to build some type of bulkhead in order to maintain the acid in place. At times it is possible to use large balloons for this purpose. Many of the surface condensers on the tube side contain organic-growth material such as algae and bacteria. In order to contact the deposit it is often necessary to remove these materials prior to chemical cleaning. This usually can be accomplished by means of pretreatment of copper sulphate, chlorine, and like chemicals. Under certain conditions it should be possible to clean these condensers while in service by injection of a weak inhibited acid solution into the inlet water. If the disposal of such a solution does not present a problem, consideration should be given to this method of cleaning.

Drain coolers are cleaned on the water (tube) side to remove deposits similar to those found in the surface condensers; i.e., silicates, calcium carbonate, iron oxides, and corrosion products.

Evaporators and evaporator-condensers often require cleaning; the evaporators on the shell side and the evaporator-condensers on the tube side.

Stage heaters and feedwater heaters usually require different solvents than normally are employed in cleaning in central stations. Some of the heaters, expressly those operating on the higher temperature steam, contain organic materials which originally were oil and have subsequently decomposed, then polymerized onto the tubes to form a varnish-like deposit which is at times difficult to remove. Whenever organic material is present, the acid solvent has to be preceded by a treatment with an oxidizing agent in an aqueous-alkaline solution. The stage heaters operating off the low-pressure end of the turbine usually do not contain the polymerized organic material and the acid solvent will remove the deposit satisfactorily.

Filters also are cleaned by the soaking technique. The filters, either sand or anthrafilt, are plugged by deposits carried over from the softening tanks. Before cleaning the filters it is advisable to determine the relative volume of plugging material within the filter in order to measure the volume of shrinkage that can be expected from the chemical-cleaning process. This procedure will indicate whether it is more economical to clean present media and replenish if necessary, or to replace entire media.

Deaerating heaters normally are cleaned by filling and soaking with acid solvent for removing deposits (carbonates, phosphates, and silicates) which have been precipitated from the softened water. Another procedure is to add the acid into the top of the unit where it can cascade over the trays.

Steam-flow nozzles at times may become fouled with iron oxides and/or metallic copper. These materials can be removed by using acid for the iron oxide and an ammoniacal-oxidizing solvent for the copper.

There are many other smaller pieces of equipment which have been cleaned chemically. Among such items may be mentioned generator and transformer cooling systems on the water side,

vent condensers, air-compressor jackets, refrigeration units, and air-conditioning units.

High-Pressure Jet Cleaning

The high-pressure jet normally is used on equipment which contains large quantities of scale. The jets operate at 2000 to 4000 psi pressure and can break up the scale deposits mechanically. There are three basic jet-nozzle designs. One type operates on the end of a flexible hose and is self-propelling in that the design of the jet pulls itself through the unit being cleaned. Another jets straightforward on a plane for cleaning ahead of the jet and the third has 2, 4, or more openings diametrically opposite for cleaning at right angles to the jets. The liquids used in the jets may be weak acid, alkaline solutions, or water. The scale deposit does not necessarily have to have high solubility in the solvent, but the choice of the solvent to use is the one which will give the best disintegration of the deposit. Since the jet breaks up the deposits some means must be used to wash out or carry out the disintegrated scale.

Feedwater lines can be cleaned either by means of the jet or by filling and soaking. The technique to use depends upon the size of the lines and the amount of scale present. In large lines containing a large amount of deposit the jet, if it can be used, is the most satisfactory method, whereas in complicated piping systems and small lines and where there is a relatively small amount of deposit the soaking procedure usually is the better one to employ.

Lines between softener tank and the filters offer a possibility of using jets for removing the large quantity of scale which very often is found.

Spray-type headers at the top of the hot lime-soda water-softening equipment at times may contain a considerable amount of deposit and have been cleaned by means of the jet.

Spray Technique

Equipment which contains a relatively small amount of surface area in relationship to its liquid-volume capacity is cleaned more easily by spraying the solvent onto the scale surface than can be accomplished by either the jet or soaking techniques. It is often impossible to fill such vessels, and the only way to contact the scale with the solvent is by spraying. In this procedure, mechanical means are not utilized for the removal of the deposit, but rather the dissolving action of the solvent.

The type of solvent sprayed upon the surface depends upon the amount of scale and its chemical composition. Whenever the scale is calcium carbonate which is readily soluble in acid an aqueous-acid solution can be used, the concentration of which depends upon the amount of scale present. Whenever the scale consists mainly of iron oxides which are much slower to dissolve than calcium carbonate, it is advisable to use a thickened acid solvent in order that the sprayed material will adhere to the surface for a sufficient length of time to remove the deposit. Such an acid solvent consists of a gellifying material and an absorbent material to take up the acids, similar to the method by which a sponge takes up water, and a third material which acts as a film-forming substance over the surface of the sprayed liquid to retard the vaporization of the acid. By means of the thickened solvent it is possible to use 20 to 25 per cent hydrochloric-acid-content solvents which greatly expedite the dissolving of the deposit. Using this spraying technique a relatively small volume of solvent will clean a large surface. For instance, 450 gal of the thickened acid were used to clean a 6000-bbl-capacity storage tank. Once the deposit has been removed the thickened solvent can be washed down with a stream of water which is then followed by an alkaline rinse.

For the removal of deposits of grease and oil it is advisable to spray an emulsion onto the surface. The emulsions used are of the acid-in-oil type, in which the oil (kerosene), being the continuous phase, will dissolve the oily materials, and the acid can remove any rust that may be present. There is sufficient viscosity of the emulsions so that they will adhere to the metal surface, vertical walls, and even overhanging roofs. The emulsifying agents used give stability to the emulsions so that they can be prepared well in advance of their use. Once the oil and rust have been removed, the emulsion can be washed off with water, followed by an alkaline rinse.

Softener tanks containing heavy deposits of carbonate or phosphates, depending upon the softening process employed, can be cleaned by spraying with a dilute acid solution.

Air preheaters often can be cleaned by washing with water but, when this does not result in a satisfactory removal of the deposit, spraying with dilute acid solvent usually is found to be successful.

Fuel-oil tanks can be cleaned either by the use of a thickened acid solvent or by the acid-in-oil type emulsions, depending upon the type of deposit being removed. If the deposit is essentially iron oxide then the thickened acid solvent is employed. However, if the deposit is mainly organic material from the oil, then the emulsion is the better solvent to use. In either case, the solvent is sprayed onto the metal surfaces, followed by washing down with water, then by an alkaline material.

Firesides of economizer and boiler tubes have been serviced to some extent by the spraying of weak acid or water solutions onto the hot surfaces in order to break loose the slag deposits.

The Circulating Technique

The circulating technique is used mainly to clean organic deposits from relatively small units in which it is possible to circulate an alkaline material or an emulsion of kerosene in an alkaline solution through the system. The purpose behind the use of an emulsion is the incorporation of the combined action of the organic liquid and the alkaline solution into a one-stage treatment. Very often it is found that the emulsion as a one-stage treatment is far superior to a two-stage treatment, one of an organic liquid and the other an alkaline material. Usually by rapid circulation it is possible to disintegrate and flush out the organic deposits.

Turbine oil-lubrication systems normally are cleaned in this manner. This includes the oil-storage tank, circulating pumps, the lubrication oil lines, filters, and oil coolers. A study of the deposit should be made prior to the treatment in order to determine which alkaline material to use and whether or not an emulsion is required. Sometimes iron oxides are present. Whenever this is the case a treatment of an acid solvent has to be used following the alkaline stage.

Oil-cooled transformer lines also can be cleaned by this technique of using an alkaline material or by an emulsion of kerosene in an aqueous-alkaline solution.

Cleaning in Service

The technique of cleaning while the equipment is in operation has not been used to any great extent to date. When such a procedure can be used there is no outage time of the equipment, thus it is an economical method. Several factors have to be considered, such as the rate of dissolution of the deposit because the contact time is very short, the temperature at which the unit operates, in order to prevent the solvent from becoming corrosive, and the disposal of the solvent since usually it is impossible to change the normal operation of the unit.

Ash-disposal lines often are cleaned while in service by introducing a weak acid solvent and disposing of the returned solution. The deposits encountered in such lines are essentially calcium carbonate which are readily soluble in acid.

Recent Advances in Inhibitors

The use of acid for removing scale deposits from steel equipment has come about as a result of the development of excellent inhibitors for the control of the attack of acid on iron (8, 9). Since the introduction of chemical cleaning there has been a considerable improvement made in acid inhibitors (10, 11, 12). In fact, it is possible from the recent research to design inhibitors to protect the stressed metals from acid attack. These metals normally are the most susceptible to corrosion.

In the construction of steel equipment it is often necessary to use stressed metals. Boilers contain a considerable amount of cold-worked or stressed metals such as rolled tube ends, the machined surfaces on hand-hole caps, man-hole plates, and the seats for these caps and plates in the headers and drums. When such metal is exposed to the inhibited hydrochloric-acid solutions pitting may occur.

In order to study the effect of acid attack upon the stressed areas the apparatus shown in Fig. 3 was employed to duplicate

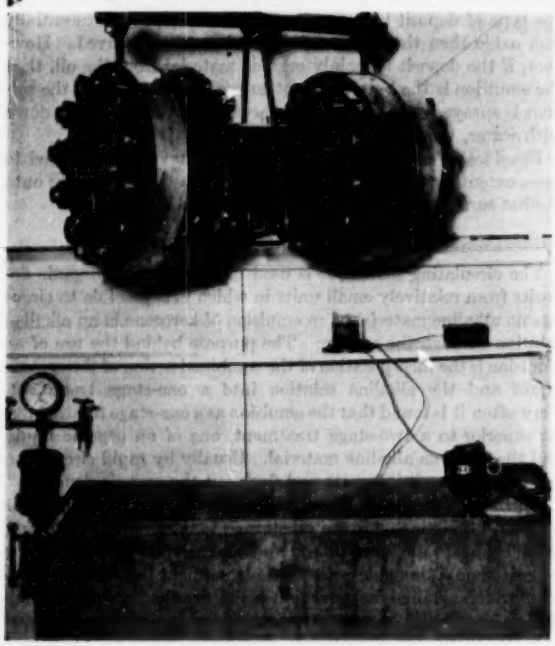

Fig. 3 Hand-Hole Cap Test Apparatus

as far as possible the conditions encountered during acid cleaning of a boiler. The complete cycle of acid cleaning could be performed in order to investigate the effects of the acid upon the hand-hole caps which with their gaskets were fastened in place in the apparatus.

Fig. 4 is a hand-hole cap which has been subjected to 5 per cent hydrochloric acid containing a nitrogen-sulphur coal-tar inhibitor for 19 periods of 8 hr each at a temperature of 150 F. It will be noted that the lip is pitted and that a deep groove is present at the point of contact between the hand-hole cap and gasket. A metallographic examination of the cap showed that the grains were medium to fine in size (ASTM No. 5–6) and angular, indicating a stressed condition within the metal. It is possible to change the crystal structure of a hand-hole cap by proper heat-treatment, resulting in caps that are more resistant to corrosion.

Similar tests, under the same conditions of exposure, were con-

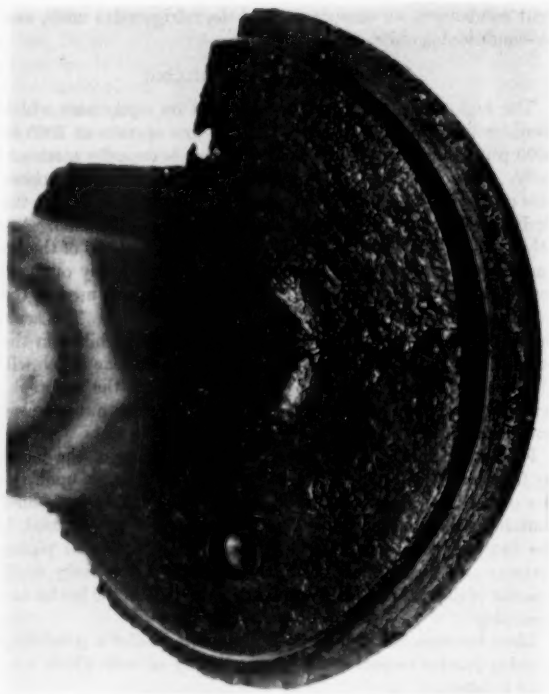

Fig. 4 Hand-Hole Cap Exposed to Coal-Tar-Inhibited Hydrochloric-Acid Solution for 152 Hr

Fig. 5 Annealed Hand-Hole Cap Exposed to Coal-Tar-Inhibited Hydrochloric-Acid Solution for 152 Hr

ducted on a hand-hole cap which had been annealed properly. The condition of this cap following the test is shown in Fig. 5. The cap was similar to the one shown in Fig. 4 before being annealed. Comparing these two illustrations, it may be noted that there is considerably less corrosion on the annealed cap.

Metallographic examination showed that the crystal structure was reduced somewhat by annealing. The grain size was ASTM No. 6 and the crystals were no longer angular. From a practical standpoint, however, it is difficult to assure that the caps used for boiler construction are properly heat-treated. Besides this, there are other stressed metals in the boiler, such as

FIG. 6 HAND-HOLE CAP EXPOSED TO POLYETHANOLAMINE-INHIBITED HYDROCHLORIC-ACID SOLUTION FOR 152 HR

the machined seats in the drums and headers, which it is impractical to relieve by annealing.

Since the industrial equipment is designed and built with steels containing different crystal structures, which are impossible to change once the unit is erected, it becomes necessary to select the inhibitor for the specific crystal-structure conditions found in these stressed metals. A similar test to that shown in Fig. 4 was performed using in place of the nitrogen-sulphur coal-tar inhibitor a rosin amine-ethylene oxide condensate product as an inhibitor (13). This polyethanolamine material is surface active and functions as a combination inhibitor and wetting agent to prevent more effectively the attack of the acid.

A hand-hole cap similar to the one shown in Fig. 4 was treated using the polyethanolamine inhibitor in 5 per cent hydrochloric-acid solution. After being subjected to the acid, the cap is shown in Fig. 6. While this cap does show slightly more acid attack than does the annealed one in Fig. 5, the cap is much better than the one exposed to the nitrogen-sulphur coal-tar inhibited hydrochloric-acid solution of Fig. 4.

Besides the stressed metal within the equipment there may be areas of varying grain size, and also the possibility exists of the presence of Widmanstätten structure, especially if the metal has been welded. Both of these facts, the varying grain size and the Widmanstätten structure, have considerable influence on the corrosion of the equipment metal. In this connection, a comparison between nitrogen-sulphur coal-tar and the polyethanolamine inhibitors was made using bifurcate tubes. Two bifurcates which had identical crystal structures were subjected to 16 periods of 6 hr each to 7.5 per cent hydrochloric-acid solutions inhibited with these two materials. The results are shown in Figs. 7 and 8. The crystal structure of the tube given in Fig. 7 is shown in Figs. 9 and 10.

It will be noted that in the case of a nitrogen-sulphur coal-tar inhibitor the acid caused pitting in the areas of the large crystals, and in these same areas Widmanstätten structure also was present. The tubes subjected to the polyethanolamine-inhibited

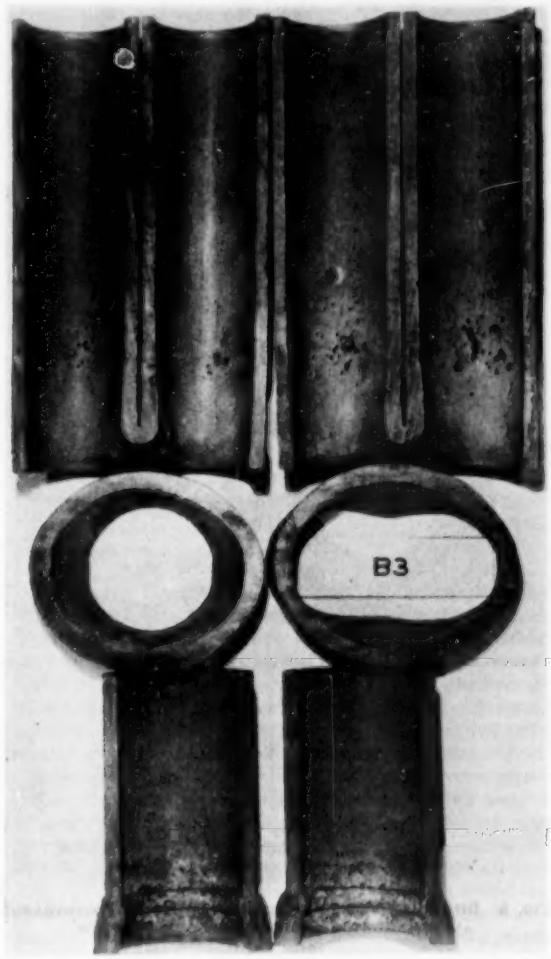

FIG. 7 BIFURCATE TUBE EXPOSED FOR 96 HR TO COAL-TAR-INHIBITED HYDROCHLORIC-ACID SOLUTION

hydrochloric-acid solution did not pit, even though the tube had the same crystal structure. An investigation of other bifurcate tubes containing only dissimilar metal structures, that is, medium and fine-grain, adjacent to one another, but no Widmanstätten structure, has shown that the polyethanolamine-inhibited hydrochloric-acid solution did not cause pitting, whereas

pitting was obtained with nitrogen-sulphur coal-tar-inhibited hydrochloric-acid solution.

This investigation indicates that whenever there are present dissimilar metal structures varying only in grain size, the pitting from acid attack takes place in the areas of the large crystals, unless an acid inhibitor is used which will prevent this from happening. The polyethanolamine material is such an inhibitor. Whenever the steel contains Widmanstätten structure, it is necessary to use polyethanolamine as the inhibitor for the hydrochloric-acid-solution.

The location of the zone of dissimilar metal structures seems to be dependent upon the temperature gradient brought about

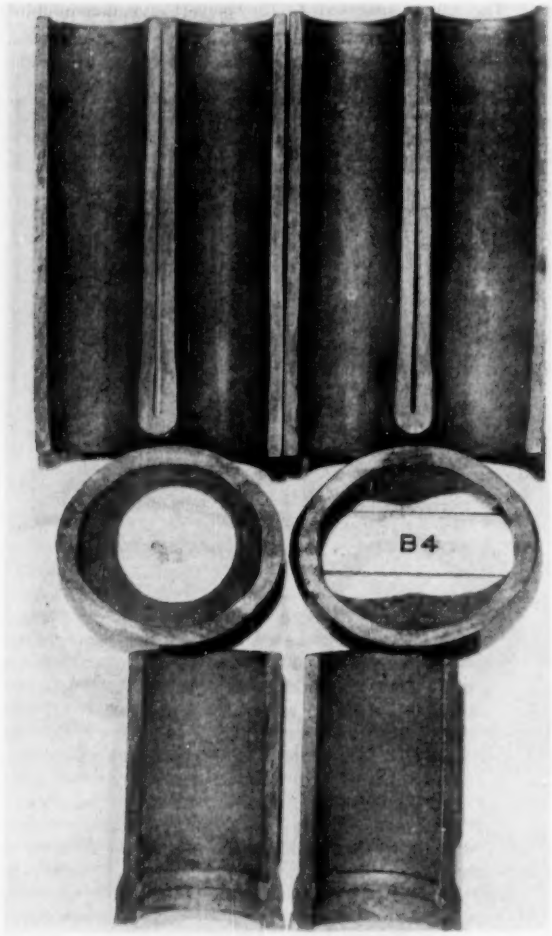

FIG. 8 BIFURCATE TUBE EXPOSED FOR 96 HR TO POLYETHANOLAMINE-INHIBITED HYDROCHLORIC-ACID SOLUTION

within the metal by the welding process. Sometimes the zone is very near the weld, whereas at other times it is some distance away.

From this investigation and other similar work (12) it is believed that the pitting occurring in the area of large crystals is due either to the large grains being more susceptible to attack, or to a galvanic effect of dissimilar metal structures in contact with each other. Possibly the pitting is due more to the latter effect than to the former.

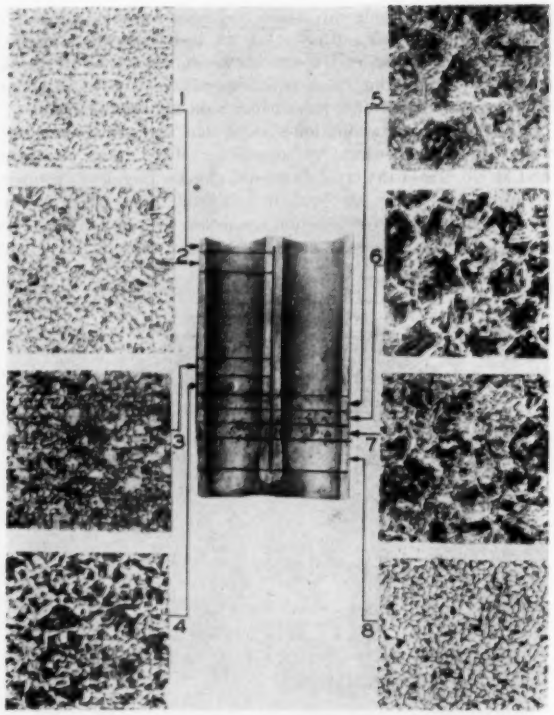

FIG. 9 MICROSTRUCTURE OF SECTION OF BIFURCATE TUBE IN FIG. 7

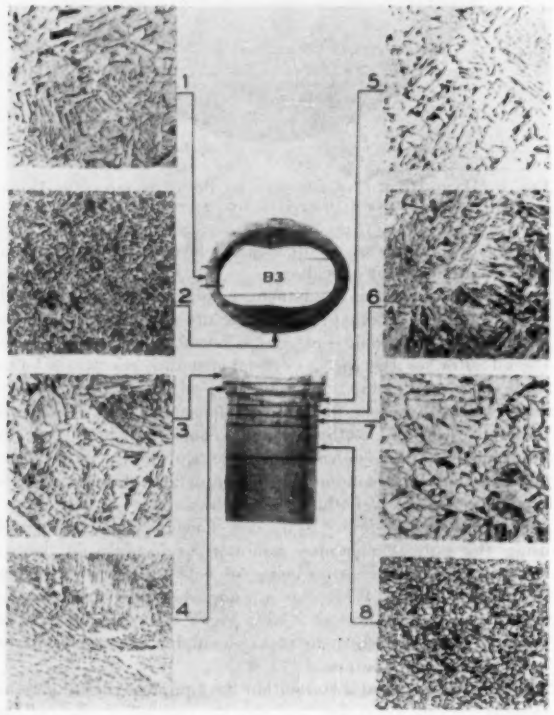

FIG. 10 MICROSTRUCTURE OF SECTION OF BIFURCATE TUBE IN FIG. 7

Possibility of Ferric-Iron Corrosion

Another possible mechanism which has been suggested that may bring about corrosion during acid cleaning is called ferric-iron corrosion (14). When scales containing ferric oxides are dissolved by hydrochloric acid, ferric chloride is formed, but from analyses of acid solutions taken during and after chemical cleaning only traces of ferric iron (of less than 0.02 per cent) have ever been found. This means that the ferric iron has been reduced to ferrous iron and the question is, whether or not the reduction has been at the expense of boiler metal.

The chemical equations for the dissolution of iron oxides in hydrochloric-acid solutions are given in the following equations. In both it will be noticed that ferric chloride ($FeCl_3$) is formed

$$Fe_3O_4 + 8HCl = 2FeCl_3 + FeCl_2 + 4H_2O \quad [1]$$

$$Fe_2O_3 + 6HCl = 2FeCl_3 + 3H_2O \quad [2]$$

The reaction between ferric chloride and iron of the boiler metal is considered as ferric-iron corrosion in that it dissolves boiler metal over and above the amount dissolved by the acid

$$Fe + 2FeCl_3 = 3FeCl_2 \quad [3]$$

Before it can be determined whether or not Reaction [3] will proceed and to what extent, it is necessary to make a complete study of the chemical system; e.g., iron oxides—inhibited hydrochloric acid—boiler metal. In order to do this it becomes necessary to write three additional equations as follows

$$Fe + 2HCl = FeCl_2 + H_2 \quad [4]$$

$$Fe + 2HCl = FeCl_2 + 2H \quad [5]$$

$$2FeCl_3 + 2H = 2FeCl_2 + 2HCl \quad [6]$$

The sum of Reactions [4] and [5] is the total amount of acid attack upon the boiler metal. Two reactions are written because of the hydrogen which is formed; a portion of it is evolved as a gas and the remainder is used according to Equation [6].

It may be noted that Equations [5] and [6] when added together give Equation [3]. The possibility of the addition of these two equations is the step which causes the confusion in the ferric-iron-corrosion problem. It will be noted that the metallic iron dissolved in Equation [4] is by acid corrosion and is not dissolved by ferric chloride. Thus the amount of ferric chloride reduced by Reaction [6] does not dissolve boiler metal as ferric-iron corrosion. It is true that the hydrogen which reduces the ferric chloride in Reaction [6] comes from the reaction of acid dissolving boiler metal, but this reaction is acid corrosion and will take place regardless of whether or not ferric chloride is present. Until such time that inhibitors can be developed to prevent all acid corrosion, Reactions [4] and [5] can proceed; thus Reaction [6] is always a possibility.

The problem of ferric-iron corrosion then becomes one of determining which of the two reactions (Equation [3] or [6]) reduces the ferric chloride. In the chemical system, iron oxides—inhibited hydrochloric acid—boiler metal, there are seven materials which can be measured at any one time, namely, the amount of each of the two iron oxides dissolved, the change in acid content, the ferrous-chloride content, the ferric-chloride content, the amount of hydrogen evolved, and the amount of metallic iron dissolved.

Even though there are seven items that can be measured, it still is not possible to explain the system, iron oxides—inhibited hydrochloric acid—boiler metal without additional chemical determinations of either the amount of ferric chloride reduced by hydrogen or the amount reduced by metallic iron. This is shown in the Appendix. As yet no chemical method has been devised by which these measurements can be made.

Since direct measurements cannot be made of the possibility of ferric-iron corrosion, the next best thing seems to be to attempt to gather information through an indirect procedure. Two series of experiments were conducted in this connection. In one series a section of boiler metal containing scale in place was filled with 5 per cent inhibited hydrochloric-acid solution for a period of 6 hr at a temperature of 150 F. In this test, determinations were made for weight loss of the scaled specimen, the total iron content, and the ferric-iron content present in the acid solution.

In another test the scale was removed from the boiler metal and the resulting clean piece of metal was filled with 5 per cent inhibited hydrochloric acid. Determinations were made in this case for weight loss of the specimen and iron content of the acid solution. The results of the tests are given in Table 1. It is to be noted that since the amount of acid corrosion on the descaled specimen (0.308 gram) was greater than the amount of iron dissolved (0.279 gram) from the metal of the scaled specimen; thus a boiler metal containing an iron-oxide scale in place corrodes at a much lower rate than does a bare piece of metal. The amount of ferric-iron corrosion, if there is any, is less than this decrease of the corrosion rate of the metal as brought about by the presence of scale.

TABLE 1 TEST WITH ACTUAL SCALED BOILER TUBE

Analysis of Scale:	
X-ray	100 per cent Fe_3O_4
Iron content	61.4 per cent
Materials other than iron (oxygen)	38.6 per cent
Analysis of acid solution—Nonscaled specimen:	grams
Total iron content	0.308
Weight loss of specimen	0.309
Analysis of Acid Solution—Scaled Specimen:	
Total iron content	0.417
Weight loss of specimen	0.504
Ferric-iron content	0.008
Iron in acid solution from scale (calculated):	
Weight loss of scaled specimen	0.504
Iron content—acid solution-scaled specimen	0.417
Materials other than iron dissolved (oxygen)	0.087
Amount scale dissolved (calculated)	0.225
Amount iron dissolved from scale (calculated)	0.138
Iron dissolved from metal of scaled specimen	0.279
Iron dissolved from metal of unscaled specimen	0.308

In another series of tests an attempt was made to prevent the ferric chloride from reacting with either the metallic iron or hydrogen and to measure the increase in the amount of hydrogen evolved. This increase in hydrogen represents the amount of ferric chloride which would have been reduced by the hydrogen. This was accomplished by immersing a scaled piece of boiler tube in 10 per cent inhibited hydrochloric acid at 175 F for 4 hr and determining the weight loss of the scaled tube, amount of iron in solution, ferric-iron content, and amount of hydrogen evolved. A similar test with the same chemical determinations was made in which the inhibited hydrochloric acid contained 4 per cent hydrazine sulphate. This material is capable of reducing ferric chloride. The results are given in Table 2.

It will be noted from these results that there is considerably more hydrogen evolved when the ferric chloride has been reduced with hydrazine sulphate than when there is no hydrazine sulphate present and the hydrogen can react with the ferric chloride. These results certainly indicate that hydrogen can reduce the ferric chloride.

There is one other approach to this ferric-iron-corrosion problem and that is to repeat the tests given in Table 2, using a material which will oxidize or absorb the hydrogen in place of the reducing agent, hydrazine sulphate. In this way it would be possible to measure the increase in amount of boiler metal dissolved. Thus far all of the agents investigated for this purpose have had a detrimental effect upon the acid inhibitor. No con-

TABLE 2 HYDROGEN EVOLUTION FROM INHIBITED HYDROCHLORIC-ACID SOLUTION ON SCALED BOILER TUBE
(Scale 68 per cent Fe_3O_4 and 32 per cent Fe_2O_3)

	Test without hydrazine sulphate, grams	Test with hydrazine sulphate, grams
Analytical data:		
Specimen weight loss	6.38	6.32
Iron in solution	5.12	5.07
Hydrogen evolved standard conditions	334[a]	716[a]
Ferric-chloride content	1.60	0.00
Amount scale dissolved (calculated):		
Specimen weight loss	6.38	6.32
Iron in solution	5.12	5.07
Materials other than iron dissolved (oxygen)	1.26	1.25
Amount scale dissolved	4.44	4.40
Amount iron dissolved from scale and boiler tube:		
Amount scale dissolved	4.44	4.40
Iron dissolved from scale	3.18	3.15
Iron in solution	5.12	5.07
Iron dissolved from boiler tube	1.94	1.92
Amount ferric chloride reduced:		
Amount scale dissolved	4.44	4.40
Amount ferric chloride formed	7.11	7.05
Amount ferric chloride reduced	5.51	7.05
Decrease amount hydrogen evolved	382[a]	....
Amount ferric chloride reduced by hydrogen	5.50	....

[a] Measured in ml.

clusions can be drawn to date from such work but the indications are that the reaction of ferric chloride and metallic iron in this chemical system is very slow.

From the results of these two series of tests it seems that the amount, if there is any, of ferric-iron corrosion normally is very small. Most of the ferric chloride is reduced by nascent hydrogen which is a powerful reducing agent. This reaction of nascent hydrogen is expedited by the fact that the formation of nascent hydrogen takes place at the cathode which is also the location of the formation of ferric iron by reaction of acid upon the iron oxide. Thus the hydrogen and the ferric iron are formed at the same electrode in the system and the reaction between them can take place without one of the ions having to move to the other electrode or diffuse into the solution.

When the time comes that better acid inhibitors are developed, and this will come about some day, there will be an insufficient amount of hydrogen formed from the reaction of acid on steel to reduce the ferric chloride. With the introduction of these better inhibitors the problem of ferric-iron corrosion will become a serious one and there will have to be added to the acid solution reducing, complexing, or chelating agents in order to control the ferric-iron corrosion.

Conclusions

In order to remove the various scale deposits found in central-station equipment it is necessary to use acid solvents, alkaline solutions, emulsions of organic liquids in an aqueous-alkaline medium, and thickened acid solvents. Besides the various solvents which have to be used, it is necessary to employ different treating techniques such as the filling and soaking method, the jetting at high pressures in order to break up the deposit mechanically, the spraying of thin or thick solvents onto the scale when it is present in large vessels or tanks, the circulating technique to remove organic materials, and, when possible, cleaning the equipment while in service.

Improved acid inhibitors are now being used in the acid solvents. These polyethanolamine products give better protection than the coal-tar nitrogen-sulphur inhibitors, especially on stressed areas, on zones having dissimilar grain sizes, and on metals containing the Widmanstätten structure.

The problem of ferric-iron corrosion has been investigated and, while it seems to be impossible to make direct chemical measurements as to the amount, if any, of this type of corrosion, experimental results indicate that the ferric chloride is reduced by nascent hydrogen which is formed by the reaction of acid with the steel. The reduction of ferric chloride by this procedure does not dissolve any additional boiler metal over that dissolved by the acid.

BIBLIOGRAPHY

1 "Chemical Removal of Scale From Heat-Exchange Equipment," by F. N. Alquist, C. H. Groom, and G. F. Williams, Trans. ASME, vol. 65, 1943, pp. 719–722.

2 "Chemical Cleaning of Heat-Exchange Equipment," by C. M. Loucks and C. H. Groom, Trans. ASME, vol. 71, 1949, pp. 831–836.

3 "Chemical De-Scaling of a Modern Steam Generator," by M. E. Brines, *Power Plant Engineering*, vol. 49, 1945, pp. 90–92, 99.

4 "Chemical Cleaning Applied to Controlled Circulation Boilers," by W. D. Bissell and M. M. Sorenson, *Combustion*, vol. 23, 1952, pp. 40–41.

5 "Iron Oxide on Water Side of a Cyclone Fired Pressurized Steam Generator," by M. E. Brines and F. N. Alquist, National Association Corrosion Engineers, Seventh Annual Conference, New York, N. Y., March 14, 1951.

6 "Chemical Removal of Copper From Boilers," by R. G. Call and W. L. Webb, *Industry and Power*, vol. 59, August, 1950, pp. 90–92.

7 "Removal of Copper From Boilers," by R. F. Andres, Engineers' Society of Western Pennsylvania, Twelfth Annual Water Conference, Pittsburgh, Pa., October, 22–24, 1951.

8 "Acid-Cleaning of Boilers and Auxiliary Equipment," by S. T. Powell, Trans. ASME, vol. 68, 1946, pp. 905–917.

9 "Investigation of Acid Attack on Boilers and the Effect of Repeated Acid Cleaning on the Metal," by H. C. Farmer, Trans. ASME, vol. 69, 1947, pp. 405–412.

10 "Corrosion of Boiler Steels by Inhibited Hydrochloric Acid," by P. H. Cardwell and S. J. Martinez, *Industrial and Engineering Chemistry*, vol. 40, 1948, pp. 1956–1964.

11 "Use of Wetting Agents in Conjunction With Acid Inhibitors," by P. H. Cardwell and L. H. Eilers, *Industrial and Engineering Chemistry*, vol. 40, 1948, pp. 1951–1956.

12 "Microstructure and the Corrodibility of Steel in Inhibited Hydrochloric Acid Solutions," by P. H. Cardwell, The Electrochemical Society, Detroit Meeting, Detroit, Mich., October 10, 1951.

13 "Rosin Amine-Ethylene Oxide Condensates as Corrosion Inhibitors for Mild Steel in Hydrochloric Acid," by E. A. Bried and H. M. Winn, *Corrosion*, vol. 7, 1951, pp. 180–185.

14 "Ferric Iron Corrosion During Acid Cleaning," by F. N. Alquist, J. L. Wasco, and H. A. Robinson, *Corrosion*, vol. 3, 1947, pp. 482–487.

Appendix

Algebraic Equations

Since in the systems of iron oxides—inhibited hydrochloric acid—boiler metal, there are seven different items which can be measured and there are only six equations, the question immediately arises as to which combinations of these measurements should be made in order to understand fully the chemical system. In order to do this it becomes necessary to set up a number of algebraic equations expressing the relationships between the various ingredients. In the algebraic equations the following nomenclature is used:

$^{M^1}FeCl_2$ represents number of moles of ferrous chloride formed in Equation [1].

Likewise

$^{M^3}FeCl_3$ is the number of moles of ferric chloride consumed in Equation [3].

For the materials which can be measured, and this will be the total amount from all reactions, the following nomenclature is used:

$^{T}FeCl_2$ is the total number of moles of ferrous chloride at any one time in the complete chemical system, iron oxides—inhibited hydrochloric acid—boiler metal.

The following relationships are present:

Amount of ferrous chloride formed

$$^{T}FeCl_2 = {}^{M^1}FeCl_2 + {}^{M^2}FeCl_2 + {}^{M^4}FeCl_2 + {}^{M^5}FeCl_3 + {}^{M^6}FeCl_2 \quad [7]$$

Amount of ferric chloride formed

$$^{T}FeCl_3 = {}^{M^1}FeCl_3 + {}^{M^3}FeCl_2 + {}^{M^3}FeCl_3 + {}^{M^3}FeCl_3 \ldots [8]$$

Equation [8] may be written

$$^{T}FeCl_3 = {}^{2M^1}FeCl_2 + {}^{M^3}FeCl_3 - {}^{2/3M^3}FeCl_3 - {}^{M^3}FeCl_2 \ldots [9]$$

Change in acid content (Δ HCl) may be expressed as follows

$$^{\Delta T}HCl = {}^{M^1}HCl + {}^{M^3}HCl + {}^{M^4}HCl + {}^{M^3}HCl + {}^{M^3}HCl \ldots [10]$$

$$^{\Delta T}HCl = {}^{8M^1}FeCl_2 + {}^{3M^3}FeCl_3 + {}^{2M^4}FeCl_2 + {}^{2M^3}FeCl_2 - {}^{M^3}FeCl_2 \ldots [11]$$

The amount of boiler metal dissolved is as follows

$$^{T}Fe = {}^{M^2}Fe + {}^{M^4}Fe + {}^{M^3}Fe \ldots [12]$$

or

$$^{T}Fe = {}^{1/3M^3}FeCl_3 + {}^{M^4}FeCl_3 + {}^{M^3}FeCl_2 \ldots [13]$$

Amount of hydrogen evolved

$$^{T}H_2 = {}^{M^4}H_2 = {}^{M^4}FeCl_3 \ldots [14]$$

Amount of Fe_3O_4 dissolved

$$^{T}Fe_3O_4 = {}^{M^1}Fe_3O_4 = {}^{M^1}FeCl_2 \ldots [15]$$

Amount of Fe_2O_3 dissolved

$$^{T}Fe_2O_3 = {}^{M^3}Fe_2O_3 = {}^{1/2M^3}FeCl_3 \ldots [16]$$

In Equations [5] and [6] there is the following relationship

$$^{2M^4}FeCl_3 = {}^{M^4}FeCl_2 \ldots [17]$$

The equations can be simplified as follows:

Equation [7]—substituting Equations [14], [15], [17]

$$^{T}FeCl_2 = {}^{T}Fe_3O_4 + {}^{M^2}FeCl_2 + {}^{T}H_2 + {}^{M^4}FeCl_2 + {}^{2M^4}FeCl_2 \ldots [18]$$

or

$$^{T}FeCl_2 = {}^{T}Fe_3O_4 + {}^{M^2}FeCl_2 + {}^{T}H_2 - {}^{3M^1}FeCl_2 \ldots [19]$$

Equation [9]—substituting Equations [15], [16], [17]

$$^{T}FeCl_3 = {}^{2T}Fe_3O_4 + {}^{2T}Fe_2O_3 - {}^{2/3M^3}FeCl_2 - {}^{2M^3}FeCl_2 \ldots [20]$$

Equation [11]—substituting Equations [14], [15], [16], and [17]

$$^{T}HCl = {}^{8T}Fe_3O_4 + {}^{6T}Fe_2O_3 + {}^{2T}H_2 + {}^{2M^2}FeCl_2 - {}^{2M^3}FeCl_2 \ldots [21]$$

Equation [21] is of little value since all of the items in it can be measured.

Equation [13]—substituting Equation [14]

$$^{T}Fe = {}^{1/3M^3}FeCl_2 + {}^{T}H_2 + {}^{M^2}FeCl_2 \ldots [22]$$

The three remaining Equations, [19], [20], and [22], show that in order to understand the chemical system, iron oxides—inhibited hydrochloric acid—boiler metal, it becomes necessary to determine experimentally only certain combinations of variables.

Four measurements only are necessary to explain this chemical system when one oxide is present. For each additional oxide one additional measurement has to be made. On the system, one iron oxide—inhibited hydrochloric acid—boiler metal, the four chemical measurements which have to be made fall into two groups.

Group I—Two items must be measured from the following:

(*a*) Amount iron oxide dissolved.

(*b*) Amount hydrogen evolved.

(*c*) Change in acid content.

Group II—Must determine all items except one in any one of the following combinations:

Combination 1

(*a*) Total ferrous-chloride content.

(*b*) Amount ferrous chloride from reduction of ferric chloride by hydrogen.

(*c*) Amount ferrous chloride from reduction of ferric chloride by iron.

Combination 2

(*a*) Ferric chloride content.

(*b*) Amount ferrous chloride from reduction of ferric chloride by hydrogen.

(*c*) Amount ferrous chloride from reduction of ferric chloride by iron.

Combination 3

(*a*) Amount metallic iron dissolved.

(*b*) Amount ferrous chloride from reduction of ferric chloride by hydrogen.

(*c*) Amount ferrous chloride from reduction of ferric chloride by iron.

Discussion

R. F. Andres.[3] This paper presents a comprehensive and enlightening summary of the current status of acid-cleaning techniques used on central-station equipment. Owing to the broad scope of the paper several difficult problems related to acid cleaning necessarily have been mentioned only briefly. Additional observations regarding some of these problems are discussed in the following.

It is apparent throughout the paper that a great deal of emphasis has been placed on development of suitable inhibitors to minimize metal loss from equipment during the chemical-cleaning process. The inhibitors currently being used are quite effective when the acid temperatures are maintained below or in the range of 150–170 F. Unfortunately, in central-station boilers, the deposits to be removed chemically usually are quite high in magnetic iron oxide, which is not rapidly soluble in hydrochloric-acid solvents used in this temperature range. Removal is predicated on sloughing the material from the metal surfaces followed by removal with the spent acid solvent in an insoluble form as the boiler is drained. Dependence on this means of removal of deposits obviously has many variables from boiler to boiler. Where magnetic iron oxide has been a problem, some companies even resort to mechanical cleaning after chemical cleaning, which is both time-consuming and expensive. Development of suitable inhibitors so that higher temperatures can be used in acid-cleaning procedures, and development of a more rapid solvent for magnetic iron oxide would go far in removing the element of uncertainty in boiler operators' minds concerning the completeness of removal of these troublesome deposits.

Copper and copper oxides are other major components of deposits found in central-station high-pressure steam-generating boilers. In conventional acid-cleaning procedures these deposits can and do dissolve and replate from the acid solvent. As mentioned in the paper, copper deposits can be removed satisfactorily by employing a two-stage chemical-cleaning treatment, using acid in the first stage for iron oxide and scale removal, and using an oxidizing ammoniacal solvent in the second stage under very carefully controlled conditions for copper removal. This

[3] Chief Chemical Engineer, Dayton Power and Light Company, Dayton, Ohio.

answer to the problem is again both time-consuming and expensive. One of the major controlling factors in the solution and replating of copper is the ferric-ion concentration present in the acid solvent. The author's statement regarding the use of a reducing agent, hydrazine sulphate, to eliminate ferric ion as it is formed in the acid solvent is of great interest in that this may be a partial answer to the copper-replating problem. Work in our laboratories and by other investigators has indicated that the solution and replating of copper during acid cleaning can be minimized by the addition of relatively slight amounts of suitable reducing agents to the acid solvent. The addition of a reducing agent to the solvent seems to be a step in the right direction, in that copper present in the boiler would remain in its normal granular or finely divided form and might be removed as the spent acid is drained from the boiler. Further work on the problem is indicated, and one possible solution may be the use of a mixed acid solvent with proper reducing and chelating agents added to dissolve and remove in solution iron oxide, scale, and copper in a single-stage treatment. An effective treatment of this type would be welcomed by many operators faced with copper deposits in boilers.

Chemical-cleaning solvents and their application to cleaning a wide variety of equipment have been developed quite thoroughly and, in general, excellent results can be obtained readily. The answers to earlier problems such as effective wetting of metal surfaces and after-rusting have been explored rather thoroughly and it is to be hoped that in the near future at least partial answers to the problems mentioned can be obtained.

E. C. Chapman.[4] The author is to be highly commended for the advancement in the science of chemical cleaning which has been proved so clearly in this interesting paper. As he has pointed out, improvements in the technique of acid washing, both as regards the materials used and their application, have been an important factor in making major boiler-design changes possible. The more efficient inhibitor, which has been demonstrated, has already served to relieve the anxiety of both the boiler operator and the manufacturers over possible damage to various parts through the use of less efficient inhibitors.

The efficiency of the polyethanolamine inhibitor as compared with the coal-tar inhibitor should in the future mean (1) less initial cost of an installation and (2) less repair cost. It is impossible to build a modern boiler with uniform metallurgical structure within even one component. For instance, consider a tube weld. The grain size is inherently different from the tube material and the analysis cannot be absolutely duplicated. This means that no form of heat-treatment administered to a weld, either in a furnace or in the field locally, will result in a structure which is closely comparable to that of the tube. The cost of heat-treating for grain refinement up to 20,000 tube and pipe welds in a boiler in order to make the structures as similar as possible to the base metal would be a major item. If small differences in structure have the effect of lowering corrosion resistance, as suggested by the author, this additional expense would be of no avail.

To eliminate all Widmanstätten structure from welds and heat-affected zones of welds, a normalizing or annealing treatment must be administered. Normalizing introduces serious problems of distortion with drums and headers and sets up shrinkage stresses which can be relieved only with a second heat-treatment. Annealing lowers tensile strength and it is doubtful that the mills would be able to meet the specified tensile strengths with this treatment under the material specification to which our materials are now furnished. According to the author, elimination of Widmanstätten structure does not assure resistance to pitting corrosion since even small differences in grain size promote susceptibility.

There are other parts in a boiler which cannot be protected or improved in their resistance by costly preventative measures. Any cross section of plate, pipe, or tube shows lower corrosion resistance than the rolled surfaces of these parts. They may be exposed where nozzles are welded to drums or headers, on the scarfed edges of plates, or where tubes are joined to these parts. Many parts of internals made of relatively light gage material can be damaged seriously by a relatively mild degree of attack, by pitting or otherwise. Some of these parts do not lend themselves to high-temperature heat-treatment. Castings, because of segregation which takes place during solidification, cannot be homogenized by heat-treatment to eliminate completely the weakness which results. Any local heat-treatment administered in the field is accompanied by temperature gradients which are unavoidable. A gradient of structure is thereby produced and stresses are only partially relieved.

It is apparent that we must endure variations in metallurgical structure and, therefore, an effective inhibitor is of immeasurable value.

It is fortunate that corrosion by oxygen and other chemicals, which has been experienced infrequently in boilers under adverse conditions, does not parallel attack by acid as regards the susceptibility of various types of structure and changes in structure. In many investigations it has never been noted that attack concentrates on Widmanstätten structure or on locations where there are sharp demarcations in structure. We have these conditions throughout the boiler, of course.

We have conducted general corrosion tests in both uninhibited 5 per cent sulphuric and 5 per cent hydrochloric acid on carbon-steel samples having wholly uniform lamellar pearlite for structure, and for comparison on samples from the same tube converted to Widmanstätten structure. The results failed to show that the latter structure is inferior in general corrosion resistance and the attack was general with no pitting in each case.

Will the author state whether he has ever observed the same type of pitting attack in boilers which have been acid-washed as shown in his tests? We have failed to find any evidence of preferential attack on Widmanstätten structure in hundreds of tube samples removed from boilers which were acid-washed regularly, nor have we observed this in our inspection of many drums and headers. There have been instances where poor control of acid temperature has resulted in considerable general loss in wall thickness and areas such as cross sections of nozzles or tubes have shown differential attack.

Also a question occurs with regard to the location of the author's photomicrographs with respect to the corroded surfaces. The structure usually varies through the wall thickness and in particular the structure at the surface is often decarburized to various degrees. The grain size and structure at the surface, therefore, may be considerably different from that at the center of the wall. Variations in structure over the surface can be as great as variations due to welding, particularly when minor surface imperfections penetrate the surface layer of decarburized or other metal of dissimilar structure. These effects may be as responsible for pitting by galvanic action as variations in structure caused by heat from welding or otherwise.

Light layer welds that normally are very fine grained, as compared with base material, are adversely affected physically by increasing the grain size by heat-treatment to compare with that of the plate. Their mechanical properties are lowered and it is important to retain the fine grain for this reason. Single-pass or very heavy layer welds are of unrefined cast structure and Widmanstätten structure predominates. If it is necessary for the metallurgical structure of welds to be the same as or to ap-

[4] Chief Metallurgist, Combustion Engineering, Inc., Chattanooga Division, Chattanooga, Tenn. Mem. ASME.

proximate the structure of the base material in order to avoid pitting, the most susceptible part of a boiler should be the boiler drums or any other parts welded by the submerged-arc process, since this method of welding normally will give a weld with structure more dissimilar to that of the base metal than any other method of arc welding, unless very light layers are used. This process is used more than any other for welding the seams of boiler drums and other pressure vessels. In our experience the seam welds of drums and other parts that are accessible for inspection have not developed pitting that could be attributed to galvanic corrosion after a number of acid-cleaning treatments.

I. B. Dick.[5] The writer's company has been cleaning power-plant equipment since 1943, and has so cleaned a total of 567 separate units of equipment of which about two thirds have been boilers and the remainder distributed principally among feedwater heaters, condensers, and economizers. The following comments relate to experiences accumulated from these jobs:

In so far as theoretical discussion goes, we wish only to point out that whether iron is lost from a boiler by direct acid attack or whether it is lost by oxidation by ferric chloride is unimportant. Every unit of magnetic or ferric-iron oxide removed by acid from a boiler requires a definite amount of reducing agent to change its ferric-iron content to ferrous. It is widely recognized that such reduction does take place because iron in acid drainings after a cleaning is always completely in the reduced (ferrous) form. Whether the reducing agent is iron from the boiler metal by direct reaction, according to the author's Equation [3], or whether it is hydrogen, according to Equation [6], seems to be of little importance, since the hydrogen in the latter instance represents a corresponding loss of iron from the boiler. In other words, the reduction of 1 lb of ferric iron requires exactly the same amount of iron loss from the boiler regardless of the mechanism of the reduction.

The author's repeated mention of the Widmanstätten structure as related to chemical cleaning calls for some clarification. This structure does not imply internal, "locked-in" or thermal stresses in steel, and, as a matter of fact, we have not encountered it in hundreds of metallographic examinations of high-pressure-boiler steels. In any case, we would not expect this steel to be any more susceptible to acid attack than normal pearlitic steels.

When first starting to clean equipment with potentially corrosive substances like mineral acids, one is quite understandably concerned over attack on the metal of the equipment being cleaned. We have cleaned some boilers as much as 18 times without any serious metal deterioration, and four series of closed feedwater heaters 11 times with similarly little attack on the metal. Some of these results we accomplished the hard way. We found it quite necessary, for example, to have an entire boiler at as nearly a uniform temperature as possible, and that not to exceed 160 F at any point. This may be accomplished in a cold boiler by filling the boiler with water to the normal water level and heating it to some temperature well above 160 F by judicious firing, then allowing it to cool down to the desired temperature before draining the water. Use of permanent and contact thermocouples to check metal temperatures is of primary importance in controlling metal attack.

We have had poor success in heating a cold boiler with hot feedwater, because the upper drums always rise more rapidly in temperature and remain considerably higher than lower parts; so that when the steam drums hit 160 F, the waterwall tubes and lower headers may be only 120—too low for effective cleaning. In the case of an operating boiler, we normally cool it down in the regular manner, using the fans to accelerate the operation, until the desired temperature is reached before emptying the boiler.

[5] Assistant Chief Chemical Engineer, Consolidated Edison Company of New York, Inc., New York, N. Y.

We also have found it impossible to prevent corrosion of stressed areas, especially the light seal welding generally used in assembling drum internals. Carryover conditions have been found attributable to openings left in drum baffles by chemical-cleaning-solution attack on seal-weld beads. The remedy for this condition at the moment appears to be a careful inspection of the unit after chemical cleaning, and repairs made of the faults disclosed by the inspection. This is even more desirable when it is considered that the chemical cleaning frequently discloses fabrication flaws which could act as stress raisers leading to ultimate metal failures unless corrected. The use of properly trained chemists or chemical engineers, who are familiar both with chemical-cleaning techniques and with boiler construction and operation, to make the post-chemical cleaning inspections is recommended.

It may be in order to ask "When does a piece of equipment need a cleaning?" The answer has to be specific for each situation, but a discussion of how we gage some of ours may be helpful. Consider boilers. Experience has shown that some of our oldest 1400-psi units can be expected to develop tube troubles when the deposits removed from one wall tube by dry-turbining exceed 50 grams. This seems a very small amount of deposit to justify a chemical cleaning, but it must be remembered that the bulk of this deposit will be removed from a few feet of the tube in the hottest part of the furnace. Other, more modern boilers in our system will tolerate upward of 2 lb of deposit per tube without developing tube troubles. In these two cases the nature of the deposit is similar chemically and physically. Why, then, the difference? Apparently it is because of circulation rate and of heat-input rate. In the first case the heat input is so great that the smallest interference with heat transfer causes overheating of the metal. In the second case a lower heat-input rate combined with a much more vigorous water circulation minimizes the effect of the tube deposit.

So, our experience indicates that careful collection of samples of deposits from dry-turbining of critical tubes, and their subsequent weighing and analysis, correlated with knowledge of the characteristics of the particular boiler, will permit us to gage when a unit requires cleaning.

As the author states, modern practice is to the complete elimination of handhole caps. This makes it impossible to collect samples by turbining. In this case a good lead can be obtained by cutting out about 3-ft sections of two or more tubes from the hottest zone of the furnace, sectioning them lengthwise (being careful to cut them dry) and examining the deposit for amount, nature, and composition, examining the inner surface of the tube that was toward the fire for attack, and examining the tube metal under the microscope for evidences of overheating.

Once having established a pattern by some such means, we believe a cleaning schedule should be set up and adhered to until other factors dictate a change.

Consider the case of closed feedwater heaters. Performance, betterment, or results group will indicate when heaters lose efficiency and how much the loss in efficiency is worth. You can then gage when the value of the loss in efficiency balances the cost of chemical cleaning. After a few cleanings, curves can be plotted to show when cleaning becomes economical.

Now let us consider the matter of how to judge the effectiveness of a chemical cleaning of a boiler. Inspection is the first step. Look for deposits as well as corrosion. Loose drifts of soft sludges in mud drums or lower headers probably represent disintegrated adherent deposits and may be considered as indicative of a good cleaning job, but they must be removed by flushing before the unit is returned to service. Dry-turbining of representative tubes for collection of residual-deposit sample is highly informative where it can be done. We believe 5 grams of turbinings so collected is a maximum permissible from any wall tube of any

length, although should they exceed 5 grams the cleaning is not normally repeated. However, on the next job on this or similar boiler the chemical treatment is adjusted to remove more deposit. In cases where visual inspection is not revealing and turbining cannot be done, the cutting out of tube sections may be helpful, but it may not be justifiable. In such case, analysis of acid drain samples from the chemical cleaning should permit a good opinion as to the effectiveness. If the residual acid concentration was reduced more than half, there may be some reason to suspect the completeness of the cleaning. Experience here will be the best guide. As a tip to chemists, the potentiometric titration is probably the only fully satisfactory means of determining free acid in the presence of acid salts.

Another consideration we must face is how to establish the cleaning procedure and chemical solutions to be used. This can be developed by the operator by analysis, experience, and trial and error. Errors in this case can be expensive, even to the point of serious damage to equipment. There was a rumor extant some few years ago of some marine boilers that were destroyed completely by improper chemical-cleaning procedures. It was even stated that one or more fatalities were connected with one of these jobs. The writer believes that if exceptionally skillful chemical talent is not available, and if there is not a reasonable background of experience to draw upon, one would be well advised to use a reliable industrial cleaning service that has the knowledge, experience, equipment, and trained personnel to do the job better and more expeditiously than a novice can do it.

We expect a complete boiler-cleaning job to take about 24 hr exclusive of copper removal. Our deposits are largely magnetic iron oxide and metallic copper. Copper content seldom exceeds 40 per cent, and to date this has not required a copper-removal operation. At this point the writer must take issue with the author. He states that copper may be dissolved by ferric chloride, and this copper will redeposit on boiler metal in the form of sheets. There is no doubt this has happened. It does not happen in most cases to the writer's knowledge. Redeposited copper seems to appear usually as crystalline or granular copper which sometimes washes out fairly completely in the draining, flushing, and neutralizing operations, and which in no case has been reported to give trouble.

With the trend toward more and more completely sealed boiler construc ion, we must agree that chemical cleaning becomes increasingly more important. The writer believes most boiler-tube failures ould b· pr vented by keeping the water-side surfaces clean. However, with this trend, inspection to determine the condition of boilers becomes more difficult, and thorough flushing to remove loose sludges also becomes more difficult. Furthermore, the sealed-type construction makes for possible points of chemical attack which, because they are sealed, may not be detected until damage is done. It has not even been demonstrated clearly in the writer's opinion, that this type of construction may not be susceptible to corrosion by some of the normal boiler-water salines. These points should be watched carefully.

Author's Closure

As Mr. Andres points out, the more difficult soluble scales are sloughed during the chemical-cleaning treatment. This is one of the reasons for emphasis being placed on the development of improved inhibitors. The use of better inhibitors not only affords greater protection to the boiler metal, but also permits the use of higher treating temperatures that will dissolve more of the scale and correspondingly give less sloughing.

The problem of copper removal is a serious one and it would be desirable if some means could be found to prevent the copper from dissolving and redepositing during the acid cleaning. A few reducing agents are available and several chelating chemicals that can be used in the acid solution either to reduce the ferric chloride or complex the copper. To date the use of such materials has not proved too satisfactory. It is believed that the reason has been the depletion, either of the reducing agent or of the chelating agent, in the immediate vicinity of the area wherein the copper is dissolved. This depletion is brought about by the reaction of the reducing agent with ferric chloride or the reaction of the chelating agent with dissolved copper. Before additional reducing or chelating materials can migrate or diffuse into this depleted area, more copper is dissolved and is redeposited. In order to prevent the copper from redepositing it is necessary to maintain a large excess of these agents in the acid solution so that no portion of the acid solution will become depleted of the chemical. The necessity of maintaining this large excess of the agent usually makes this procedure uneconomical for the removal of the copper during the acid stage in the chemical-cleaning procedure.

Mr. Chapman's point is well made that variations in metallurgical structure will always be present in boilers. This means that extreme care must be taken in the proper selection of the acid inhibiter in order to give the maximum protection to all of the boiler metals, taking into consideration such items as presence of Widmanstätten structure, cold-worked areas, welds, including the structure in the temperature-gradient zones, and in addition, differences in grain sizes adjacent to one another. At this time it is not known whether or not a specimen that is completely converted to the Widmanstätten structure is more susceptible to attack by inhibited hydrochloric-acid solution than a uniform lamellar pearlite structure. As pointed out by Mr. Chapman, uninhibited hydrochloric-acid solution does not differentiate between the two structures. It may be that the presence of the inhibitor brings this about or it may be that both these metallurgical structures have to be present within the same specimen. It is true that a specimen containing both of these structures is much more susceptible to attack than a specimen containing only the lamellar pearlite structure. With the specimen containing both the Widmanstätten and the lamellar pearlite structures the majority of the acid attack always takes place in the area containing the Widmanstätten structure.

The type of pitting on the Widmanstätten structure reported in the paper has been observed in several boilers which have been acid-cleaned. The pitting observed in the boilers has been on the handhole caps or the manhole plates. These are the parts of the boilers that usually contain the Widmanstätten structure. It is believed that the differential attack is not caused by excessive acid temperatures since several cases have been on mill scale-removal treatments. In this type of treatment the boiler is subjected to a single acid treatment and there should be very little chance of any excessive temperatures.

In regard to the location of the photomicrographs with respect to the corroded areas, the pictures were taken at the very edge of the specimen. The pictures were taken of the surface which was exposed to the acid. It was noted at the time the pictures were taken that the amount of decarburization was small for many of the specimens. In the early part of the work it was expected that some correlation would be found between the amount of decarburization and corrodibility, but no such relationship was found.

The discussion by Mr. Dick, who has been one of the pioneers in the large-scale application of chemical cleaning in power plants, points out the importance of this method for scale removal in his statement of the number of units that have been treated.

It is very true, as pointed out by Mr. Dick, no matter how the boiler metal is dissolved, whether by ferric iron corrosion or by acid attack, it still is boiler metal removed. With the present information, it is now possible to pin-point the problem, indicating

the direction for future research to be along the lines of improved inhibiters rather than methods of preventing the reaction between ferric ions and metallic iron.

In regard to copper plating, it should have been pointed out in the paper that the form in which the copper is redeposited depends partly upon the amount of copper present. When large quantities of copper are dissolved and redeposited, the copper is usually found in the form of sheets, following the chemical cleaning treatment. Other times, when small quantities of copper are present, the copper is deposited in small crystals or leaflets. Frequently, much of this type of copper can be removed from the boiler by flushing.

An Interferometric Study of the Boundary Layer on a Turbine Nozzle Blade

By C. R. FAULDERS,[1] CAMBRIDGE, MASS.

The boundary layer on a turbine nozzle blade was investigated with an optical interferometer over a range of Reynolds numbers and subsonic downstream Mach numbers. The ratio of laminar boundary-layer thickness to distance downstream from the minimum pressure point on the suction side of the blade was found to be essentially a unique function of a length Reynolds number based on this distance. Thickness critical Reynolds numbers for transition increased, with throat Reynolds number, from 3000 to 9000 on the suction side and from 1200 to 3100 on the pressure side. A laminar velocity profile was computed from a density profile measured at a point of zero pressure gradient, and satisfactory agreement with theoretical profiles was obtained.

Nomenclature

The following nomenclature is used in the paper:

- M = Mach number of nozzle exit stream
- p = local static pressure
- p_o = stagnation pressure upstream of nozzle
- p_s = static pressure downstream of nozzle
- Re_t = throat Reynolds number, based on downstream velocity and density, throat width, and stagnation viscosity. All values of Re_t based on a throat width of 0.500 in.
- Re_x = length Reynolds number, based on local free-stream velocity and density, distance downstream from minimum pressure point on suction side and from profile inflection point on pressure side, and stagnation viscosity
- $Re_{\delta c}$ = thickness critical Reynolds number for transition based on local free-stream velocity and density, thickness of laminar boundary layer at transition, and stagnation viscosity
- t = throat width
- u = velocity in direction parallel to blade surface
- u_∞ = local free-stream velocity
- $u^* = \frac{u}{u_\infty}$
- x = distance along surface, measured from minimum pressure point on suction side and from profile inflection point on pressure side
- y = perpendicular distance from blade surface
- $y^* = \frac{y}{\delta}$
- δ = boundary-layer thickness
- λ = Pohlhausen number
- μ = coefficient of viscosity

Introduction

Two-dimensional losses in a cascade of turbine blades result from fluid friction concentrated in the boundary layer on the blade surface. Furthermore, the flow coefficient of a nozzle or rotor-bucket passage is affected by boundary-layer thickness. Means for the prediction of the behavior of the boundary layer on a blade surface are therefore important. To this end, the designer must know of the development of a boundary layer under the influence of pressure gradient and profile curvature. Knowledge of the location at which a boundary layer flowing along a blade surface changes from laminar to turbulent and an understanding of the significant factors upon which this location depends are of particular importance. Specifically, maintenance of a laminar boundary layer, with accompanying wall shear stresses that are low in comparison to those in a turbulent boundary layer, provides minimum loss as long as separation, resulting from an adverse pressure gradient, is not encountered. On the other hand, transition to turbulence upstream from the point where a laminar boundary layer would separate will, in general, offset separation.

A Mach-Zehnder optical interferometer was used to obtain measurements of the boundary layer on a turbine nozzle blade, a cascade of which was installed in the variable density wind tunnel at the M.I.T. Gas Turbine Laboratory. Previous interferometric measurements of blade pressure distribution, downstream density contours, and wake characteristics are described in reference (1).[2] In the boundary-layer study, the variation of the thickness of the boundary layer over the blade surface and the effect thereon of Mach number and throat Reynolds number were determined. Observations were made with downstream Mach numbers of 0.3, 0.6, and 0.75, and with throat Reynolds numbers varying from 80,000 to 250,000. Locations of the transition points on the pressure and suction sides of the blade were observed over the range of Mach numbers and throat Reynolds numbers. A laminar velocity profile was computed from a measured density profile and compared with theoretical results.

Experimental Apparatus

The experimental cascade consisted of eight blades which were twice-normal-size models of a particular steam-turbine nozzle profile. Dimensions of the experimental nozzle are shown in Fig. 1, and the test section with one side removed is shown in Fig. 2. A detailed description of the experimental equipment is given in reference (1). In Fig. 3 is shown a typical blade pressure distribution, measured with pressure taps in the blade surface.

The installation of the test section in the wind-tunnel circuit is illustrated in Fig. 4. The honeycomb of $2^1/_2$-in-diam tubes shown in Fig 4 was held in place by a coarse grille and covered at the top by a 0.1-in-mesh screen.

The turbulence level of the test section was measured by determining the critical Reynolds number of a 1.7-in-diam sphere placed 12 in. upstream from the leading edges of the blades. The critical Reynolds number of a sphere is, by convention, the sphere diameter Reynolds number at which the drag coefficient

---

[1] Research Assistant, Massachusetts Institute of Technology. Jun. ASME.

Contributed by the Gas Turbine Power Division and presented at the Spring Meeting, Columbus, Ohio, April 28–30, 1953, of The American Society of Mechanical Engineers.

Note: Statements and opinions advanced in papers are to be understood as individual expressions of their authors and not those of the Society. Manuscript received at ASME Headquarters, January 18, 1953. Paper No. 53—S-36.

[2] Numbers in parentheses refer to the Bibliography at the end of the paper.

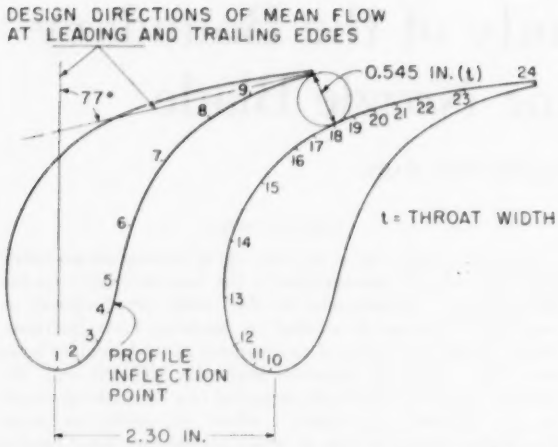

FIG. 1 BLADE PROFILE AND DIMENSIONS OF EXPERIMENTAL NOZZLE (Span, 6.00 in. Numbers indicate pressure-tap locations.)

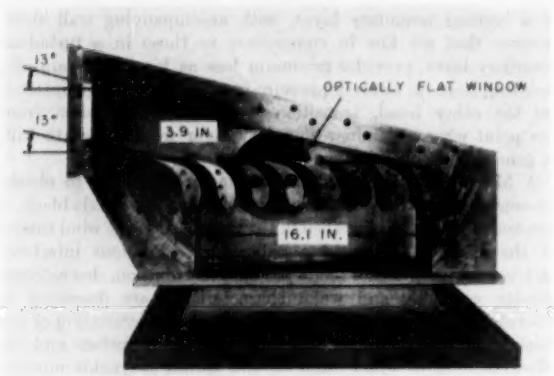

FIG. 2 TEST SECTION, SIDE PLATE REMOVED

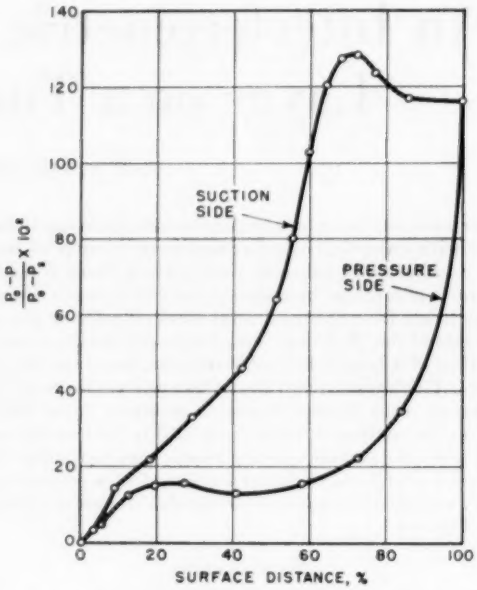

FIG. 3 TYPICAL PRESSURE DISTRIBUTION; M = 0.60

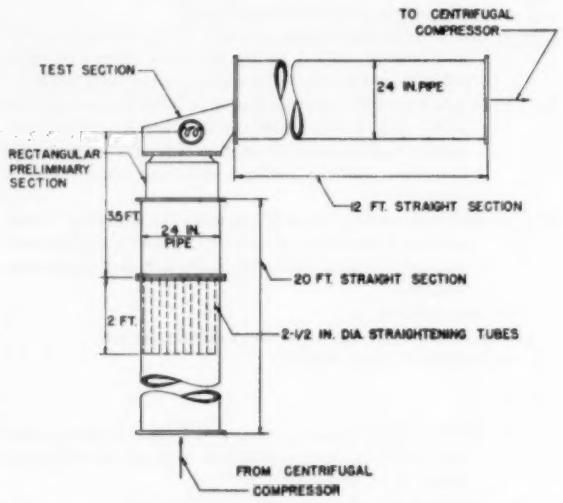

FIG. 4 SCHEMATIC DIAGRAM OF TEST-SECTION INSTALLATION IN WIND TUNNEL

drops to 0.30. The measured critical Reynolds number of 195,000 permits the classification of the wind tunnel as one of medium turbulence by comparison to aerodynamic wind tunnels in general (2). In order to obtain Reynolds numbers in the critical range, the sphere was located in a sheet-metal insert having a cross-sectional area nearly the same as that immediately ahead of the cascade. No contraction correction had to be made on the measured turbulence level, therefore, in order to give a result representative of the flow at inlet to the cascade.

APPLICATION OF INTERFEROMETER TO BOUNDARY-LAYER STUDY

A general description of the principle and method of application of the interferometer to the study of two-dimensional compressible flow is given in reference (1). Briefly, the interferometer enables quantitative measurement of the density variation throughout the flow field.

Observation of the boundary layer on the blade surface was accomplished by aligning the no-flow interference bands perpendicular to the surface. Thus, with flow over the surface, laminar and turbulent boundary layers could be distinguished readily by the shape that interference bands assumed in passing through the boundary layer. In the laminar layer there is a rounded velocity distribution somewhat resembling a parabola. Corresponding to this velocity distribution the density profile, and thus an interference band, takes on an S-shape. Furthermore, if the surface is adiabatic, the density gradient will be zero at the surface, and an interference band will intersect the surface at an angle of 90 deg. In the turbulent layer the velocity decreases from the free-stream value by only a small fraction until the laminar sublayer is reached, wherein it decreases rapidly to zero. Since the laminar sublayer is imperceptible in an interferometer photograph because of a diffraction band along the blade surface, the constant density lines in the turbulent layer, and again the interference bands, have only a slight curvature with no inflection. An interferometer photograph showing both types of boundary layer, together with an enlargement of one portion of the boundary

layer, appears in Fig. 5. The transition point can be distinguished in the photograph.

The distribution of density in the boundary layer was obtained from the measurement, at a given distance from the surface, of the displacement of an interference band from a straight-line continuation of the free-stream portion of the band. The ratio of this displacement to the no-flow band spacing gave the local band shift, which, in turn, could be related to the difference between free-stream and local density by straightforward computation (3).

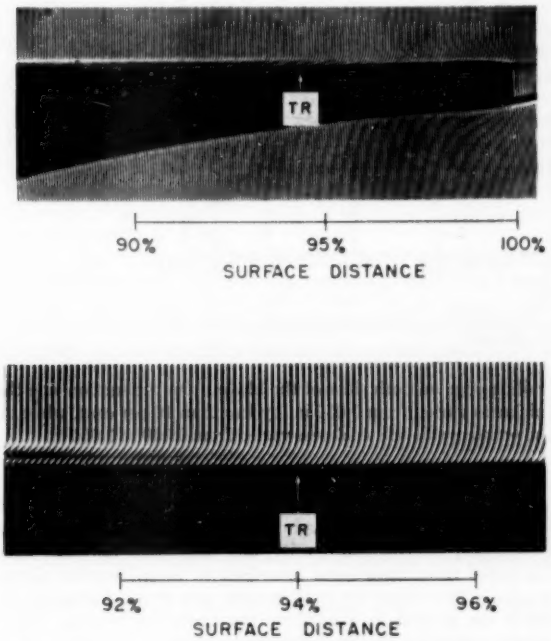

FIG. 5 INTERFEROMETER PHOTOGRAPHS OF BOUNDARY LAYER DOWNSTREAM FROM MINIMUM PRESSURE POINT ON SUCTION SIDE OF BLADE

Lower photograph is enlargement of part of upper photograph; M = 0.60, Re_l = 120,000. TR indicates transition.)

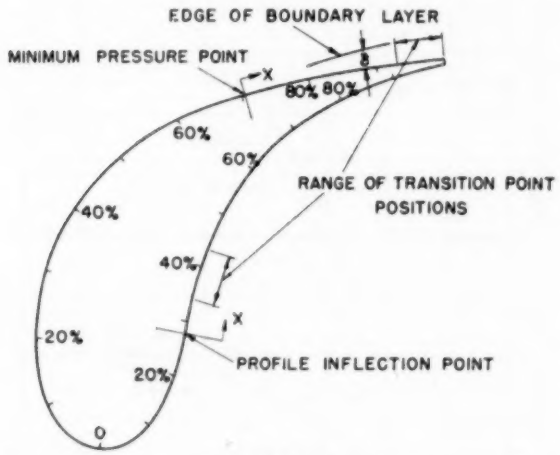

FIG. 6 OUTLINE DRAWING OF BLADE SHOWING TRANSITION-POINT POSITIONS

(Distance co-ordinates, x, are indicated. Distances along surface from leading to trailing edge: 5.45 in., suction side, 4.42 in., pressure side.)

GENERAL CHARACTERISTICS OF BOUNDARY LAYER ON NOZZLE BLADE

The general characteristics of the boundary layer can be summarized briefly. On the suction side ahead of the minimum pressure point and on the pressure side ahead of the point of inflection of the blade profile, shown in Fig. 1, the boundary layer was always too thin to be observed. Following these points the boundary layer, still laminar, suddenly thickened. The building up of the boundary layer downstream from the minimum pressure point and profile inflection point strongly resembled the growth of a boundary layer starting from the leading edge of a flat plate. The point of inflection of the profile coincides with the minimum pressure point located at approximately 27 per cent surface distance, shown in Fig. 3. The sudden thickening of the boundary layer on the pressure side of the blade, as well as on the suction side, was due therefore to an adverse pressure gradient.

Transition of the boundary layer from laminar to turbulent on the suction side of the blade moved from the trailing edge to approximately 0.4 in. upstream from the trailing edge with an increase in throat Reynolds number from 100,000 to 200,000. On the pressure side a transition moved from 0.7 in. to 0.3 in. downstream from the profile inflection point as the throat Reynolds number was increased from 80,000 to 250,000. The ranges of transition-point positions are shown in Fig. 6.

BOUNDARY-LAYER THICKNESS

The boundary-layer thickness at various parts of the blade was measured on interferometer photographs taken at a magnification ratio of 2.88. The outer edge of the boundary layer was taken to be the point where the interference bands first departed noticeably from forming straight lines. Since a diffraction band at the immediate edge of the blade obscured the location of the surface in the photographs, an estimate had to be made of the diffraction band width. Preliminary estimates used in obtaining the results presented here were found later to have given thicknesses approximately 10 per cent too small.

The thickness of the laminar boundary layer in the region downstream from 80 per cent surface distance on the suction side of the blade was found to vary from 0.015 to 0.030 in. over the experimental range. Because of the way in which the boundary layer in this region built up from the minimum pressure point, the distance from this point rather than from the leading edge of the blade appeared to be a controlling factor. Therefore, the ratio of boundary-layer thickness to this distance was plotted against a Reynolds number based on this same length, average values of free-stream density and velocity for the region downstream from the minimum pressure point, and the stagnation viscosity. The resulting data are plotted on logarithmic co-ordinates in Fig. 7 and are correlated by a straight line having the equation

$$\frac{\delta}{x} = 288\,(\mathrm{Re}_x)^{-0.748} \qquad [1]$$

As the measurements include several thicknesses along the blade at single downstream Mach numbers and throat Reynolds numbers as well as measurements at a variety of operating conditions, the correlation in Fig. 7 represents both the growth of the boundary layer along the blade and the effect of Reynolds number on the thickness at a given position on the blade. The four points at Mach number 0.75 that lie far below the line correspond to the lowest throat Reynolds number at which measurements were made, or 26,400. The throat Reynolds number thus appears to have a slight effect.

For the flat plate in incompressible flow, the ratio of laminar boundary-layer thickness to distance downstream from the lead-

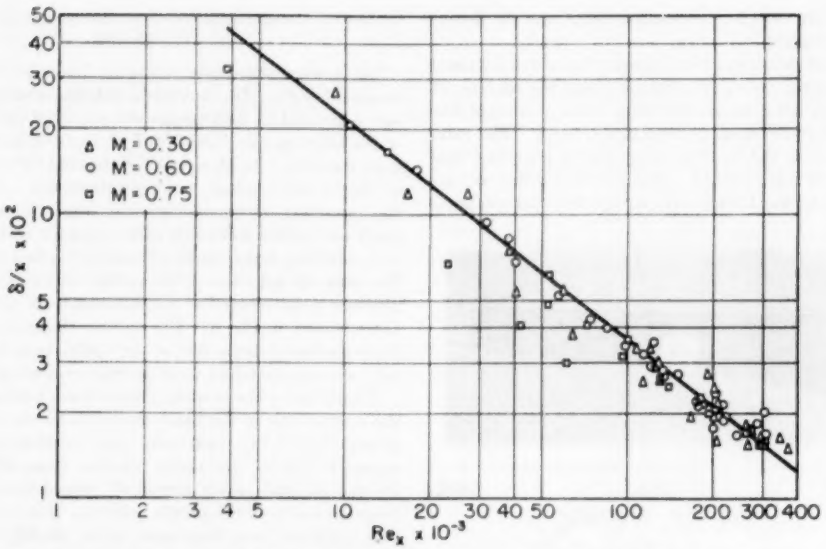

FIG. 7 LAMINAR BOUNDARY-LAYER THICKNESS DOWNSTREAM FROM MINIMUM PRESSURE POINT ON SUCTION SIDE OF BLADE

ing edge is a power function of the length Reynolds number (4). It is interesting to note that this type of functional relationship also applies to the laminar boundary layer downstream from the minimum pressure point on the suction side of the blade, in spite of an adverse pressure gradient over the first part of this region and in spite of a variation in Mach number from 0.3 to 0.75.

In view of the apparent controlling influence on the laminar boundary layer of the distance downstream from the minimum pressure point, the correlation indicated by Fig. 7 perhaps would find application to other designs of blading where the position of the minimum pressure point relative to the leading edge may be different. However, since boundary-layer behavior is influenced significantly by pressure gradients, application of the correlation in Fig. 7 would require dynamical similitude of the pressure gradient. Such similitude would be assured by comparable Pohlhausen numbers. The Pohlhausen number, a dimensionless modulus characterizing the ratio of the resisting force of the pressure gradient on the boundary layer to the average viscous shear in the boundary layer, is defined by

$$\lambda = -\frac{\delta^2}{\mu u_\infty}\frac{dp}{dx} \quad \ldots\ldots\ldots\ldots\ldots\ldots [2]$$

Values of this number ranged from negative 10 in the steep gradient region at approximately 80 per cent surface distance to zero at the trailing edge. In comparison, the Pohlhausen number for separation is negative 12.

The thickness of the laminar boundary layer downstream from the profile inflection point on the pressure side of the blade could not be correlated as in Fig. 7, for here the boundary layer would, while flowing downstream under some conditions, actually get thinner before reaching a transition. The apparent cause for this decrease in thickness was the beginning of the negative pressure gradient. The thickness of the laminar boundary layer just before transition on the pressure side was found to average 0.017 in. and to deviate from this figure by less than 30 per cent over the experimental range. The Pohlhausen number ahead of transition varied in this region from negative 7 to zero.

Turbulent boundary-layer thicknesses were measured at the trailing edge on both sides of the blade. On the suction side the thickness varied from 0.030 in. by less than 10 per cent, while on the pressure side the thickness varied from 0.030 to 0.050 in.

BOUNDARY-LAYER TRANSITION

Critical thickness Reynolds numbers, defined on the basis of the thickness of the laminar boundary layer at transition, local free-stream velocity and density, and stagnation viscosity, were computed from thicknesses measured on interferometer photographs. The results for both suction and pressure sides of the blade are plotted in Fig. 8 for the three downstream Mach numbers at which the nozzles were operated.

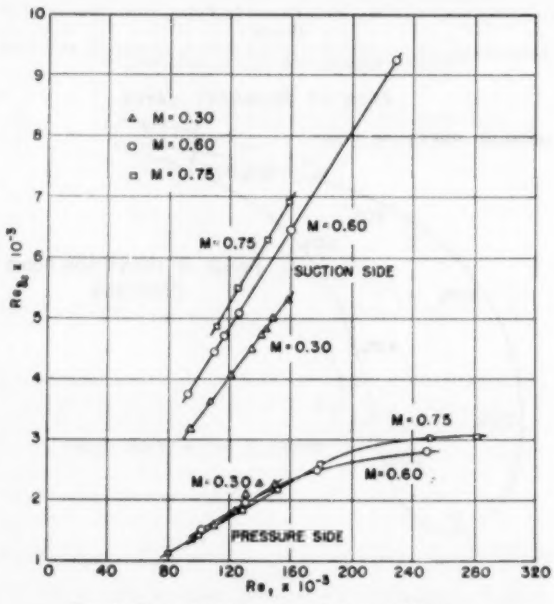

FIG. 8 THICKNESS CRITICAL REYNOLDS NUMBERS

The critical thickness Reynolds number on a flat plate with zero pressure gradient falls between 1650 and 5750, the actual value depending only on the turbulence level (5). Values obtained on airfoils fall in the same range (6). In contrast, critical thickness Reynolds numbers on the suction side of the blade vary from 3000 to over 9000 and appear as if they would go steadily higher with larger throat Reynolds numbers. On the pressure side of the blade, values varying from 1200 to almost 3100 lie in the same range as the flat-plate values. A possible upper limit of 3100 is indicated by the pressure-side data.

A constant value of critical Reynolds number based on momentum thickness is used frequently as a criterion for boundary-layer transition in the theoretical design of turbine and compressor blades. Since the momentum thickness is, to first approximation, one ninth of the boundary-layer thickness, the foregoing transition data result in critical momentum thickness Reynolds numbers varying from 350 to 1060 on the suction side and from 140 to 360 on the pressure side. The experimental results thus cast some doubt on the validity of using any one particular value of critical momentum thickness Reynolds number as a transition criterion.

The reason for the very strong dependence of thickness critical Reynolds number on throat Reynolds number indicated by Fig. 8 is not clear. That the turbulence level should change sufficiently over the range of throat Reynolds numbers to cause the resulting variation in critical thickness Reynolds number is not at all likely, for, at constant Mach number, the throat Reynolds number was varied by changing only the density level in the wind-tunnel circuit. Furthermore, to attribute the observed variations to a movement of the transition point from a region of one amount of pressure gradient to a region of another amount of pressure gradient does not seem possible, for with increase in throat Reynolds number the transition point moves from a region of zero pressure gradient to one of positive pressure gradient. The latter would be expected to act in the direction of decreasing the thickness critical Reynolds number (7). The only factor to which the increases in thickness critical Reynolds number can be attributed is the throat Reynolds number itself. It appears most likely that the effect of this variable is realized by a change in the excitation that causes turbulence, be it the wake, the secondary flow, or some other factor.

An increase in critical thickness Reynolds number with throat Reynolds number on the suction side of the blade can be explained, at least in part, if the significant excitation is assumed to arise from the turbulence of the secondary flow. Noticeable formation of secondary flow generally appears immediately downstream from a blade passage. The secondary-flow regions decrease in width as the throat Reynolds number is increased, and the strength at the center of the blade span of disturbances propagated from the turbulent secondary-flow regions can thereby be expected to diminish. Because the strength of a disturbance is dependent upon the distance of propagation, the values of thickness critical Reynolds number on the suction side may depend to some extent on the aspect ratio of the blade passage.

The principal turbulence-producing excitation on the pressure side of the blade is most likely the formation of three-dimensional vortices in the boundary layer caused by flow over a concave surface (8). According to reference (8), the thickness Reynolds number necessary for these vortices to cause transition, for a given radius of curvature of a concave surface, is inversely proportional to the square root of the boundary-layer thickness. Since the latter decreases with increasing throat Reynolds number, the trend shown in Fig. 8 appears.

The variations of transition point position with throat Reynolds number are shown in Figs. 9 and 10 for suction and pressure sides, respectively. The pressure side curve at $M = 0.30$ is peculiar in that the negative slope is continually increasing along this curve, while continually decreasing along the others. A drop in the two-dimensional nozzle efficiency was observed

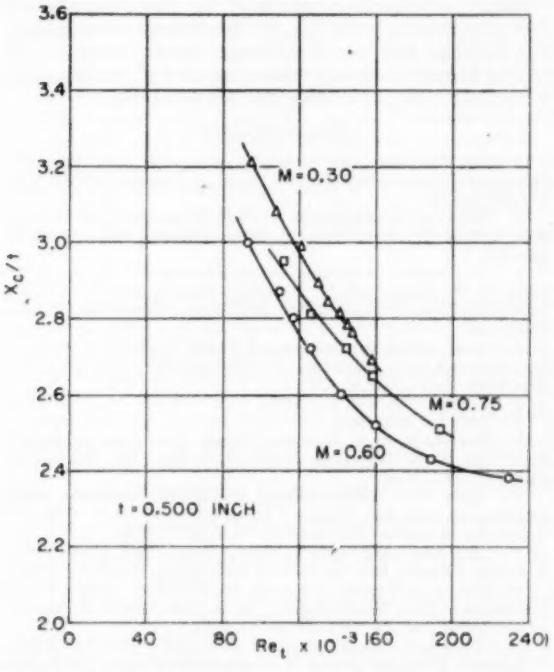

FIG. 9 TRANSITION-POINT POSITION, SUCTION SIDE OF BLADE

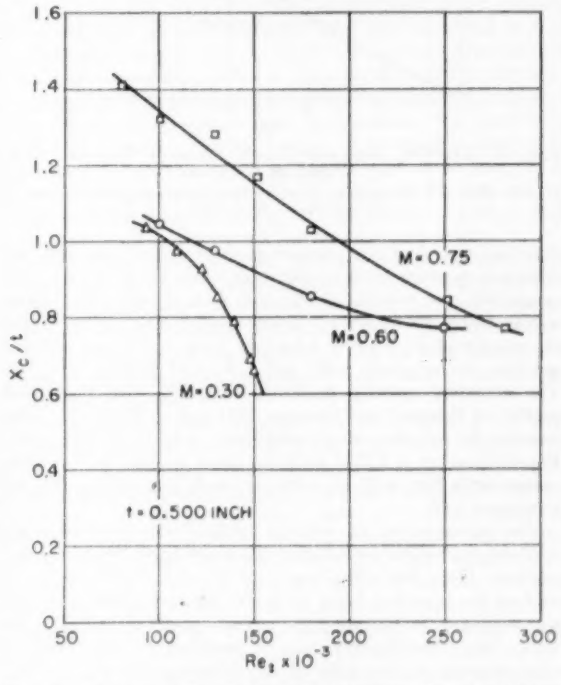

FIG. 10 TRANSITION-POINT POSITION, PRESSURE SIDE OF BLADE

previously at this same Mach number and throat Reynolds number and may well have been due to the continually increasing rate of forward motion of the transition point on the pressure side.

The transition points on the suction side of the blade were found to lie in a region of either small or zero pressure gradient. Specifically, the Pohlhausen number of the laminar boundary layer immediately ahead of transition varied from zero at the trailing edge to negative one with the transition point observed the farthest distance upstream. With continued increase in throat Reynolds number, the transition point would move toward continually steeper pressure gradients, and the curves of Fig. 8 might level out.

The foregoing transition data would be affected by turbulence level. Although the effect of increased turbulence would be a reduction in thickness Reynolds numbers at transition, the magnitude of the effect cannot be stated with any degree of assurance.

Laminar Velocity Profile

A laminar boundary-layer velocity profile, computed from the density profile measured on an interferometer photograph, is presented in Fig. 11. This particular velocity profile was obtained at a point of zero pressure gradient downstream from the minimum pressure point on the suction side of the blade. The computation of velocity distribution from density distribution was accomplished by using a theory developed by Crocco (9) for the compressible, laminar boundary layer with zero pressure gradient, an adiabatic wall, and a Prandtl number of 0.725. The measured velocity profile is compared with theoretical profiles of Brainerd and Emmons (10) and of Weil (11). The former is for flat-plate compressible flow, an adiabatic wall, and a Prandtl number of 0.733, while the latter is again for flat-plate compressible flow with an adiabatic wall, but with a Prandtl number of 1.00.

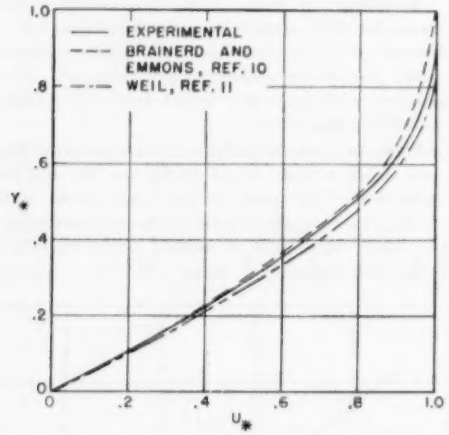

Fig. 11 Laminar Boundary-Layer Velocity Profile, Zero Pressure Gradient
(Profile measured downstream from minimum pressure point on suction side of blade; $M = 0.60$.)

The measurement of velocity profiles from interferometer photographs was hindered by the diffraction band adjacent to the surface. Since this diffraction band obscured the lower 20 per cent of the boundary-layer thickness, an extrapolation process was necessary for extending the velocity profile of Fig. 11 to the wall. The possible error thereby resulting in this profile is approximately on the order of the difference between the two theoretical curves of Fig. 11.

The conditions under which the laminar boundary layer on the blade developed up to the point at which the velocity profile in Fig. 11 was measured, differed greatly from the flow conditions on a flat plate. The good comparison with profiles computed for a flat plate indicate, therefore, that the previous history of a laminar boundary layer has no significant effect on the shape of the velocity profile.

Conclusions

The ratio of the thickness of the laminar boundary layer downstream from the minimum pressure point on the suction side of the blade to the distance downstream from this point was found to be a function of only a length Reynolds number based on this distance.

The thickness critical Reynolds number on both sides of the blade turned out to be a strong function of throat Reynolds number, whereas according to the traditional concept of boundary-layer behavior, the thickness critical Reynolds number is dependent upon turbulence level only. The experiments showed the Mach number to have negligible effect on transition.

The values of thickness critical Reynolds number on the suction side of the blade varied from 3000 to 9000, while on a flat plate or on an airfoil, values vary from 1650 to 5750. Owing to a possible effect on transition of secondary flow in the nozzle passage, suction-side values of thickness critical Reynolds number may be affected by aspect ratio.

The pressure-side-thickness critical Reynolds number varied from 1200 to 3100 and appeared to approach the latter value as an upper limit.

A laminar boundary-layer velocity profile measured near the trailing edge on the suction side of the blade, at a point of zero pressure gradient, compared well with profiles computed for a flat plate, showing previous history of the boundary-layer development to have no effect.

Acknowledgments

The author expresses gratitude to Mr. Earl Cole, now with North American Aviation, Inc., for his assistance in obtaining the data presented here, and to the Steam Turbine Division of the General Electric Company, Schenectady, N. Y., for sponsorship of the research project on which the data were taken.

Bibliography

1 "An Interferometric Investigation of the Flow Through a Cascade of Turbine Nozzle Blades," by C. R. Faulders, ASME Paper No. 52—SA-36.

2 "Modern Developments in Fluid Dynamics," by S. Goldstein, Oxford University Press, London, England, vol. 2, 1950, pp. 493–503.

3 "A Portable Mach-Zehnder Interferometer," by L. A. DeFrate, F. W. Barry, and D. Z. Bailey, Massachusetts Institute of Technology Guided Missiles Program, Meteor Report No. 51, February, 1950.

4 "Engineering Applications of Fluid Mechanics," by J. C. Hunsaker and B. G. Rightmire, McGraw-Hill Book Company, Inc., New York, N. Y., 1947, p. 188.

5 Reference (2), vol. 1, p. 326.

6 Ibid., vol. 2, p. 483.

7 "Investigation of Boundary Layer Transition on Concave Walls," by H. W. Liepmann, NACA ACR No. 4J28, Wartime Report No. W-87, 1945.

8 "Über eine dreidimensional Instabilität laminarer Grenzschichten an koncaven Wänden," by H. Görtler, Ges. d. Wiss. Göttingen, Nachr. an dem Mathematik, vol. 2, no. 1, 1940.

9 "The Laminar Boundary Layer in Gases," by L. Crocco, North American Aviation, Inc., Aerophysics Laboratory, Report CF-1038.

10 "Effect of Variable Viscosity on Boundary Layers, With a Discussion of Drag Measurements," by H. Brainerd and H. Emmons, Trans. ASME, vol. 64, 1942, pp. A-1 to A-6.

11 "Effects of Pressure Gradient on Stability and Skin Friction in Laminar Boundary Layers in Compressible Fluids," by H. Weil, General Electric Company Report No. R49A0533, April, 1950.

Discussion

C. C. Lin.[3] The author has provided us with very interesting and useful data regarding the boundary layer over the blades of turbine nozzles. It is interesting that he could correlate the boundary-layer thickness with the distance downstream of the point of minimum pressure. No convincing theoretical justification has yet been advanced for such a correlation, which is very useful, if its general validity can be established. It seems desirable to carry out an analysis based on conventional boundary-layer theory to explain all the phenomena found in the experiments of the author, and, in particular, to explore the extent of the generality of his formula for the boundary-layer thickness.

Charles Shulock.[4] The turbine designer welcomes this investigation into the growth of boundary layer over a turbine nozzle. The optical methods employed herein seem well suited to the study of the phenomenon, since the measuring instruments themselves introduce no disturbance to the flow. In addition, surveys can be extended over the entire passage, rather than being confined to or near the plane of the trailing edges.

However, precautions are still necessary. From Fig. 2 of the paper, it appears that the "optically flat window" forms one side wall of the cascade, and that the boundary layer would be photographed through this window. This side wall, and adjacent sections of the blade profile, would be subjected to boundary-layer growths quite different from that existent over the blade at mid-span. Is this disturbance eliminated by some feature of testing technique, or has it otherwise been shown of limited consequence?

The author correctly associates low shear stresses with a laminar boundary layer, and retarded separation with a turbulent boundary layer. Still undecided, however, is whether the corresponding "skin-friction" drag or "form" drag are the major source of losses in turbine blading. The relative importance of the two types of losses can vary widely with the detail design of each blade passage. In the present investigation, for instance, viscous losses appear prevalent. However, this could be changed by simply varying the passage solidity, or ratio of chord length to blade pitch. Therefore, the range of transition points indicated in Fig. 6 of the paper should be associated not with the nozzle profiles, themselves, but with the particular passage geometry which ensues when these nozzles are assembled into a cascade.

As a matter of interest, a pitch-axial width ratio of 0.72 was obtained by rough scaling Figs. 1 and 2. For comparison, optimum two-dimensional spacing for these same fluid angles, as deduced by O. Zweifel,[5] is at a pitch-width ratio of approximately 1.7.

J. C. Truman.[6] This paper represents a valuable contribution to the literature, both for readers who are interested in boundary-layer behavior, and those interested in interferometric techniques.

The conclusions which are drawn appear to be quite significant and to indicate that further work may be worthwhile. For example, the laminar boundary layer was observed to build up downstream from the minimum pressure point on the suction side, and from the blade-profile inflection point on the pressure side. It should be of value to investigate whether this also holds for blade profiles which differ considerably from the one studied here in respect to chordwise location of these points. Also, the dependence of δ/x on Re_x (using the nomenclature of the author) on the suction side of the blade should be investigated for several different blade profiles. As the author points out, a correlation between these quantities, under proper conditions of dynamical similitude, might be of value as a design criterion.

A comparison of the boundary-layer behavior, as determined from the present study, with that on a blade of the same profile mounted singly, rather than in cascade, also might be of interest. Such a comparison perhaps would not be of immediate value in the design of blades to be mounted in cascade. However, an indication might be gained as to whether the observed departures from the usual concepts of boundary-layer behavior may be in part due to interference effects between blades.

Author's Closure

The author extends his appreciation to Dr. Lin, Mr. Shulock, and Mr. Truman for their interesting and pertinent discussions.

Dr. Lin's comment on the desirability of theoretical justification of the experimental results is indeed appropriate. In addition to contributing to an understanding of the flow phenomena, such an analysis could well serve as an indication of the generality of the results.

In reply to Mr. Shulock's question regarding the effect of side-wall boundary layers on the interferometer data, the interference fringes are displaced in proportion to the integral of the density along the path of any particular light ray passing from one side wall to the other. Since the wall boundary layers in the experimental cascade occupied on the order of from 10 to 20 per cent of the span, the interferometer data measured primarily the two-dimensional flow over the central part of the span. Removal of the side-wall boundary layers would, in the author's estimation, have had no significant effect on the data.

Mr. Shulock is correct in stating that the transition-point range of Fig. 6 should be associated with the blade in the particular cascade in which it was tested, not with the blade alone. Actually, the results presented in the paper have been associated with the distribution of the pressure around the blade and the significant local pressure gradients, for it is the pressure distribution itself, along with whatever turbulence-producing excitation is present, that determines boundary-layer development. The pitch-width ratio is, in turn, a significant factor in the establishment of the pressure distribution. With too large a pitch-width ratio, for example, the pressure distribution necessary for the flow to follow the blade surface would involve excessive adverse pressure gradients, and boundary-layer separation would take place.

The author agrees with Mr. Truman that an investigation to determine the effect of different chordwise positions of the minimum pressure point and profile inflection point on boundary-layer development would be of great value. Until the results of such an investigation are available, in fact, no definite conclusions can be drawn regarding the range of application of the information presented here.

A question is raised regarding the dependence of boundary-layer behavior on the interference of neighboring blades in cascade. As mentioned earlier, the influence of multiple blades in cascade upon the boundary layer on a particular blade is effected by means of the pressure distribution that is established, the boundary layer then being a function of this pressure distribution. The determination of the boundary-layer behavior on a single blade would not seem to have any merit, as here the flow would certainly separate from the suction side long before reaching the trailing edge. The turbulence-producing excitation causing transition might be influenced by the presence and degree of proximity of adjacent blades, but probably to a minor degree.

[3] Professor of Mathematics, Massachusetts Institute of Technology, Cambridge, Mass.

[4] Development Department Engineer, Elliott Company, Jeannette, Pa. Jun. ASME.

[5] "The Spacing of Turbo-Machine Blading, Especially With Large Angular Deflection," by O. Zweifel, *Brown Boveri Review*, vol. 32, December, 1945, pp. 436–444.

[6] General Engineering Laboratory, General Electric Company, Schenectady, N. Y.

The Solubility of Oxygen in Water[1]

By L. M. ZOSS,[2] S. N. SUCIU,[3] AND W. L. SIBBITT[4]

The solubility of oxygen in water was measured at pressures of 1000, 1500, and 2000 psia and at temperatures from 32 to 625 F.

Introduction

THE increasing application of high temperatures and pressures has made a knowledge of the solubilities of compressed gases in water necessary for the purpose of engineering design.

A survey of the literature has revealed that data for the solubility of oxygen in water are meager. These investigations are summarized in Table 1.

TABLE 1 SOLUBILITIES STUDIES OF OXYGEN

Year	Author	Pressure range, in atm	Temperature range, deg F
1891.....	Winkler (5)	0–1	0–212
1904.....	Cassuto (6)	0–10.5	77
1909.....	Fox (5)	0–1	0–212
1931.....	Frolich, et al (7)	0–70	77
1950.....	Pray, et al (8)	6.8–27.2	77–650

This work is a continuation of the investigation previously reported (1).[5]

Experimental Apparatus and Procedure

The apparatus which was developed for the hydrogen and nitrogen-solubility studies was used for most of this investigation (1). It consisted of a high-pressure vessel with integral vapor and liquid sample chambers, heaters, and temperature controls, auxiliary pumps, and analytical equipment.

The sequence of operations follow: (*a*) The pressure vessel was evacuated, (*b*) charged with a known volume of water, (*c*) brought to a selected temperature level, (*d*) charged with gas (under conditions of constant total pressure, constant temperature, and continual agitation) until phase equilibrium was attained, (*e*) fastened in a vertical position until the vapor and liquid phases separated.

The liquid-sample chamber was then isolated and the sample expanded into the liquid phase-analysis apparatus to the final conditions of tap-water temperature and atmospheric pressure. The gas and liquid portions of the sample were brought into phase equilibrium and then each phase was measured. Corrections were applied to both measurements in order to account for the water vapor in the gas phase. The gas which remained dissolved in the water was negligible under all conditions of these experiments.

The solubility of the gas in the liquid phase was then calculated and expressed as cubic centimeters of gas (as measured at 0 C and 1 atm) per gram of water.

The vapor phase was analyzed by expanding the compressed gas and vapor mixture through a drying train, water-saturation chamber, and a wet-test gas meter. The sample chamber and tubing were then dried and thus the total amounts of gas and water in the vapor sample were determined. These measurements were not of sufficiently high accuracy to establish the effect of pressure upon the vapor pressure of water. The errors involved in the vapor-sample analysis were due partly to the corrosive nature of oxygen gas in the presence of water vapor.

The high-pressure vessel was attacked severely by the oxygen. The valve seats and valve stems were corroded rapidly. Another saturation vessel was constructed of stainless steel, Fig. 1. With a single-chamber saturation vessel it was necessary to use separate sample vessels. The use of separate sample vessels is not the best procedure, since it introduces additional sources of error.

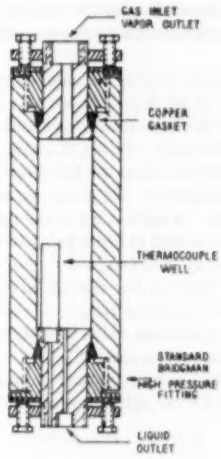

FIG. 1 NEW SATURATION VESSEL

A series of tests were made to evaluate the error in sampling. The error was not appreciable—somewhat less than ½ per cent.

Results

The data obtained are shown in Fig. 2. The effect of temperature upon the solubility is shown in Fig. 3 and the effect of pressure is shown in Fig. 4.

A limited amount of data was obtained on the vapor phase. However, these data did show that the vapor pressure of the compressed liquid phase (at constant temperature) was not a linear function of the total pressure.

The pressures shown in Fig. 2 are the total pressures of the system as measured with a gage. The "partial pressures" in Figs. 3 and 4 are ficticious values which were obtained by subtracting the saturation vapor pressure of water from the total pressure. The true vapor pressure of the water in the solution may have been greater or less than the saturation vapor pressure of pure water.

[1] The material contained herein was used by L. M. Zoss in partial fulfillment of the requirements for the PhD degree.

[2] Research Engineer, Taylor Instrument Company, Rochester, N. Y.; formerly, du Pont postgraduate fellow in mechanical engineering, Purdue University, Lafayette, Ind. Jun. ASME.

[3] Research Engineer, General Electric Company, Schenectady, N. Y.; formerly, Westinghouse research fellow in mechanical engineering, Purdue University. Jun. ASME.

[4] Professor of Mechanical Engineering, Purdue University. Jun. ASME.

[5] Numbers in parentheses refer to the Bibliography at the end of the paper.

Contributed by the Power Division and presented at the Spring Meeting, Columbus, Ohio, April 28–30, 1953, of THE AMERICAN SOCIETY OF MECHANICAL ENGINEERS.

NOTE: Statements and opinions advanced in papers are to be understood as individual expressions of their authors and not those of the Society. Manuscript received at ASME Headquarters, November 6, 1952. Paper No. 53—S-30.

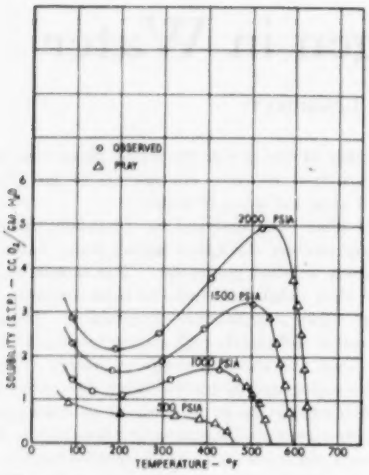

FIG. 2 SOLUBILITY OF OXYGEN IN WATER

DISCUSSION

Oxygen shows unusually high solubility at 32 F. The solubility decreases with increasing temperature in the range from 32 to 233 F and then increases with increasing temperature as shown in Figs. 3 and 4.

At room temperature where the gas solubility is small the fugacity of the water in the liquid phase may be calculated from Raoult's law. If the pressure change is small then Henry's law applies to the dissolved gas. When the solubilities of gases are measured at high pressures then the influence of pressure cannot be disregarded; consequently, the usual expression for Henry's law must be corrected. A knowledge of the partial molal volume of the dissolved gas is needed in order to make this correction (2). These data for oxygen are not available.

Fig. 4 shows that Henry's law cannot be used to predict the solubility over a wide pressure range. Actually, the solubility would increase to a maximum value and then decrease with increasing partial pressure of oxygen (3, 4).

At the present time we must depend completely upon experimental investigations for our solubility information.

ACKNOWLEDGMENTS

The authors are grateful to the E. I. du Pont de Nemours and Company, the Westinghouse Electric Corporation, and the Argonne National Laboratory for making this investigation possible.

BIBLIOGRAPHY

1 "A Study of the Nitrogen and Water and Hydrogen and Water Systems at Elevated Temperatures and Pressures," by Spiridon Suciu and W. L. Sibbitt, Argonne National Laboratory, ANL-4603, Part II, February 15, 1951, pp. 1–21.

2 "Thermodynamical Calculations of Solubilities of Nitrogen and Hydrogen in Water at High Pressures," by I. R. Krichevsky and J. S. Kasarnovsky, *Journal of the American Chemical Society*, vol. 57, 1935, pp. 2168–2171.

3 "The Existence of a Maximum in the Gas Solubility-Pressure Curve," by I. R. Krichevsky, *Journal of the American Chemical Society*, vol. 59, 1937, p. 596.

4 "Solubility of Nitrogen in Water Under High Pressures," by J. Basset and M. Dode, Comptes Rendus, vol. 203, 1936, p. 775.

5 "Solubilities of Inorganic and Metal Organic Compounds," by A. Seidell, D. Van Nostrand Company, Inc., New York, N. Y., vol. 1, 1940, third edition.

6 "Properties of Ordinary Water Substances," compiled by N. E. Dorsey, ACS Monograph Series, Reinhold Publishing Corporation, New York, N. Y., 1940.

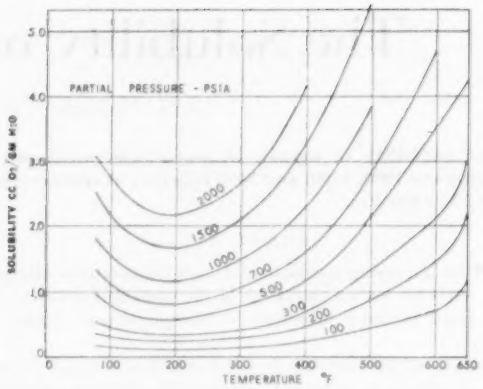

FIG. 3 SOLUBILITY OF OXYGEN IN WATER AS A FUNCTION OF TEMPERATURE

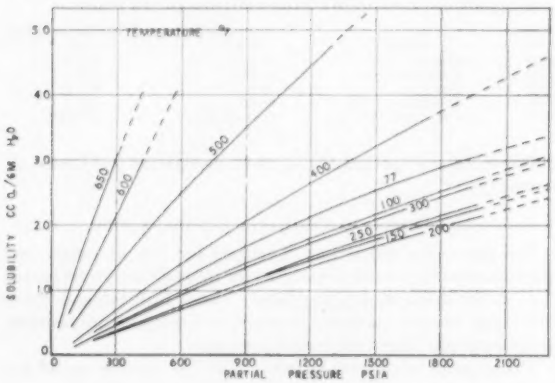

FIG. 4 SOLUBILITY OF OXYGEN IN WATER AS A FUNCTION OF PRESSURE

7 "Solubilities of Gases in Liquids at High Pressure," by K. Frolich, E. J. Tauch, J. J. Hogan, and A. A. Peer, *Industrial and Engineering Chemistry*, vol. 23, 1931, pp. 548–550.

8 "The Solubility of Hydrogen, Oxygen, Nitrogen and Helium in Water at Elevated Temperatures," by H. A. Pray, C. E. Schweichert, and B. H. Minnich, Battelle Memorial Institute, BMI–T–25, May 15, 1950, and *Industrial and Engineering Chemistry*, vol. 44, 1952, pp. 1146–1151.

Discussion

A. WATSON.[6] It is encouraging to see the authors' results—additional data to fill in the largely unchartered regions of high temperature and pressure. The writer is wondering about the details of the analytical procedures used. Even though they may appear elsewhere, a brief discussion should prove helpful. Along the same lines, what measures were taken to assure that at any one time only liquid or vapor phase was removed from the equilibrium chamber in sampling?

The authors speak of corrosion of the equipment with the use of oxygen under high pressure. Undoubtedly, some hydrogen was produced and this would affect the solubility of oxygen to some extent. Was the effect of hydrogen considered in finally evaluating the oxygen solubility? Perhaps this is what the authors had in mind when they state, "The errors involved in the vapor-sample analysis were due partly to the corrosive nature of oxygen gas in the presence of water vapor."

[6] Hall Laboratories, Inc., Pittsburgh, Pa.

The authors state, "The pressures shown in Fig. 2 are the total pressures of the system as measured with a gage." With a carbon-steel bomb, this would be a measure of water vapor, oxygen, and hydrogen. The writer believes different results would be secured in a noncorrosive environment, for example, with the stainless-steel chamber. Were the results obtained primarily with the stainless-steel saturation vessel?

The writer does not understand the statement, "At room temperature where the gas solubility is small the fugacity of the water in the liquid phase may be calculated from Raoult's law." At room temperature the gas solubility is relatively large.

The applicability of the authors' data and those of other investigators to many practical problems is undoubtedly great. However, it should be remembered that the values obtained represent equilibrium conditions with rather large partial pressures of oxygen. In a field with which the writer is familiar—boiler operation—only very small amounts of oxygen ordinarily can be present in the feedwater going to high-pressure, high-temperature units. Therefore, in the operating boiler proper, the partial pressure of oxygen in the steam must be quite low, and the solubility of oxygen in the water is, for all practical purposes, zero. This behavior is, of course, advantageous since corrosion is thereby minimized.

Authors' Closure

When the period of agitation was terminated (5 to 20 hr period) and the vessel fastened in a vertical position, a representative liquid sample could be obtained immediately. Consecutive liquid samples were duplicates.

A considerable period of time (10 to 20 min) was required for the liquid phase to drain from the wall of the vapor sample chamber. Usually a period of one to two hours was allowed for complete drainage.

The liquid-phase analysis apparatus consisted of a water-cooled burette, leveling bulbs, and a drying train. The sample was collected over mercury. The last traces of water vapor were obtained by passing dry gas through the sample chamber, the tubing, and through the drying train.

All of the high-pressure equipment was stainless steel. The type 347 steel was satisfactory but the 304 was severely corroded by the oxygen. The initial corrosion was very rapid. Hydrogen could not be detected after a few hours of operation at high temperatures.

The large errors involved in the vapor sample analysis resulted from leakage past corroded valve stems and seats. Drops of condensate were lost as a result of this leakage.

The relative solubility of oxygen in water is not small at room temperature; however, the mole fraction of oxygen in the water is very small. Therefore the liquid phase may be treated as a dilute solution. Thus, since the concentration of the solute is small, the fugacity of the solvent can be calculated by means of Raoult's law and the relationship of the fugacities of the components obtained from the Gibbs-Duhem equation.

Heat Transfer and Fluid Friction for Fully Developed Turbulent Flow of Air and Supercritical Water With Variable Fluid Properties

By R. G. DEISSLER,[1] CLEVELAND, OHIO

A previous analysis for fully developed turbulent flow and heat transfer in smooth tubes with variable fluid properties for a Prandtl number of one is generalized in order to make it applicable to air and supercritical water. Calculated velocity and temperature distributions as well as relations among Nusselt number, Reynolds number, and friction factor for both air and supercritical water with variable fluid properties are presented. Experimental local heat-transfer coefficients, friction factors, and velocity and temperature distributions, which were measured for air flowing turbulently in a smooth tube with heat transfer at large temperature differences, are included and compared with the analysis. Good agreement between analytical and experimental results was obtained for Reynolds numbers above 15,000.

Nomenclature

The following nomenclature is used in the paper:

c_p = specific heat of fluid at constant pressure (Btu/lb deg F)
c_{p_0} = specific heat of fluid at constant pressure at wall (Btu/lb deg F)
C, C_1 = constants of integration
d = exponent, the value for which depends on variation of viscosity of fluid with temperature
D = inside diameter of tube, ft
e = base of natural logarithms
g = acceleration due to gravity (32.2 ft/sec^2)
h = heat-transfer coefficient (Btu/sec-ft^2-deg F)
k = thermal conductivity of fluid (Btu-ft/sec-ft^2-deg F)
k_0 = thermal conductivity of fluid at wall (Btu-ft/sec-ft^2-deg F)
k_b, k_x = thermal conductivity of fluid evaluated at t_b, t_x, respectively (Btu-ft/sec-ft^2-deg F)
κ = von Kármán constant
n = const
q = total rate of heat transfer toward tube center per unit area, Btu/(sec-ft^2)
q_0 = total rate of heat transfer at wall toward tube center per unit area, Btu/(sec-ft^2)
r = radius, distance from tube axis, ft
r_0 = inside tube radius, ft
t = absolute static temperature, deg R
t_b = bulk or average static temperature of fluid at cross section of tube, deg R
$t_{0.4}$ = $0.4(t_0 - t_b) + t_b$, reference temperature, deg R
t_x = $x(t_0 - t_b) + t_b$, reference temperature, deg R
t_0 = absolute wall temperature, deg R
u = velocity parallel to axis of tube, fps
u_b = bulk or average velocity at cross section of tube, fps
x = quantity defining t_x
y = distance from tube wall, ft
ϵ = coefficient of eddy diffusivity for momentum, sq ft/sec
ϵ_h = coefficient of eddy diffusivity for heat, sq ft/sec
ρ = mass density (lb-sec^2/ft^4)
ρ_0 = mass density of fluid at wall (lb-sec^2/ft^4)
ρ_b = bulk or average density at cross section of tube (lb-sec^2/ft^4)
$\rho_{0.4}$, ρ_x = density of fluid evaluated at $t_{0.4}$, t_x, respectively (lb-sec^2/ft^4)
μ = absolute viscosity of fluid (lb-sec/sq ft)
μ_b = absolute viscosity of fluid evaluated at t_b (lb-sec/sq ft)
μ_0 = absolute viscosity of fluid at wall (lb-sec/sq ft)
$\mu_{0.4}$, μ_x = absolute viscosity of fluid evaluated at $t_{0.4}$, t_x, respectively (lb-sec/sq ft)
τ = shear stress in fluid, psf
τ_0 = shear stress in fluid at the wall, psf

Dimensionless groups

$\alpha \equiv \epsilon_h/\epsilon$

$\beta \equiv \dfrac{q_0\sqrt{\tau_0/\rho_0}}{c_{p_0}g\tau_0 t_0}$ = heat-transfer parameter

$f \equiv \dfrac{2\tau_0}{\rho u_b^2} = -\dfrac{D\,\dfrac{dp}{dx_{fr}}}{2\rho u_b^3}$ = friction factor

$f_b \equiv \dfrac{2\tau_0}{\rho_b u_b^2}$ = friction factor with density evaluated at t_b

$f_{0.4}$, f_x = friction factor with density evaluated at $t_{0.4}, t_x$, respectively

$\mathrm{Nu} \equiv hD/k$ = Nusselt number

$\mathrm{Nu}_b \equiv hD/k_b$ = Nusselt number with thermal conductivity evaluated at t_b

Nu_0 = Nusselt number with thermal conductivity evaluated at t_0

$\mathrm{Nu}_{0.4}$, Nu_x = Nusselt number with thermal conductivity evaluated at $t_{0.4}$, t_x, respectively

$\mathrm{Pr}_0 \equiv c_{p_0}\mu_0 g/k_0$ = Prandtl number with properties evaluated at wall

---

[1] Research Engineer, NACA, Lewis Flight Propulsion Laboratory. Jun. ASME.

Contributed by the Heat Transfer Division and presented at the Spring Meeting, Columbus, Ohio, April 28–30, 1953, of The American Society of Mechanical Engineers.

Note: Statements and opinions advanced in papers are to be understood as individual expressions of their authors and not those of the Society. Manuscript received at ASME Headquarters, July 16, 1952. Paper No. 53—S-41.

$\mathrm{Re}_b \equiv \rho_b u_b D/\mu_b$ = Reynolds number with density and viscosity evaluated at t_b

Re_0 = Reynolds number with density and viscosity evaluated at t_0

$\mathrm{Re}_{0.4}$, Re_x = Reynolds number with density and viscosity evaluated at $t_{0.4}$, t_x, respectively

$r_0^+ \equiv \dfrac{\sqrt{\tau_0/\rho_0}}{\mu_0/\rho_0} r_0$ = tube radius parameter

$t^+ \equiv \dfrac{(t_0 - t)c_{p_0}g\tau_0}{q_0\sqrt{\tau_0/\rho_0}} = \dfrac{1 - t/t_0}{\beta}$ = static temperature parameter

t_1^+ = value of t^+ at y_1^+

$t_b^+ \equiv \dfrac{1}{\beta}\left(1 - \dfrac{t_b}{t_0}\right)$ = static bulk-temperature parameter

$u^+ \equiv \dfrac{u}{\sqrt{\tau_0/\rho_0}}$ = velocity parameter

u_1^+ = value of u^+ at y_1^+

$u_b^+ \equiv \dfrac{u_b}{\sqrt{\tau_0/\rho_0}}$ = bulk-velocity parameter

$v = du^+/dy^+$

v_1 = value of v at y_1^+

$y^+ \equiv \dfrac{\sqrt{\tau_0/\rho_0}}{\mu_0/\rho_0} y$ = wall-distance parameter

y_1^+ = value of y^+ at intersection of curves for flow close to wall and a distance from wall

Introduction

Current interest in heat transfer between fluids and surfaces at very high fluxes has indicated a need for determining the effect of the variation of fluid properties across the stream on the heat-transfer and fluid-friction processes. The fact that the variation of fluid properties due to temperature variation has an effect on these processes has been recognized in reference (1).[2]

The material presented in this paper is a continuation of the work described in reference (2). In reference (2) some of the results of an analytical and experimental heat-transfer investigation made at the NACA Lewis Flight Propulsion Laboratory were given. An analysis was made for predicting heat transfer and fluid friction for fully developed turbulent flow with variable fluid properties in a smooth tube for a Prandtl number of 1. Velocity and temperature distributions were measured for turbulent flow without heat transfer in order to evaluate the constants appearing in the analysis.

In the present paper the previous analysis is generalized in order to make it applicable to air, which has a Prandtl slightly less than 1. In order to verify the analysis, local heat-transfer coefficients, friction factors, and velocity and temperature distributions were measured for air flowing turbulently with high rates of heat transfer in a smooth tube. The analysis also is applied to supercritical water because of current technical interest in the use of supercritical water as a coolant and because of the very large variation with temperature of the physical properties of supercritical water.

Basic Equations

For obtaining velocities and temperatures in the tube as functions of the distance from the wall, the differential equations for shear stress and heat transfer are often written in the following form

$$\tau = \mu\, du/dy + \rho\epsilon\, du/dy \quad [1]$$

$$q = -k\, dt/dy - \rho g\, c_p\, \epsilon_h\, dt/dy \quad [2]$$

where ϵ and ϵ_h are known as the coefficients of eddy diffusivity for momentum and heat transfer, the values for which are dependent upon the amount and kind of turbulent mixing at a point. Equations [1] and [2] can be considered as definitions of ϵ and ϵ_h. When written in dimensionless form, Equations [1] and [2] become

$$\frac{\tau}{\tau_0} = \frac{\mu}{\mu_0}\frac{du^+}{dy^+} + \frac{\rho}{\rho_0}\frac{\epsilon}{\mu_0/\rho_0}\frac{du^+}{dy^+} \quad [3]$$

and

$$\frac{q}{q_0} = \left(\frac{k}{k_0}\frac{1}{\mathrm{Pr}_0} + \frac{\rho}{\rho_0}\frac{c_p}{c_{p_0}}\alpha\frac{\epsilon}{\mu_0/\rho_0}\right)\frac{dt^+}{dy^+} \quad [4]$$

where the subscripts 0 refer to values at the wall, and the dimensionless quantities are defined in the Nomenclature.

Expressions for Eddy Diffusivity

In order to make practical use of Equations [3] and [4], the eddy diffusivity ϵ must be evaluated for each portion of the flow.

For the region at a distance from the wall the most reasonable expression for ϵ available at present is the similarity expression of von Kármán (3)

$$\epsilon = \kappa^2 \frac{(du/dy)^3}{(d^2u/dy^2)^2} \quad [5]$$

In dimensionless form, Equation [5] becomes

$$\frac{\epsilon}{\mu_0/\rho_0} = \kappa^2 \frac{(du^+/dy^+)^3}{(d^2u^+/dy^{+2})^2} \quad [6]$$

Equation [5] is obtained readily from dimensional analysis by assuming that the mechanism for turbulent transfer at a point depends only on the velocities in the vicinity of the point relative to the velocity at the point and is independent of the velocity relative to the wall u, the distance from the wall y, and the properties of the fluid, μ, ρ, etc. Equation [5] has been verified experimentally in references (4) and (5) for flow without heat transfer for the region at a distance from the wall. It appears to be applicable also to flow with heat transfer with variable fluid properties inasmuch as the radial variation of properties should not affect ϵ when the property values themselves do not affect it.

In the region close to the wall, Equation [5] cannot apply because the turbulent transfer must approach zero at the wall and u becomes very nearly a linear function of y. The denominator in Equation [5] therefore approaches zero, giving a very large value of ϵ at the wall where it should be zero. It appears that the effects of the velocity relative to the wall u and the distance from the wall y cannot be neglected in the region close to the wall. Inasmuch as the second derivative approaches zero and the first derivative approaches the value u/y in the vicinity of the wall, ϵ is considered, as a first approximation, to be a function only of u and y for the region close to the wall, or

$$\epsilon = n^2 uy \quad [7]$$

In dimensionless form this equation becomes

$$\frac{\epsilon}{\mu_0/\rho_0} = n^2 u^+ y^+ \quad [8]$$

[2] Numbers in parentheses refer to the Bibliography at the end of the paper.

Equation [8] has been verified experimentally in reference (4) for flow without heat transfer for the region close to the wall. In this expression for flow close to the wall the effect of kinematic viscosity μ/ρ on ϵ has been neglected. A preliminary investigation (not reported herein) indicates that the effect of μ/ρ close to the wall becomes important at high Prandtl numbers.

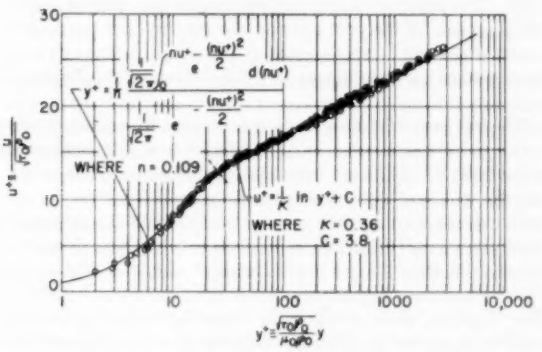

FIG. 1 GENERALIZED VELOCITY DISTRIBUTION FOR FULLY DEVELOPED ADIABATIC TURBULENT FLOW IN SMOOTH TUBES
(Reynolds-number range for data, 8000 to 200,000.)

Fig. 1, which is taken from reference (2), gives a comparison between equations for constant fluid properties derived by using Expressions [6] and [8] and experimental data. It is seen that the equation for flow close to the wall agrees with the data for $y^+ < 26$ and the equation for flow at a distance from the wall agrees with the data for $y^+ > 26$. The values of the constants in the equations are $n = 0.109$ and $\kappa = 0.36$ as determined from the experimental data. These values will be used for flow with variable fluid properties.

ANALYSIS FOR FLOW OF AIR IN SMOOTH TUBES

Assumptions. The following assumptions are made in addition to the assumption concerning the expressions for the eddy diffusivity (Equations [6] and [8]):

1 The eddy diffusivities for momentum ϵ and heat transfer ϵ_h are equal, or $\alpha = 1$. Previous analyses for flow in tubes based on this assumption yielded heat-transfer coefficients that agree with experiment (6). At low Reynolds or Peclet numbers (Pe = Re Pr), α appears to be a function of Peclet number (7) but for Reynolds numbers above 15,000 α is nearly constant.

2 The variations across the tube of the shear stress τ and the heat transfer per unit area q have a negligible effect on the velocity and temperature distributions. The effect of these variations will be investigated in the Appendix and in the section Predicted Effect of Variation of Shear Stress and Heat Transfer Across Tube.

3 The molecular shear-stress and heat-transfer terms in Equations [3] and [4] can be neglected in the region at a distance from the wall. The effect of these terms also will be investigated in the Appendix and in the section Predicted Effect of Molecular Shear Stress and Heat Transfer in Region at a Distance From Wall.

4 The static pressure can be considered constant across the tube.

5 The Prandtl number and specific heat can be considered constant with temperature variation. The variations with temperature of the specific heat and Prandtl number are of a lower order of magnitude than the variations of viscosity, thermal conductivity, and density.

Velocity and Temperature Distributions. For obtaining the velocity and temperature distributions close to a smooth wall the expression for ϵ from Equation [8] is substituted into Equations [3] and [4] to give

$$1 = \left(\frac{\mu}{\mu_0} + \frac{\rho}{\rho_0} n^2 u^+ y^+\right) \frac{du^+}{dy^+} \quad [9]$$

and

$$1 = \left(\frac{k}{k_0}\frac{1}{\mathrm{Pr}_0} + \frac{\rho}{\rho_0} n^2 u^+ y^+\right) \frac{dt^+}{dy^+} \quad [10]$$

where assumptions 1, 2, and 5 have been used.

From viscosity data it is found that μ/μ_0 can be represented approximately by $(t/t_0)^d$, and from the assumption of constant Prandtl number and specific heat this also is equal to k/k_0. From the assumption of constant static pressure and the perfect gas law, ρ/ρ_0 can be replaced by t_0/t. From the definitions of β and t^+, $t/t_0 = 1 - \beta t^+$. Equations [9] and [10] then become

$$1 = \left[(1 - \beta t^+)^d + \frac{1}{1 - \beta t^+} n^2 u^+ y^+\right] \frac{du^+}{dy^+} \quad [11]$$

and

$$1 = \left[\frac{(1 - \beta t^+)^d}{\mathrm{Pr}_0} + \frac{1}{1 - \beta t^+} n^2 u^+ y^+\right] \frac{dt^+}{dy^+} \quad [12]$$

Equations [11] and [12] can be written in integral form as

$$u^+ = \int_0^{y^+} \frac{dy^+}{(1 - \beta t^+)^d + \dfrac{n^2 u^+ y^+}{1 - \beta t^+}} \quad [13]$$

and

$$t^+ = \int_0^{y^+} \frac{dy^+}{\dfrac{(1 - \beta t^+)^d}{\mathrm{Pr}_0} + \dfrac{n^2 u^+ y^+}{1 - \beta t^+}} \quad [14]$$

Equations [13] and [14] can be solved simultaneously by iteration; that is, assumed relations between u^+ and y^+ and t^+ and y^+ are substituted into the right sides of the equations and the new values of u^+ and t^+ are calculated by numerical integration. These new values are then substituted into the right sides of the equations and the process is repeated until the values of u^+ and t^+ do not change appreciably. Equations [13] and [14] give the relations among u^+, t^+, and y^+ for various values of the heat-transfer parameter β for flow close to the wall.

For the region at a distance from a wall the expression for ϵ from Equation [6] is substituted into Equations [3] and [4] to give

$$1 = \frac{\rho}{\rho_0} \kappa^2 \frac{(du^+/dy^+)^3}{(d^2u^+/dy^{+2})^2} \frac{du^+}{dy^+} \quad [15]$$

and

$$1 = \frac{\rho}{\rho_0} \kappa^2 \frac{(du^+/dy^+)^3}{(d^2u^+/dy^{+2})^2} \frac{dt^+}{dy^+} \quad [16]$$

where assumptions 1, 2, and 3 have been used. Dividing Equation [15] by Equation [16] and integrating result in

$$t^+ - t_1^+ = u^+ - u_1^+ \quad [17]$$

where t_1^+ and u_1^+ are the values of t^+ and u^+ at y_1^+, which is the lowest value of y^+ for which Equations [15] and [16] apply. Then

$$\frac{t}{t_0} = 1 - (u^+ - u_1^+ + t_1^+)\beta \quad [18]$$

or, from the assumption of constant static pressure and the perfect-gas law

$$\frac{\rho}{\rho_0} = \frac{1}{1 - (u^+ - u_1^+ + t_1^+)\beta} \quad \ldots\ldots [19]$$

Substitution of Equation [19] in Equation [15] and one integration result in

$$C_1\beta \frac{du^+}{dy^+} = -e^{\frac{2\kappa}{\beta}\sqrt{1 - \beta(u^+ - u_1^+ + t_1^+)}} \quad \ldots\ldots [20]$$

where the negative sign was selected on taking the square root in order to make κ positive. Integration of Equation [20] gives

$$y^+ = -\frac{C_1\beta^2}{2\kappa^2} e^{-\frac{2\kappa}{\beta}\sqrt{1 - \beta(u^+ - u_1^+ + t_1^+)}} \left[\frac{2\kappa}{\beta}\sqrt{1 - \beta(u^+ - u_1^+ + t_1^+)} + 1\right] + C \quad \ldots [21]$$

As the wall is approached the velocity gradient becomes very large compared with that at a distance from the wall so that dy^+/du^+ approaches zero as y^+ approaches zero. If dy^+/du^+ is substituted from Equation [20] into Equation [21] and dy^+/du^+ is set equal to zero when y^+ and $u^+ = 0$, $C = 0$. (In the section Predicted Effect of Molecular Shear Stress, ... C is obtained by matching the slopes at the intersection of the equations for flow close to and far from the wall rather than by the foregoing procedure.) To determine C_1, set $u^+ = u_1^+$ when $y^+ = y_1^+$. Then

$$y^+ = \frac{y_1^+ e^{-\frac{2\kappa}{\beta}\sqrt{1 - \beta(u^+ - u_1^+ + t_1^+)}} \left[\frac{2\kappa}{\beta}\sqrt{1 - \beta(u^+ - u_1^+ + t_1^+)} + 1\right]}{e^{-\frac{2\kappa}{\beta}\sqrt{1 - \beta t_1^+}} \left(\frac{2\kappa}{\beta}\sqrt{1 - \beta t_1^+} + 1\right)} \quad \ldots\ldots [22]$$

Equation [22] gives the relation between u^+ and y^+ for various values of β for flow at a distance from the wall. The parameter t^+ and thus the temperature distribution can be calculated from Equation [17].

For a Prandtl number of 1, $t_1^+ = u_1^+$ and Equation [22] reduces to the equation for a Prandtl number of 1 given in reference (2). For $\beta = 0$, Equation [22] is indeterminate. For this case ρ/ρ_0 in Equation [15] is set equal to 1 before integrating and the well-known logarithmic equation is obtained

$$u^+ = \frac{1}{\kappa} \log_e y^+ + C$$

Calculated temperature and velocity distributions for a Prandtl number of 0.73 are plotted in Figs. 2 and 3. The values for the constants ($n = 0.109$ and $\kappa = 0.36$) which were found from the experimental data for flow without heat transfer are used for plotting the equations. The same ranges of applicability for the equations close to and far from the wall are also used ($y^+ < 26$ for flow close to the wall and $y^+ > 26$ for flow at a distance from the wall). The effect of various assumptions for the range of applicability of each of the equations on the velocity and temperature distributions will be investigated in the section Effect of Various Assumptions for the Ranges of Applicability of the Equations, ...

The exponent d in the equations was found from viscosity data for air to have an average value of 0.68 for temperatures between 0 and 2000 F. Although this value was obtained specifically for air, the values of d for most common gases do not vary greatly from this value, so that the curves plotted should be applicable to most gases with Prandtl numbers close to 0.73. The plots of the equations in Figs. 2 and 3 indicate that t^+ and u^+ are not equal as was the case for a Prandtl number of 1, reference (2). Both profiles, however, show trends with increasing values of the heat-transfer parameter β which are similar to those for a Prandtl number of 1.

Nusselt Number, Reynolds Number, and Friction Factor. The bulk temperature, as used in this paper, is given by

$$t_b = \frac{\int_0^{r_0} tc_p\rho u(r_0 - y)dy}{\int_0^{r_0} c_p\rho u(r_0 - y)dy} \quad \ldots\ldots [23]$$

In dimensionless form this becomes

$$t_b^+ = \frac{\int_0^{r_0^+} t^+(c_p/c_{p_0})(\rho/\rho_0)u^+(r_0^+ - y^+)dy^+}{\int_0^{r_0^+} (c_p/c_{p_0})(\rho/\rho_0)u^+(r_0^+ - y^+)dy^+} \quad \ldots\ldots [24]$$

For air, $c_p/c_{p_0} = 1$ and $\rho/\rho_0 = 1/(1 - \beta t^+)$. By using the definitions of the various quantities involved, the following expressions are obtained for Nu_0, Re_0, and f_0

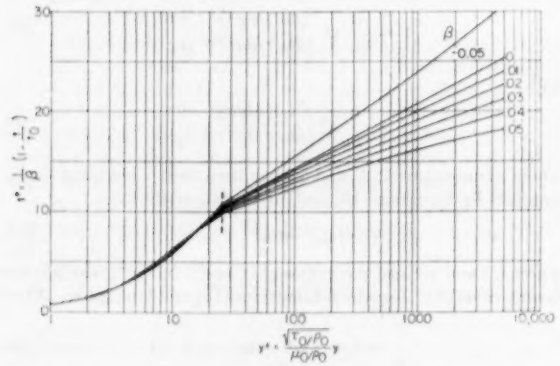

FIG. 2 PREDICTED GENERALIZED TEMPERATURE DISTRIBUTIONS FOR FLOW OF GASES WITH HEAT TRANSFER
(Prandtl number = 0.73.)

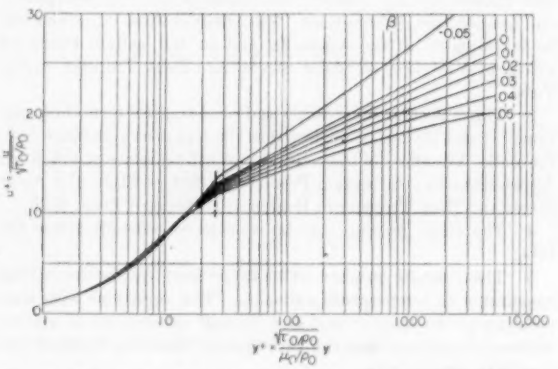

FIG. 3 PREDICTED GENERALIZED VELOCITY DISTRIBUTIONS FOR FLOW OF GASES WITH HEAT TRANSFER
(Prandtl number = 0.73.)

$$Nu_0 = 2r_0^+Pr_0/t_b^+ \quad [25]$$

$$Re_0 = 2u_b^+r_0^+ \quad [26]$$

$$f_i = 2/u_b^{+2} \quad [27]$$

where

$$u_b^+ = \frac{2}{r_0^{+2}}\int_0^{r_0^+} u^+(r_0^+ - y^+)dy^+ \quad [28]$$

Nusselt numbers, Reynolds numbers, and friction factors with the properties in their definitions evaluated at some temperature other than the wall temperature may be obtained readily by using the relation, $t_b/t_0 = 1 - \beta t_b^+$.

Comparison of Analytical and Experimental Results for Air. In order to verify the foregoing analysis for air, local heat-transfer coefficients and friction factors, as well as velocity and temperature distributions, were measured at the Lewis laboratory for air flowing turbulently in a smooth electrically heated tube having an inside diameter of 0.87 in. and a length of 87 in. The tests were made near the exit of the tube where the flow was fully developed. The apparatus and test procedure are described fully in reference (8).

Although the analysis for air was carried out for the case where the compressibility effects resulting from high velocities can be neglected, it is shown in reference (9) that the same correlations apply, in general, to flow at high subsonic velocities. For the latter case, except for small temperature differences, it is necessary only to replace the static bulk temperature by the total bulk temperature in the definition of the heat-transfer coefficient h. The experimental data, some of which were obtained at high velocities, therefore can be compared with the analysis.

In Figs. 4, 5, and 6 experimental and predicted Nusselt numbers for air (Pr = 0.73) are plotted against Reynolds number for various values of the heat-transfer parameter β. In Fig. 4 the physical properties including density, in the Reynolds number and Nusselt number, are evaluated at the static bulk temperature. Both the experimental and predicted Nusselt numbers at a given Reynolds number show a decrease with increasing values of β or of ratio of wall to bulk temperature.

In Fig. 5 the physical properties, including density, in the Reynolds and Nusselt numbers are evaluated at the wall temperature. For this case both the experimental and predicted Nusselt numbers at a given Reynolds number increase with increasing β.

In Fig. 6 the properties in the Nusselt and Reynolds numbers are evaluated at $t_{0.4}$, which is slightly closer to the bulk temperature than the average of the wall and bulk temperatures. It is observed that the effect of β or of ratio of wall to bulk temperature on both the experimental and predicted Nusselt numbers is practically eliminated when the properties are evaluated at this temperature. The data follow the predicted line very closely for Reynolds numbers above 15,000. For low Reynolds numbers the separation of the data from the predicted line is probably caused by a partial transition from turbulent to laminar heat transfer, which was not considered in the analysis. The same trend at low Reynolds numbers was observed in the data for average heat-transfer coefficients given in reference (10). It is shown in reference (7) that this may be an effect of Peclet number on α.

It should be emphasized that, in order for the foregoing correlation to hold, the same assumptions for the variation of physical properties with temperature must be made for calculating the experimental results as were made in the analysis: Constant specific heat and both thermal conductivity and viscosity proportional to $t^{0.68}$. If the conductivity had been assumed proportional to $t^{0.81}$ as sometimes given in the literature, the effects of ratio of wall to bulk temperature on the Nusselt-number correlation would have been eliminated by evaluating the fluid properties at a tem-

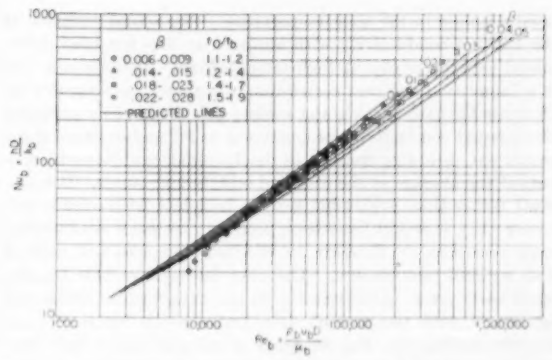

FIG. 4 VARIATION OF NUSSELT NUMBER WITH REYNOLDS NUMBER FOR FLOW OF AIR WITH HEAT ADDITION AND PROPERTIES EVALUATED AT STATIC BULK TEMPERATURE
(Prandtl number = 0.73.)

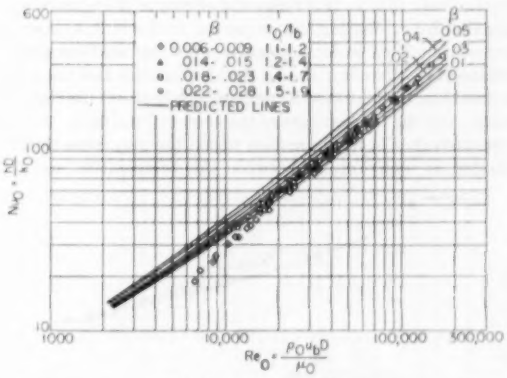

FIG. 5 VARIATION OF NUSSELT NUMBER WITH REYNOLDS NUMBER FOR FLOW OF AIR WITH HEAT ADDITION AND PROPERTIES EVALUATED AT TUBE-WALL TEMPERATURE
(Prandtl number = 0.73.)

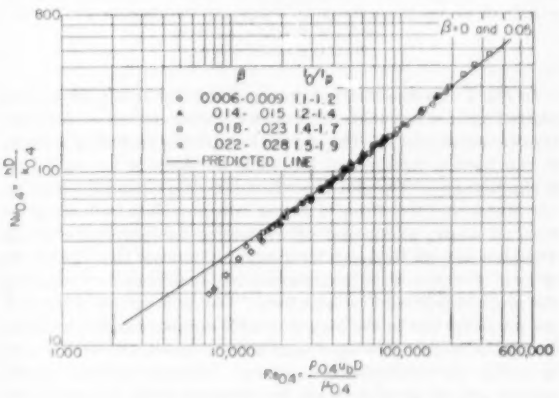

FIG. 6 VARIATION OF NUSSELT NUMBER WITH REYNOLDS NUMBER FOR FLOW OF AIR WITH HEAT ADDITION AND PROPERTIES EVALUATED AT $t_{0.4} = 0.4\ (t_0 - t_b) + t_b$
(Prandtl number = 0.73.)

perature close to the wall temperature. The actual variation of the thermal conductivity with temperature has not been determined experimentally at high temperatures. In reference (10) it is found that the best correlation of average heat-transfer coefficients for both heating and cooling was obtained by assuming the thermal conductivity proportional to $t^{0.5}$ and evaluating the properties, including density, in the Reynolds and Nusselt numbers at the average of the wall and bulk temperatures. If a constant rather than a variable specific heat had been used in reference (10), it would have been necessary to use a conductivity proportional to $t^{0.6}$ in order to eliminate the effect of ratio of wall to bulk temperature. The data for average heat-transfer coefficients given in reference (10) are therefore in substantial agreement with the present data and analysis for local heat-transfer coefficients. For the range of ratios of wall to bulk temperatures used in the present tests, as good a correlation could be obtained by evaluating the properties at the average of the wall and bulk temperatures as by evaluating them at $t_{0.4}$.

Although extensive data were not obtained in the low Reynolds-number range at high ratios of wall to bulk temperature, the data taken indicate that in this range the effects of β are more nearly eliminated by evaluating the properties at the bulk temperature than at $t_{0.4}$. This is in agreement with the analysis given in reference (11) where it is shown that for laminar flow the properties should be evaluated at a temperature between the bulk temperature and the temperature at the center of the tube. It would be expected that in the transition region the properties should be evaluated at temperatures between this temperature and $t_{0.4}$.

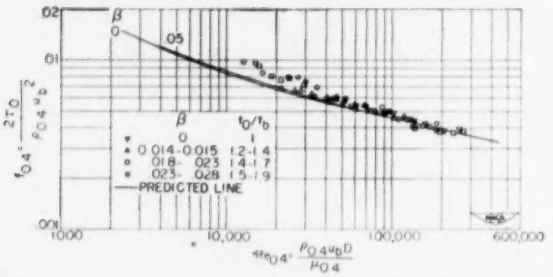

Fig. 7 Variation of Friction Factor With Reynolds Number for Flow of Air With Heat Addition and Properties Evaluated at $t_{0.4} = 0.4(t_0 - t_b) + t_b$
(Prandtl number = 0.73.)

In Fig. 7 experimental and predicted friction factors for air are plotted against Reynolds numbers for various values of the heat-transfer parameter β. The physical properties, including density, in the friction factors and Reynolds numbers in the figure are evaluated at $t_{0.4}$. The plot of predicted friction factors given in Fig. 7 indicates that the effects of β or of ratio of wall to bulk temperature are nearly eliminated by evaluating the properties at $t_{0.4}$. The data at high Reynolds numbers also indicate that the effects of ratio of wall to bulk temperature are eliminated by evaluating the properties at that temperature. The data agree closely with the predicted line in the high Reynolds-number range. At lower Reynolds numbers the agreement is not as good, although it may be within the experimental accuracy. Measurements of friction factors are, in general, much less accurate than those of heat-transfer coefficients because of difficulties in measuring static pressure gradients. In reference (10) it is found that some of the data for average friction factors at low Reynolds numbers lie both below and above the predicted line in Fig. 7, when the fluid properties are evaluated at the average of the wall and bulk temperatures.

Experimental and predicted velocity distributions for various values of β are shown in Fig. 8. The velocity distributions were measured with a small total-head probe having a 0.005-in. opening. Rectangular rather than semilogarithmic co-ordinates are used inasmuch as data are not shown for flow close to the wall;

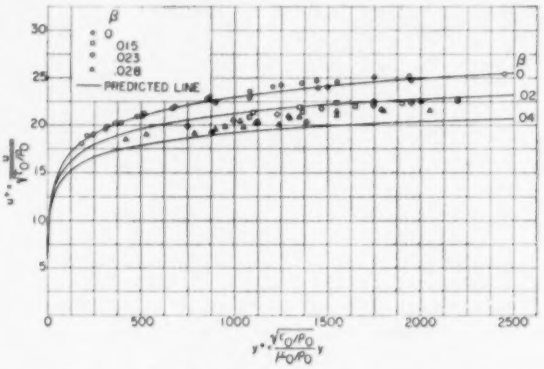

Fig. 8 Generalized Velocity Distributions for Flow of Air With Heat Addition
(Prandtl number, 0.73; Reynolds numbers for data, 100,000-250,000.)

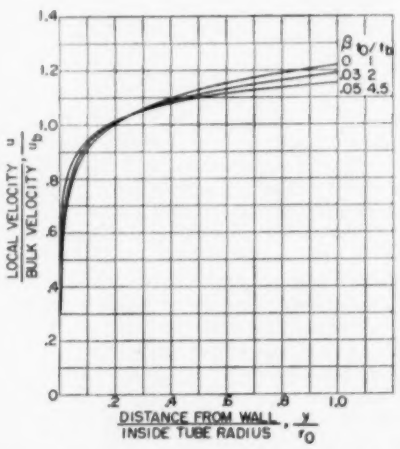

Fig. 9 Predicted Effect of Heat Transfer on Shape of Velocity Profile; Tube-Radius Parameter r_0^+, 2000
(Prandtl number = 0.73.)

these data are not shown because the distributions were measured at high Reynolds numbers where the severe velocity gradients and the presence of the hole in the tube wall make the accuracy of the measurements doubtful.

It can be seen that the experimental and predicted values are in substantial agreement although there is some scatter in the data. Inasmuch as the experimental distributions were measured in the high Reynolds-number range where the experimental friction factors fell on the predicted line, the agreement between the experimental and predicted velocity distributions might be expected. It appears that measurement of velocity distributions with heat transfer yields little information in addition to that obtained by measurement of friction factors and heat-transfer coefficients other than possible information concerning changes in shape of the velocity profile with heat transfer. However, as indicated in Fig. 9, changes in profile shape should be very small over most of the tube cross section for the range of values of β ob-

tained in the tests (0 to 0.028) and probably could not be measured experimentally.

Experimental and predicted temperature distributions are plotted in Fig. 10. The temperature distributions were measured with a thermocouple probe consisting of 0.001-in. chromel-and-alumel wire butt-welded between chromel-and-alumel prongs. Data for temperature distributions close to the wall are shown only at low flow rates because at high flow rates the severe velocity and temperature gradients and the presence of the hole in the tube wall make the accuracy of the measurements doubtful. The distributions shown for the region close to the wall may be subject to errors due to conduction along the thermocouple-probe prongs inasmuch as the velocities in that region were very small. Temperature distributions were not measured for high values of β or of ratio of wall to bulk temperature because of the delicacy of the temperature probe and because it appeared that such measurements would not yield appreciable information beyond that obtained by measuring heat-transfer coefficients and friction factors at high values of β. Changes in temperature-profile shape with heat transfer should be small as in the case of velocity profile, Fig. 9.

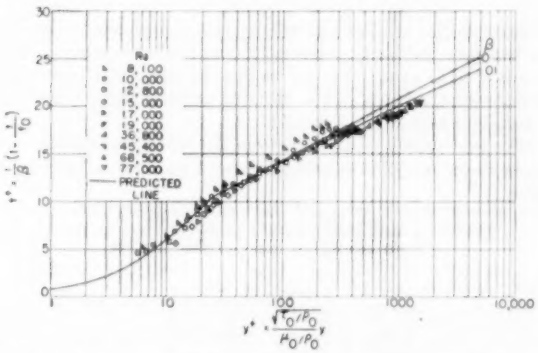

FIG. 10 GENERALIZED TEMPERATURE DISTRIBUTION FOR FLOW OF AIR WITH LOW RATES OF HEAT ADDITION
(Prandtl number, 0.73; β for data, 0.0075–0.0093; t_b/t_0 for data, 1.1–1.2.)

It is seen in Fig. 10 that the experimental temperature distributions agree fairly well with those predicted except in the low Reynolds-number range where transition from turbulent to laminar heat transfer is taking place. This separation of data from the predicted line at low Reynolds numbers is not present in the velocity-distribution data given in reference (4), so it appears that the eddy diffusivities for heat and momentum transfer cannot be considered equal in the low Reynolds or Peclet number range (7).

Predicted Effect of Variation of Shear Stress and Heat Transfer Across Tube. An analysis which includes the effect of variation of shear stress and heat transfer across the tube for a Prandtl number of 1 is given in the Appendix. A comparison between equations from that analysis and equations which assume uniform shear stress and heat transfer (2) is shown in Fig. 11. For variable shear stress and heat transfer the intersection of the curves for flow close to and far from the wall is taken at $y^+ = 30$ rather than 26. It is seen that the effect of variable shear stress and heat transfer on the velocity distributions is small and probably within the accuracy of flow and pressure measurements. The effect is greater for heat extraction (negative β) than for heat addition to the gas.

Although the foregoing calculations were carried out for a Prandtl number of 1, it is evident that the effects of variable shear stress and heat transfer also would be small for a Prandtl number of 0.73.

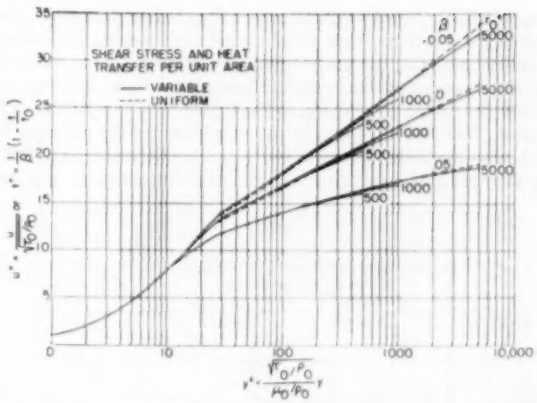

FIG. 11 CURVES SHOWING PREDICTED EFFECT OF VARIATION OF SHEAR STRESS AND HEAT TRANSFER ACROSS TUBE ON VELOCITY AND TEMPERATURE DISTRIBUTIONS OF GASES
(Prandtl number = 1.)

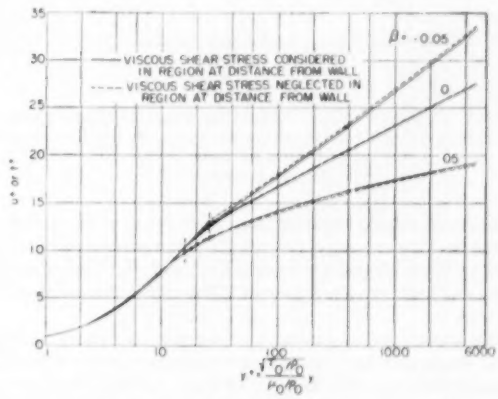

FIG. 12 CURVES SHOWING EFFECT OF NEGLECTING MOLECULAR SHEAR STRESS AND HEAT TRANSFER IN REGION AT A DISTANCE FROM WALL
(Prandtl number = 1.)

Predicted Effect of Molecular Shear Stress and Heat Transfer in Region at Distance From Wall. An analysis which includes the effect of molecular shear stress and heat transfer in the region at a distance from the wall for a Prandtl number of 1 is given in the Appendix. The results of this analysis are given in Fig. 12. By including the molecular shear stress in the equation for flow at a distance from the wall, the region of applicability of the von Kármán similarity expression is extended from $y^+ > 26$ to $y^+ > 16$. At $y^+ = 16$, the curve joins smoothly with the curve for flow close to the wall with no discontinuity in slope; that is, the eddy diffusivity is continuous from the wall to the center of the tube. Only a small difference in the velocity or temperature distribution is produced by including the effect of molecular shear stress and heat transfer in the region at a distance from the wall. Although the preceding calculations were carried out for a Prandtl number of 1, it is evident that the same conclusions would hold for a Prandtl number of 0.73.

Effect of Various Assumptions for Ranges of Applicability of Equations for Flow Close to and at a Distance From Wall. In all of the foregoing considerations the value of y^+ at the intersection of the curves for flow close to and at a distance from the wall y_i^+, was assumed to be constant as β varied. It is desirable to obtain

the effect of various assumptions for the variation of y_1^+ on the velocity and temperature distributions. One assumption which might be made is that the intersection occurs at a given constant ratio of turbulent shear stress to viscous shear stress; that is, the value of $\epsilon/(\mu/\rho) = n^2 u y \rho/\mu$ at the intersection is constant as β varies. The results of using this assumption for the variation of y_1^+, with the molecular shear stress and heat transfer considered in the region at a distance from the wall, are shown in Fig. 13.

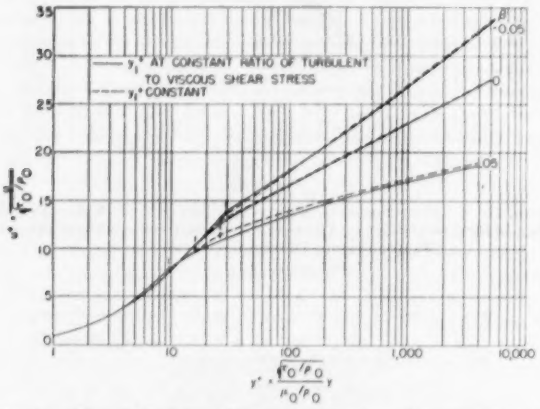

FIG. 13 CURVES SHOWING EFFECT OF VARIOUS ASSUMPTIONS FOR VARIATION OF y_1^+ ON GENERALIZED VELOCITY OR TEMPERATURE DISTRIBUTION
(Prandtl number = 1.)

The vertica. dotted lines indicate the variation of y_1^+ with β. It is seen that the curves plotted using the foregoing assumption are close to those plotted for constant y_1^+ with the molecular shear stress and heat transfer neglected in the region at a distance from the wall.

The assumption of constant y_1^+ for the case where molecular shear stress and heat transfer are neglected in the region at a distance from the wall should give quite accurate results.

ANALYSIS FOR FLOW OF SUPERCRITICAL WATER IN SMOOTH TUBES

The analysis for supercritical water is somewhat more complicated than that for air because of the peculiar variation of the physical properties of supercritical water with temperature. The variation of properties of supercritical water with temperature at a pressure of 5000 psi is shown in Fig. 14. The property values,

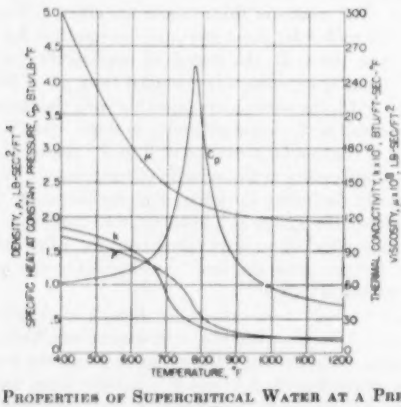

FIG. 14 PROPERTIES OF SUPERCRITICAL WATER AT A PRESSURE OF 5000 PSI

except the thermal conductivities at the lower temperatures which were taken from reference (12), were taken from tables and equations given in reference (13). There is considerable uncertainty in the property values of supercritical water, especially for viscosity and thermal conductivity, so that the accuracy of the computed results may be affected to some extent by errors in those values.

Assumptions 1, 2, and 4 in the analysis for air will be used also for supercritical water.

Velocity and Temperature Distribution. For the region close to the wall the expression for ϵ from Equation [8] is substituted into Equations [3] and [4]. By using assumptions 1 and 2 from the analysis for air, and integrating

$$u^+ = \int_0^{y^+} \frac{dy^+}{\frac{\mu}{\mu_0} + \frac{\rho}{\rho_0} n^2 u^+ y^+} \quad \ldots\ldots [29]$$

$$t^+ = \int_0^{y^+} \frac{dy^+}{\frac{k}{k_0}\frac{1}{\mathrm{Pr}_0} + \frac{\rho}{\rho_0}\frac{c_p}{c_{p0}} n^2 u^+ y^+} \quad \ldots\ldots [30]$$

Equations [29] and [30] can be solved simultaneously by iteration in the same way as Equations [13] and [14] were solved. Inasmuch as μ/μ_0, ρ/ρ_0, and so on, are functions of t/t_0 for a given wall temperature, and $t/t_0 = 1 - \beta t^+$, the property ratios can be calculated for each value of β and t^+.

For the region at a distance from the wall the expression for ϵ from Equation [6] is substituted into Equations [3] and [4] to give

$$1 = \frac{\mu}{\mu_0}\frac{du^+}{dy^+} + \frac{\rho}{\rho_0}\kappa^2 \frac{(du^+/dy^+)^4}{(d^2u^+/dy^{+2})^2} \quad \ldots\ldots [31]$$

and

$$1 = \left[\frac{k/k_0}{\mathrm{Pr}_0} + \frac{\rho}{\rho_0}\frac{c_p}{c_{p0}}\kappa^2 \frac{(du^+/dy^+)^3}{(d^2u^+/dy^{+2})^2}\right]\frac{dt^+}{dy^+} \quad \ldots\ldots [32]$$

where assumptions 1 and 2 from the analysis for air have been used. In these equations the molecular shear-stress and heat-transfer terms have been retained so that the slopes can be matched at y_1^+. (The procedure used for evaluating the constant C in Equation [21] cannot be used unless analytical expressions are given for the variation of properties with temperature.) Substitution of $du^+/dy^+ = v$ in Equation [31] and rearrangement give

$$\frac{dv}{v} = -\kappa \frac{du^+}{\sqrt{\frac{1 - (\mu/\mu_0)v}{\rho/\rho_0}}} \quad \ldots\ldots [33]$$

or

$$v = v_1 e^{-\kappa \int_{u_1^+}^{u^+} \frac{du^+}{\sqrt{\frac{1 - (\mu/\mu_0)v}{\rho/\rho_0}}}} \quad \ldots\ldots [34]$$

Substitution of $du^+/dy^+ = v$ in Equation [32] and rearrangement give

$$\frac{dv}{v} = -\kappa \sqrt{\frac{(\rho/\rho_0)(c_p/c_{p0})}{\frac{v}{dt^+/dy^+} - \frac{vk/k_0}{\mathrm{Pr}_0}}}\, du^+ \quad \ldots\ldots [35]$$

Eliminating dv/v from Equations [33] and [35], rearranging, and integrating, result in

$$t^+ = t_1^+ + \int_{u_1^+}^{u^+} \frac{du^+}{\frac{c_p}{c_{p0}} + v\left(\frac{k/k_0}{\mathrm{Pr}_0} - \frac{c_p}{c_{p0}}\frac{\mu}{\mu_0}\right)} \quad \ldots\ldots [36]$$

Equations [34] and [36] can be solved simultaneously by iteration by using assumed relations among v, u^+, and t^+. After the relation among v, t^+, and u^+ has been determined, y^+ can be calculated by integrating the expression $v = du^+/dy^+$, or

$$y^+ = y_1{}^+ + \int_{u_1{}^+}^{u^+} \frac{du^+}{v} \quad \ldots\ldots\ldots\ldots [37]$$

Because of the unusual variation of the properties of supercritical water, the velocity and temperature distributions must be calculated for each wall temperature. Velocity and temperature distributions for various values of β for a wall temperature of 900 F and a pressure of 5000 psi are shown in Figs. 15 and 16. For plotting these curves $y_1{}^+$ is taken at 16 as in Fig. 12. In general,

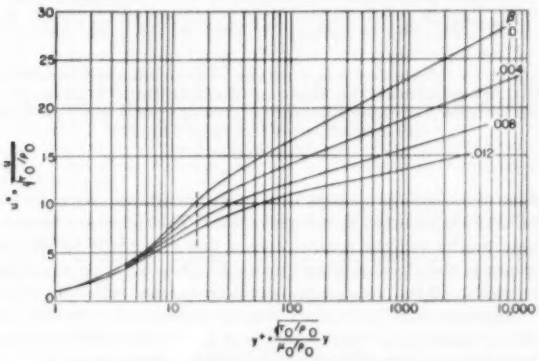

FIG. 15 PREDICTED GENERALIZED VELOCITY DISTRIBUTIONS FOR FLOW OF SUPERCRITICAL WATER WITH HEAT ADDITION
(Pressure, 5000 psi, wall temperature, 900 F.)

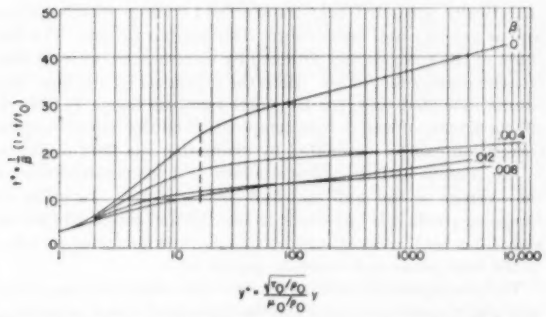

FIG. 16 PREDICTED GENERALIZED TEMPERATURE DISTRIBUTIONS FOR FLOW OF SUPERCRITICAL WATER WITH HEAT ADDITION
(Pressure, 5000 psi; wall temperature, 900 F.)

the appearance of the velocity distribution curves is similar to those for air. However, the variation of the temperature distributions with β is more complex than for air; for a β of 0.012, t^+ for some values of y^+ is higher than for $\beta = 0.008$. This effect can be explained by the decrease in specific heat with a decrease in temperature at the lower temperatures. The specific heat appears in the denominator of Equation [36].

Nusselt Numbers, Reynolds Numbers, and Friction Factors. For supercritical water the Nusselt numbers, Reynolds numbers, and friction factors are calculated from the same equations as were used for air. A plot of Nusselt numbers against Reynolds number for a pressure of 5000 psi and a wall temperature of 900 F is shown in Fig. 17. As was the case for the variation of temperature distributions, the variation of Nusselt number with β is complex. A single reference temperature, which can be used for evaluating

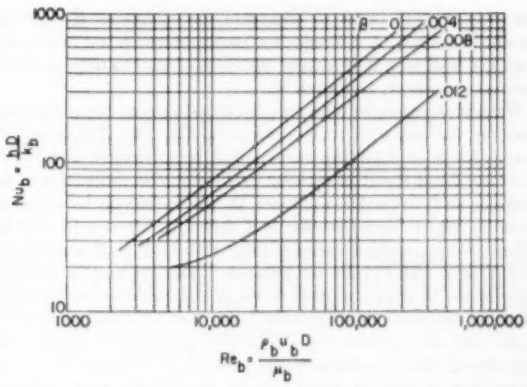

FIG. 17 PREDICTED VARIATION OF NUSSELT NUMBER WITH REYNOLDS NUMBER FOR FLOW OF SUPERCRITICAL WATER WITH HEAT ADDITION AND PROPERTIES EVALUATED AT BULK TEMPERATURE
(Pressure, 5000 psi; wall temperature, 900 F.)

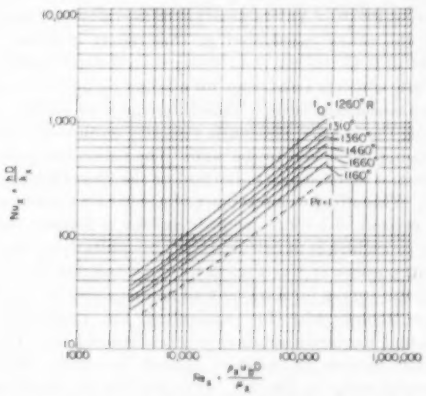

FIG. 18 PREDICTED VARIATION OF NUSSELT NUMBER WITH REYNOLDS NUMBER FOR FLOW OF SUPERCRITICAL WATER WITH HEAT ADDITION AT VARIOUS WALL TEMPERATURES AND PROPERTIES EVALUATED AT REFERENCE TEMPERATURES t_x GIVEN IN FIG 19
(Pressure, 5000 psi.)

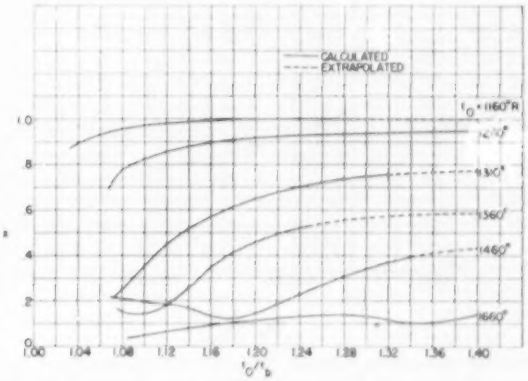

FIG. 19 VARIATION OF $x(t_x = x(t_0 - t_b) + t_b$ WITH WALL TEMPERATURE AND t_b/t_0 FOR USE WITH FIG. 18

the properties in order to eliminate the effects of β therefore cannot be found. A reference temperature which is a function of both the wall temperature and the ratio of wall to bulk temperature can, however, be found.

Nusselt numbers for 5000 psi are plotted against Reynolds numbers for various wall temperatures in Fig. 18. These are the curves for $\beta = 0$ for the various wall temperatures and can be used for β not equal to zero by evaluating the properties in the Nusselt and Reynolds numbers at the reference temperature given in Fig. 19 as a function of t_s and t_0/t_b. It is seen that the reference temperature varies greatly with both wall temperature and ratio of wall to bulk temperature. Figs. 18 and 19 might be generalized to apply to other fluids in the supercritical region by dividing the wall temperatures by the critical temperature of water and the pressure by the critical pressure of water. The validity of this procedure would depend on whether or not the properties of various fluids can be determined with sufficient accuracy from generalized plots.

The variation of the level of the curves for Nusselt numbers versus Reynolds number in Fig. 18 is caused by the variation in Prandtl number. These curves indicate that Nusselt number varies approximately as $Pr_0^{0.55}$ for the range of Prandtl numbers shown whereas experimental data for various fluids indicate a variation of $Pr^{0.40}$. (An examination of the data for Prandtl numbers in the range considered in this report indicates that an exponent of 0.45 fits the data better than the commonly used exponent 0.4, which is an average for a larger range of Prandtl numbers than considered here.) This difference is probably caused by neglecting the effect of kinematic viscosity on the eddy diffusivity in the region very close to the wall. The region very close to the wall becomes increasingly important as the Prandtl number is increased. This effect is the subject of a separate investigation but for the present, if a more accurate answer is desired, the recommended procedure is to calculate Nu_x by multiplying the Nu_x for a Prandtl number of 1 in Fig. 18 by the correction $Pr_0^{0.40}$, instead of using the curves for various wall temperatures in Fig. 18. The reference temperature for evaluating the properties in the Nusselt and Reynolds numbers can be obtained from Fig. 19.

Friction factors are plotted against Reynolds numbers for supercritical water in Fig. 20. As in the case of Nusselt numbers it is possible nearly to eliminate the effects of variable properties by evaluating the properties at a temperature which is a function of wall temperature and ratio of wall to bulk temperature, Fig. 21.

Several other analyses of heat transfer and friction for supercritical water using somewhat different assumptions for the effect of variable properties were made simultaneously with this one and are reported in reference (14). The difference between those results and the present ones is due principally to the difference in the physical properties used; when the same properties are used in all the analyses the results are in reasonable agreement.

Experimentally determined Nusselt numbers and friction factors for supercritical water would be of great value for establishing the validity of the analysis given in the present paper.

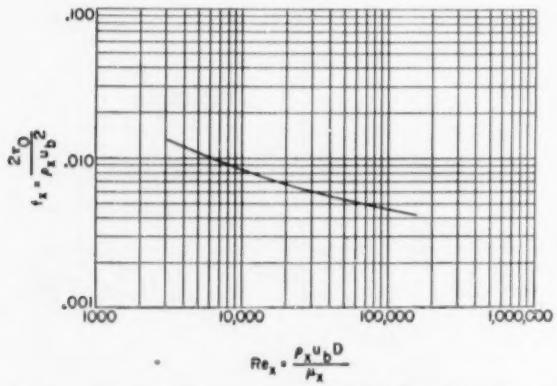

FIG. 20 PREDICTED VARIATION OF FRICTION FACTOR WITH REYNOLDS NUMBER FOR FLOW OF SUPERCRITICAL WATER WITH HEAT ADDITION AND PROPERTIES EVALUATED AT REFERENCE TEMPERATURE GIVEN IN FIG. 21

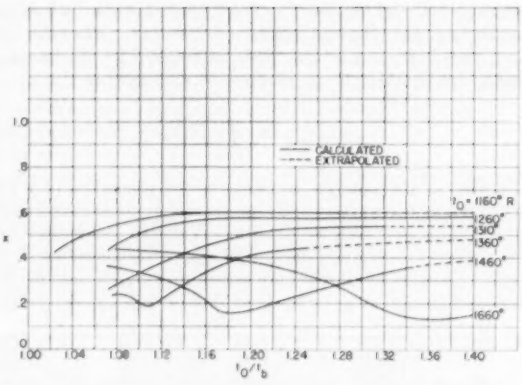

FIG. 21 VARIATION OF x AS DEFINED BY $t_x = x(t_s - t_b) + t_b$ WITH WALL TEMPERATURE AND RATIO OF WALL TO BULK TEMPERATURE FOR DETERMINATION OF REFERENCE TEMPERATURES FOR USE WITH FRICTION FACTOR CURVE IN FIG. 20

(Pressure, 5000 psi.)

SUMMARY OF RESULTS

Substantial agreement was obtained between experimental and analytically predicted heat-transfer and friction correlations as well as velocity and temperature distributions for air. The best check of the analysis was obtained by measurement of local heat-transfer coefficients for air. Both the experimental and analytical results indicated that, for Reynolds numbers above 15,000, the effects of ratio of wall to bulk temperature on the Nusselt-number correlation can be eliminated by evaluating the fluid properties in the Nusselt and Reynolds numbers at a temperature close to the average of the wall and bulk temperatures. In using the foregoing result it is important to use thermal conductivities and viscosities both proportional to the absolute temperature raised to the 0.68 power and constant specific heat.

The analysis indicated that the effect of variation of shear stress and heat transfer across the tube on the velocity and temperature distributions is slight for turbulent flow with variable fluid properties. It also indicated that the effect of molecular shear stress and heat transfer in the region at a distance from the wall is slight.

The analysis for supercritical water indicated that the effects of variable fluid properties on the Nusselt-number and friction-factor correlations are eliminated by evaluating the properties in the Nusselt and Reynolds number at a reference temperature which is a function of both the wall temperature and the ratio of wall to bulk temperature.

BIBLIOGRAPHY

1 "Der Einfluss der Gastemperatur Auf den Wärmeübergang im Rohr," by W. Nusselt, *Technische Mechanik und Thermodynamik*, vol. 1, August, 1930, pp. 277–290.

2 "Investigation of Turbulent Flow and Heat Transfer in Smooth Tubes, Including the Effects of Variable Fluid Properties," by R. G. Deissler, Trans. ASME, vol. 73, 1951, pp. 101–107.

3 "Turbulence and Skin Friction," by Th. von Kármán, *Journal of the Aeronautical Sciences*, vol. 1, January, 1934, pp. 1–20.

4 "Analytical and Experimental Investigation of Adiabatic Turbulent Flow in Smooth Tubes," by R. G. Deissler, NACA TN 2138, 1950.

5 "Gesetzmassigkeiten der Turbulenten Stromung in Glatten Kohren," by J. Nikuradse, VDI Forschungsheft 356, 1932.

6 "The Analogy Between Fluid Friction and Heat Transfer," by Th. von Kármán, Trans. ASME, vol. 61, 1939, pp. 705–710.

7 "Analysis of Fully Developed Turbulent Heat Transfer in Smooth Tubes at Low Peclet Numbers With Application to Liquid Metals," by R. G. Deissler, NACA RM E52F05.

8 "Analytical and Experimental Investigation of Fully Developed Turbulent Flow of Air in a Smooth Tube With Heat Transfer With Variable Fluid Properties," by R. G. Deissler and C. S. Eian, NACA TN 2629, 1952.

9 "Analytical Investigation of Turbulent Flow in Smooth Tubes With Heat Transfer With Variable Fluid Properties for a Prandtl Number of One," by R. G. Deissler, NACA TN 2242, 1950.

10 "Measurements of Average Heat Transfer and Friction Coefficient for Subsonic Flow of Air in Smooth Tubes at High Surface and Fluid Temperatures," by L. V. Humble, W. H. Lowdermilk, and L. G. Desmon, NACA Report 1020, 1951. (Formerly RM's E7L31, E8L03, E50E23, and E50H23.)

11 "Analytical Investigation of Fully Developed Laminar Flow in Tubes With Heat Transfer With Fluid Properties Variable Along the Radius," by R. G. Deissler, NACA TN 2410, 1951.

12 "A Survey of the Thermodynamic and Physical Properties of Water," by E. J. Wellman, MS thesis, Purdue University, Lafayette, Ind., 1950.

13 "Thermodynamic Properties of Steam," by J. H. Keenan and F. G. Keyes, John Wiley & Sons, Inc., New York, N. Y., first edition, 21st printing, 1950.

14 "Comparison of Heat Transfer Coefficients and Wall Shear Stresses Computed by the Methods of K. Goldman and H. Elrod," by R. C. Ross, NDA-10-9, Nuclear Development Associates, 1952.

Appendix A

Analysis Including Effect of Variation of Shear Stress and Heat Transfer Across Tube for Prandtl Number = 1

The following analysis was made to determine the effect of variation of shear stress and heat transfer across the tube on the velocity and temperature distributions with variable fluid properties. The variations of shear stress and heat transfer in the region close to the wall are negligible so that only the region at a distance from the wall is considered.

The relation for the variation of shear stress with radius for fully developed flow is obtained by equating the shear forces to the pressure forces acting on a cylinder of fluid of arbitrary radius and differential length. This relation gives

$$\tau = \tau_0(1 - y/r_0) \quad [38]$$

The heat transfer per unit area varies in approximately the same way as the shear stress although the variation is not linear. For the purpose of determining the general effect of the variation of heat transfer the following relation is assumed

$$q = q_0(1 - y/r_0) \quad [39]$$

Substituting Equations [38] and [39] into Equations [1] and [2], dividing Equation [2] by Equation [1], and integrating the result between the wall and a point in the fluid give, for a Prandtl number and α of 1

$$t/t_0 = 1 - \beta u^+ \quad [40]$$

With substitution of Equations [6], [38], and [40], Equation [3] can be written with the molecular shear stress neglected as

$$\frac{d^2u^+}{dy^{+2}} = -\kappa \frac{1}{\sqrt{(1 - \beta u^+)(1 - y^+/r_0^+)}} \left(\frac{du^+}{dy^+}\right)^2 \quad [41]$$

In order to solve Equation [41] let

$$du^+/dy^+ = v \quad [42]$$

Integration of Equation [42], gives

$$y^+ = y_1^+ + \int_{u_1^+}^{u^+} \frac{du^+}{v} \quad [43]$$

Substituting Equations [42] and [43] into Equation [41] and integrating result in

$$v = v_1 e^{-\kappa \int_{u_1^+}^{u^+} \frac{du^+}{\sqrt{(1 - \beta u^+)\left(1 - \frac{y_1^+}{r_0^+} - \frac{1}{r_0^+}\int_{u_1^+}^{u^+} \frac{du^+}{v}\right)}}} \quad [44]$$

Equation [44] can be solved by iteration by substituting assumed values for u^+ and v into the right side of the equation and calculating new values of v. After the relation between u^+ and v has been obtained for various values of β and r_0^+, y^+ can be calculated from Equation [43].

Analysis Including Effect of Molecular Shear Stress and Heat Transfer in Region at a Distance From Wall for Prandtl Number = 1

The effect of the molecular shear-stress and heat-transfer terms in Equations [3] and [4] on the velocity and temperature distributions is investigated in this section. A solution which includes the effect of these terms has been obtained already in Equation [34]. For gases with a Prandtl number of 1, $\rho/\rho_0 = 1/(1 - \beta u^+)$ and $\mu/\mu_0 = (1 - \beta u^+)^d$ and Equation [34] becomes

$$v = v_1 e^{-\kappa \int_{u_1^+}^{u^+} \frac{du^+}{\sqrt{[1 - (1 - \beta u^+)^d v](1 - \beta u^+)}}} \quad [45]$$

which is solved by iteration. The quantity y^+ is then calculated from Equation [43].

Discussion

E. R. G. Eckert.[3] The calculations presented in the author's paper give significant information on the influence of variable-property values on heat transfer and fluid friction in fully developed turbulent tube flow. The results of the author's calculations obtained for air flow have been checked by experiments so that the results for supercritical water should be acceptable with confidence, although no experimental verification has been obtained. The procedure, well established in the field of heat transfer, of using generally the relationships obtained for constant-property values and adapting them to variable properties by introducing these properties at an appropriately determined reference temperature, again proved profitable in the presentation of the results obtained by the author. This reference temperature at which the properties have to be introduced was found to be located approximately halfway between the fluid bulk temperature and the wall temperature for turbulent air flow. The corresponding relationship for supercritical flow of water was found to be more complex and is presented in Figs. 19 and 21.

In an attempt to obtain a presentation which is more easily interpretable, the writer has replotted the figures and obtained after some attempts the diagram shown in Fig. 22 of this discussion. In this diagram, the parameter x (expressing the ratio of the difference of the reference temperature minus bulk temperature t_b to wall temperature t_0 minus bulk temperature) is plotted over the parameter $(t_m - t_b)/(t_0 - t_b)$. In this parameter, t_m is that temperature at which the specific heat assumes its maximum value of 780 F, as indicated in Fig. 14 of the paper. The upper part of the diagram shown in Fig. 22 refers to the reference temperature which has to be used in the dimensionless

[3] Mechanical Engineering Department, Institute of Technology, University of Minnesota, Minneapolis, Minn. Mem. ASME.

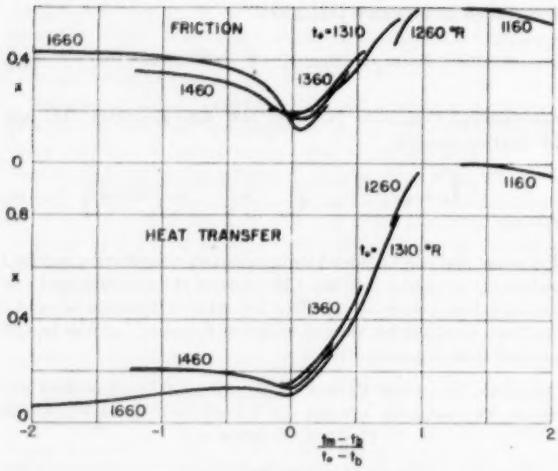

FIG. 22

parameters for the friction coefficient; the lower part indicates the reference temperature for the heat-transfer parameters. Only the calculated range of x-values in Figs. 19 and 21 of the paper, and not the extrapolated values, were used in the preparation of the diagram. It may be observed that in this presentation the influence of the second parameter t_0 has become quite insignificant, since all the curves for different t_0 values align quite well along a single curve. It is also interesting to note that the temperature which exerts the largest influence on the location of the reference temperature is the value t_m. The lower part of Fig. 22 indicates that the reference temperature to be used for heat-transfer calculations is near the bulk temperature ($x \sim 0$) when the bulk temperature coincides with the temperature t_m

$$\left(\frac{t_m - t_b}{t_0 - t_b} = 0\right)$$

and that it is equal to the wall temperature ($x = 1$) when the wall temperature coincides with the temperature t_m

$$\left(\frac{t_m - t_b}{t_0 - t_b} = 1\right)$$

The influence of the temperature t_m on the location of the reference temperature to be used for the calculation of friction, and to be obtained from the upper part of Fig. 22 is less strong than for heat transfer. This may be expected, since the specific heat influences directly the heat flow, but only indirectly the velocity field.

K. GOLDMANN.[4] The author is to be congratulated for his extensive work in the field of turbulent flow and heat transfer for fluids with variable properties to which the present paper is another valuable contribution.

The validity of the author's analysis rests primarily on his assumption that the empirical constants κ and n, which are obtained from isothermal tests, have the same values for nonisothermal flow of fluids with variable properties. The only justification for this assumption appears to be the good agreement between predicted and actually measured values for air heat-transfer coefficients and friction factors as reported by the author.

A somewhat different approach to a similar analytical method has been proposed and used by the writer. In this approach it is assumed that the universal turbulent-velocity profile $u^+ = f(y^+)$, which has been verified for isothermal flow, may be used to describe nonisothermal-flow fields with variable properties provided the velocity and distance parameters are redefined as

$$u^{++} \equiv \int_0^u \frac{du}{\sqrt{\tau/\rho}} \quad \text{and} \quad y^{++} \equiv \int_0^y \frac{\sqrt{\tau/\rho}}{\mu/\rho}\, dy$$

This assumption implies that a local value of eddy diffusivity ϵ at any point in the flow field is not only a function of distance, velocity, and velocity derivatives, but is also a function of the fluid properties at that point. Results obtained with this assumption check the experimental data for air and are in reasonably good agreement with the analytical results for water at 5000 psi, as presented in the paper.

It should be pointed out that neither of these analytical approaches would be applicable to supercritical water, if actual experimental results should indicate the existence of a boiling-like phenomenon. Above the critical pressure, a liquid phase and a vapor phase cannot co-exist in stable equilibrium. However, under high rates of heat transfer, it is conceivable that macroscopic clusters of liquidlike molecules "explode" at the heat-transfer surface, move as gaslike aggregates into the bulk of the fluid where they "collapse" again into liquidlike clusters. One may speculate that the growth and collapse of these clusters, like the growth and collapse of bubbles during boiling at subcritical pressures, cause enough agitation to result in heat-transfer coefficients that are significantly higher than predicted in the paper.

The writer does not share the author's optimism concerning the possibility of finding reduced property functions that will allow a general correlation for all fluids above their critical pressure. Without this incentive, there is no advantage in presenting the supercritical-water results as Nu_x or $f_x - \mathrm{Re}_x - t_0 - t_0/t_b - x$ correlations, as has been done in the paper. Such correlations have the distinct disadvantage of requiring a cumbersome trial-and-error method in applying them to the solution of particular heat-transfer problems. A more direct, and perhaps more useful, correlation might consist of plots of a heat-tranfser parameter $q_0 D^{1-m}/G^m$ and a shear-stress parameter $\tau_0 D^{2-n}/G^n$ versus wall temperature t_0 at constant values of bulk temperature t_b.

J. C. MATHESON.[5] The author's objective of extending the analysis of turbulent flow and heat transfer in tubes to include the effect of variable fluid properties and fluids of Prandtl number other than 1 has been accomplished with remarkable success. The agreement between the analytical and experimental results for air is exceptionally good.

It is easy to understand why the von Kármán similarity theory, the assumption of equal diffusivity for heat and momentum, and the assumption of constant shear stress and heat transfer across the tube are so popular in works of this kind. It is because they have proved to be profoundly successful. The difficult thing to understand is why they have been so successful.

The von Kármán similarity theory is today the best mathematical conception of the turbulence mechanism available to the investigator. Still, it is known to be inaccurate. The author has cited Nikuradse's results (5) as verifying the similarity expression for the eddy diffusivity. There has been much doubt concerning Nikuradse's "corrected" values until recent months,[6] and even

[4] Senior Engineer, Nuclear Development Associates, Inc., White Plains, N. Y. Jun. ASME.

[5] Mechanical Research Engineer, Research Laboratory, United Aircraft Corporation, East Hartford, Conn. Jun. ASME.

[6] "Turbulent Flow in Smooth Pipes, A Reanalysis of Nikuradse's Experiments," by D. Ross, Ordnance Research Laboratory, The Pennsylvania State College, School of Engineering, September 8, 1952.

though a modern analysis of his work has helped to dispel this doubt it has revealed other inconsistencies which require some revision of the interpretation, at least with regard to verification of the similarity theory.

There certainly is precedent for the assumption $\epsilon = \epsilon_h$; however, this assumption is contrary to the published results of several investigators.[7, 8, 9, 10] Values of α have been quoted from 1.1 to 2.0, most of these being in the range 1.3 to 1.6. The effect of using too low a value for α may be masked in heat-transfer correlations by the use of too large a laminar-film thickness. The limit of the laminar-boundary layer ordinarily is taken as $y^+ = 5$, but Reichardt's measurements show this limit at $y^+ = 2$.

There is no intention in these statements to detract from the obvious value of the paper. The extension of the conventional analysis of turbulent heat transfer to include the effect of temperature-dependent fluid properties is an important contribution. The gist of the discussion may be summarized in the query, "Why does analysis based on a foundation known to be inadequate agree so well with the results of experiment?"

Author's Closure

The author wishes to thank Dr. Eckert and Messrs. Goldmann and Matheson for their discussions. Dr. Eckert's correlation of the reference temperatures for supercritical water considerably simplifies the presentation of the results for that part of the analysis. In the case of heat transfer a particularly simple result is obtained: The properties in the Nusselt and Reynolds numbers are evaluated at t_m, the temperature at which the specific heat assumes its maximum value as long as t_m remains between t_0 and t_b. If t_m is higher than t_0 the properties are evaluated at t_0; if lower than t_b they are evaluated at approximately t_b. The importance of t_m in the reference temperature correlation might be due partly to the fact that the fluid properties are all varying rapidly with temperature at or near that temperature.

If the preceding reference temperatures are used for evaluating the properties in the conventional Nusselt-type correlation, it should be stressed that the Prandtl number should be evaluated at the wall temperature rather than at t_x, that is, $Nu_x = C\,Pr_0^a Re_x^b$.

The author agrees with Mr. Goldmann, in that he feels the assumptions in the analysis find their justification in the agreement between predicted and measured values. However, he would prefer to consider the fundamental assumptions as $\epsilon = f(u, y)$ close to the wall and $\epsilon = f(du/dy, d^2u/dy^2)$ in the region at a distance from the wall. Equations [5] and [7] of the paper then follow directly by dimensional analysis and there is no question about the variability of the constants n and κ in the case of nonisothermal flow.

In connection with the possibility of applying the results of the supercritical-water analysis to other supercritical fluids, as discussed by Mr. Goldmann, it would seem that Dr. Eckert's correlation of reference temperatures throws considerable light. If the correlation in his Fig. 22 is, as it appears, more than an accident, one would expect it to apply as well to fluids other than supercritical water. It would be of interest to check this correlation for fluids and pressures other than those considered in this paper.

[7] "Values for the Eddy Diffusion Coefficient," by W. Karush, USAEC, AECD-3256, June 8, 1945.

[8] "Heat Transfer Through Turbulent Friction Layers," by H. Von Reichardt, Translation as NACA-TM 1047, 1942.

[9] "Temperature Distributions for Air Flowing Turbulently in a Smooth Heated Pipe," by R. A. Seban and T. T. Shimazaki, General Discussion on Heat Transfer, London Conference, IME-ASME, 1951.

[10] "Turbulent Transfer Mechanism and Suspended Sediment in Closed Channels," by H. M. Ismail, Proceedings—Separate, ASCE, No. 56, February, 1951; also Trans. ASCE, vol. 117, 1952, p. 409.

The author shares Mr. Matheson's opinion that more fundamental studies must be made before the turbulence mechanism is understood. The von Kármán expression for ϵ at a distance from wall, Equation [5] of the paper, should be considered as a first approximation. One could obtain a better approximation by including in the expression derivatives of higher order than the first and second. In that way, minor incongruities such as a nonzero slope at the tube center and a slightly better agreement with the data for constant shear stress than for a linearly varying shear stress could be eliminated. These deviations are, however, unimportant for most applications so that the additional complications involved in including higher-order derivatives, do not seem to be justified. The agreement between theory and experiment is, in most cases, within a few per cent.

Incidentally, it is often stated that other expressions for ϵ such as $\kappa^2 (du/dy)\, y^2$ and $\kappa\sqrt{\tau_0/\rho}\, y$ could be used as well as Equation [5], inasmuch as they all lead to the logarithmic profile. It should be mentioned, however, that the same profile is obtained only when the shear stress is considered constant; when a linearly varying shear stress is used, as it must be in an exact analysis, Equation [5] is found to be superior in representing the data.

Mr. Matheson's comments concerning the ratio α of eddy diffusivities for heat and momentum transfer have led the author to attempt to obtain the ratio from his own measurements (Figs. 1 and 10 of the paper). The ratio was obtained by working out the analysis for various values of α and comparing with the data, rather than by measuring the slopes of the velocity and temperature profiles, which is difficult to do accurately. By using this procedure, α was found from the data in Fig. 10 to be about 1.04 for $r_0^+ = 1000$ or Re = 40,000. (It can be seen from Fig. 10 that the data lie slightly below the predictions for $\alpha = 1$.) When a value of α of 1.04 is used for calculating Nusselt numbers the predicted curve is still in good agreement with the data in Fig. 6 at the higher Reynolds numbers. At low Reynolds or Peclet numbers the data in Figs. 6 and 10 indicate an α less than 1, in agreement with the analysis in reference (7) of the paper.

It might be mentioned that the author also has attempted to obtain values for α by measurement and analysis of temperature-recovery factors. This investigation (as yet unpublished) indicates a value of α of about 1.07 at a Reynolds number of 300,000. The slight difference between this value and the foregoing value obtained (1.04) might be caused by the difference between the Reynolds or Peclet numbers in the two cases. At a Reynolds number of 40,000, α appears to depend to a slight extent on Peclet number which tends to lower the value of α, reference (7). Both of the preceding methods used give mean effective values for α and do not indicate whether a variation occurs across the tube.

One more point which requires comment is the definition of bulk temperature with variable specific heat. The true cup-mixing temperature for supercritical water should be obtained by defining a bulk enthalpy

$$H_b = \int_0^{r_0} H\,\rho\,u\,(r_0 - y)\,dy \Big/ \int_0^{r_0} \rho\,u\,(r_0 - y)dy$$

and finding the bulk temperature t_b corresponding to H_b from steam tables rather than from Equation [23] of the paper. The bulk velocity should then be obtained from

$$u_b = (2/r_0^2\rho_b) \int_0^{r_0} \rho\,u\,(r_0 - y)\,dy$$

where ρ_b corresponds to the t_b from the steam tables. It was found that the use of these equations for t_b and u_b, rather than Equations [23] and [28], produced no significant changes in the results of the analysis.

The Unsteady-Flow Water Tunnel at the Massachusetts Institute of Technology

By J. W. DAILY[1] and K. C. DEEMER[2]

A project to investigate fluid friction and cavitation phenomena in unsteady motion is under way in the Hydrodynamics Laboratory at the Massachusetts Institute of Technology. Its objective is to obtain for transient-flow conditions through conduits and around immersed bodies the same kinds of basic information that have been determined for steady-flow cases. A pilot-model water tunnel of unconventional design has been developed to produce flow in which the basic motion is accelerating or decelerating. It is of the blowdown type and consists essentially of two tanks 20 in. diam and 6 ft 8 in. long mounted vertically, one above the other, and connected by a tube, or working section of 1 in. ID. The velocity and acceleration of the flow through the tube are governed by the difference in air pressure above the water surfaces in the upper and lower tanks. This differential pressure, in turn, is controlled by a servosystem. High-frequency-response electronic cells were developed for measuring differential water pressures directly. These cells have been employed in experiments to determine loss of head along the test section and for measuring the instantaneous average velocity.

Introduction

STEADY flow in conduits, channels, and around submerged bodies has been the subject of many studies and substantial contributions have been made toward understanding the phenomena of loss of head in channels and conduits and of separation, cavitation, and forces on submerged bodies. Unsteady flow has not been given the equivalent attention and, consequently, is not so well understood. Practical interest in unsteady behavior exists in the prediction of transient drag, of deceleration rates, and of other hydrodynamic characteristics of underwater projectiles, ships, and planing surfaces and in determining transient energy dissipation and cavitation along boundaries exposed to rapidly varied flow.

A project for investigation of fluid friction and cavitation phenomena in unsteady motion has been in progress since 1948, at the M. I. T. Hydrodynamics Laboratory under the sponsorship of the Office of Naval Research. Its object is to obtain for transient-flow conditions through conduits and around immersed bodies the same kinds of basic information that have been obtained for steady-flow cases. Unsteady-flow experiments require special laboratory apparatus and techniques, and the initial phase of this program involved the design and construction of a pilot-model unsteady-flow water tunnel, together with suitable instrumentation for producing and observing accelerating and decelerating motions. The following description gives details of this unusual equipment and describes some of the initial experiments.

General Specifications and Type of Apparatus

The unsteady-flow test apparatus was designed to incorporate the following desirable features:

1 The water stream should have rectilinear motion and initially be free of turbulence.

2 The acceleration and velocity of the stream should be controlled at either arbitrarily fixed values or according to some programmed variation.

3 The local pressure in the test stream should be controllable such that cavitation can be produced or prevented as desired.

The ranges of variables initially specified were as follows:

1 Velocities up to 100 fps.

2 Accelerations up to 5 fps per sec with at least a 20-sec test duration or higher accelerations for shorter intervals.

3 Local pressure intensities in the unobstructed test stream ranging from 4 psia upward.

The apparatus chosen for this purpose is a nonreturn unsteady-flow water tunnel. The erected equipment is shown in Fig. 1, with a schematic section in Fig. 2. The tunnel proper consists of two cylindrical tanks mounted one above the other and connected by a vertical pipe or working section extending into the lower tank. Water is caused to flow from one tank to the other under pneumatic control; compressed air in the spaces above the water surfaces in the two tanks is used to provide an adequate driving force for desired accelerations and degree of control. Flow is established on release of a quick-opening valve in the pipe below the working section. This basic arrangement permits flow in either direction, although in the design of the equipment, downward flow was given primary consideration. Thus the entrance nozzle is located at the bottom of the upper tank to insure proper flow into the working section.

The apparatus constructed is actually a small-scale model of a proposed larger apparatus. The small size is a consequence of the early realization that the main problems with this unconventional equipment were to be those of instrumentation, essentially independent of the size of apparatus. On the other hand, with the exception of tests involving flow around suspended bodies, most of the contemplated boundary-friction and cavitation experiments would be possible in a small unit. Consequently, a model having a "working section" of 1 in. diam was constructed in preference to a larger, costlier design.

As for the steady-flow tunnel, the apparatus can be adapted to measurements of boundary-layer phenomena, of resistance, or of cavitation on bodies supported in the stream within the working section, or to measurements along the working-section walls themselves. The cylindrical working section can be replaced by a venturi section or by any other shape of transition. The vertical working section facilitates pressure measurements over any plane normal to the stream since the gravitational effect is constant. This is of importance in making cavitation studies. Also, for

[1] Associate Professor, Civil and Sanitary Engineering Department, Massachusetts Institute of Technology, Cambridge, Mass. Mem. ASME.

[2] Professor and Chairman, Department of Applied Mechanics, University of Kansas, Lawrence, Kans. Mem. ASME.

Contributed by the Hydraulic Division and presented at the Spring Meeting, Columbus, Ohio, April 28–30, 1953, of The American Society of Mechanical Engineers.

 Manuscript received at ASME Headquarters, March 5, 1953. Paper No. 53—S-31.

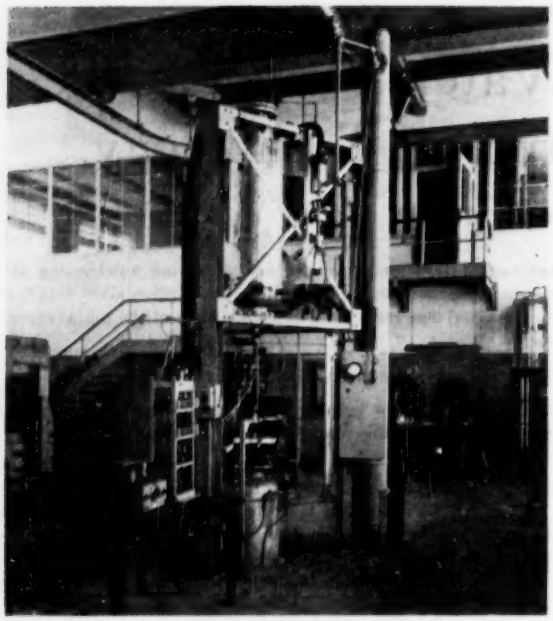

FIG. 1 THE UNSTEADY-FLOW WATER TUNNEL

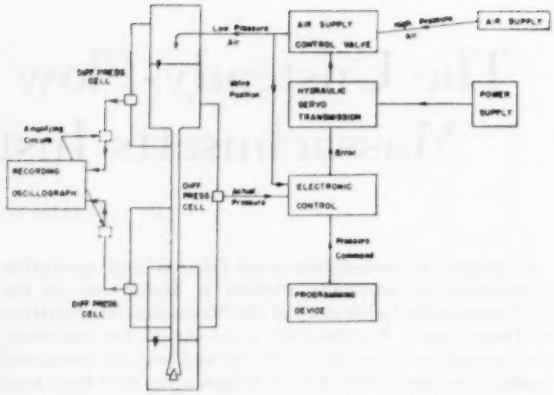

FIG. 3 BLOCK DIAGRAM OF CONTROL AND DATA-MEASURING SYSTEMS

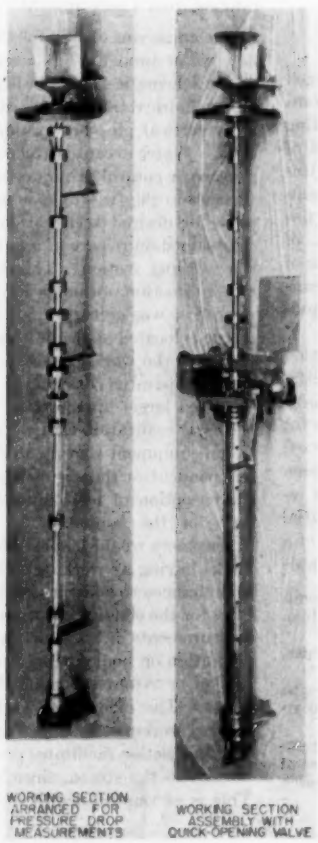

FIG. 2 (*right*) SCHEMATIC SECTION OF TUNNEL CIRCUIT

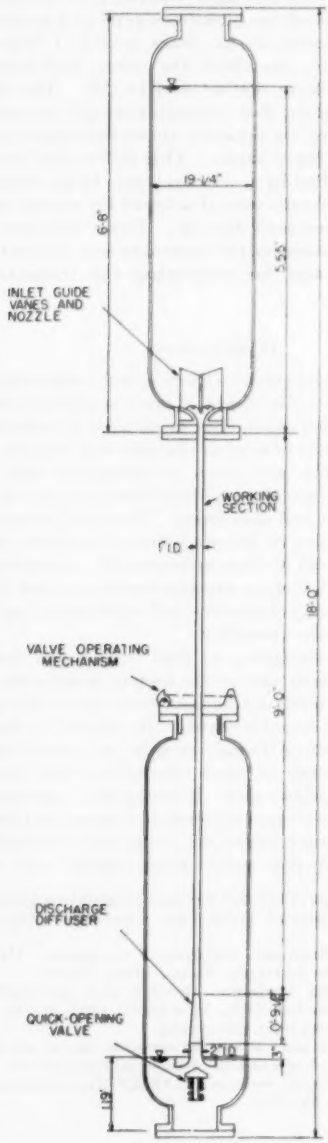

downward flow the hydrostatic pressure increase in the direction of flow tends to compensate for the pressure drop due to friction. Of course, exact compensation is obtained only for one rate of steady motion.

An essential part of the equipment is its control system. To obtain the desired ranges of acceleration and pressure in the working section, the compressed air or gas must be admitted to or rejected from either tank according to some time schedule. Furthermore, it is desirable to be able to duplicate test runs. This calls for repeating exactly the time histories of velocity and acceleration, so as to assure the same stage of boundary-layer growth and intensity of turbulence at corresponding times. For these reasons, a closed-loop automatic control for velocity and acceleration is provided, operating on the "error" between scheduled and actual tank-pressure differences. This control loop is indicated schematically in Fig. 3. Simultaneous automatic control of the test-section pressure is not provided although this is a desirable feature which is expected to be added later.

Auxiliary instruments including provision for instantaneous measurement of velocity and pressure complete the basic elements of the water-tunnel equipment.

Description of Tunnel and Its Operation

The unsteady-flow water tunnel is erected in the main research hall of the new M. I. T. Hydrodynamics Laboratory (1).[2] The laboratory is arranged with water-supply tanks, circulating pumps, and other mechanical and electrical services on the basement level. The main hall on the floor above is an unobstructed space 120 ft × 56 ft with 21 ft clearance to the roof beams. Access to the basement area is by means of a set of 30-in. × 30-in. floor openings (with steel covers) placed approximately on 15-ft centers.

The water tunnel is a structure having an over-all height of 21 ft and supported by a three-legged steel frame which forms a 5-ft equilateral triangle in plan. The 6-in. H-beam columns of the structural frame are 13 ft high. As shown in Fig. 1, water and air tanks project a distance of 4 ft above this frame while the lower water tank projects below the frame and through one of the 30-in. × 30-in. floor openings a distance of 4 ft.

For descriptive purposes, the tunnel components may be considered to form three systems, the "hydraulic system," the "control system," and the "data-measuring and recording system." The main hydraulic circuit and the compressed-air supply for powering the circuit are considered here to be the hydraulic system.

Hydraulic System. The purpose of the main hydraulic circuit is to store the water supply prior to and after the test run and to provide for conducting the water to and from a suitable test section under specified transition conditions. An analysis based on the arbitrarily chosen velocity, acceleration, and test-duration specifications indicated that the maximum pressure in the main tanks of the tunnel circuit would be of the order of 200 to 250 psi, while the volume of each of these tanks should be approximately 12 cu ft. The decision to conduct friction-loss experiments for the initial tests called for a test section with appropriate pressure connections. The details of these elements together with inlet nozzle and quick-opening foot valve are described as follows:

Tanks: Two tanks 20 in. OD × 6 ft 8 in. long, Fig. 4, were designed and constructed according to ASME and Massachusetts Standard Specifications for 250-psi air. At each end of each tank is an 8-in-diam nozzle; the lower nozzle on the top tank and the upper nozzle on the bottom tank were machined after welding to the heads so that they would be smooth as well as axial. A number of couplings were welded into the shell and heads to permit connections to gage glasses, pressure cells, and so on. A third 8-in. nozzle was inserted in the shell of the lower tank near the bottom for inspection purposes. After fabrication, the tanks were galvanized and the coupling threads and machined surfaces were wiped before cooling of the coating.

Inlet Nozzle and Guide Vanes: The inlet nozzle shown in Fig. 4 is designed (2) to assure a continuous decrease in pressure from the tank to the 1-in-ID test section and at the same time to give a uniform velocity distribution at the test section. It is preceded by guide vanes whose function is to prevent local eddies and vortex motion at the entrance to the nozzle. The nozzle is machined from a bronze casting while the guide vanes are made from 1/16-in. sheet brass, soldered together and also soldered into grooves machined in the nozzle.

The inlet nozzle is also employed for flow metering. At the 1-in-diam junction between the nozzle and test section, the end of the nozzle is relieved to provide a 0.010-in-wide gap for use as a

[2] Numbers in parentheses refer to the Bibliography at the end of the paper.

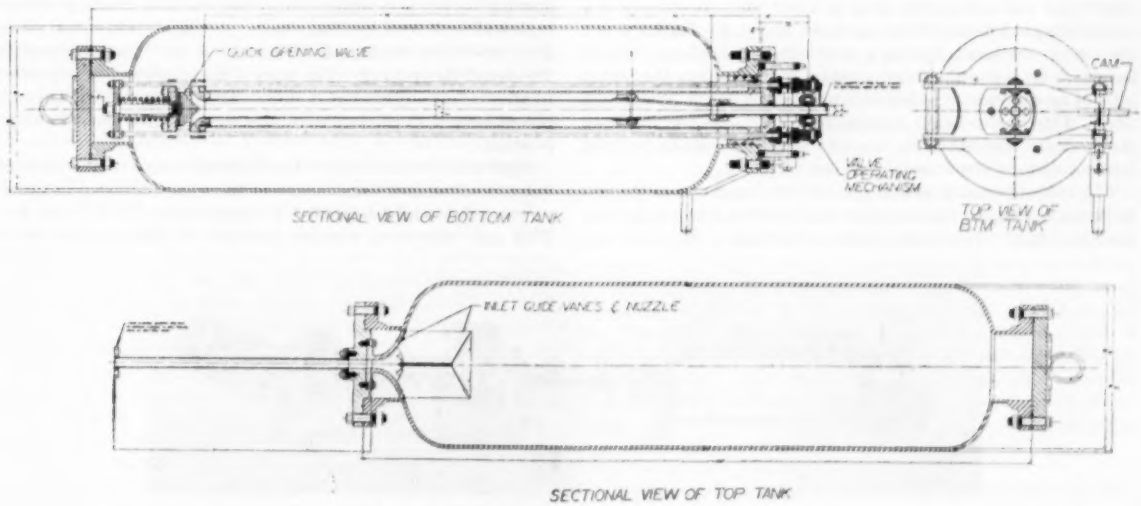

Fig. 4 Sectional Drawing of Hydraulic Circuit

piezometer tap. This permits measurement of the pressure drop across the nozzle.

Test Section: The test section shown assembled in Fig. 2 was made from 1-in-ID × $^1/_8$-in-wall drawn brass tubing, and the section below the diffusion cone from 2-in-ID × $^1/_8$-in-wall drawn brass tubing. The 1-in. tubing was made in three sections and connected by flanges designed to minimize disturbances of the boundary layer. The flanges were machined and bored in pairs to provide a smooth joint and at the same time permit inspection and lapping of the joint between each flange and adjacent section of tubing.

For pressure-drop measurements, eight sets of four piezometer holes are located along the 1-in. test section. The four holes are drilled at 90-deg intervals around the tube and connected into a manifold. The first ring is 1 in. from the end of the entrance nozzle and the spaces between subsequent taps are 9, 12, 12, 12, 15, 19.5, 19.5 in., giving a total length of 99 diam. The holes were drilled and reamed $^1/_{16}$ in. diam through an effective wall thickness of 0.400 in. formed by soldering the piezometer ring to the test-section tube. It has been found (3) that a slightly rounded hole gives a more accurate pressure indication than one with sharp edges. However, in this small tube rounding with any degree of uniformity would be difficult. Consequently, it was decided to rely upon obtaining consistent results with carefully made holes with sharp edges.

In the manufacture, the holes were drilled with a jig to make them fall on the axis of the tube and to be perpendicular to it. The tube was then polished with light oil and lapping paper fastened to a plug so that it just fit the bore. In this process, the tube was turned in a lathe while the plug was advanced through it. The piezometer holes then were reamed and the tube polished again, the process being repeated several times.

The piezometer holes were made $^1/_{16}$ in. diam after dynamic tests indicated this size would accommodate sufficient flow of water to give pressure indications on the diaphragm gages without intolerable lag or attenuation. The diffuser cone having a total angle of 6 deg connects the 1-in. tube to the 2-in-diam discharge piece. The connection at the 1-in-diam end is rounded to avoid a sharp change in flow curvature and possible flow separation at this juncture. This cone can be placed in any position depending on the desired length of the 1-in. tube.

Quick-Opening Foot Valve: The foot valve at the outlet of the expanded 2-in. test section holds the water under pressure in the upper tank and test section prior to a test run. It consists of a cone seating in a flared diffuser as shown in Fig. 4. During a test the cone is retracted, leaving a streamlined conical exit diffuser passage. Owing to the short duration of test runs at the higher rates of acceleration, it is desirable to establish flow in a minimum time. This valve design permits opening to be accomplished over various time intervals down to about 0.01 sec in free air; opening under water is somewhat less rapid.

The valve-operating mechanism and the lower end of the test section are designed for assembly and lowering into the bottom tank as a unit. This permits pressure-testing of the valve and all the piezometer connections and joints on the test pipe prior to installation in the relatively small receiving tank. The conical plug ordinarily is held open under a coil spring loading. It is closed against this loading (to 750 lb when closed) by means of a cam-operated linkage and the two tension rods shown. The valve cone is made of rubber molded around a stainless-steel stem and flange, and this rubber serves to lessen the impact shock of opening.

Air-Supply System: The compressed-air supply for powering the circuit must be sufficient to provide the highest rates of acceleration regardless of the head-tank pressure in the water system. For this purpose, a high-pressure reservoir was provided wherein gas could be stored in such quantities that the storage pressure need never drop below about 500 psi. This would permit throttling into the water head tank through a critical-flow control valve thus making the air flow independent of the downstream pressure. The reservoir is the 10-in. × 16-ft 6-in. upright tank attached, as shown in Fig. 1, to the right-hand column of the tunnel's structural frame. It is constructed according to ASME and Massachusetts Standard Specifications for 900-psi air.

Control System. The control-system elements shown schematically in Fig. 3 operate as follows:

A cam-driven programming device produces a "command" voltage according to an instantaneously desired pressure difference between the upper and lower tanks. A diaphragm-type pressure transducer is used to measure the actual instantaneous difference (or simply the pressure in the upper tank if atmospheric pressure is maintained in the bottom tank). This instrument gives a voltage output which is subtracted from the pressure-command voltage. The difference is the pressure "error" which is amplified to control the solenoid-stroke control of a standard hydraulic transmission. The motor of this transmission operates a special air valve to regulate the admission of air to the upper tunnel tank. The pressure error is in effect the valve position command. To improve stability of operation, there has been incorporated recently (4) a secondary loop within the main pressure loop which measures the error in valve position and applies a suitable correction to the valve-position command being fed to the hydraulic transmission. The individual components are described as follows:

Air-Inlet Control Valve: Fig. 5 shows the air-inlet valve which, as mentioned, always operates with the downstream pressure less than critical. Air flows at sonic velocity through an annular opening between an orifice and a tapered plug which is driven back and forth by a hydraulic motor through a lead screw. For given upstream conditions, the mass-flow rate is proportional to the area of the opening. The taper of the plug is sufficiently small to allow a fine adjustment of flow. The plug stem is linked to a potentiometer to produce a voltage signal proportional to valve position.

Hydraulic Transmission: The hydraulic drive on the air-inlet valve is a standard transmission of the type employed in turret power unit Model AA-16850-A 17 manufactured by Vickers, Inc. This unit delivers a variable quantity of high-pressure oil in

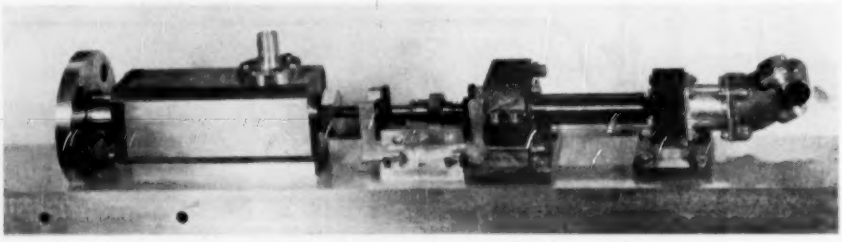

FIG. 5 AIR-INLET CONTROL VALVE

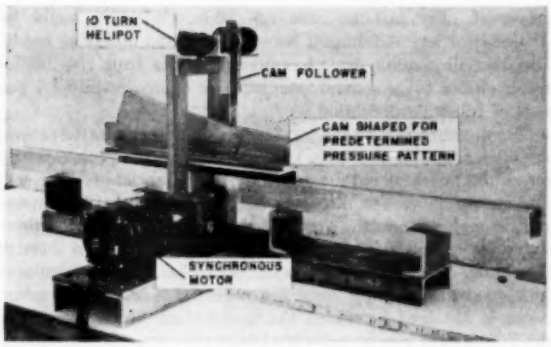

FIG. 6 CYCLE-PROGRAMMING DEVICE

accordance with the setting of a stroke-control mechanism incorporated in the transmission. The high-pressure oil pumped from this unit drives the positive-displacement hydraulic motor on the air-inlet control valve described previously. The transmission is capable of reversing the direction of the hydraulic motor, and hence the valve plug, 20 times per sec, or of driving the valve through a complete cycle of opening and closing in less than 1 sec.

Cycle-Programming Device: The device for producing an electrical signal proportional to a desired top tank pressure-time curve is shown in Fig. 6. A synchronous motor drives a long plate cam through a rack and gear. The cam follower is geared to a potentiometer and in this way delivers a voltage which is a function of time as prescribed by the plate cam.

Pressure Transducer: This consists of a diaphragm-type differential-pressure cell, employing a linear variable-differential transformer as the sensing element. An oscillator and a preamplifier energize the cell transformer.

These elements are the same as used for other sets of transducers built for data-measuring purposes and are described later.

Electronic Control: The pressure transducer-transformer field is excited with an 8-kc carrier and the output is the modulated pressure signal. This signal, stepped up approximately 10 times with a transformer, and the program signal, excited by the same 8-kc signal and shifted 180 deg out of phase from the pressure signal, are summed to produce the error. This low-level a-c error signal is amplified by three conventional triode stages. The next stage is a cathode follower which reduces source impedance. This a-c error must be detected since the stroke-control solenoids require direct current. The sense (positive or negative) of the a-c pressure error must be preserved in the detection, so a phase-sensitive detector is used which produces a d-c error that decreases with a negative a-c pressure error and increases with a positive error. Two d-c amplifier stages follow the phase-sensitive detector to supply a d-c input error to the valve-position loop. A positional helipot, attached to the rotating shaft of the valve, feeds back a d-c signal proportional to the valve position. The amplified d-c pressure-error signal is subtracted from the valve-position voltage and fed into a d-c phase-inverter amplifier. This signal drives the grids of two push-pull solenoid control tubes. The difference in the total current in each tube is used to drive the solenoids which position the stroke.

With this control, the resonant frequency of the system is about 2.2 cps which is approximately the closed-loop frequency response of the hydraulic transmission. Satisfactory operation has been achieved for a system loop gain as high as 10 decibels.

Indicating and Recording Equipment and Procedures. Differential-Pressure Cell: In unsteady-flow studies, it is desirable to know the time history of pressure, velocity, and acceleration throughout the flow field. In general, determination of these variables involves measurement of the instantaneous values of pressure and pressure differences. Consequently, a reliable and accurate pressure-transducing system is the most essential measuring device. Moreover, in order to reduce the error in measuring pressure differences, it is desirable to have instruments which can measure this difference directly. The several types of electronic pressure cells in common use were considered but the desirability of obtaining differential pressures directly led to the development of a new cell (5, 6).

This cell is known as the "diaphragm differential transformer

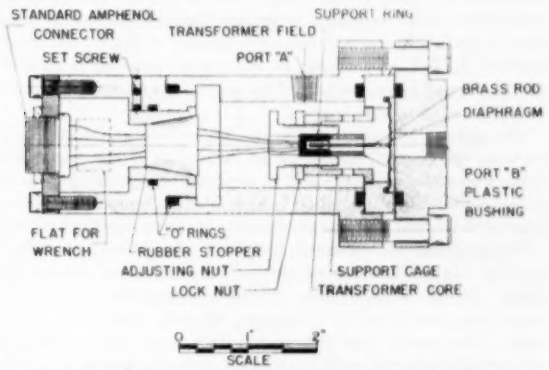

FIG. 7 CROSS-SECTIONAL VIEW OF TYPE DDT DIFFERENTIAL-PRESSURE CELL

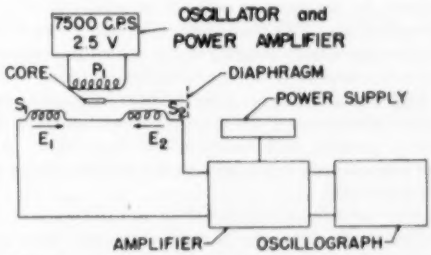

FIG. 8 SCHEMATIC DIAGRAM OF ELECTRONIC COMPONENTS OF DIFFERENTIAL-PRESSURE CELL

(DDT) type differential-pressure cell" and the experimental model is shown in Fig. 7. Water is admitted to both sides of a corrugated diaphragm through ports A and B. A brass rod soldered to the bottom of the diaphragm carries a small iron transformer core and as the diaphragm deflects as a result of unbalanced pressures at A and B, the core travels in a small differential transformer,[4] consisting of three coils mounted on a common axis. As shown in Fig. 8, the center coil acts as the transformer primary, while the two outside coils are connected in phase opposition and act as the secondaries. When the core is centered exactly with respect to the three coils, no current flows. As the core is moved off center toward one secondary coil, more current is induced in that secondary, and this current can be amplified for recording purposes. The secondary output is a linear function of core travel within certain limits depending on transformer size. By combining three sizes of transformers with four diaphragms, it was possible to cover a wide range of differential pressures, all within the linear range of both transformer and diaphragm.

[4] Manufactured by Schaevitz Engineering Corporation, Camden, N. J.

The diaphragms are made from inconel and beryllium copper with diameters ranging from 0.5 in. to 1.0 in. and thickness is from 0.0043 in. to 0.0075 in. Originally designed for aeronautic instrument capsules, the diaphragms were manufactured with a skirt around the periphery. In assembly some initial radial tension was provided by pressing this skirt over the heavy brass ring to which the diaphragm was soldered. These metals exhibit low hysteresis, the effects being less than 1 per cent of maximum applied pressure for these gages. The corrugated diaphragms deflect more linearly under load than flat diaphragms.

Diaphragm deflections are kept to about 4 per cent of their free diameters to avoid residual set. For the 0.5-in. diameter, this amounts to 0.020 in. which is the full range of the largest transformer used. In normal use, the volume of fluid required to register the full-scale change of differential pressure is 0.002 cu in. (or about 0.03 cc) for any of the gages, and in many cases it is only a fraction of this volume.

The natural frequency of the assembled cells was measured to be from 400 to 6200 cps for air on both sides of the diaphragm. With water on both sides and in the lead lines, this figure is reduced considerably, but in all combinations of cells and lead lines employed to date, the natural frequencies have exceeded 165 cps.

The pressure-cell housing is designed for pressures up to 200 psi and the rugged construction avoids the necessity of special handling. It will be noted that provision is made for adjusting the transformer null position by moving the coils with respect to the core. The transformer unit is especially coated for underwater application and the cells have been operated satisfactorily for periods of several months with the electrical units under water.

Electronic Equipment for Pressure Transducing: The differential transformers for the pressure cells are supplied with 2 to 7 volts at 7500 to 8000 cps. This frequency represents a compromise between deflection-output linearity range, output per unit of input, and frequency sensitivity for the transformers used. A General Radio high-stability Type 1304-A beat-frequency oscillator powers the transformers. In practice, several pressure cells are operated in parallel with resulting low impedance. A power amplifier is introduced to supplement the oscillator to assure up to 7.0 volts to the cells.

A separate amplifying and detecting unit follows each pressure gage. Electrically, the modulated pressure signal from the transformer of the pressure cell undergoes two stages of voltage amplification, after which the carrier frequency is removed by an infinite-impedance detector. The detector output is a d-c signal proportional to the pressure-cell diaphragm deflection. A differential amplifier provides the current transformation required by the low-impedance galvanometers of a recording oscillograph. The output of this system to a 5-ohm load is linear between ± 8 ma.

Two 300-volt d-c, 70-ma electronically regulated power supplies are used in conjunction with the six pressure-cell amplifiers employed to date.

Recording Oscillograph: A Hathaway Type S-8B 24-channel oscillograph is used to record the variables on a 10-in-wide roll chart. Record traces are produced on photosensitive paper by light beams reflected from galvanometer mirrors which are deflected by input current. Number OA-2 galvanometers having coils ranging from 5 to 7 ohms and natural frequencies of 750 cps are used. Full-scale deflection is obtained with 14-ma direct current. In addition to the galvanometer trace, time lines appear on the chart at 0.01-sec intervals governed by a tuning-fork and shutter arrangement.

In applying the complete transducing and recording system, the combination of pressure-cell transformer, metal diaphragm, and amplifier gain were adjusted to provide full-scale oscillograph-chart deflection for the particular pressure differential to be measured. For instance, the full 10-in. deflection could be obtained for any differential between 0.75 and 300 ft of water. The over-all possible error in converting data from the oscillograph charts to numerical quantities is approximately $^2/_3$ per cent of full-scale deflection.

Determination of Velocity and Acceleration: As indicated earlier, the inlet nozzle is used as a metering device, the pressure drop across the nozzle being measured by a differential-pressure cell. For steady flow, the discharge is calculated using the usual venturi-meter formula. For unsteady flow, the measured pressure drop contains a component due to the acceleration through the nozzle. This inertia component is small and can be calculated with good accuracy by assuming potential flow. A correction factor is obtained by which the true instantaneous velocity in the test section can be calculated from the measured differential pressure. The method involves a calculation of the average instantaneous velocity from the measured differential and an adjustment of this velocity as indicated by the acceleration. One correction is usually sufficient. Average instantaneous velocity also is obtained volumetrically from recording-tank levels as a function of time. Inasmuch as the diameter of the tank is nearly 20 times that of the test section, the volumetric method does not give good results over short time intervals. However, it does provide a check on the entrance-nozzle measurements for time increments of 1 sec or more. The initial experiments have involved only the determination of the average acceleration for the conduit cross section. To date this acceleration has not been measured directly, but has been calculated from the slope of the instantaneous velocity-time record.

The Experimental Program

Initial Pipe-Friction Measurements. The first experimental work (5) was the measurement and comparison of fluid friction due to steady and unsteady fully developed turbulent flow in a smooth conduit. Measurements were made over the last 19.5 and 39 diam of the 99-diam-long test section and at Reynolds numbers well above the laminar range. The steady-flow experiments covered the Reynolds-number range from 75,000 to 750,000 (average velocities about 9 to 85 fps). The unsteady-flow runs were made with average velocities from about 15 to 72 fps and average accelerations ranging from zero to about 35 fps per sec. The initial unsteady-flow experiments were exploratory, designed to cover a variety of conditions to determine, in general, if there is a measurable difference between steady and unsteady-flow friction loss.

The steady-flow tests were made by keeping the pressure drop constant across the working section, care being taken to hold the pressure in the lower tank sufficiently high to avoid cavitation. For unsteady-flow runs, a steady velocity was established first and then the pressure drop was varied to cause the flow to accelerate through some range and, in general, to level off at a higher velocity. To increase the accuracy of recording for these tests, some portion of the run was selected as the "running range" and the electronic-data-measuring equipment adjusted so as to give as nearly full-scale oscillograph deflection as possible. The period included a change in tank level of about 0.75 ft. Starting and ending the test run with a constant velocity served as a check on the condition and operation of the equipment since any difference from the established steady-flow loss was an indication of a possible calibration shift or accidental overloading of a pressure-cell diaphragm. These first runs were undertaken before the final developments of the control system were completed and were carried out with hand rather than automatic control of the air pressures. Furthermore, the entire test series represented, as well, a period of calibration and trial of the tunnel setup.

Fig. 9 shows the results of the steady-flow tests on familiar pipe-

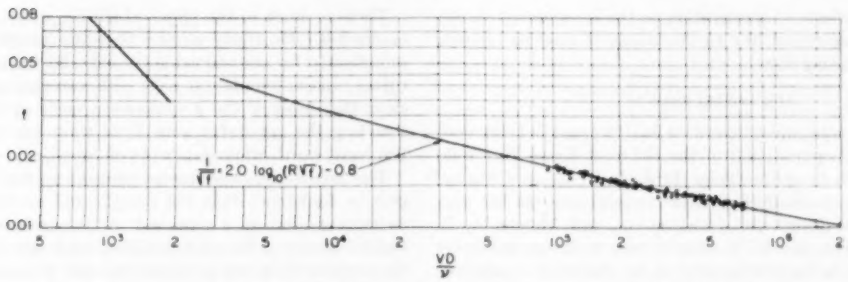

FIG. 9 EXPERIMENTAL STEADY-FLOW FRICTION FACTORS PLOTTED ON SMOOTH PIPE CURVES

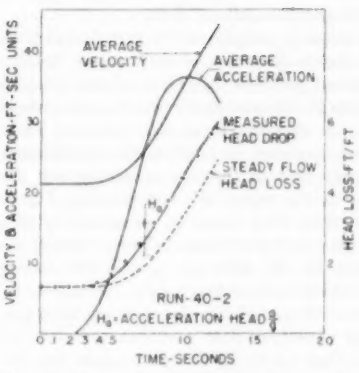

FIG. 10 UNSTEADY-FLOW RUN—INITIAL IMPULSE FROM STEADY TO ACCELERATED FLOW

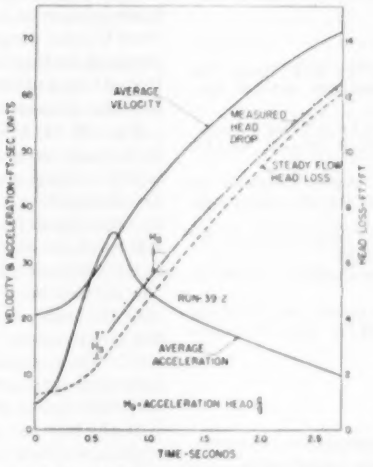

FIG. 11 UNSTEADY-FLOW RUN—ESTABLISHED ACCELERATION PHASE

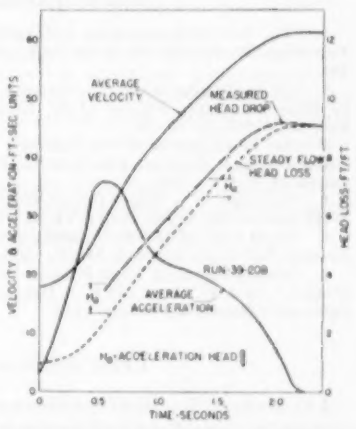

FIG. 12 UNSTEADY-FLOW RUN—TRANSITION FROM ACCELERATED TO STEADY FLOW

friction factor versus Reynolds-number curve. It is seen that the results agree well with the von Kármán-Prandtl logarithmic law for smooth pipes. The maximum deviation of the test data from the curve is 3.5 per cent while most data fall within 1 to $1^1/_2$ per cent of the logarithmic law. This is considered good since the tunnel and instrumentation were designed primarily for unsteady motion and do not incorporate all the features normally considered necessary for precise steady-flow experiments. Furthermore, it is interesting that consistent data can be obtained using this equipment without long periods of waiting for establishing either a steady flow or steady indications by the instruments of the usual type.

Figs. 10, 11, and 12 are typical plots of the data obtained from unsteady-flow runs. In these figures, curves were drawn for values of the average velocity, Q/A, average acceleration over the cross section, measured head drop, and the equivalent steady-flow head loss. The latter is calculated using the instantaneous velocities in the steady-flow head loss equation. The sum of the equivalent steady-flow head loss and the acceleration head are shown by the small crosses at 0.1-sec intervals, and the curve of measured instantaneous head drop is broken to accommodate these crosses where the values nearly coincide.

The limited amount of data obtained to date indicates that the friction factor for unsteady flow based on the average instantaneous velocity is essentially equal to that for steady flow based on the same velocity. Only in the region of initial impulse, Fig. 10, does the head loss differ from what would be calculated by using the instantaneous velocity and the steady-velocity friction factor.

An analysis of the implications of these preliminary results in terms of the turbulent velocity fluctuations and the shear stresses is to be found in references (5) and (6).

Subsequent to these initial experiments several equipment refinements were made. Consequently, the tests with fully developed turbulent flow are being continued and ultimately will include both acceleration and deceleration studies.

Future Studies. The initial experiments with fully developed turbulent flow are to be followed up immediately in three areas:

1 Conduit transitions at which separation occurs.

2 Regions of boundary-layer development such as at the entrance to a uniform-diameter conduit.

3 Conduit transitions at which cavitation occurs.

Studies are currently under way using sharp-edged orifices singly and in series to determine any effect of unsteady motion on the energy dissipation associated with the high shear and turbulence generation accompanying separation and jet formation. These experiments were selected as the first follow-up of the initial findings, namely, that steady and unsteady friction losses for fully developed flow are essentially the same. If the loss associated with orifice jet-energy dissipation is also essentially unaffected by acceleration, the unsteady-flow testing procedure may be useful in the unanticipated application of obtaining steady flow losses over wide Reynolds-number ranges by one rapid test. These current experiments also include deceleration tests.

Both items 2 and 3 will be investigated as soon as possible. One interest in item 2 lies in the question of drag and energy dissipation during the acceleration phase of projectile motion.

For item 3, any effects of acceleration on the inception of cavitation can be an important key to the unsolved question of scale effects with cavitating flows.

Acknowledgments

The water-tunnel project described in this paper is being conducted under the sponsorship of the Office of Naval Research. The authors wish to acknowledge Prof. A. T. Ippen's original suggestion of an unsteady-flow water tunnel and for his contributions to the design and construction, and Messrs. A. L. Keller, D. L. Favin, and W. H. Seaver, who were responsible for successive stages in the development of the electronic equipment and controls. They also are indebted to Messrs. W. L. Hankey and R. W. Olive for aid in preparation of this manuscript.

Bibliography

1 "The New Hydrodynamics Laboratory," by A. T. Ippen, *The Technology Review*, vol. 53, June, 1951, pp. 399–403, 429–430, 432, 434.

2 "On the Design of the Contraction Cone for a Wind Tunnel," by Hsue-Shen Tsien, *Journal of the Aeronautical Sciences*, vol. 10, February, 1943, pp. 68–70.

3 "An Investigation of the Influence of Orifice Geometry on Static Pressure Measurements," by R. E. Rayle, Jr., MS thesis, Course II, M.I.T., 1949.

4 "Redesign of a Water-Tunnel Pressure-Control System," by W. H. Seaver, MS Thesis, Course VI, M.I.T., 1953.

5 "Fluid Friction Due to Unsteady Flow in Conduits," by K. C. Deemer, ScD thesis, Course I, M.I.T., 1952.

6 "Measurements of Fluid Friction With Steady and Unsteady Motion," by J. W. Daily and K. S. Deemer, M.I.T. Hydrodynamics Laboratory Report No. 9, July, 1952.

Discussion

J. O. Jones.[5] This paper describes a remarkable achievement. The solution of a difficult problem was boldly conceived and carried to a convincing conclusion. The detailed description of the means employed emphasizes the promise of success that can be achieved in microtechnic by utilizing all scientific equipment available; but, in turn, this demands that the experimenter have an ever-wider knowledge of the tools of modern research. In short, the emphasis nowadays must be on instrumentation.

In laboratory work in all fields, always there is the question: Are the measurements accurate or merely consistent? In this instance the remarkable agreement of the pipe-friction measurements with the von Kármán-Prandtl equation for steady flow in smooth pipes gives confidence that the measurements are not only consistent, but also are as precise as can be desired. In view of the fact that the measurements are practically instantaneous, the agreement is amazing.

The writer hopes that future experiments will include measurements of pipe friction for values of Reynolds numbers as great as 10^7 and even greater.

R. W. Powell.[6] Since the writer recommended Professor Deemer for this research job at M.I.T., he naturally read this paper with great interest, and rates it as very important. For years we have been collecting data as to the resistance to flow in pipes and channels when the flow was steady. Flow in nature and in the works of man is seldom steady, but in our designs and investigations we have said "in the absence of any data as to resistance to unsteady flow, we will assume that the resistance will be the same as for steady flow at the same velocity." At last, in this paper we have data on the resistance to accelerated flow.

There is much in the paper which the writer will not attempt to discuss. He freely admits that the instrumentation is too complicated for one trained in the old school to understand. The writer can contemplate it only with awe and amazement. It is clear that most of the 4 years were spent in designing and constructing the apparatus, and little time was left for using it. But some worth-while data were obtained.

The runs at zero acceleration give us no new information, but give us confidence that the complicated mechanism actually is measuring what it is supposed to. Considering the extremely short duration of the runs, and that the length of pipe over which the pressure drop was measured was only 39 diam, the agreement, shown in Fig. 9 of the paper, is remarkable. It may be noted that although the von Kármán-Prandtl formula plotted in that figure is regarded by most as the best available for smooth pipes, there is some disagreement. For example, refer to the formulas proposed by Harris[7] and some of the discussers of his paper, and that of Chu and Streeter.[8] It should be added that most of these formulas also agree well with the authors' data.

Figs. 10, 11, and 12 are only samples of ten such figures given in the more complete papers (5 and 6 of the authors' Bibliography). They are typical samples, however. From all their data the authors conclude that when the acceleration is constant, or approximately so, the shearing resistance indicated (after correction for the force necessary to produce the acceleration) is the same as for steady flow at that instantaneous velocity. The authors say, "only in the region of initial impulse, Fig. 10, does the head loss differ from what would be calculated by using the instantaneous velocity and the steady-velocity friction factor." Their explanation for the difference is that with rapidly increasing acceleration the increase in mechanical viscosity of the turbulent flow in the central core of the pipe does not keep pace with the increase in the velocity of flow, and that, therefore, the resistance to flow is less than for steady flow at the same velocity.

Fig. 11 does not bear out the authors' statement because there is a large difference at the very point where the rate of change of acceleration is zero. But perhaps this was a purely instrumental difficulty. In the thesis (5 of the Bibliography), it is stated that it was "difficult to attain a high degree of accuracy in the early portions of the unsteady-flow runs." It would be interesting to know if subsequent tests have been made with negative acceleration, and, if so, whether the authors' theory was verified by the resistance to unsteady flow being greater than for steady flow.

One other minor point is that, with rapidly changing pressure difference, it is important that the pressures on the two sides of the differential gage represent simultaneous pressures at the two ends of the test length, and the velocity measurements correspond to that same time. It would seem that the leads to the differential gage should have been of equal length, and that the leads from the measuring nozzle should have been longer than these by about 90 in. Actually, they were somewhat shorter. As the velocity of pressure waves in copper pipe is of the order of 3700 fps, this might have put the pressure and velocity measurements some 0.003 sec out of phase. This is probably negligible in these experiments, but should be considered if further refinements are made.

Authors' Closure

The authors are grateful to Professors Jones and Powell for their objective discussions. In particular, they have raised certain questions regarding the test results which the following paragraphs will attempt to answer.

[5] Professor of Hydraulics, University of Kansas, Lawrence, Kan.

[6] Professor, Department of Mechanics, Ohio State University, Columbus, Ohio.

[7] "An Engineering Concept of Flow in Pipes," by C. W. Harris, Trans. ASCE, vol. 115, 1950, pp. 909–958.

[8] "Fluid Flow and Heat Transfer in Artificially Roughened Pipes," by H. Chu and V. L. Streeter, Final Report of Project No. 4918, Illinois Institute of Technology, 1949.

Accuracy in measurement of the difference between the pipe-friction factor for steady flow and that for unsteady flow depends on the ratio of acceleration head to total head drop. In order to keep this ratio reasonably high, the experimental program did not include unsteady flow velocities above approximately 75 ft per sec; consequently, inasmuch as the steady-flow results were considered only a necessary part of the unsteady-flow data, the steady-flow measurements did not extend far beyond those velocities.

Professor Jones' suggestion that more complete steady-flow pipe-friction data, especially at higher Reynolds numbers, should be obtained with the DDT cell, may be followed. Certainly, extensive high-caliber experimental work has been done on steady flow, but it would be interesting to see how rapidly an entire set of experiments could be run and still maintain a fair degree of accuracy.

Professor Powell is justified in pointing out the discrepancy in Fig. 11, but there appears to be ample evidence that the discrepancy is an experimental error rather than a phenomenon of the flow. As mentioned in Bibliography (5) and (6), the ranges of the electronic cells were set to give full-scale oscillograph chart deflection for the range of differential pressures desired in a given group of runs. In setting these ranges, the amplifiers and power supplies used in this experimental work frequently approached saturation at the extreme signals (at zero and max differential pressures). During runs, the extreme signals did cause some saturation, but no such saturation occurred in the central portions of the set ranges. In addition, as mentioned in this paper and in greater detail in Bibliography (5) and (6), the overall error in converting data from the oscillograph chart to numerical quantities is approximately $^3/_4$ per cent of full-scale deflection. The "fat and wiggly" nature of the line accounts for most of this error. Of course, the lower the differential pressure, the greater the actual error in converting data. Hence both the saturation and the data-conversion factors indicate that more weight should be given to data obtained in the central regions of the test range (such as shown in the central regions of Fig. 10) than that obtained in the lower ranges (such as in the early portions of Fig. 11). It might be noted that the power supplies and amplifiers have been redesigned recently to give greater capacity and to have more stability. The authors wish to emphasize that the experimental work reported herein was exploratory and the results were meant to be preliminary.

It is true that an impulse traveling through two different lengths of lead line will arrive at the cell diaphragm at different times and the magnitude of the possible error should be checked. In this work the precision with which the data could be obtained and plotted was not of sufficient order as to make a time delay of 0.003 sec significant. The cells were mounted on a sturdy framework independent of the tunnel structure, and the lead lines were made as short as possible to minimize inertial effects and difficulties arising from air entrainment.

A Photographic Study of Events in a 14-In. Two-Cycle Gas-Engine Cylinder

By R. L. BOYER,[1] D. R. CRAIG,[2] and C. D. MILLER[3]

The more important results are presented from a 2-year research program involving, it is believed, the first high-speed photographic records of events occurring within a very large engine cylinder. This research was performed on a co-operative basis by The Cooper-Bessemer Corporation and Battelle Memorial Institute. Involved in this study was a Cooper-Bessemer GMV engine, a two-cycle, spark-ignited engine of 14-in. bore and 14-in. stroke, which operates on natural gas. This engine is widely used for pumping natural gas through cross-country pipe lines. The photographs were made with the Battelle Isotran camera. Schlieren photographs were taken of combustion, exhaust blowdown, scavenging, gas turbulence, and fuel injection, through large glass windows mounted at various positions in the cylinder head and cylinder wall. All of these phenomena were rendered clearly visible in slow-motion pictures, and exact data were secured for all gas and flame velocities, as well as the crank angles involved in these events. The most important indication from the photographs is the basic nature of flow of scavenging air through the cylinder volume in turbulent jets, which apparently cannot be circumvented.

Introduction

PROBABLY the major problem confronting builders of two-cycle engines today is that of effective scavenging. Scavenging is of great importance in the engine because of its effect on the quantity of fresh air that is available for combustion. In surveying the field we find two principal methods of performing this function—loop scavenging and uniflow scavenging—each with its peculiar advantages and disadvantages. Likewise, there are many means for determining the effectiveness of the scavenging method used—static flow tests, charging-efficiency tests, fuel-air measurements—each again with its own idiosyncrasies.

In the design of its line of two-cycle angle compressors, the company chose to lean heavily on the static flow test as a means of design analysis. It was found that cylinders resulting from such design testing would compete successfully with cylinders designed by a variety of other means. It was not known, however, how the results of the static flow test compared with the actual aerodynamics of engine operation.

Because of interest in results obtained with high-speed photographic methods of analysis in smaller engines, it was proposed that such methods be used to analyze the scavenging processes and other events in large two-cycle engines. By making the photographs directly with a large cylinder, for example, a 14-in. GMV cylinder, problems would be avoided in correlating results involving a smaller cylinder.

High-speed photographs had been taken of combustion in engine cylinders up to 5 in. in diam. Never had photographs been made that showed the flow of air and gases in an operating engine cylinder. Nor had photographs shown engine combustion with natural gas. It was proposed that this investigation be directed toward obtaining photographs of the air and gas movements, including the combustion processes, in the much larger cylinder. A camera was needed capable of unusually high repetition rates and high resolution. Battelle Memorial Institute designed and built a camera having the required characteristics for photographic analysis of scavenging and combustion in the GMV engine.

The type-GMV angle compressor, the prototype of a series of angle compressors, integrates a 14-in. × 14-in., loop-scavenged, two-cycle gas engine with the compressor unit. These angle compressors have many applications as pumping engines, but cross-country gas pipe lines use the greater percentage of the engines built. Although the specific fuel consumption of the GMV engine was only 8300 Btu/bhphr (since reduced to 7500 Btu/bhphr), the importance of research contributing to better scavenging was recognized. The importance of such research is obvious when it is considered that 12,000,000 cu ft of gas per day would be saved as the result of a decrease in fuel consumption of only $^1/_2$ cu ft per bhphr in the more than 1,250,000 hp in installed GMV engines.

Much use has been made of the findings of this study, and it is believed that the results will continue to be useful. The more important information contained in the 4000 ft of 8-mm film exposed over the 2-year period of the investigation can now be released.

Summary

High-speed photographs were used in a study of ignition, flame propagation, fuel injection, exhaust blowdown, cylinder scavenging, and turbulence in a Cooper-Bessemer GMV engine. Photographs were exposed, through glass windows installed in cylinder walls and cylinder heads, with the Isotransport camera designed and built by Battelle Memorial Institute. The research, sponsored by The Cooper-Bessemer Corporation was conducted jointly by Cooper-Bessemer and Battelle personnel.

An important step accomplished during the early phases of the research was the complete elimination of lubricating oil in the combustion chamber of the engine. Such elimination of oil was essential to avoid its rapid deposit on the window and mirror surfaces within the chamber, which rendered photography impossible. An important incidental result of the research, therefore, was an indication as to where improvements might be made relative to oil consumption.

From the photographs, exhaust blowdown was seen to follow a pattern of laminar flow. Scavenging air, however, was found to enter the cylinder in turbulent jets. The inevitability of such jet action was fully predictable on a theoretical basis for any con-

[1] Vice-President and Chief Engineer, The Cooper-Bessemer Corporation, Mt. Vernon, Ohio. Mem. ASME.

[2] Assistant to Chief Research Engineer, The Cooper-Bessemer Corporation, Mt. Vernon, Ohio.

[3] Assistant Supervisor, Battelle Memorial Institute, Columbus, Ohio.

Contributed by the Oil & Gas Power Division and presented at the Spring Meeting, Columbus, Ohio, April 28–30, 1953, of The American Society of Mechanical Engineers. Re-presented at the ASME Oil and Gas Power Conference, May 25–28, 1953, Milwaukee, Wis.

 Manuscript received at ASME Headquarters, March 24, 1953. Paper No. 53—S-45.

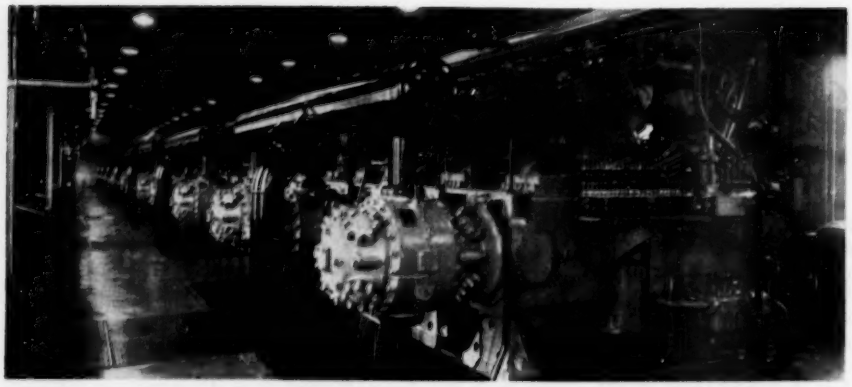

FIG. 1 TYPICAL COMPRESSOR STATION ON A CROSS-COUNTRY GAS-TRANSMISSION LINE

ceivable method of introducing air into the engine cylinder. Nevertheless, the existence of this phenomenon does not appear to have been recognized earlier. Recognition of such a nature of flow of air into any engine cylinder, suggested by the photographs obtained in this test program, is believed to be a significant advance in the understanding of engine operation.

The nature of scavenging-air flow shown by the high-speed photographs appears to support loop scavenging in preference to other types that have been considered and tested by other means.

Photographs have indicated that satisfactory turbulence is achieved, from a combustion standpoint, together with satisfactory mixing of the injected natural gas with the cylinder contents. The jet action of the scavenging air apparently contributes greatly toward turbulence.

APPARATUS AND EQUIPMENT

This joint research was done in the experimental laboratory of The Cooper-Bessemer Corporation, to which the Isotran camera was taken from Battelle. The tests were made on one cylinder of a standard four-cylinder Cooper-Bessemer GMV engine, a two-cycle gas-burning engine of 14-in. bore and 14-in. stroke.

A typical installation of ten-cylinder GMV engines, as used for the pumping of natural gas through transmission pipe lines, appears in Fig. 1. A transverse section of the engine is shown in Fig. 2. The master connecting rod drives the compressor crosshead; the connecting rods from the power cylinders are attached to the master rod with an articulated construction. Scavenging air is supplied by a reciprocating blower designed to function in the same space with the compressor crosshead. The engine operates on gaseous fuels that are delivered to the power cylinders under pressure and admitted to the cylinders when the piston is at low crank-angle positions. Exterior views of the engine are shown in Figs. 3 and 4.

High-Speed Camera. Fig. 5 shows the Isotransport camera designed and built by Battelle and first used in this study.[4] The Isotran camera exposes a series of approximately 500 frames, on standard 8-mm motion-picture film, in a single burst. The resolution of the photographs is approximately 20 lines per mm in all directions on the film. The repetition rate is variable from about 10,000 frames per sec to 100,000 frames per sec.

Modifications of GMV Engine for Schlieren Photography. Because of the normally invisible nature of the gases in the combustion chamber, the schlieren method[5] was needed to make visible

[4] "Isotransport Camera for 100,000 Frames Per Second," by C. D. Miller and A. Scharf, *Journal of the Society of Motion Picture and Television Engineers*, vol. 60, February, 1953, pp. 130–144.

[5] "Introduction to Aerodynamics of a Compressible Fluid," by H. W. Liepmann and A. E. Puckett, John Wiley & Sons, Inc., New York, N. Y., 1947, pp. 89–101.

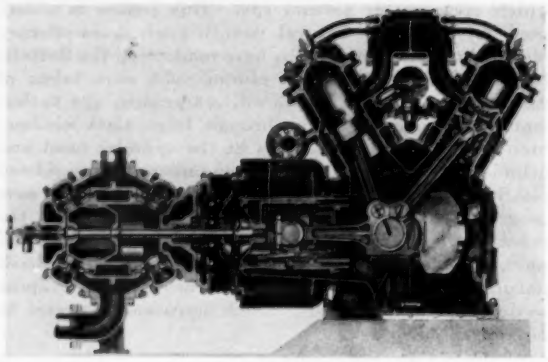

FIG. 2 TRANSVERSE SECTION OF GMV ENGINE WITH COMPRESSOR CYLINDER ATTACHED

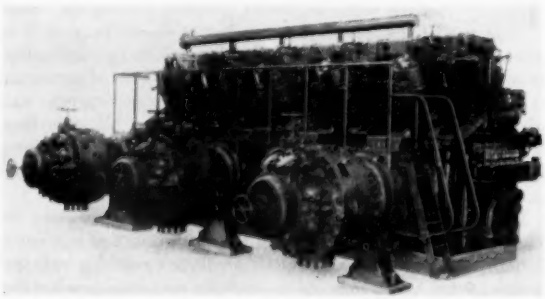

FIG. 3 EXTERIOR VIEW OF GMV ENGINE, COMPRESSOR SIDE

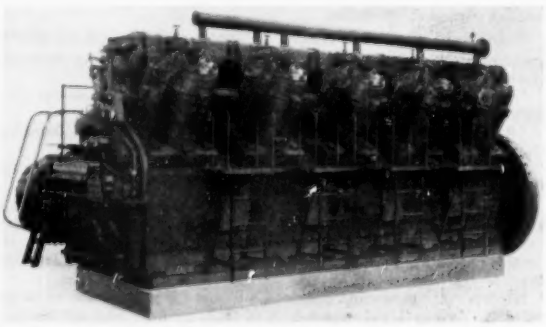

FIG. 4 EXTERIOR VIEW OF GMV ENGINE, OPERATING SIDE

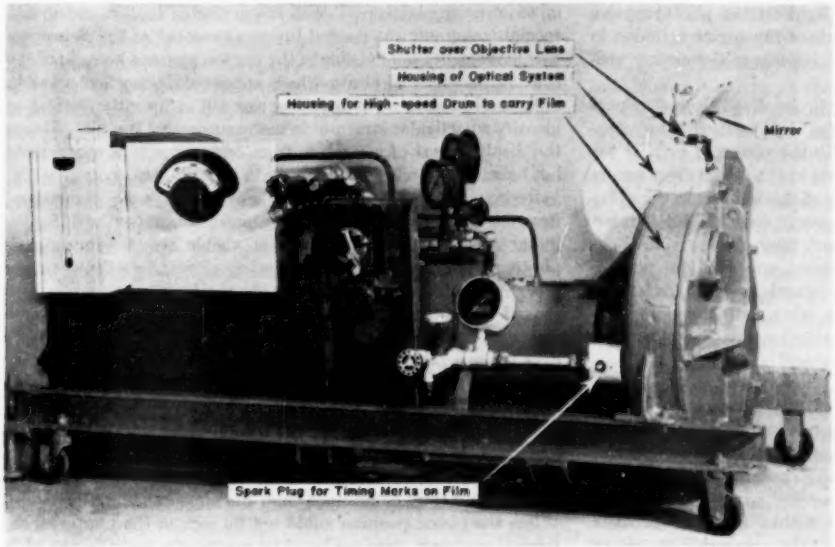

FIG. 5 ISOTRANSPORT CAMERA FOR OPERATION IN SPEED RANGE FROM 10,000 TO 100,000 FRAMES PER SEC

the processes of exhaust blowdown, scavenging, fuel injection, and turbulence. The schlieren method allows some invisible processes to become visible by utilizing the variations in optical density, or index of refraction, of the gases. The schlieren method, involving the use of a light source external to the engine, also was used for photography of combustion. The light radiated by the burning gases was not sufficient for exposure at the rates used.

Only one cylinder of the test engine was used for photography. The engine was brought up to speed by use of the other three cylinders. The test cylinder was then operated for only a few cycles before and after the cycle photographed.

Special cylinders, heads, and pistons were cast and machined for the test engine to accommodate glass windows and mirrors used in the construction of five schlieren optical arrangements. These optical setups provided three views into the test cylinder through the head, and two views through the cylinder wall.

A considerable amount of work was done on the test engine to eliminate the passage of oil into the combustion chamber. Oil in quantities so small as to be of no importance whatever in normal engine operation formed a fog on the glass windows in the cylinder head and walls so quickly that photographs could not be taken.

Photographic Test Setups. In all of the photographic test setups, two of which are illustrated in Figs. 6 and 7, an external light source was used. An image of this light source was formed by the condensing lenses shown in these figures upon the surface of a mirror located just above the lens of the camera. Light reflected from that mirror was collimated by the schlieren-head lens and passed on to the test engine by one or more plane mirrors. After passing into the engine cylinder through a glass window, the light was reflected back out through the same window by a mirror on the top of the piston or in the cylinder wall. The light then followed its earlier path in reverse, passed again through the schlieren-head lens, and was refocused by that lens to form a second image of the light source just above the objective lens of the camera. The mirror just above the camera lens now served the additional function of a knife-edge relative to the light returning from the engine, as required in a schlieren system. The camera

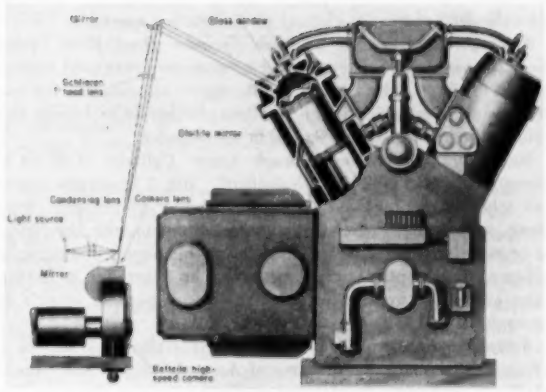

FIG. 6 EXPERIMENTAL ARRANGEMENT FOR SCHLIEREN PHOTOGRAPHY THROUGH CYLINDER HEAD OF GMV ENGINE

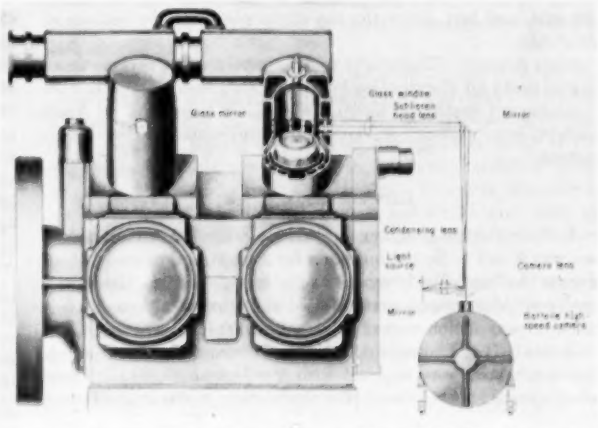

FIG. 7 EXPERIMENTAL ARRANGEMENT FOR SCHLIEREN PHOTOGRAPHY THROUGH LOWER CYLINDER WALL IN DIRECTION PARALLEL TO AXIS OF CRANKSHAFT

lens then was enabled to focus this light on the photosensitive film, forming an image of the contents of the engine cylinder, in a manner such as to render optical inhomogeneities clearly visible.

Setup for Photographs Through Cylinder Head Opposite Spark Plug. Fig. 6 shows one of the optical setups used for photography through the cylinder head with the piston at or near top center. A stellite mirror was mounted in the top of the piston as shown. The exact angular positions of the window in the cylinder head and of the stellite mirror, however, were 135 deg counterclockwise from the position of the spark plug, as seen from above the cylinder. This optical arrangement was used for photography of turbulence and of flame travel in its later stages. Throughout this paper, photographs taken with this optical arrangement will be referred to as having been exposed "through the cylinder head opposite the spark plug."

Setup for Photographs Through Cylinder Head in Vicinity of Igniting Spark. For photography of turbulence and of flame travel in its earliest stages, an arrangement similar to that of Fig. 6 was used, but with the glass window and the stellite mirror in the same angular position as the igniting spark. For these photographs a special spark plug was provided with long electrodes that projected to a position well within the field of view. Throughout this paper, photographs taken with this optical arrangement will be referred to as having been exposed "through the cylinder head in the vicinity of the igniting spark."

Setup for Photographs Through Cylinder Head With Piston Near Bottom Center. Yet another arrangement was used similar to that of Fig. 6 but with the stellite mirror relocated on the top of a piston of an older design to allow photography through the cylinder head with the piston low in the cylinder.

Setup for Photographs Through Lower Cylinder Wall in a Direction Parallel to Axis of Crankshaft. Fig. 7 illustrates one of the schlieren arrangements for photography of exhaust blowdown, scavenging, turbulence, and fuel injection with the piston at or near bottom center. Throughout this paper, photographs taken with this optical arrangement will be referred to as having been exposed "through lower cylinder wall parallel to axis of crankshaft."

Setup for Photographs Through Lower Cylinder Wall, in a Direction Perpendicular to Plane of Axes of Cylinder and Crankshaft. A schlieren arrangement similar to the one shown in Fig. 7 was used in some tests, but with the optical axis perpendicular to the optical axis shown in Fig. 7. In this case, also, the optical axis passed through the cylinder perpendicular to the cylinder axis, and just above the top of the piston at the bottom of its stroke.

Light Sources. Three light sources were used at various times in this study for illumination in the schlieren system: A 500-watt incandescent projection lamp, a carbon-arc lamp, and an Ames high-pressure mercury-arc lamp of approximately 20,000-lumen output.

Experimental Work

Early in the test program, a repetition rate of 20,000 frames per sec was found to be the optimum for a slow-motion study of all events that could be observed in the test cylinder. Hence virtually all photographs were exposed at that rate, although a few shots of combustion were obtained at 50,000 frames per sec.

A total of 648 photographic shots, each comprising 6 ft of standard 8-mm film, were exposed with the Isotran camera. These photographs showed clearly the combustion, turbulence, exhaust blowdown, scavenging, and fuel injection. Flame fronts were defined sharply, and their velocities could be measured easily.

Although turbulence, exhaust blowdown, scavenging, and fuel injection were plainly visible in the projected motion pictures, a special technique was needed for measurement of the velocities. The movements were visible in the motion pictures because of the shifting positions of strata which appeared as mottled areas in individual frames. The mottling was not sufficiently distinct to identify a particular stratum[6] in many successive frames. Hence the displacement of a stratum from one frame to another could not be measured with a linear scale in the still photographs.

Reproducible velocities of all movements were determined from the projected motion pictures, notwithstanding the difficulty in measuring the displacements of visible strata between one photographic frame and another when viewed as stills. An observer projected a spot of light on the motion-picture screen, and moved this spot by hand in the same direction and at the same speed as the moving strata. It proved easy for the observer's eyes to integrate the motion of all visible strata in the motion pictures, even though an individual stratum remained visible throughout only a comparatively few frames. A second observer used a stop watch to note the time required for transit of the projected spot of light across a marked distance on the screen.

Whenever possible in the analysis of the photographs, the crank angles were determined from the appearance of the piston. When the piston position could not be seen in the photographs, fiducial markings were produced by means of a special spark plug and a miniature projector mounted in the camera. The spark plug was energized by a contactor on the engine.

In addition to directions and speeds of flame and gas movements, crank angles were determined for various events, such as the start of visible combustion, the beginning and end of the exhaust blowdown, the beginning and end of visible flow of scavenging air, and the appearance of injected fuel.

Findings and Results

The high-speed photographs obtained in the test program have fully provided the information that was expected of them. Much of this information is believed to be of wide general interest.

When the photographs are projected on a screen as a motion picture, the movements of gases are clearly visible. However, the motion pictures are of little value in the form of reproductions as "still" photographs. The photographs must be projected as a motion picture to allow study of the motions that will be discussed, or even to permit those motions to be seen. Hence reproductions of the high-speed photographs as figures in this paper will be minimal.

Elimination of Lubricating Oil in Combustion Chamber. During the first few days of the experimental work it became apparent that the luminosity of the flame was too feeble to permit photography at the speeds needed, or even at much lower speeds. Hence preparations were made to obtain schlieren photographs of the flame. However, success with the schlieren system demands scrupulously clean optical elements throughout, including the glass window in the cylinder head and the stellite mirror mounted on the top of the piston. It was soon found that the slight amount of oil reaching the combustion chamber quickly created a fog on the glass window and on the stellite mirror, preventing schlieren photography.

During a period of many weeks, the manner in which oil reached the combustion chamber was investigated and various

[6] Throughout this paper the term "stratification" will be used in a manner common in the terminology of engine operation, for which the term "striation" might be more accurate. Stratification will be understood here to refer to three-dimensional inhomogeneity, rather than to two-dimensional layers. Likewise, the term stratum will be used to refer to a three-dimensional region appearing homogeneous within itself in the schlieren photographs, but appearing to be of different optical density from its environment.

means were invented and tried to eliminate the difficulty. Virtually complete success was achieved finally in keeping oil out of the combustion chamber, to a greater extent even than would be desirable in a continuously operating engine. Moreover, the means used were more involved than would be justified in a practical operating engine.

The most important of the various means to reduce the passage of oil into the combustion chamber included circumferential grooves around the exterior surface of the piston, extending at intervals of 1 in. from a point just above the ring band at the bottom of the piston to a point just below the upper ring band. These grooves were utilized as part of a drainage system created by means of the following:

1 A longitudinal groove cut in the wall of the piston, on the exhaust side, extending from the uppermost circumferential groove to the lowest such groove just above the upper oil-control ring.

2 Each of the circumferential grooves in turn during each cycle of operation.

3 A groove cut in the interior cylinder wall below the inlet ports and extending around one quarter of the circumference of the cylinder.

refraction in a direction perpendicular to the light rays through which the light rays traveled only a short distance.

With the necessarily qualitative nature of the schlieren indications understood, the photographs indicate that stratification of residual combustion products and scavenging air persists in the cylinder of a two-cycle engine up to the time of combustion. The scale of the individual strata, as projected on a plane perpendicular to the optical axis of the photographic setup, was always of the order of a few tenths of an inch.

In photographs exposed through the cylinder head opposite the spark plug, without fuel injection either on the test cycle or on the preceding cycle, stratification usually was visible throughout the crank-angle range from 50 deg BTC to top center, but not earlier. The crank angle at which stratification became visible was advanced somewhat ahead of 50 deg BTC with fuel injection during the test cycle, but without firing on the preceding cycle. The crank angle at which stratification appeared became still further advanced, to about 80 deg BTC, with fuel injection on the test cycle and firing on the preceding cycle. These facts support the opinion that stratification visible throughout the crank-angle range near top center involves strata of both residual combustion products and injected fuel as well as scavenging air.

FIG. 8 SCHLIEREN SYSTEM IN FORM USED FOR PHOTOGRAPHS TAKEN IN THIS INVESTIGATION ILLUSTRATING STRATA OF TWO TYPES WHICH ARE VISIBLE IN PHOTOGRAPHS

(A, Stratum of uniform optical density. B, Stratum with gradient of index of refraction in direction perpendicular to light rays.)

4 A drain hole drilled through the side of the cylinder below the inlet ports and registering with the groove mentioned in item 3.

A vacuum pump was connected to the drain hole (item 4). A flow of air originated at one of the exhaust ports and progressed through the longitudinal groove in the piston, to each circumferential groove. As the individual grooves on the piston reached the level of the drain hole and the groove in registration with it, the oil was removed. Continuous removal of oil in this manner virtually eliminated passage of oil into the combustion chamber.

Stratification of Residual Products of Combustion and Scavenging Air. If no stratification whatever existed in the engine cylinder, involving either the residual products of combustion or the injected gaseous fuel, no schlieren photographs would have been possible except those of flame. However, the indications of the schlieren photographs are irretrievably qualitative as to the nature of the stratification that exists.

Fig. 8 illustrates two types of strata which become visible in schlieren photographs, a wedge-shaped stratum of uniform optical density but of different optical density from its surroundings, and a stratum having parallel surfaces through which light rays pass into and out of the stratum but having a gradual variation of optical density within itself at right angles to the light rays. Combinations of these two types of strata also can be seen. No data are available in a schlieren photograph to determine whether a particular light spot, or dark spot, is caused by (1) a sharp wedge of very high or very low optical density relative to its surroundings, (2) a blunt wedge differing less from its surroundings in optical density, (3) a parallel-sided stratum having a low gradient of index of refraction in a direction perpendicular to the light rays but through which the light rays traveled a great distance, or (4) a parallel-sided stratum having a high gradient of index of

Why stratification becomes more clearly visible as top center is approached is not well understood. This occurrence may be caused by the fact that the distance of travel of the light beam through the gases within the cylinder diminishes as the piston approaches top center. The optical arrangement was adjusted for the best focus on the film with the piston at top center. Hence with the piston down a considerable distance from top center, most of the strata within the cylinder would be out of focus on the film. Their optical effect would be that of obscuring to some extent the strata that were in focus.

Stratification of Injected Fuel and Scavenging Air. The effect of injection of fuel in causing stratification of the cylinder charge to become visible at an earlier crank angle was mentioned in the discussion of the stratification of residual combustion products with scavenging air.

In the photographs exposed in both directions through the lower cylinder wall, the flow of injected fuel was distinctly visible even near the top of the piston. The photographs indicated that the gaseous fuel tended to flow down through the center of the cylinder to the piston top, rather than to mix thoroughly with the air within the cylinder on its way down. However, the photographs indicated that the subsequent turbulence and swirl of the cylinder contents provided adequate mixing of the fuel and air.

Moreover, efforts to eliminate the flow of injected fuel through the cylinder contents by redesign of the injection valve were not fruitful in the sense of improving performance. Apparently the mixing effect of turbulence and swirl subsequent to fuel injection is so effective that the actual manner of entrance of fuel is not of great importance.

Disappearance of Stratification After Top Center. A phenomenon observed with the igniting spark unduly retarded was the disappearance of visible stratification after top center and before

the passage of the flame through the visible gases. The reason for this occurrence is not known.

Velocities of Flow From Inlet Ports and Toward Exhaust Ports. Fig. 9 shows directions and the speed of flow of combustion products during the exhaust blowdown period as determined from

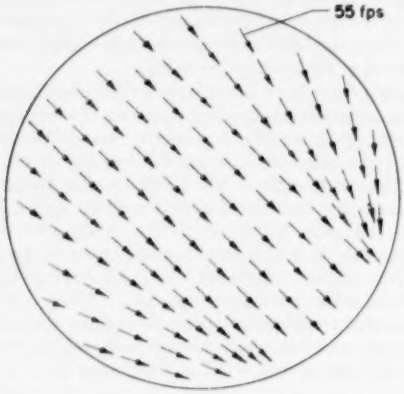

FIG. 9 VECTORS REPRESENTING AVERAGE DIRECTIONS AND SPEED OF FLOW OF PRODUCTS OF COMBUSTION DURING EXHAUST BLOWDOWN IN GMV ENGINE, AS DETERMINED FROM PHOTOGRAPHS EXPOSED THROUGH LOWER CYLINDER WALL PARALLEL TO AXIS OF CRANKSHAFT

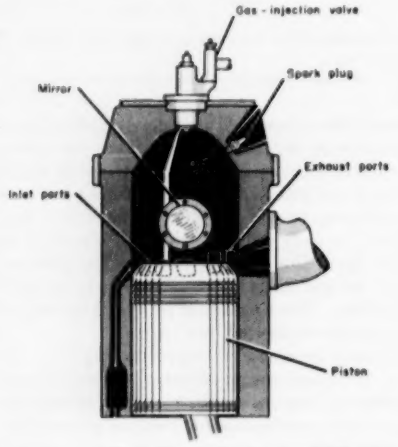

FIG. 10 SECTION OF TEST CYLINDER SHOWING ORIENTATION OF FIELD OF VIEW FOR PHOTOGRAPHY THROUGH CYLINDER WALL

ten high-speed photographic shots exposed through the lower cylinder wall parallel to the axis of the crankshaft.

Fig. 10 shows the location and orientation of the projected area included in the photographs used for the construction of Fig. 9. The mirror shown in Fig. 10, of 5 in. diam, is identical with the projected area covered by the photographs.

For each photographic shot used in the construction of Fig. 9, the average velocity of gas movement was determined for the entire blowdown period. The resulting averages for the individual cases were then combined to form the average of 55 fps used in the figure. The blowdown started at 125 deg ATC and ended at 151 deg ATC on the average, as seen in the photographs.

Fig. 11 shows the four dominant motions during the scavenging period determined from high-speed photographs exposed through the lower cylinder wall parallel to the axis of the crankshaft. The vectors directed diagonally upward and toward the right represent

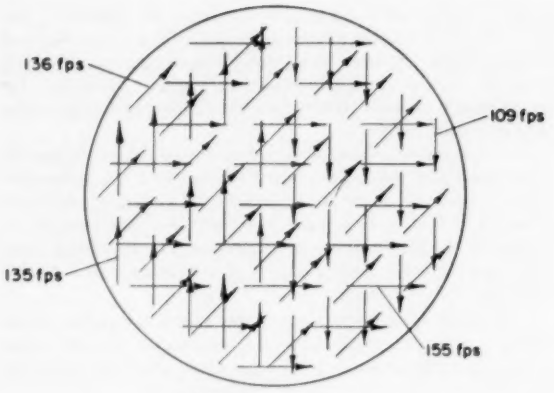

	Diagonal movement upward toward right throughout field	Upward movement in left half of field	Movement toward right throughout field	Downward movement in right half of field
Average speed, fps	136	135	155	109
Average crank angle for beginning of movement, deg ATC	156	156	156	156
Average crank angle for end of movement, deg ATC	226	226	226	226

FIG. 11 DOMINANT GAS MOVEMENTS WITHIN CYLINDER OF GMV ENGINE DURING SCAVENGING PERIOD, AS DETERMINED FROM HIGH-SPEED PHOTOGRAPHS THROUGH LOWER CYLINDER WALL PARALLEL TO AXIS OF CRANKSHAFT

the motion most apparent of all in the motion pictures, directly away from the inlet ports. The vectors extending directly upward in the left-hand side of the field of view, and those extending directly downward in the right-hand side of the field, represent other motions clearly visible. These motions are in accordance with the design intent of loop scavenging. The fourth type of vector in the figure extending directly toward the right represents a motion, not prominent, following a short circuit from inlet ports to exhaust ports. From 6 to 25 high-speed photographic shots were used for the determination of each average represented in Fig. 11. The averages shown in the tabulation in the figure were determined from averages of the individual cases, as with Fig. 9.

Combustion Quality. All photographs of combustion obtained through the cylinder head, both in the vicinity of the igniting spark and opposite the spark plug, have demonstrated that flame reaches all parts of the combustion chamber. Hence stratification cannot be of such a degree that nonflammable strata of appreciable dimensions exist within the combustion chamber at the time of the flame travel.

No definite indication of autoignition of the cylinder charge was found in the photographs under any of the test conditions.

Fig. 12 is a reproduction of 220 individual frames from a high-speed photographic shot exposed at 20,000 frames per sec with the Isotran camera through the cylinder head in the vicinity of the igniting spark. The intervals between consecutive frames in this figure are only 50 microsec. The order of succession of the frames is from 1 to 20 through each row of the photographs. The ignition spark occurred at the location within the chamber indicated in frame A-5, at the intersection of two electrodes consisting of long wires which are visible in each frame. The time of the igniting spark, however, is not established, and probably did not occur at the same time as the exposure of frame A-5. The first visible flame appears at about frame C-4 as a dark mottled area. The flame spreads throughout the visible part of the chamber in frames C-4 to about H-8, and disappears during the exposure

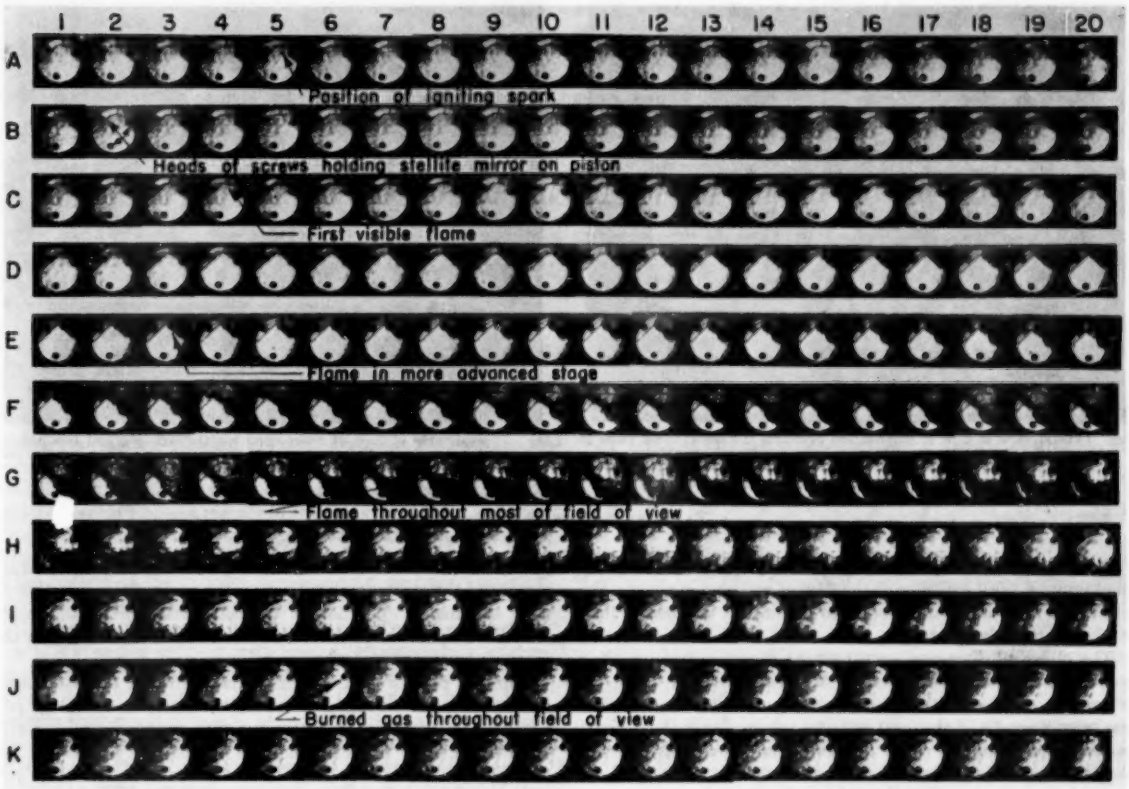

FIG. 12 HIGH-SPEED SCHLIEREN PHOTOGRAPH OF FLAME TAKEN THROUGH WINDOW IN CYLINDER HEAD OF COOPER-BESSEMER GMV ENGINE AT 20,000 FRAMES PER SEC WITH ISOTRAN CAMERA

of frames H-8 to J-6. The mottled appearance throughout the field of view in the frames before the appearance of the flame, A-1 to C-4, and after the disappearance of the flame, J-6 to K-20, is caused by stratification of the gaseous contents of the combustion chamber. It is the movement of this mottling in the projected motion pictures that makes possible the determination of velocities of gas motion, not only within the combustion chamber just before and just after burning, but also in the lower part of the cylinder during the processes of exhaust blowdown, scavenging, and fuel injection.

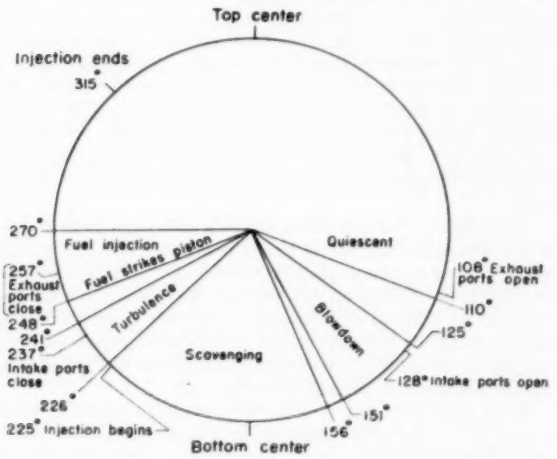

FIG. 13 AVERAGE CRANK-ANGLE RANGES COVERED BY EXHAUST BLOWDOWN, SCAVENGING, TURBULENCE AFTER SCAVENGING, AND FUEL INJECTION, AS SEEN IN ALL HIGH-SPEED PHOTOGRAPHS EXPOSED THROUGH LOWER CYLINDER WALL PARALLEL TO AXIS OF CRANKSHAFT

Quality of Scavenging. Of much importance in any two-cycle engine is any possible improvement in the scavenging efficiency. Some of the most interesting and valuable data available from the high-speed photographs are concerned with scavenging.

Crank-Angle Ranges Covered by Exhaust Blowdown and Scavenging. Fig. 13 shows graphically the average crank-angle ranges covered by exhaust blowdown, scavenging, turbulence after scavenging, and fuel injection, as seen in all of the photographs exposed through the lower cylinder wall parallel to the axis of the crankshaft. Also shown in Fig. 13 are the known crank angles for opening and closing of the exhaust and inlet ports, and the known crank angle for the beginning of fuel injection.

Of interest, among the results shown in Fig. 13, is the discrepancy between the crank angles for the beginning and end of various events as seen in the photographs and the known crank angles for opening and closing of the exhaust and inlet ports. The first indication of exhaust blowdown appears in the photographs 20 crankshaft deg after the first opening of the exhaust ports. Blowdown continues until 23 deg after the first opening of the inlet ports. Even so, a period of complete quiescence in the visible part of the cylinder is reached after the end of the blowdown period, and persists until 28 deg after the first opening of the inlet ports, at which time the first indication of the flow of

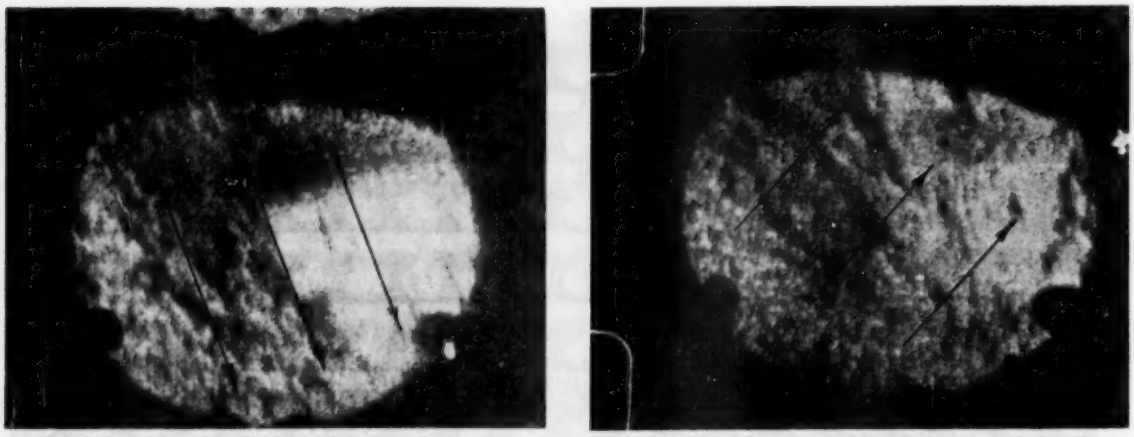

(*a*) Typical view of flow of combustion products toward exhaust ports in laminar streamlines. Stratification is predominantly parallel to direction of flow shown by arrows.

(*b*) Typical view of flow of scavenging air through residual products of combustion in turbulent jets. Stratification is predominantly perpendicular to direction of flow shown by arrows.

FIG. 14 ENLARGED FRAMES FROM HIGH-SPEED PHOTOGRAPHS EXPOSED THROUGH LOWER CYLINDER WALL PARALLEL TO AXIS OF CRANKSHAFT

scavenging air into the visible part of the cylinder appears in the photographs. All evidence of the flow of scavenging air into the visible part of the cylinder ends 13 crankshaft deg before final closing of the inlet ports.

The observed discrepancies cannot be considered as revealing weird and unexpected behavior of the gases. Instead, these discrepancies emphasize the facts that gases possess inertia, that gas must flow out of the local cylinder volumes near the exhaust ports before it can flow out of the more remote parts of the cylinder, that time must elapse between the flow of scavenging air through the inlet ports and the arrival of the air in the visible part of the cylinder, that both inlet and exhaust ports have comparatively minute flow areas until a considerable number of crankshaft degrees after their first opening, and that the ports also have comparatively minute flow areas for a considerable number of crankshaft degrees before their final closing.

Flow of Scavenging Air in Turbulent Jets. Of greatest interest among all the facts revealed by the high-speed photographs is the discovery that the scavenging air in any engine must project from the inlet ports through the cylinder contents in high-speed turbulent jets.

Fig. 14 presents greatly enlarged prints of two frames of typical high-speed photographs exposed through the lower cylinder wall parallel to the axis of the crankshaft. Frame (*a*) in this figure is a typical view of the flow of the combustion products toward the exhaust ports. The visible stratification aligns well with the directions of the arrows that have been drawn on the photograph, directed toward the exhaust ports. Frame (*b*) is a typical view of the flow of scavenging air through the residual combustion products. The arrows that have been drawn in this photograph are directed away from the inlet ports, in the observed predominating direction of flow of scavenging air. In this photograph the visible stratification forms lines perpendicular to the direction of flow of the scavenging air.

No theoretical reason is offered for the alignment of stratification parallel with the laminar flow of gases toward the exhaust ports, and perpendicular to the turbulent flow of the scavenging air from the inlet ports. Although this condition is observed in the photographs, it was not depended upon for the conclusions as to the nature of the flow.

For a true appreciation of the jet-type flow of scavenging air from the inlet ports, the photographs must be viewed as motion pictures. The condition then is evident on the basis of actual motion of the strata, rather than on the basis of the direction of their alignment. The flow of the combustion products toward the exhaust ports in perfect streamlines also is seen clearly in the motion pictures on the same basis.

Laminar flow of combustion products toward exhaust ports, and the flow of scavenging air from inlet ports in turbulent jets constitute a condition in harmony with experience with fluids outside engines. For example, the air leaving an electric fan proceeds for many feet away from the fan as a turbulent jet. The air approaching the fan from the rear, however, flows in streamlines. Likewise, the flow of a liquid out of a tank through a small aperture involves only laminar movement of the liquid within the tank. However, water flowing into a tank through a small aperture inevitably projects through a large part of the body of water within the tank in turbulent jets.

In any high-speed flow through an orifice, kinetic energy must be acquired by the fluid as it passes through the orifice. Such kinetic energy can be dissipated only in turbulence, unless the fluid issuing from the orifice can be made to encounter a positive gradient of pressure to slow it down without turbulence, as in a diffuser. Before the necessary turbulence can be created, for dissipation of this kinetic energy of the fluid issuing from the orifice, the fluid must flow some distance through the surrounding substance as a jet, gradually entraining the surrounding, comparatively stagnant, fluid and setting up a swirl-and-eddy pattern.

Hence issuance of scavenging air from inlet ports as turbulent jets is probably unavoidable in any practical design. The only known way of avoiding such jets would be by means of a diffuser, which is impractical to construct within the cylinder volume. Because of the difficulty of eliminating turbulence in the scavenging air, the condition probably should be accepted as inevitable, and the engine design should be evolved around the concept of using the turbulent jets in the most effective manner.

In the best scavenging systems, the scavenging efficiency is only a little better than that computed on the assumption that all inlet air is mixed uniformly with all the contents of the cylinder at the instant it passes through the inlet ports. This fact is not difficult to understand in view of the discovery of the flow of the inlet gas in turbulent jets. This nature of the flow of the scavenging air is of particular interest relative to the question of substituting uni-

flow scavenging for the loop scavenging now used in the GMV engine.

The theoretical advantage of uniflow scavenging is based on the assumption that the inlet air will decelerate to a virtual standstill immediately after passing through the inlet ports or inlet valves, and that the inlet air will assume the form of a laminar piston to push the combustion products ahead of it toward the exhaust ports. A true understanding of the unavoidable nature of the flow of gas into the cylinder not only removes the assumed theoretical advantage of the uniflow type of scavenging, but suggests an actual theoretical advantage for loop scavenging.

The jet effect of the scavenging air as seen in projected motion pictures is so great that the scavenging air may reach the upper parts of the cylinder before it becomes excessively mixed with the residual combustion products from the preceding cycle, and before its kinetic energy is materially dissipated in a swirl-and-eddy pattern. Hence the result of admission of scavenging air through ports at the bottom of the cylinder, directed upward, appears to be much the same as that anticipated in the principle of uniflow scavenging. During the early stages of the scavenging process, except within the jets where the scavenging air is unavoidably on its way upward, the concentration of scavenging air probably builds up more rapidly in the upper part of the cylinder volume than elsewhere. As a consequence, during the early part of the scavenging process, the gas flowing out of the exhaust ports at the bottom of the cylinder should consist preponderantly of combustion products from the preceding cycle.

Although no photographs have been taken of scavenging action in a GMV engine cylinder with uniflow scavenging, extensive tests have been made with such a cylinder. Entrance of scavenging air should be expected to occur in the form of jets, just as with loop scavenging. In this case, as with the loop-scavenged cylinder, a high concentration of scavenging air should be expected to build up early in the scavenging process at the opposite end of the cylinder from the inlet. Exhaust at the opposite end of the cylinder, therefore, should permit the gases containing this higher concentration of scavenging air to leave the cylinder throughout a large part of the scavenging period.

In agreement with this reasoning, tests made with uniflow scavenging with a GMV engine cylinder[7] indicated somewhat reduced efficiency and power output as compared with the loop-scavenged cylinder. Although tests with uniflow and other scavenging methods are continuing, the results of the tests already made, the apparent theoretical advantage for the loop-scavenged cylinder on the basis of the photographic results, and the expense involved in setting up the uniflow-scavenged cylinder for photographic tests have discouraged effort in this direction.

Although the turbulent jets issuing from the inlet ports are undesirable from the standpoint of any effort to produce a laminar "piston of air" to push the residual combustion products out of the cylinder, this jet-type flow is of inestimable value in setting up the turbulence necessary for good combustion and regularity of firing. The need of turbulence to obtain satisfactory combustion in engine cylinders has long been known.

Maximal velocity of scavenging-air jets may tend to produce a swirl-and-eddy pattern involving the entire contents of the cylinder, even in the earliest stages of the scavenging process. From the standpoint of scavenging efficiency, such a condition would be inferior to that in which the scavenging jets enter the cylinder at a more moderate velocity, beginning to lose appreciable kinetic energy by the time they reach the opposite end of the cylinder.

Large port areas and comparatively low scavenging pressures should provide the desired compromise between the extreme conditions of (1) insufficient velocity of scavenging air to produce satisfactory turbulence; and (2) excessive velocity of scavenging air which might reduce scavenging efficiency.

Nature of Fuel Injection. As with the scavenging air, injected gaseous fuel inevitably must project through the contents of the cylinder in turbulent jets. The indicated slight importance of this fact from the standpoint of mixing in the GMV engine has been discussed already.

The photographs, as shown in Fig. 13, indicate that the injected fuel strikes the top of the piston at 248 deg ATC on the average. Although the exhaust ports are not fully closed until 9 crankshaft deg later, probably little injected fuel is lost through the exhaust ports for three reasons; i.e., (1) because the fuel, at 248 deg ATC, strikes the piston only in its axial area, (2) because the exhaust ports present only a small flow area during the 9 crank-angle deg preceding their final closing, and (3) because 11 crankshaft deg after the final closing of the inlet ports the pressure within the cylinder is not much greater than the pressure in the exhaust manifold. Earlier tests by other methods had shown that virtually no unburned fuel is lost through exhaust.

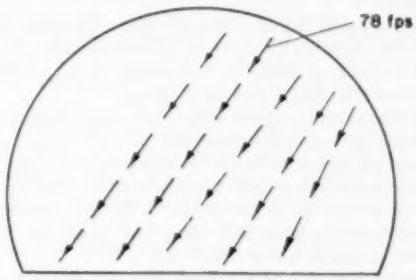

FIG. 15 VECTORS REPRESENTING AVERAGE DIRECTIONS AND SPEED OF FLOW OF INJECTED FUEL, AS SEEN IN HIGH-SPEED PHOTOGRAPHS THROUGH LOWER CYLINDER WALL PARALLEL TO AXIS OF CRANKSHAFT

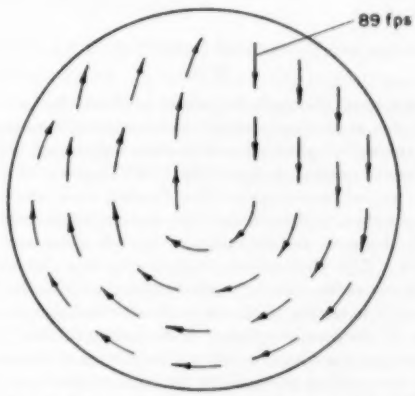

FIG. 16 VECTORS REPRESENTING AVERAGE DIRECTIONS AND SPEED OF AIR SWIRL AFTER SCAVENGING, AS SHOWN BY PHOTOGRAPHS EXPOSED THROUGH LOWER CYLINDER WALL PARALLEL TO AXIS OF CRANKSHAFT

Fig. 15 shows the average directions and the speed of flow of injected fuel at the time the fuel strikes the top of the piston, as determined from the photographs exposed through the lower cylinder wall parallel to the axis of the crankshaft. The average velocity was 78 fps. The average direction of flow is at a considerable angle to the axis of the cylinder because of the effect of the air swirl produced by closing of the scavenging loop after the closing of the inlet ports.

[7] The results of these tests will be reported in detail by J. D. Hines and T. O. Kuivinen in a later publication.

Turbulence of Fuel-Air Charge. As has long been known, a considerable degree of turbulence of the fuel-air mixture is necessary for good combustion in an engine cylinder. Even with a perfectly premixed charge, the rate of flame propagation in a stagnant gas is too low for the completion of combustion within the brief period available with the piston in the vicinity of top center.

According to the design intention for the GMV engine, upon final closing of the inlet and exhaust ports the scavenging loop should close to form a circular flow of the air charge. It was hoped that this flow would break up into small-scale eddies, so that adequate turbulence would exist for satisfactory combustion at top center.

The photographs indicate that the design intention has been accomplished fully with respect to turbulence, although the jet effect of scavenging probably contributes more to turbulence than does the closing of the scavenging loop.

Fig. 16 shows vectors representing the average directions and the speed of gas movements representing air swirl after the end of the scavenging period, as shown by photographs exposed through the lower cylinder wall parallel to the axis of the crankshaft. The average speed of the gases was 89 fps. This figure illustrates that the intended closing of the scavenging loop to produce a circular swirl of the air charge was well achieved.

Movements of the fuel-air charge were determined from schlieren photographs exposed through the cylinder head opposite the spark plug. Rapid motions were visible simultaneously in several different directions. At times the speeds of some of the local motions were twice as great as the general speed of the entire mass of gas.

Discussion and Evaluation of Results of Experimental Work

The high-speed photographs present evidence that is in general support of a static-flow method of analysis of scavenging, involving the use of pitot tubes and other equipment, which was applied in the original design of the GMV engine. Observation of many feet of photographic film showing cycle after cycle of engine operation indicates that the scavenging pattern is substantially the same as that indicated by this static-flow method of analysis. The photographs show clearly, however, that scavenging air enters the cylinder in highly turbulent jets, thus causing an unavoidable mixing of the fresh air with the remnant exhaust products of the previous cycle. This finding substantiates previous evidence pointing to nearly perfect mixing of the scavenging air with the exhaust products as the usual rather than the rare case. With this point brought so clearly to mind by the photographs, resort to the four-cycle principle naturally was considered. This principle, of course, does not depend upon an air piston for scavenging. The four-cycle engine, however, is regarded as being subject to serious weight and space handicaps as compared to the two-cycle engine of the same horsepower.

The photographic evidence that the gaseous combustion is continuous throughout the range of burnable fuel-air ratios indicates that satisfactory mixing is achieved in the cylinder. Inadequate mixing would result in areas of rich and lean mixtures, some of which might not propagate the flame. Of importance in consideration of fuel economy are the pictures showing fuel gas striking the crown of the piston. This indication is a striking example of the value of high-speed photography in research. These pictures confirm with great certainty the fact that no fuel is lost to the exhaust.

Conclusions

The following conclusions appear to be justified on the basis of the high-speed photographs which have been studied in this investigation:

1 Stratification of residual combustion products and injected fuel in the scavenging air at the time of combustion is of small scale, individual strata having dimensions not greater than one or two tenths of an inch.

2 Stratification, either of the fuel or of the residual gas, in the scavenging air, is not of sufficient degree to prevent burning within any part of the combustion chamber.

3 Scavenging air enters the cylinder through the inlet ports in the form of turbulent jets, which project through the entire cylinder charge at high speed and promote intimate mixing of the scavenging air with the residual combustion products.

4 The design intention of a scavenging loop in the GMV engine cylinder is achieved approximately, but is modified by the jet effect of the scavenging air.

5 A highly satisfactory degree of turbulence at the time of combustion is achieved.

Acknowledgments

E. M. Bash of Battelle was of inestimable aid in the conduct of the experimental work. He conducted the details of the high-speed photographic part of the work earnestly, with great competence, industry, and enthusiasm. Also, the authors are indebted to J. D. Hines and B. C. Bicksler of The Cooper-Bessemer Corporation, and to R. A. Lawrence of Battelle, for continuous close co-operation, helpful suggestions, and active and capable participation in the test work.

Discussion

W. M. Kauffmann.[8] The authors are to be congratulated on a significant approach to the study of two-cycle spark-ignition combustion.

Certain conclusions and inferences have been made with respect to uniflow scavenging (based on preliminary research) which are at variance with our own experience. After many years of port-scavenged diesel and spark-ignition-engine manufacture, research was started in 1940 on uniflow-scavenged spark-ignition gas engines by the Worthington Corporation.

Continuous development of the uniflow type in bore sizes up to 16 in. has resulted in over 250,000-hp installed capacity in continuous heavy-duty operation from 1950 to date.

The inference has been made that uniflow engines indicate somewhat reduced efficiency and power output. Possibly this could be applied to the test engine in question. However, research tests have been made in our shop, showing fuel consumption under 7500 Btu/bhp/hr and delivered output in excess of 100 bmep. These tests have confirmed the improved performance expected from this design.

The importance of the nature of stratification prior to combustion, fuel-injection phenomena, and swirl of the scavenge air charge has been stressed. We believe these to be essential factors in making our uniflow results possible.

In the port-scavenged engine, unless an auxiliary rotating valve is used for exhaust-port closing, pressure phenomena are experienced from the gas-wave movement in exhaust pipe. These oscillations may return exhaust gas to the cylinder, causing turbulence, and contaminating the fuel-air charge.

A direct effect would be increased initial compression temperature of the charge. This will result in reduced knock limit as compression ratio is increased, thereby limiting efficiency.

If the gas-injection pressure is high enough, the gas jet will penetrate to the piston top. This is not as important as "where it is" when the spark ignites the mixture. The location of the spark plug, whether in the center, or at the side, determines

[8] Chief Engineer, Worthington Corporation, Buffalo, N. Y.

the nature of combustion—whether it will be smooth or rough. We have found the port-scavenged engine particularly sensitive to load condition. At light load, conditions change materially in the fuel-air mixture, and the operation of the engine becomes rough. This may be stratification, or erratic turbulence, or both. The uniflow system permits the designer to select an adequate blowdown period, and a supercharged closing. The inlet ports extend 360 deg around the cylinder, providing a maximum opening area for low-velocity scavenging. The ports can be shaped to vary path of swirl during opening, from tangential to radial, depending on the position of piston travel.

This swirl is definitely orderly. As evidence, the pattern has been observed on the piston top. We have found that the gas-injection valve placed directly above this path of swirl will, if properly introduced, give optimum combustion efficiency. Smooth operation, equal to that of four-cycle gas engines, is possible even at light loads. This is probably one of the severest tests for two-cycle gas-engine performance. Exhaust temperatures are lower and high compression ratio may be used due to cooler piston and cylinder walls. The lack of exhaust openings in the cylinder liner promotes more uniform heat gradient throughout the cylinder walls.

The writer does not wish to detract from the excellent work presented here by the authors. He does, however, suggest that any conclusions regarding uniflow scavenging be based on an actual record of performance of this type of engine.

This record includes millions of horsepower of automotive, locomotive, and industrial diesels and spark-ignition engines.

L. G. Kaplan.[9] Through the use of schlieren photography, the authors have made a worth-while contribution to the general understanding of the flow phenomena, as they transpire inside the cylinder of a two-cycle diesel or gas engine, both during scavenging and combustion. Although the steady-flow technique and various modifications thereof have been used for a number of years for evaluating the scavenging properties of various cylinder sleeve and port designs, it was a matter of speculation as to how closely the flow thus obtained duplicated conditions as they exist in an actual engine. Confirmation of the validity of these techniques in itself constitutes an important contribution.

From studies carried out on a similar-type engine at the Armour Research Foundation, in which the dynamic behavior of the gases was simulated in a transparent engine-cylinder model, without actuating the engine piston, it was established that scavenging air flow in different planes taken at various distances from the cylinder center line and parallel to a center line through the ports, varied appreciably. The schlieren photographs, which covered a relatively small cylindrical volume perpendicular to and through these planes, were incapable of distinguishing between them, but merely superimposed the flow patterns one over the other. In spite of this inherent limitation a qualitative picture of the flow phenomena in a running engine, procurable thus far by no other method, was obtained.

Our own limited observations of the air-flow patterns in one design of a loop-scavenged engine showed the lower portion of the cylinder to be fairly well cleansed of residual gases, while the upper cylinder regions served mainly as a mixing chamber. The high-velocity incoming air jets seemed to sweep the lower cylinder regions clear in a relatively short time, while the reduced air velocities coupled with indiscriminate turbulence in the upper portions of the cylinder resulted in intimate mixing with the residual gases rather than the formation of a so-called laminar piston of fresh air. As the exhaust gases or mixture from the top of the cylinder were forced downward, a large portion thereof was re-entrained by the incoming air jets and carried back to the top of the cylinder. It appeared that in this particular engine roughly the lower third of the cylinder was scavenged of residual gases while the upper two thirds served as a mixing chamber. It further appeared that this tendency toward re-entrainment of the residual gases is inherent in the loop-scavenging system and that great care in port and cylinder design would be required to give the residual gases a clear passage to the exhaust ports, and keep the re-entrainment within reasonable bounds. We further speculated that the uniflow design, by permitting the residual gases to escape directly through the upper portion of the cylinder, would result in a more complete scavenging. The higher mep's attainable with uniflow-type engines seem to attest to the validity of this contention. (This hypothesis, which is speculative in nature, we hope to investigate shortly by photographing the scavenging flow patterns in a uniflow-type engine.)

The schlieren photography technique, by permitting visual observation of the flow inside an operating engine, is useful in validating or verifying the other scavenging study methods, and in studying the blowdown interval, as well as the squish action near top dead center. The dynamic-flow technique, on the other hand, can serve as an economical and convenient method of qualitative evaluation of cylinder-sleeve and port designs, and hence can constitute a useful laboratory tool for the engine designer. The two methods are of different capabilities, each suitable for particular applications.

[9] Assistant Supervisor, Armour Research Foundation of Illinois Institute of Technology, Chicago, Ill.

Authors' Closure

It is agreed that the characteristic of the pressure wave in the exhaust manifold is of extreme importance to the operation of any two-cycle engine, and that it must be given special consideration during the development of such an engine. We have not observed the loop-scavenged engine to be particularly sensitive to this wave.

Good mixing of the fuel and air in the cylinder must be attained if the entire charge of air is to be burned and the maximum load-carrying ability of the engine is to be attained. Much work has been done to eliminate stratification of the gas and air charge, and such stratification is regarded as being detrimental to engine operation. The question of the location of a pocket of ignitible fuel-air mixture is not of importance, since the cylinder contents should be homogeneous and contain no such pockets.

The problem of proper cylinder design for two-cycle engines has been the subject of considerable controversy for many years. It always has been more or less assumed that the uniflow type of construction was advantageous from the standpoint of scavenging efficiency and over-all performance, and that the loop-scavenged type of construction, although inferior in performance, was often chosen because of its simplicity. We have come to believe, however, that the uniflow type offers no better performance characteristics than the loop-scavenged type and that the long-standing assumptions regarding the superiority of the uniflow construction are not valid. We have not observed that higher mean effective pressures are attainable with uniflow scavenging than with loop scavenging.

Mr. Kauffmann reports that uniflow-scavenged engines have achieved loads over 100 bmep and fuel rates under 7500 Btu/bhp-hr. We find that loads well in excess of 100 bmep can be carried with the standard production loop-scavenged engine, and that fuel rates below 7500 Btu/bhpbr are not extreme. It is interesting to note that one of the largest manufacturers of small, high-speed two-cycle engines has switched to loop scavenging for its latest-model engine.

Poor light-load operation in two-cycle gas engines is a result of

the decrease in fuel-air ratio with load. Since adequate scavenging must be achieved at any load condition, the problem becomes one of decreasing the weight of air that is trapped in the cylinder without affecting the scavenging efficiency. Engines have been built which performed well on light load, but it always has been at the expense of reduced maximum load or excessive paraphernalia.

Cylinder-design studies have shown effects similar to those described by Mr. Kaplan, but the detrimental effects of these flows have been minimized by careful port design. The photographs show no re-entrainment and only a small amount of crossflow. Some crossflow is desirable for the proper scavenging of the lower portion of the cylinder and for prevention of re-entrainment of exhaust gases by intake air. The amount of this crossflowing air must be regulated carefully, however, to prevent excessive losses of inlet air to the exhaust ports.

Phase-Plane Analysis—A General Method of Solution for Two-Position Process Control

By D. P. ECKMAN,[1] CLEVELAND, OHIO

The phase-plane method of analysis requires transforming the differential equations for the closed loop into coordinates of rate of change of deviation versus deviation. Then, by integral equations the period and amplitude of oscillation of process control may be evaluated. Five interesting problems in process control are discussed. The limitations of the analysis are that process-control problems involving differential equations of higher order than second cannot be evaluated exactly. For process-control problems, an approximation of the response by a Ziegler-Nichols method of approach can be used in a very simple manner. Problems involving various nonlinearities also may be solved.

Nomenclature

The following nomenclature is used in the paper:

A = amplitude of oscillation = $(A_1 + A_2)/2$
A_1 = maximum positive error
A_2 = maximum negative error
c = controlled variable
C = process capacitance
e = $c - V$ = error
G = differential gap (one-half total differential gap)
L = dead time
n = number relating valve size to load variable
N = maximum process-reaction rate
P = period of oscillation = $P_1 + P_2$
P_1 = period in which control is on
P_2 = period in which control is off
m = manipulated variable
u = process load
R = process resistance
t = time
T = process time constant = RC
V = set point
$x = \bar{e}$
$y = \bar{\dot{e}} = \frac{\bar{de}}{dt}$

Introduction

Two-position or on-off control is one of the most important and simplest modes of control in both industrial and domestic applications. Two-position control frequently is employed in engine and other machine controllers. In spite of its wide use, two-position control has not been treated adequately from the analytical viewpoint because of the essential nonlinearity of the system; that is, because the operation of the system is not described by a single linear differential equation.

The analysis of two-position control has been made for certain simple cases by the method of differential equations by Oldenbourg and Sartorius (1)[2] and by the method of Fourier series by Ivanoff (2). Although these analyses are valid for the cases considered, they are not sufficiently general to enable the solution of important industrial applications.

The phase-plane analysis presented in this paper follows the approach to nonlinear systems presented by Minorsky (3) and by MacColl (4).

When two-position control is applied to a process, a steady oscillation of the controlled variable results as shown in Fig. 1, if the differential gap G is not zero or if there is a finite dead-time lag L in the control system. A steady oscillation is obtained after the transient state has disappeared providing the system is stable.

For steady-state oscillation, the change of controlled variable is repeated each period of oscillation, although it is not necessary that the oscillation be symmetrical. In the latter case the control is said to be nonsymmetrical.

In general, the operation of the controlled system may be represented by two differential equations, either linear or nonlinear. Each equation is valid only during the appropriate half period.

Phase-Plane Analysis

Suppose that a two-position controlled system can be represented by two differential equations

$$a\ddot{e} = f_1(\dot{e}, e) \quad 0 \leqq t \leqq P_1 \ldots\ldots\ldots\ldots [1a]$$

$$a\ddot{e} = f_2(\dot{e}, e) \quad P_1 \leqq t \leqq P_2 \ldots\ldots\ldots\ldots [1b]$$

It is not necessary for these equations to be linear but they must not be of a higher order than second.

The order of the equations can be suppressed by one if

$$y = \bar{\dot{e}} = \dot{c} \ldots\ldots\ldots\ldots [2a]$$

$$x = \bar{e} = c - V \ldots\ldots\ldots\ldots [2b]$$

The negative signs are employed so that deviation e and phase coördinates y and x carry the same sign as the controlled variable c. The set point V is almost always a fixed value.

Substituting in Equations [1a] and [1b]

$$ay\frac{dy}{dx} = -f_1(-y, -x) \quad x_2 < x < x_1 \ldots\ldots\ldots [3a]$$

$$ay\frac{dy}{dx} = -f_2(-y, -x) \quad x_3 < x < x_{13} \ldots\ldots\ldots [3b]$$

Often these equations are integrable in y and x and may be plotted in y, x co-ordinates. This is termed the phase plane and Equations [3a] and [3b] are called the phase lines. Fig. 1(*b*) illustrates typical phase lines. When the two phase lines are connected, a phase trajectory is formed. Note that a phase trajectory always proceeds in a clockwise direction in a conventional rectangular co-ordinate system.

Time co-ordinates also are represented in the phase plane since

$$t_n - t_{n-1} = \int_{n-1}^{n} dt = \int_{n-1}^{n} \frac{dx}{y} \ldots\ldots\ldots [4]$$

---

[1] Associate Professor of Mechanical Engineering, Case Institute of Technology. Mem. ASME.

Contributed by the Review Committee of the Industrial Instruments and Regulators Division and presented at the Spring Meeting, Columbus, Ohio, April 28–30, 1953, of The American Society of Mechanical Engineers.

Note: Statements and opinions advanced in papers are to be understood as individual expressions of their authors and not those of the Society. Manuscript received by ASME Applied Mechanics Division, February 10, 1953. Paper No. 53—8-17.

[2] Numbers in parentheses refer to the Bibliography at the end of the paper.

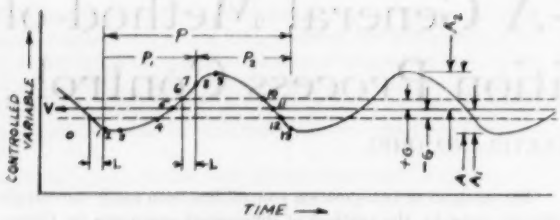

a) Steady oscillation in two-position control

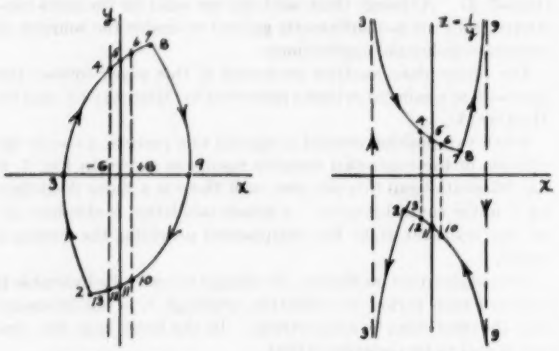

(b) Phase trajectory (c) Period trajectory

FIG. 1 THE PHASE PLANE

Therefore time co-ordinates are represented by the normals at any point of the phase-plane trajectory (5).

It should be noted that if the phase lines are plotted on ($z = 1/y$, x) co-ordinates as in Fig. 1(*c*), areas under the phase lines represent time differences. Unfortunately, in two-position control there are points similar to x_3 and x_9 in Fig. 1 where $y = 0$ and Z is infinite. This makes the representation awkward in that the phase trajectories close through infinity.

The period of oscillation of two-position control now is found

$$P = P_1 + P_2 = \int_2^7 \frac{dx}{y} + \int_8^{13} \frac{dx}{y} \quad \ldots\ldots [5]$$

The dead-time lag must be

$$L = \int_6^7 \frac{dx}{y} = \int_{12}^{13} \frac{dx}{y} \quad \ldots\ldots [6]$$

The amplitude may be found from

$$A = \frac{|A_1| + |A_2|}{2} = \frac{1}{2}\int_3^5 dx + \frac{1}{2}\int_9^{11} dx \quad \ldots\ldots [7]$$

and the differential gap is

$$G = -\int_4^5 dx = \int_5^6 dx = \int_{11}^{10} dx = -\int_{12}^{11} dx \quad \ldots\ldots [8]$$

With these equations the amplitude and period of oscillation may be determined in terms of the parameters of the system, the dead-time lag L and the differential gap G.

For a symmetrical cycle

$$\frac{f_1(y, x)}{y} = \frac{-f_2(-y, -x)}{(-y)} \quad \ldots\ldots [9]$$

and Equations [5], [6], [7], and [8] are simplified appropriately.

DERIVATION OF PHASE EQUATIONS

Consider the two-position control of a single-capacitance process shown in Fig. 2. The operational diagram might represent a liquid-level process with manipulated inlet flow m, and a constant outlet flow U. A dead time L may exist anywhere within the closed-loop portion of the circuit. The equation for the process is

$$C\dot{c}(t - L) = m(t) - u(t) \quad \ldots\ldots [10]$$

where

C = process capacitance
c = controlled variable
t = time
L = dead time (lag)
m = manipulated variable
u = load (disturbance) variable

For the purpose of the analysis, the load variable u may be considered constant

$$u(t) = U \quad \ldots\ldots [11]$$

The process reaction rate is then

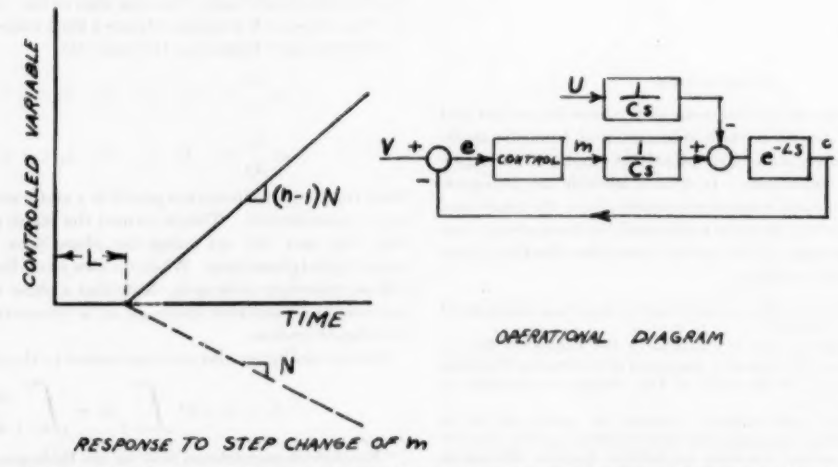

FIG. 2 TWO-POSITION CONTROL OF SINGLE-CAPACITANCE PROCESS, SHOWING RESPONSE TO STEP CHANGE OF m IN OPERATIONAL DIAGRAM

$$N = \frac{U}{C} \quad [12]$$

and is the rate of change of the controlled variable when the manipulated variable is zero (control valve off).

Two-position control is specified by two equations

$$m(t) = nU \qquad \text{when } e \leq V - G,\ \dot{e} < 0 \quad [13a]$$

$$m(t) = 0 \qquad \text{when } e \geq V + G,\ \dot{e} > 0 \quad [13b]$$

where n is a fraction specifying the maximum value of the manipulate variable (essentially a valve size) in terms of the value of the load variable U. The set point V is constant and is equal to the reference input.

Combining Equations [10] through [13], the differential equations for the controlled system are obtained

$$C\dot{e}(t - L) = (n - 1)u(t) \quad [14a]$$

$$C\ddot{e}(t - L) = -u(t) \quad [14b]$$

where the controlled variable has the same limits as in Equations [13].

The deviation is given by the usual equation

$$e = V - c \quad [15]$$

where e is the deviation (actuating signal).

Combining Equations [14] and [15] in Equations [12]

$$\dot{e} = -N(n - 1) \quad [16a]$$

$$\dot{e} = N \quad [16b]$$

The phase equations are found by employing the definition of Equations [2]

$$y = N(n - 1) \quad [17a]$$

$$y = -N \quad [17b]$$

By integrating the phase equations suitably, the period and amplitude of oscillation may be calculated.

Case 1 Single-Capacity Process Without Self-Regulation. The phase equations are developed in the previous section

$$y = (n - 1)N \quad [17a]$$

$$y = -N \quad [17b]$$

and are plotted in Fig. 3 together with the oscillation in the time domain. The vertical lines are not in reality phase lines, but are shown here to complete the phase trajectory.

The dead time L is computed from

$$L = \int_G^{A_1} \frac{dx}{(n - 1)N} = \int_{-G}^{-A_1} \frac{dx}{(-N)} \quad [18]$$

Integrating and solving for amplitude

$$A = \frac{n}{2}(NL) + G \quad [19]$$

where A is the amplitude of oscillation (one half the peak-to-peak amplitude).

The period of oscillation is found by

$$P = \int_{-A_1}^{A_1} \frac{dx}{(n - 1)N} + \int_{A_1}^{-A_1} \frac{dx}{(-N)} \quad [20]$$

where P is the period of oscillation (peak-to-peak time). Integrating and eliminating amplitude A

$$P = \left(\frac{2n}{n - 1}\right)\frac{A}{N} \quad [21]$$

Equations [19] and [21] are easily checked by calculating directly from the time oscillation shown in Fig. 3. The amplitude of oscillation is plotted in Fig. 4.

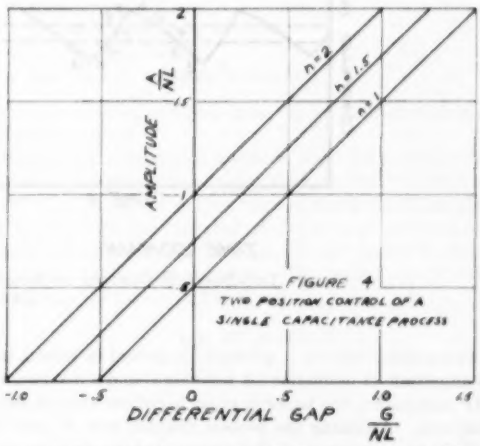

Fig. 4 Two-Position Control of Single-Capacitance Process, Showing Amplitude of Oscillation

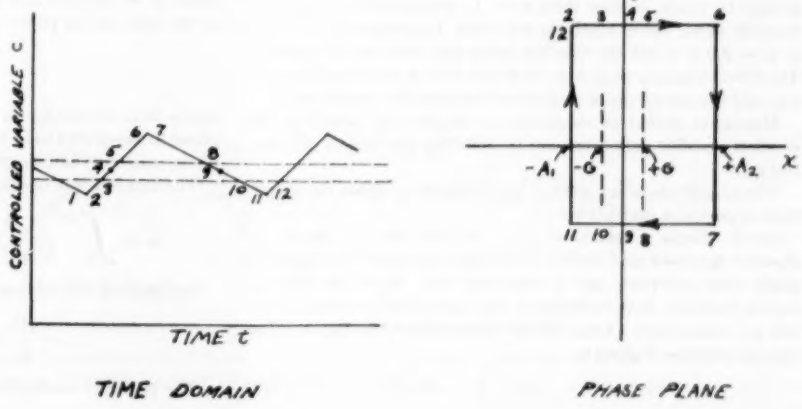

Fig. 3 Two-Position Control of Single-Capacitance Process, Showing Time Domain and Phase Plane

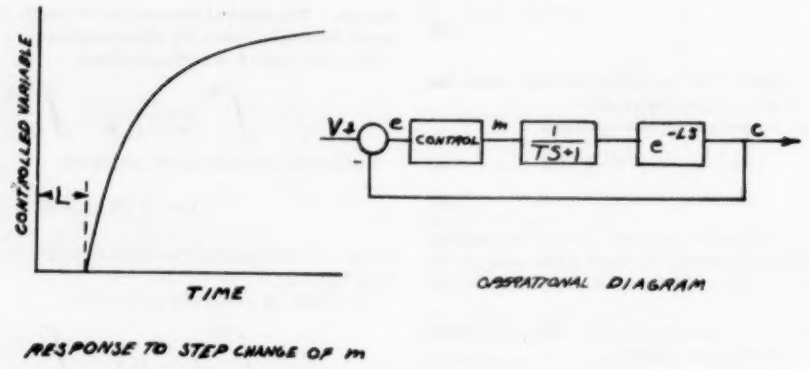

FIG. 5 TWO-POSITION CONTROL OF SINGLE TIME-CONSTANT PROCESS, SHOWING RESPONSE TO STEP CHANGE OF m IN OPERATIONAL DIAGRAM

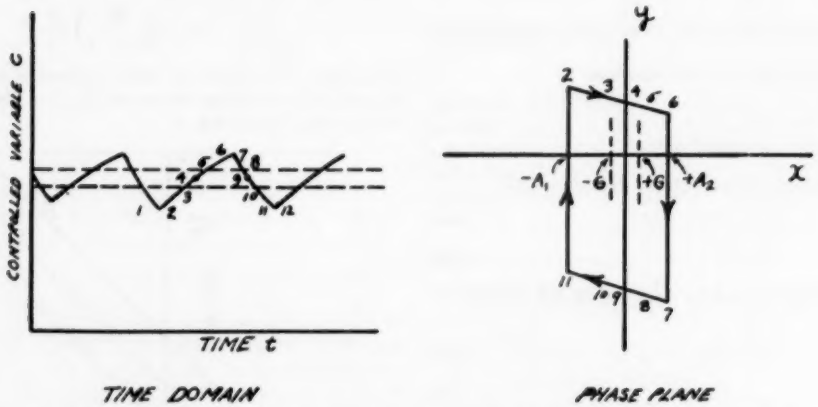

FIG. 6 TWO-POSITION CONTROL OF SINGLE TIME-CONSTANT PROCESS, SHOWING TIME DOMAIN AND PHASE PLANE

In two-position control it generally is desired to have a minimum amplitude of oscillation (A minimum) and a maximum period (P maximum), the latter in order to reduce wear on control mechanisms. Assuming the process reaction rate N, and dead time L, fixed parameters of the process, values of valve size n and differential gap G may be selected.

Minimum amplitude is obtained when valve size n and differential gap G are as small as possible. However, the valve size cannot be made smaller than $n = 1$, otherwise the controlled variable would never reach the set point. Consequently, $n = 1.5$ or $n = 2.0$ is about the smallest valve size that can be selected. The differential gap should be small and, in fact, can be made negative and the amplitude of oscillation theoretically is reduced.

Maximum period of oscillation is obtained by selecting the smallest possible valve size and by selecting the largest differential gap.

The magnitude of set point V does not affect either the amplitude or period of oscillation.

Case 2 Single Capacity Process—Self-Regulation. Many industrial processes may consist of a single capacitance providing a single time constant, and a dead-time lag. Such processes as simple furnaces, heat exchangers, and liquid-level-controlled vessels are of this type. Consider the process shown in Fig. 5. The process response is given by

$$T\dot{c}(t - L) + c(t - L) = Rm(t) \quad [22]$$

where T = process time constant and R = process outflow resistance.

Combining with Equations [13] for two-position control, the phase equations may be derived

$$Ty + x = V(n - 1) \quad [23a]$$

$$Ty + x = -V \quad [23b]$$

where V = set point and n specifies the control-valve size in terms of the value of set point

$$M = n\frac{V}{R} \quad [24]$$

where M is the maximum value of the manipulated variable. The phase lines referred to in Equations [23] are plotted in Fig. 6. The phase trajectory is a simple parallelogram.

The amplitude of oscillation is found from

$$L = \int_G^{A_2} \frac{T\,dx}{V(n-1) - x} = \int_{-G}^{-A_1} \frac{T\,dx}{-(V + x)} \quad [25]$$

Integrating and solving for amplitude

$$A = \frac{nV}{2}(1 - e^{-L/T}) + Ge^{-L/T} \quad [26]$$

The period of oscillation is found from

$$P = \int_{-A_1}^{A_2} \frac{T\,dx}{(n-1)V - x} + \int_{A_2}^{-A_1} \frac{T\,dx}{-V - x} \quad \ldots [27]$$

Integrating

$$P = T \ln \left| \frac{\left(n - 1 + \frac{A_1}{V}\right)\left(1 + \frac{A_2}{V}\right)}{\left(n - 1 - \frac{A_2}{V}\right)\left(1 - \frac{A_1}{V}\right)} \right| \quad \ldots [28]$$

If the cycle is symmetrical ($n = 2$), then the period is given by

$$P = 4T \tanh^{-1} \frac{A}{V} \quad \ldots [29]$$

and the amplitude is

$$A = V(1 - e^{-L/T}) + Ge^{-L/T} \quad \ldots [30]$$

The amplitude of oscillation is plotted in Fig. 7.

Assuming again that dead time L, time constant T, and set point V are determined by the particular process under investigation, then only the differential gap G and valve-size factor n may be selected to produce minimum amplitude of oscillation. It is again apparent from Equation [26], plotted in Fig. 7, that the valve size should be as small as possible. The differential gap also should be as small as possible. Smallest amplitude of oscillation is insured by a negative differential gap. However, the smallest differential gap is limited by

$$G \geq \frac{nV}{2}(1 - e^{L/T}) \quad \ldots [31]$$

Comparing Case 2 with Case 1 for a process with and without self-regulation, it is shown that self-regulation is desirable because it generally reduces the amplitude of oscillation.

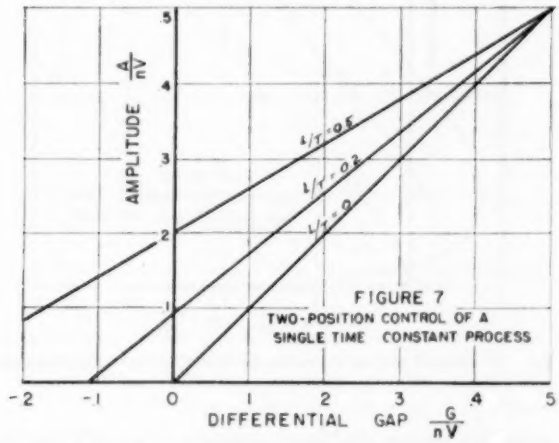

Fig. 7 Two-Position Control of Single Time-Constant Process, Showing Amplitude of Oscillation

Case 3 Two-Capacity System. The controlled system in Fig. 8 might represent a two-capacity process consisting of a time-constant element and a self-regulation element, or it may represent a single-capacity process with a control-valve lag. The latter is common when pneumatic two-position control is employed. The time-constant lag is then the lag of the pneumatic transmission line and control-valve mechanism. In either case the phase equations for symmetrical operation may be shown to be

$$Ty\frac{dy}{dx} + y = N \quad \ldots [32]$$

$$Ty\frac{dy}{dx} + y = -N \quad \ldots [33]$$

where

T = time constant
N = process reaction rate = U/C
C = process capacitance
U = value of load variable (constant)

The phase equations are plotted in Fig. 9 together with the cycle in the time domain.

Symmetrical operation is provided when the control-valve size is twice that necessary to accommodate the load variable ($n = 2$) or, $M = 2U$, where M = max value of manipulated variable.

The amplitude and period of oscillation may be found by integrating the equations for dead time L and period P, using the same general procedure as before. The results, for symmetrical operation of the system of Fig. 8, are

$$A = NT \ln \cosh Z \quad \ldots [34]$$

and

$$\frac{G}{NT} = \frac{e^{-L/T}}{e^{z}\cosh Z} + Z - \frac{L}{T} - 1 \quad \ldots [35]$$

where

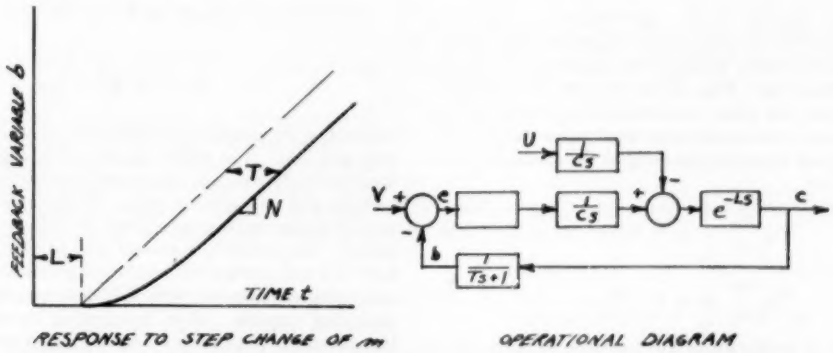

Fig. 8 Two-Position Control of Two-Capacitance Process, Showing Response to Step Change of m in Operational Diagram

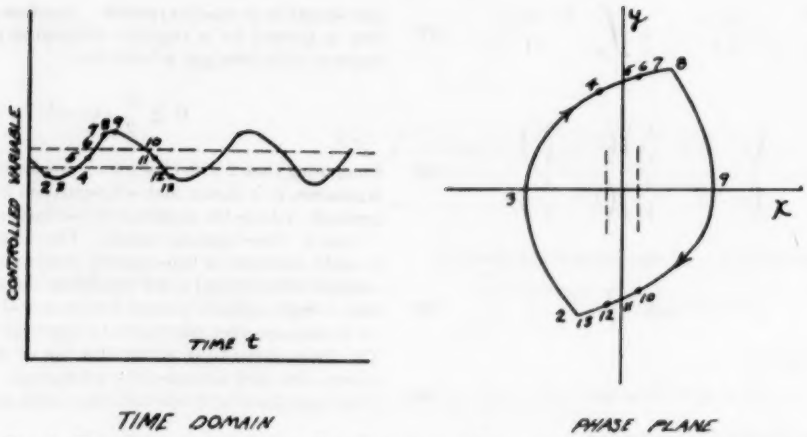

FIG. 9 TWO-POSITION CONTROL OF TWO-CAPACITANCE PROCESS, SHOWING TIME DOMAIN AND PHASE PLANE

Z = $P/4T$
A = amplitude of oscillation
N = process reaction rate = U/C
T = time constant
P = period of oscillation
G = differential gap
L = dead time

The amplitude calculated from the equations is plotted in Fig. 10. Note that it is possible to obtain a double amplitude of oscillation when the differential gap is small and either positive or negative. For example, if a given process has $L/T = 0.5$, and $NT = 1.0$ unit, then the following are the amplitude and period of oscillation:

A	P	G
0	0	0.15
0.03	T	0
0.25	$3T$	0.15
0.64	$5T$	0
0.85	$6T$	0.15

Thus the smaller amplitude is accompanied by a shorter period. Such points generally are unstable and the large amplitude tends to predominate. In the author's experience, systems with negative-differential gap may alternate from one amplitude to the other in a continuous transient state. As shown in Fig. 10, the double-amplitude condition exists only when appreciable dead time is present.

Case 4 Single-Capacity Process and Measuring Lag. The controlled system in Fig. 11 represents a single-capacity process and a two-position controller in which the measuring element has a single time-constant lag. This may be the case in two-position control of furnaces and other temperature-controlled systems where heat losses are not greatly dependent upon temperature. In this case the phase equations applying to the feedback (measured) variable b, are

$$T y_b \frac{dy_b}{dx} + y_b = N \quad \text{[36]}$$

$$T y_b \frac{dy_b}{dx} + y_b = -N \quad \text{[37]}$$

The amplitude of oscillation of the feedback variable can be calculated with the same results as Case 3. Assuming that the oscillation of the controlled variable is nearly sinusoidal, which

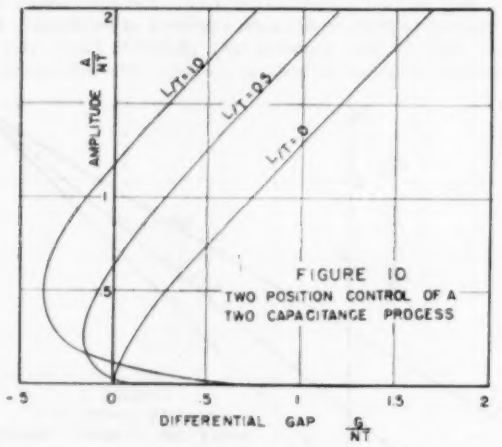

FIG. 10 TWO-POSITION CONTROL OF TWO-CAPACITANCE PROCESS, SHOWING AMPLITUDE OF OSCILLATION

generally is the case, the Fourier harmonics are negligible and the amplitude of oscillation of the controlled variable may be computed from

$$A_c = A_b \sqrt{1 + (WT)^2} \quad \text{[38]}$$

$$A_c = A_b \sqrt{1 + \frac{\pi^2}{2Z}} \quad \text{[39]}$$

where A_b is the amplitude of oscillation calculated from Equations [34] and [35]. The results are shown in Fig. 12. There is an appreciable difference in amplitude of oscillation of the controlled variable and its indicated value. Unfortunately, as the amplitude of oscillation becomes smaller, the difference tends to be maintained. For example, a process with $G = 0.2$, $NT = 1.0$, and $L/T = 0$ will oscillate with 0.38 unit amplitude indicated by the measuring element but with 0.74 unit amplitude of the actual controlled variable. Thus, interpreting the results of two-position control by inspection of a measuring element indication may be inconclusive.

Case 5 Two-Capacity Process With Self-Regulation. For any

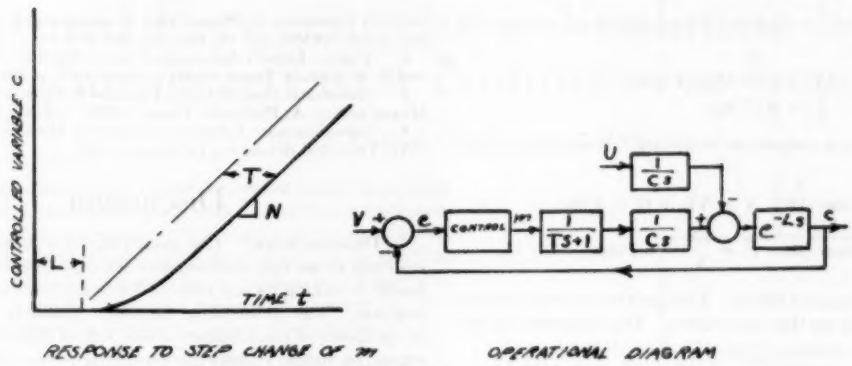

FIG. 11 TWO-POSITION CONTROL WITH MEASURING LAG

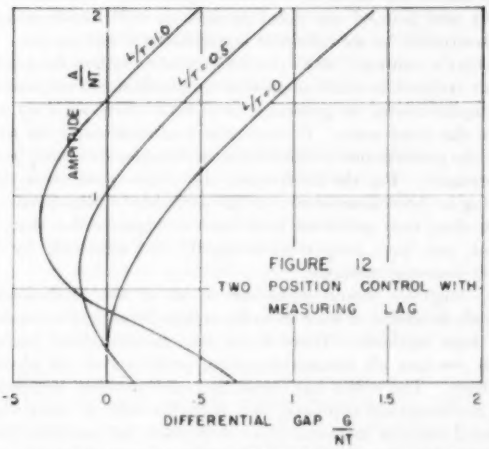

FIG. 12 TWO-POSITION CONTROL WITH MEASURING LAG, SHOWING AMPLITUDE OF OSCILLATION

two-capacitance process with self-regulation, cascade or not, the phase equations for symmetrical operation may be written

$$T_1T_2y\frac{dy}{dx} + (T_1 + T_2)y = (\pm K - x) \quad [40]$$

By substituting

$$y = u(\pm K - x) \quad [41]$$

The phase equations are made separable and may be integrated

$$\ln(\pm K - x) = \int \frac{T_1T_2u\,du}{(T_1u - 1)(T_2u - 1)} + C_1 \quad [42]$$

However, the evaluation of this integral in the general case yields a rather complex algebraic function which is difficult to handle in subsequent integrations for period and amplitude of oscillation. In any particular case for numerical values of T_1, T_2, and K, the problem is solved more easily. A graphical solution of any particular case also is made possible by the method given by Jacobson (5).

APPROXIMATE SOLUTIONS FOR TWO-POSITION CONTROL

For many industrial processes the Ziegler-Nichols approximation is considered satisfactory (6). This method requires approximating the process-reaction curve by an apparent dead time L and a reaction rate N, for processes without self-regulation as shown in Fig. 13(*a*). For processes with self-regulation the process-reaction curve may be approximated by an apparent dead time L, a process sensitivity K, and a time constant T, as shown in Fig. 13(*b*). The process-reaction curve is obtained by disconnecting the controller from the process, opening the final control element (a valve or an electrical relay), and recording the resulting change in controlled variable. This procedure is performed best with a small change of manipulated variable and with the controlled variable always near the set point. Sometimes in two-position control, this is not possible because the final control element may have only two fixed positions, either open or closed. Also, it is advisable to employ both an increase and a decrease in controlled variable in order to account for possible nonsymmetrical operation.

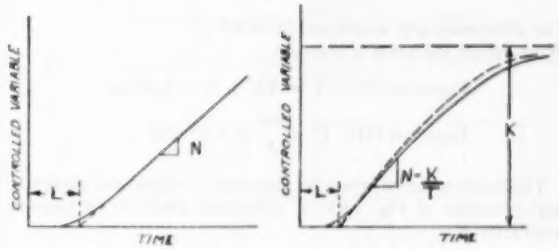

(*a*) Without self-regulation (*b*) With self-regulation

FIG. 13 APPROXIMATION OF RESPONSE BY ZIEGLER-NICHOLS METHOD

Three examples are given herewith. The data for these processes are given elsewhere (6). The process-reaction curve is approximated by a dead-time lag L and a reaction rate N, as shown in Fig. 2. This approximation ignores the process self-regulation.

Wet-Bulb Temperature Control. The apparent lag and reaction rate are

$$N = 0.24 \text{ deg per min}$$
$$L = 4.5 \text{ min}$$

The differential gap is assumed to be 0.5 deg. Symmetrical operation ($n = 2$) is assumed.

$$\text{Equation [19]: } A = NL + G = 1.6 \text{ deg}$$

$$\text{Equation [20]: } P = \frac{4A}{N} = 27 \text{ min}$$

This control might prove unsatisfactory because of the very large period of oscillation.

Dry-Bulb Temperature Control. The apparent lag and reaction rate are

$$N = 2.64 \text{ deg per min}$$
$$L = 0.77 \text{ min}$$

The differential gap is assumed to be 2.0 deg. Symmetrical operation is assumed.

$$\text{Equation [19]: } A = NL + G = 4 \text{ deg}$$

$$\text{Equation [20]: } P = \frac{4A}{N} = 6.1 \text{ min}$$

Column-Vent Pressure Control. Two-position control probably would not be used on this application. The apparent lag and reaction rate are

$$N = 2.4 \text{ psi per min}$$
$$L = 0.08 \text{ min}$$

The differential gap is assumed to be 0.5 psi. Symmetrical operation is assumed.

$$\text{Equation [19]: } A = NL + G = 0.69 \text{ psi}$$

$$\text{Equation [21]: } P = \frac{4A}{N} = 1.15 \text{ min}$$

The three examples presented also could be calculated using the approximation of Fig. 13(*b*) if data were available for process sensitivity K.

Conclusions

The phase-plane method of analysis offers many possibilities for the solution of problems in both process control and servomechanisms. The exact solution of any two-position-control problem is obtained if the system (process and controller) does not involve differential equations of higher order than 2. Although no examples are given in this paper, nonlinear systems of certain types also may be solved. For process control, in general, the approximation method of Ziegler and Nichols may be used.

Acknowledgment

The author acknowledges the suggestions of N. B. Nichols, Director of Research, Raytheon Manufacturing Company.

BIBLIOGRAPHY

1 "The Dynamics of Automatic Controls," by R. C. Oldenbourg and H. Sartorius, The American Society of Mechanical Engineers, New York, N. Y., 1948.

2 "Theoretical Foundations of the Automatic Regulation of Temperature," by A. Ivanoff, *Journal of the Institute of Fuel*, vol. 7, February, 1934, pp. 117–130.

3 "Introduction to Nonlinear Mechanics," by N. Minorsky, Edwards, Ann Arbor, Mich., 1947.

4 "Fundamental Theory of Servomechanisms," by L. A. MacColl, D. Van Nostrand Company, Inc., New York, N. Y., 1945.

5 "On a General Method of Solving Second-Order Ordinary Differential Equations by Phase-Plane Displacements," by L. S. Jacobson, Trans. ASME, vol. 74, 1952, pp. 543–553.

6 "Process Lags in Automatic Control Circuits," by J. G. Ziegler and N. B. Nichols, Trans. ASME, vol. 65, 1943, p. 433.

7 "Automatic Control in the Presence of Process Lags," by C. D. Mason and G. A. Philbrick, Trans. ASME, vol. 62, 1940, p. 295.

8 "Discontinuous Automatic Control of Missiles," by I. F. Lots, ONR Technical Report no. 14, August, 1950.

Discussion

R. Oldenburger.[3] It is gratifying for a former pure mathematician to see that mathematics developed 100 or 200 years ago finally is making its way into the kit bag of tools employed by the engineer. The phase-plane approach probably had its origin in the theory of the existence of solutions of differential equations, where, by simple transformations, a high-order differential equation is reduced to a set of first-order equations.

The author has made an excellent exposition of this important subject and pointed out disadvantages as well as advantages. The restriction to second-order equations is a serious one. At the writer's company, when the differential equations for a problem are reduced as much as possible by physical and mathematical simplifications, we generally, or at least often, wind up with one of the third order. If we arrive at a lower order, we often make the problem one of the third order because we obtain better performance. For the third order, the phase approach requires plotting in three dimensions, for the nth order n-dimensions.

Our dead-time problems have been of higher order than the second, and have been treated rapidly and efficiently by frequency-response methods.

The engineer should make use of all of the mathematical methods available, at least in so far as time permits him to assimilate these methods. There is no one mathematical panacea which resolves all automatic-control problems or all physical problems. The writer has found that each problem requires its own mathematical approach, but, unfortunately, it takes a professional research mathematician to develop the mathematics to fit the problem.

The experience of each of us is necessarily very limited. An approach that enables one person to treat many of his problems on the back of an envelope will not enable another, working in a different area, to do the same. Where the two first-order differential equations, equivalent to a given second-order differential equation, can be solved in closed form (by formulas), the phase-plane approach may be very useful. Unfortunately, the number of problems that can be thus solved is extremely limited. Of course, approximate solutions are often satisfactory.

The phase-plane approach is one of the important techniques available to the designer. It has its definite areas of application. The author is to be commended for bringing it forcefully to the attention of the automatic-control designer.

[3] Chief Mathematician, Woodward Governor Company, Rockford, Ill. Mem. ASME.

Natural Frequency of a Nonlinear System Subjected to a Nonmassive Load

By C. E. CREDE,[1] WATERTOWN, MASS.

This paper discusses a single-degree-of-freedom system with nonlinear elasticity such that the stiffness increases as the deflection increases. This stiffness increase, without a change in the mass, effects an increase in natural frequency. Graphical means are presented to evaluate the increase in natural frequency when the support for the system experiences a sustained constant acceleration.

Nomenclature

The following nomenclature is used in the paper:

- a = sustained acceleration of support, expressed as dimensionless multiple of acceleration of gravity
- f = natural frequency at any deflection, cps
- f_0 = natural frequency at zero deflection, cps
- F = sustained force applied to mounted body, lb
- g = acceleration of gravity
- h = thickness of resilient material in isolator, in.
- k = stiffness of isolator, any deflection, lb/in.
- k_0 = stiffness of isolator, zero deflection, lb/in.
- m = mass of supported body, lb sec^2/in.
- T = transmissibility, dimensionless
- δ = deflection of isolator, in.
- ω = forcing frequency, radians/sec
- Ω = natural frequency of isolator, any deflection, radians/sec
- Ω_0 = natural frequency of isolator, zero deflection, radians/sec

Introduction

In a vibration isolator whose force-deflection curve exhibits nonlinear characteristics, the stiffness of the isolator is a function of its deflection, or of the load it supports. Many isolators that embody resilient material loaded in compression exhibit a gradual increase in stiffness when the deflection increases. Large deflections may result from the dead-weight load of the supported equipment: from an external force, such as belt pull in belt-driven machinery; or from the inertia forces derived from sustained acceleration, such as that embodied in the take-off of a rocket or missile. In some of these applications the force applied to the isolator is greater than the dead weight of the supported load. A particular type of nonlinear isolator is discussed in the following paragraphs, and the influence of the nonlinearity upon natural frequency and transmissibility is analyzed.

Analysis of Nonlinear System

The following analysis refers to the single-degree-of-freedom system shown in Fig. 1. A rigid body of mass m is supported by a nonlinear vibration isolator of stiffness k and having resilient material of thickness h. A sustained force F may be applied to the supported body, or a sustained acceleration a may be experienced by the support for the system. The interval during which F or a endures is great, relative to the natural period of the system k, m.

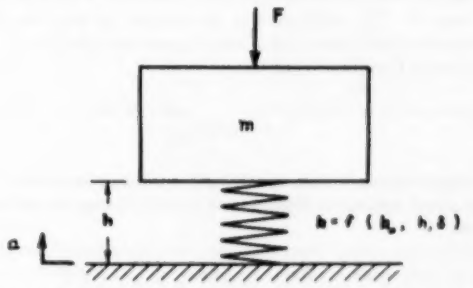

Fig. 1 Schematic Diagram of Rigid Body Supported by Nonlinear Isolator

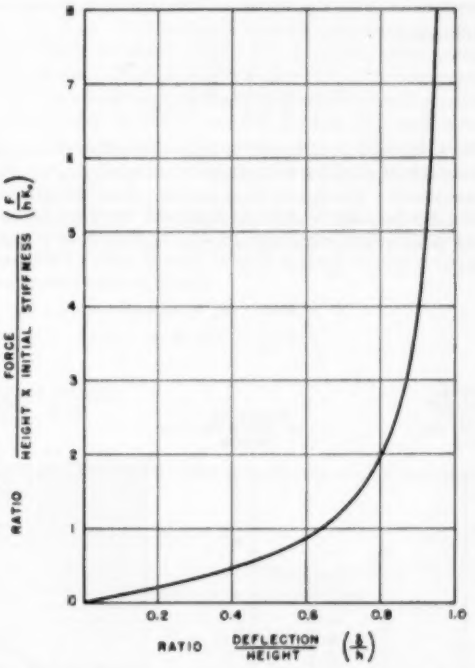

Fig. 2 Force-Deflection Curve for Nonlinear Isolator Plotted in Dimensionless Parameters

An equation that has been found to define approximately the force-deflection characteristic of a typical isolator with increasing stiffness, such as one using rubber in compression as the load-carrying element, is

$$F = \frac{2k_0h}{\pi} \tan \frac{\pi\delta}{2h} \quad \ldots\ldots\ldots\ldots\ldots\ldots [1][2]$$

[1] Chief Engineer, The Barry Corporation. Mem. ASME.

Contributed by the Machine Design Division and presented at the Spring Meeting, Columbus, Ohio, April 28–30, 1953, of The American Society of Mechanical Engineers.

Note: Statements and opinions advanced in papers are to be understood as individual expressions of their authors and not those of the Society. Manuscript received at ASME Headquarters, February 7, 1952. Paper No. 53—S-10.

[2] "Dynamics of Package Cushioning," by R. D. Mindlin, *Bell System Technical Journal*, New York, N. Y., vol. 24, July–October, 1945, equation 1.4.3, p. 363.

Equation [1] may be rearranged with dimensionless parameters, and plotted as shown in Fig. 2. The stiffness k_0 is the slope of the force-deflection curve at the origin, and, therefore, determines the natural frequency of the system when the isolator is not deflected statically. The product hk_0 is equal to the force required to deflect completely a hypothetical linear isolator of stiffness k_0.

Assuming that a sustained force F is applied to the mass m, the isolator experiences a sustained deflection δ in response to the force F. The stiffness k of the isolator at the deflection δ is the derivative of the force F with respect to deflection δ. Differentiating Equation [1] gives

$$k = k_0 \sec^2 \frac{\pi\delta}{2h} \quad \ldots\ldots [2]$$

The following expressions involving the tangent and secant functions which appear in Equations [1] and [2] may be written as follows

$$\tan \frac{\pi\delta}{2h} = \frac{F\pi}{2k_0h}; \quad \sec^2 \frac{\pi\delta}{2h} = 1 + \left(\frac{F\pi}{2k_0h}\right)^2 \quad \ldots\ldots [3]$$

Substituting from Equations [3] in Equation [2] to obtain an expression for k in the equation[5] for natural frequency, $\Omega = \sqrt{k/m}$, gives

$$\Omega = \sqrt{\frac{k_0}{m}\left[1 + \left(\frac{F\pi}{2k_0h}\right)^2\right]} \quad \ldots\ldots [4]$$

The foregoing equations can be made applicable to a condition wherein the support for the system k, m experiences a sustained acceleration a. The inertia force resulting from the mass m then has a value amg which may be considered, for purposes of computing isolator deflection, equal to the applied force F. Substituting

$$F = amg; \quad \Omega_0 = \sqrt{k_0/m} \quad \ldots\ldots [5]$$

Equation [4] becomes

$$\Omega = \sqrt{\Omega_0^2\left[1 + \left(\frac{\pi ag}{2h\Omega_0^2}\right)^2\right]} \quad \ldots\ldots [6]$$

The foregoing equation for natural frequency may be written as a ratio of the natural frequency at any deflection to the natural frequency at zero deflection. This is expressed in engineering units by substituting $g = 386$ in/sec^2, $\Omega_0 = 2\pi f_0$ and $\Omega = 2\pi f$, giving

$$\frac{f}{f_0} = \frac{\Omega}{\Omega_0} = \sqrt{1 + \left[15.37\left(\frac{a}{f_0^2h}\right)\right]^2} \quad \ldots\ldots [7]$$

The significance of the natural frequencies Ω and Ω_0 in the determination of transmissibility may be evaluated by reference to the following equation for transmissibility

$$T = \frac{1}{1 - (\omega/\Omega)^2} \quad \ldots\ldots [8][4]$$

The effective transmissibility of the isolator when subjected to a sustained acceleration a and a forcing frequency ω may be calculated from Equation [8] by substituting the value of Ω determined from Equation [6].

The deflection of the isolator under the influence of sustained acceleration may be determined by substituting expressions from Equations [3] and [5] in Equation [1], and letting $g = 386$ in/sec^2 and $\Omega_0 = 2\pi f_0$, to give

$$\frac{\delta}{h} = \frac{2}{\pi}\tan^{-1}\left[15.37\left(\frac{a}{f_0^2h}\right)\right] \quad \ldots\ldots [9]$$

The relations given by Equations [7] and [9] are shown by the

[5] "Mechanical Vibrations," by J. P. Den Hartog, McGraw-Hill Book Company, New York, N. Y., 1947, equation 16, p. 43.

[6] "Vibration and Shock Isolation," by C. E. Crede, John Wiley and Sons, Inc., New York, N. Y., 1951, equation [2.15], p. 37.

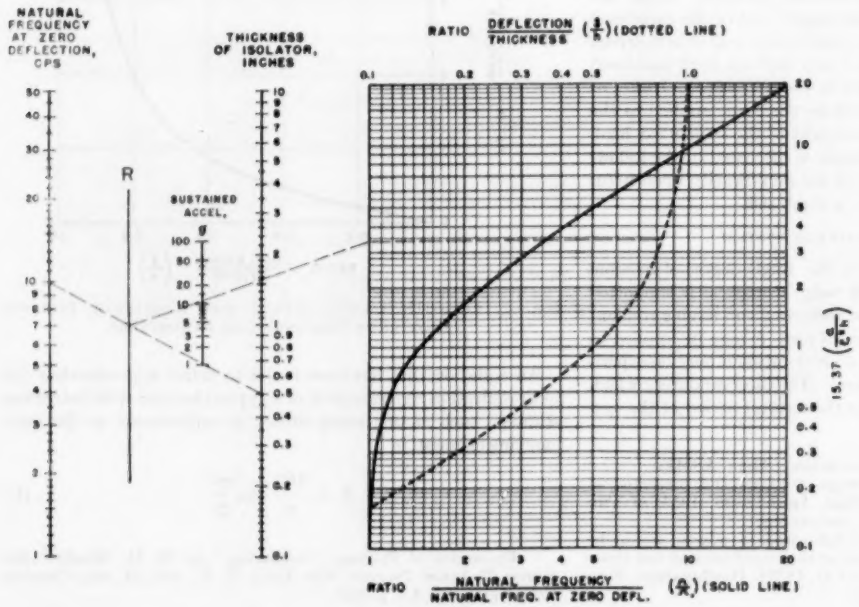

FIG. 3 NOMOGRAPH AND CURVES FOR DETERMINING RATIO OF NATURAL FREQUENCIES AND RATIO OF DEFLECTION TO HEIGHT

combined nomograph and curves in Fig. 3. The nomograph evaluates the parameter

$$15.37\left(\frac{a}{f_0{}^2h}\right)$$

which appears in Equations [7] and [9]. This is transferred by a horizontal projection to the co-ordinate system for the curves; values for the ratio of natural frequencies Ω/Ω_0 are read from the lower abscissa scale, and values for the deflection ratio δ/h are read from the upper abscissa scale. The method of employing Fig. 3 is illustrated by the following example:

Application of Nomograph

An isolator using rubber in compression $^1/_2$ in. thick has a natural frequency at zero deflection of 10 cps; it is subjected to a sustained acceleration of 11 g. It is desired to determine the transmissibility of the isolator to vibration having a forcing frequency of 100 cps, and to determine the deflection of the isolator under the sustained acceleration. Referring to Fig. 3, a straight line is drawn from 10 on the "natural frequency" scale to 0.5 on the "thickness" scale. A second straight line is drawn from the intersection of the first line with the R scale, and is extended through the value 11 on the "sustained acceleration" scale. The second line intersects the left side of the co-ordinate system and is extended horizontally to the intersection with the solid and dotted curves. This indicates a ratio of natural frequency Ω to natural frequency Ω_0 at zero deflection equal to 3.5, and a ratio of deflection δ to thickness h of 0.81. The deflection of the isolator as a result of the sustained acceleration is $0.81 \times 0.5 = 0.405$ in. The transmissibility is calculated from Equation [8] by substituting $\omega = 100 \times 2\pi$ and $\Omega = 10 \times 3.5 \times 2\pi$. Making these substitutions, the transmissibility T is 0.140. In the absence of the sustained acceleration, the corresponding transmissibility would be obtained by substituting $\omega = 100 \times 2\pi$ and $\Omega_0 = 10 \times 2\pi$. The transmissibility of 0.011 obtained from this latter calculation compares with the transmissibility of 0.140 when the system is subjected to sustained acceleration of 11 g.

The expression for the force-deflection characteristic of an isolator, Equation [1], is an approximation. The characteristic for a rubber member in compression may be made to coincide quite closely with this expression by care in design. In general, however, some deviation from the characteristic defined by the expression may be expected. This deviation does not destroy the usefulness of the foregoing data as a design procedure, because the dynamic properties of rubber are such that other uncertainties of equal magnitude are introduced into the determination of natural frequency on the basis of static properties of the rubber.

Discussion

D. C. Kennard, Jr.[6] The system treated in this paper has considerable practical significance in vibration protection of delicate equipment. When the protected equipment is subjected to a sustained acceleration while vibrating, the appropriate stiffening spring must be used in mounting the equipment to minimize static deflections and yet provide the necessary degree of vibration protection.

In this paper it has been assumed that the vibratory displacements are small enough to permit the dynamic spring action to be considered as linear. Hence only one resonant frequency results at a given sustained acceleration in a single-degree-of-freedom system. However, in many applications the vibratory displacements are large enough to warrant consideration of the nonlinear spring effects.

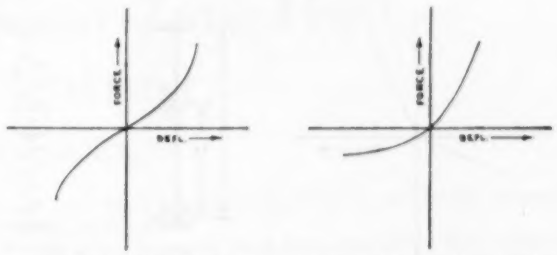

Symmetrical nonlinear spring Asymmetrical nonlinear spring

Fig. 4

This type of nonlinearity is "asymmetrical" about the neutral position of the mass, i.e., the position of rest when the mass does not vibrate. In contrast, the usual nonlinearity treated in text books is symmetrical, Fig. 4 of this discussion.

Assume that asymmetrical nonlinearity of spring rate may be approximated by two straight lines forming an obtuse angle, as shown in Fig. 5(*a*). Two simple systems having such a spring-rate characteristic are shown in Fig. 5(*b*), herewith, where a simple pendulum has a different length on one side of its swing than on the other or where a spring-suspended mass contacts another spring at its neutral position. In such systems, free oscillations take place where the half-sine excursion has a different period and amplitude on one side of the neutral position than on the other, as shown in Fig. 6.

The kinetic energy of the mass passing through neutral position just prior to contact with the stiffened-spring rate is $^1/_2\, mv^2$.

The potential energy stored in both springs at the point of maximum downward excursion is

$$^1/_2(K_1 + K')d_1{}^2 = \frac{1}{2}\, K_2 d_2{}^2$$

Equating the energies

$$mv^2 = K_2 d_2{}^2 \qquad [10]$$

For the upward excursion above the neutral position, the energy equation is

$$mv^2 = K_1 d_1{}^2 \qquad [11]$$

From Equations [10] and [11] the following expression for amplitude ratio in terms of spring-rate ratio is obtained

$$\frac{d_1}{d_2} = \sqrt{\frac{K_2}{K_1}} \qquad [12]$$

The periods may be expressed as

$$2T_1 = 2\pi\sqrt{\frac{m}{K_1}} \quad \text{and} \quad 2T_2 = 2\pi\sqrt{\frac{m}{K_2}}$$

Hence

$$\frac{T_1}{T_2} = \sqrt{\frac{K_2}{K_1}} \qquad [13]$$

With a forcing frequency having a period $T_f = T_1 + T_2$, a net amount of energy can be fed into the system each cycle, thus producing resonance at a frequency which corresponds to the natural frequency treated in the paper.

Now assume a forcing frequency having a half period equal to

[6] Physicist, Equipment Laboratory, Wright Air Development Center, Wright-Patterson Air Force Base, Dayton, Ohio. Mem. ASME.

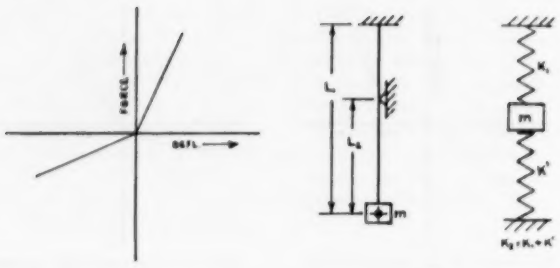

(a) Asymmetrical nonlinear spring approximation

(b) Typical systems with spring characteristics shown in (a)

FIG. 5

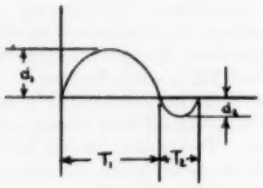

FIG. 6 FREE OSCILLATION OF ASYMMETRICAL NONLINEAR SYSTEM

T_1, i.e., $T_f = 2T_1$. The forcing frequency will be in phase with the first half cycle of velocity only when the following ratio is integral

$$n\left(\frac{T_{f1}}{T_1 + T_2}\right) = N; \quad N = 1, 2, 3 \ldots\ldots\ldots [14]$$

where n is the number of forcing cycles required to make the ratio integral. In other words, T_{f1} will be in phase with the velocity of T_1 every nth cycle of the forcing frequency.

If the forcing frequency has a half period $T_{f2} = 2T_2$, the forcing frequency will be in phase with the second half of the velocity cycle only when the following ratio is integral

$$n\left(\frac{T_{f2}}{T_1 + T_2}\right) = N \ldots\ldots\ldots\ldots\ldots [15]$$

The same number n is required in Equations [14] and [15] to make the ratios integral.

This system responds with a pseudobeating effect at two frequencies of maximum excursion. The first frequency has a period T_{f1} which corresponds to the slow part of the cycle T_1. But as the forcing frequency enters the fast portion of the cycle, its phasing with the velocity response is lost so that even when the slow cycle repeats, the forcing frequency is not phased with response although the half-cycle periods are the same. Hence the slow-cycle displacement is decreased by the opposing effect of the unphased force cycle. This opposing effect continues as the oscillations progress until an integral number of response cycles has taken place during an integral number of force cycles. At this point the velocity cycle receives an in-phase force cycle which boosts the displacement response to a maximum, thus completing the pseudobeat cycle. A similar beat is encountered with the higher frequency resonance where T_{f2} corresponds to the fast part of the cycle T_2.

Thus with large amplitudes such a system has three resonant frequencies or frequencies of maximum excursion. These are the resonant frequency having a period $T_f = T_1 + T_2$, a lower beating-type resonance where $T_{f1} = 2T_1$, and a higher beating-type resonance where $T_{f2} = 2T_2$.

This discussion is intended to provide a simple explanation for the presence of beats which otherwise are unexplainable in nonlinear systems. It in no way detracts from the importance, validity, and timeliness of the paper.

C. D. PENGELLEY.[6] The title of the paper is somewhat misleading since it seems to indicate a general study of the natural frequency of nonlinear systems. In actual practice, it provides a solution for a specific system consisting of a mass supported by a pad of rubber in compression.

A valuable contribution has been made for design purposes. The nomograph, presented in Fig. 3 of the paper, provides much useful information, and the procedures are set forth clearly. Of particular interest is the empirical relationship contained in Equation [1] of the paper which has been set forth graphically in Fig. 2. This provides an approximate force-deflection function for typical rubber springs in compression. It would have been interesting if the author had discussed in more detail the limitations of this expression. What are the effects of changes in the ratio of spring height to cross-sectional area? May it be applied with equal confidence to a "sheet" of rubber and a "block?"

The frequency equations are based upon the assumption that under any given static deflection, the stiffness may be assumed constant during vibration. This, of course, limits the application to vibrational amplitudes which are very small compared with the initial static deflection. Needless to say, a more precise nonlinear analysis which would be applicable to large amplitudes probably would be too complex for practical purposes. Nevertheless, a discussion based on empirical data or qualitative reasoning, which would indicate whether the nonlinearities tend to raise or lower the natural frequencies, would be desirable. An analogy of this would be of considerable practical importance.

AUTHOR'S CLOSURE

It is well known that a complete analysis of a nonlinear system involves many complex phenomena. Certain of these can be simplified by assuming small displacements. The present paper implies but does not state explicitly that the analysis refers only to vibration of small displacement. Mr. Kennard's interesting discussion points out some of the considerations that must be taken into account when analyzing the motion of a nonlinear system with large displacements.

Mr. Pengelley points out that the title of the paper suggests a more general treatment of nonlinear systems than that included in the paper. This criticism is justified in a sense. The explicit results set forth in the nomograph and curves are, of course, limited to one particular type of nonlinearity. In a broader sense, however, the paper points out generally the effect of a nonmassive load and suggests an analytical approach that may be applied to any known type of nonlinearity.

It is suggested by Mr. Pengelley that information be included on the application of Equation [1] to rubber shapes in general. This equation is empirical and has been found to be approximate for rubber elements loaded in compression. The stiffnesses of rubber blocks of the same elastomer and same load-carrying area tend to vary inversely as the thickness. There is an additional consideration resulting from the fact that Poisson's ratio for rubber is one half; i.e., the rubber is incompressible and deflects only by bulging. The lateral area of the block is thus a very important factor in determining the stiffness. Equation [1] may be made to fit the resulting force-deflection curves of blocks and pads empirically by assignment of appropriate values to k_0 and k.

[6] Chairman, Engineering Mechanics, Southwest Research Institute, San Antonio, Texas. Mem. ASME.

Distribution of Shear-Zone Heat in Metal Cutting[1]

By W. C. LEONE,[2] PITTSBURGH, PA.

The paper presents an expression for the fraction of thermal energy developed at the shear zone in orthogonal metal cutting which is conducted back into the workpiece. The shear-zone temperatures calculated using this expression are found to compare favorably with those measured indirectly by Trigger and with those calculated by use of Hahn's inclined-source solution.

SINCE practically all of the energy involved in metal cutting is expended in heating the workpiece, tool, and chips, the temperatures near the cutting region are quite high and have been the subject of research for many years. Herbert (1),[3] Schwerd (2), and Boston (3) did much of the early work. More recently Trigger, Chao, and Zylstra (4, 5, 6, 7, 8, 9), Trent (10), Svakov (11), and Hahn (12) have made contributions to the study.

In orthogonal metal cutting where a continuous chip is produced, there are two sources of heat generation, Fig. 1. At the shear zone AB the metal is deformed plastically and practically all of the strain energy involved in the deformation appears in the form of heat. The second source is at the chip-tool interface AC and is due to the friction of the chip rubbing against the face of the tool.

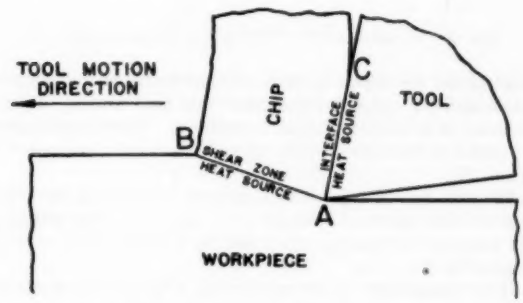

FIG. 1 SOURCES OF HEAT GENERATION

Undeformed and unheated workpiece material passes through AB where its temperature is raised by the heat of deformation at the shear zone. After passing through AB this same material becomes the deformed and heated chip material which acquires more heat at AC. Therefore the chip at AC is quite hot and may even attain a temperature as high as the melting temperature of the chip or tool.

The energy expended along shear zone AB is that which is almost entirely available as thermal energy to be distributed partly into the workpiece and partly into the chip. If the fraction of this energy which goes into the workpiece is known, the shear-zone temperature can be found. If the workpiece is held stationary and the tool moves with a constant horizontal velocity, a moving heat source is involved. The workpiece is large in the plane of tool motion and the depth of cut is very small compared with the other dimensions of the system. The width of the heat source in the direction of motion is small, Fig. 2. Therefore the heat source can be taken as a moving-line source uniformly distributed across the thickness w of a semi-infinite plate, Fig. 3.

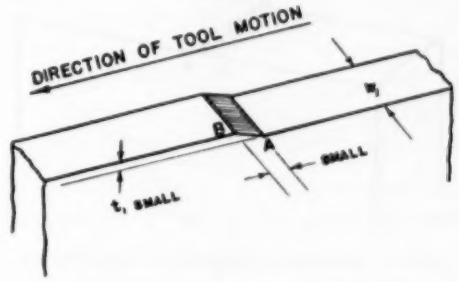

FIG. 2 HEAT SOURCE MOVING ON WORKPIECE

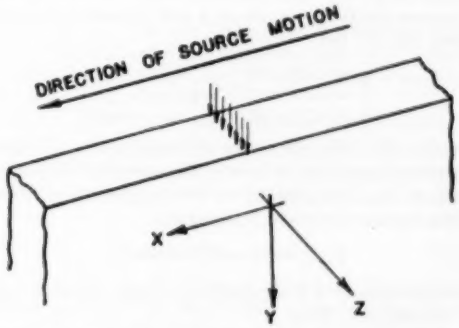

FIG. 3 LINE HEAT SOURCE MOVING ON WORKPIECE

LINE-SOURCE SOLUTION

Assuming a quasi-stationary state (13), the line-source solution is

$$T - T_0 = \frac{q'}{\pi k} e^{\frac{-V_s s}{2a}} K_0\left(\frac{V_s |s|}{2a}\right) \quad \ldots\ldots\ldots [1]$$

where

T = temperature on surface of workpiece at distance s from source, deg F

[1] Research underlying this paper was done in partial fulfillment of the requirements for the degree of Doctor of Science at Carnegie Institute of Technology.

[2] Assistant Professor, Department of Mechanical Engineering, Carnegie Institute of Technology. Jun. ASME.

[3] Numbers in parentheses refer to Bibliography at end of paper.

Contributed by the Production Engineering Division and presented at a joint session with the Research Committee on Metal Processing at the Spring Meeting, Columbus, Ohio, April 28–30, 1953, of THE AMERICAN SOCIETY OF MECHANICAL ENGINEERS.

NOTE: Statements and opinions advanced in papers are to be understood as individual expressions of their authors and not those of the Society. Manuscript received at ASME Headquarters, January 15, 1953. Paper No. 53—S-7.

s = distance from source in direction of tool motion, in.
T_0 = ambient temperature, deg F
q' = rate of heat per unit length of line source, Btu/in sec deg F
k = thermal conductivity of workpiece material, Btu/in sec deg F
V_c = velocity of tool with respect to workpiece, ips
a = thermal diffusivity of workpiece material, sq in. per sec
K_0 = modified Bessel function of second kind and zero order

Of course, the line-source solution will yield the result that the shear-zone temperature is infinite. The solution is still useful, however, in that it enables us to make a rough calculation of the relative temperatures in front of and behind the source. For example, using information corresponding to data of Merchant (14), the heat source is one of dimensions $w = 0.25$ in. and $t_1 \cot \phi$ = 0.0121 in. Taking the line heat source in the middle of the shear-zone area over which the heat source actually spreads, we can compare the temperatures at A and B which are only 0.0121 in. apart, Fig. 4. Let

$\rho = 0.281$ pci
$c = 0.12$ Btu/lb deg F
$k = 5.7 \times 10^{-4}$ Btu/in sec deg F

which should be of the right order of magnitude for NE 9445 steel.

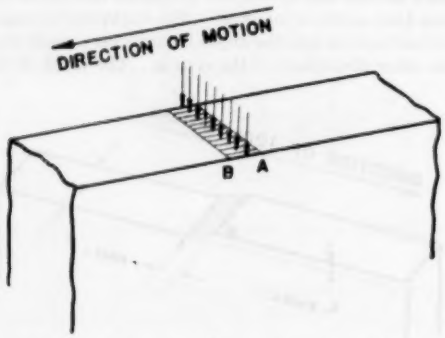

FIG. 4 ASSUMED LINE SOURCE AND AREA SOURCE

The temperature at B in front of the source will be the value of T obtained from Equation [1] for $s = (t_1/2) \cot \phi = 0.00605$ in. Substitution into Equation [1] shows that

$$T_{at\ B} - T_0 = 2.2 \times 10^{-4} q'$$

The temperature at A is obtained in the same manner except that $s = -0.00605$ in. Then

$$T_{at\ A} - T_0 = 268\ q'$$

Certainly T_B can be considered negligible when it is compared with T_A. It appears that the material in front of the shear zone is essentially unheated.

Therefore, in so far as the thermal problem is concerned, the material *E-B-A-D*, Fig. 5, serves only as a means of supplying the material from which the chip is formed. Thus the system can be represented as in Fig. 6 where the chip moves along the surface of the workpiece with a constant horizontal velocity and is itself continuously formed such that its velocity of flow is V_f as shown.

Suppose that σ is the fraction of q which goes into the workpiece, where q is the heat rate at the source in units of Btu/in² sec. Then $(1 - \sigma)$ must go into the chip.

The temperature of the workpiece at the center of source AB can be found for a heat source of a given intensity with the aid

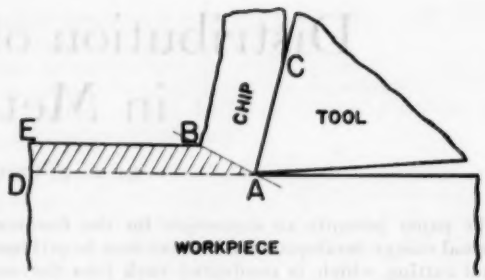

FIG. 5 CHIP FORMED FROM MATERIAL *E-B-A-D*

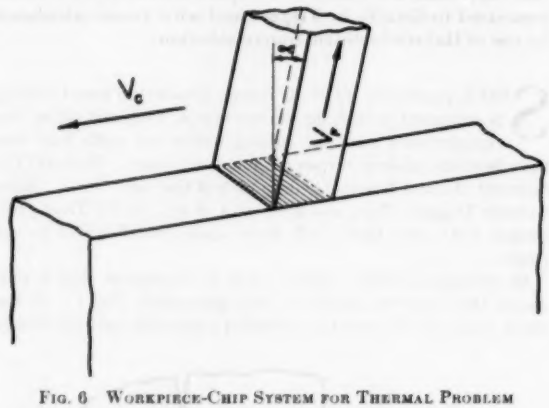

FIG. 6 WORKPIECE-CHIP SYSTEM FOR THERMAL PROBLEM

of a method developed by Blok (15) for the rubbing of unlubricated surfaces. For the workpiece this heat source, which is assumed to be uniform, has an intensity q. The temperature at the center of the source, which will be in terms of σ, is denoted by $(T_w + T_0)$.

The chip can be treated as a uniform bar moving through a uniform heat source of intensity $(1 - \sigma)q$. The temperature at the center of the source, which will be in terms of $(1 - \sigma)$, is denoted by $(T_c + T_0)$.

If the temperature at the center of the source for the workpiece and chip are used as a basis for comparison, T_w can be set equal to T_c. The equation relating T_w and T_c will have only one unknown, σ. The fractional distribution of heat energy to workpiece and chip, and therefore, the temperature $(T_w + T_0)$ can be found.

Suppose that an evenly distributed and continuously applied source of heat (square-shaped with sides $2L$) moves over the plane surface of a large body at a uniform velocity in a direction parallel to one of the sides; it is assumed that the heat supply is started simultaneously with the motion. Blok (15) found the temperature T_H at the center C at a time H after starting the motion. For a velocity $V \geq 4a/L$, he found that

$$T_{H=\infty} \approx \frac{\sqrt{\frac{4a}{VL}}}{\sqrt{\pi}} \frac{qL}{k} \quad \ldots\ldots\ldots\ldots\ldots\ldots [2]$$

where $T_0 = 0$. At increasing velocities, the "side flow" of heat into the body is increasingly reduced so that the square source of heat may be approximately compared with that of an infinitely band-shaped source of heat (width $2L$), moving with the same high velocity V at right angles to its longitudinal axis.

Since only σq Btu/in² sec goes into the workpiece, the temperature rise T_w will be

$$T_w \approx \frac{\sigma q L}{k} \frac{\sqrt{\frac{4a}{VL}}}{\sqrt{\pi}}$$

or

$$T_w \approx 1.13 \frac{\sigma q}{k} \sqrt{\frac{aL}{V_c}} \quad \ldots\ldots [3]$$

In so far as the chip is concerned, we can assume it to be of uniform cross section and that it flows from the location of the heat source continuously with a velocity V_f. We are not concerned with motion of the chip in the direction V_c because the heat source moves right along with the chip. Since the rake angle α is small the heating of the chip can be treated as a linear heat-flow problem.

If the origin of a Cartesian co-ordinate system is taken at the center of the source with the x-axis in the direction of V_f, and if the quasi-stationary state is again assumed

$$T - T_0 = \frac{aq}{V_f k} e^{\frac{-V_f s'}{a}} \quad \ldots\ldots [4]$$

where s' is the distance from the source and the boundary conditions used are that

$$T = T_0 \text{ at } s' = \infty$$

$$\frac{dT}{ds'} \to 0 \text{ as } s' \to \infty$$

$$-k \frac{dT}{ds'} \to q \text{ as } s' \to 0$$

The rise of temperature at the location of the source will be the value of $T - T_0$ for $s' = 0$. Since the fraction of q that goes into the chip is $(1 - \sigma)$

$$T_c = \frac{aq\,(1 - \sigma)}{V_f k}$$

or, since $a = k/\rho c$

$$T_c = \frac{(1 - \sigma)\, q}{V_f \rho c} \quad \ldots\ldots [5]$$

By setting T_w from Equation [3] equal to T_c from Equation [5] we arrive at a simple equation for σ, which determines the distribution of heat to the workpiece and chip

$$T_w = \frac{\sigma q L}{k} \frac{\sqrt{\frac{4a}{V_c L}}}{\sqrt{\pi}} = T_c = \frac{(1 - \sigma)\, q}{V_f \rho c}$$

$$\sigma = \frac{1}{1 + 2\, LV_f \sqrt{\frac{1}{V_c L \pi a}}}$$

But $V_f = rV_c$, therefore

$$\sigma = \frac{1}{1 + 1.13\, r \sqrt{\frac{LV_c}{a}}} \quad \ldots\ldots [6]$$

The portion of heat that goes into the workpiece can be determined from Equation [6]. Of course the portion that goes into the chip is found by subtracting σ from 1. It is interesting to note that the total heat expended q need not be known to find the distribution determined by σ. Since

$$r \sqrt{\frac{LV_c}{a}}$$

is dimensionless, it is possible to show the variation of σ with this dimensionless group. This is shown in Fig. 7. For a given cutting test, r, V_c, and L are known or easily found. If an estimate is made for the diffusivity of the material for the given cutting conditions

$$r \sqrt{\frac{LV_c}{a}}$$

is easily computed and σ can be taken directly from the curve in Fig. 7.

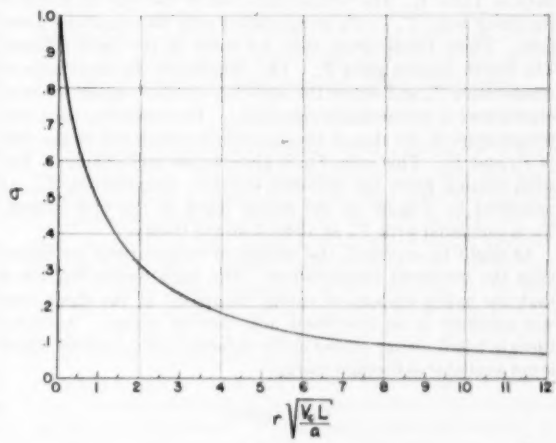

FIG. 7 FRACTION OF HEAT TO WORKPIECE VERSUS $r\sqrt{\frac{V_c L}{a}}$

As pointed out by Chao and Trigger (9), the fraction of heat generated at the shear zone and conducted back into the workpiece depends on the thermal number since LV_c/a is really the thermal number times $(\cot \phi)/2$.

Of course, q must be known for finding the actual temperature rises T_w and T_c. With σ known, either Equation [3] or [5] can be used for finding the temperature of the chip as it leaves the shear zone. If this temperature is denoted by T_s, $T_s = T_w + T_0 = T_c + T_0$.

CHECKING EQUATIONS

As a partial check on the equations given here, it is desirable to calculate temperatures for which observations have been made. The tests made by Trigger (5, 6) are rather complete in that F_c, F_t, r, α, w, and the temperatures were all measured over a range of operating speeds. It is possible to work back from his recorded and plotted results to obtain the pertinent data needed in our calculations. These data are shown in Table 1. For specific-heat and thermal-conductivity values, the ASM Metals Handbook curves used by Trigger and Chao (7) are used here.

TABLE 1 DATA CORRESPONDING TO TRIGGER'S EXPERIMENTAL DATA

V_c	F_c	F_t	r	ϕ	$W_s/10^3$	q	L	V_f	F	FV_f
20	475	330	0.235	13.4	390	199	0.214	4.7	362	1700
40	410	235	0.330	18.6	323	466	0.151	13.2	263	3470
60	378	192	0.375	21.0	296	730	0.133	22.5	218	4910
80	360	170	0.398	22.2	283	990	0.125	31.8	194	6160
100	345	155	0.415	23.1	271	1240	0.120	41.5	179	7440
120	338	142	0.425	23.6	268	1510	0.117	51.0	166	8460

NOTE: For all cases $t = 0.102$ in., $w = 0.0098$ in., $\alpha = 4$ deg.

TABLE 2 COMPARISON OF EXPERIMENTAL AND CALCULATED TEMPERATURES

V_s, fpm	T_f, deg F	$T_s - T_0$, deg F	T_s, deg F	T_{1c}, calculated, deg F	T_{1x}, experimental, deg F
100	269	810	875	1144	1030
200	507	747	812	1319	1190
300	626	726	791	1417	1300
400	713	703	768	1481	1380
500	781	682	747	1528	1445
600	827	679	744	1571	1502

NOTE: Room temperature = 65 F = T_0.

In Table 2 the second column gives the temperature rise at the contact surface of the chips caused by rubbing friction of the tool T_f, as theoretically calculated by Trigger and Chao (7) for the data in Table 1. The temperature rise of the chip as it leaves the shear zone, $T_s - T_0$, is calculated with the equations given here. These temperature rises are listed in the third column. The fourth column gives T_s. The chip leaves the shear zone at temperature T_s and enters the tool-chip interface region where it experiences a temperature rise of T_f. Theoretically, then, the temperature of the chip at the tool-chip interface will be the sum of T_f and T_s. This sum, T_{1c}, is given in the fifth column. The sixth column gives the tool-chip interface temperature, T_{1x}, as measured by Trigger at the speeds listed in the first column. T_{1c} is compared with T_{1x} as a check on the theory.

As might be expected, the calculated temperatures are higher than the measured temperatures. The main reason for this is that the entire amount of energy dissipated at the shear zone was assumed to be converted into thermal energy. Actually, there is latent energy stored in the deformed chip material which is not available as thermal energy.

CONCLUSION

The calorimetric measurements for total chip temperature made by Hahn (12) were not made in Trigger's tests. However, it is possible to compare the shear-zone temperature as obtained here with that using Hahn's inclined-source method. Additional curves for Hahn's "average dimensionless temperature" had to be drawn to cover the range required by using Trigger's data. The comparison, however, was reasonably good considering the many approximations and assumptions that had to be made in both derivations. Also, as expected, Hahn's "dimensionless adiabatic temperature" is at all times higher than the shear-zone temperature found here. Therefore it is felt that the curve in Fig. 7 is reliable in giving approximately the fraction of shear-zone heat conducted back into the workpiece.

BIBLIOGRAPHY

1 "The Measurement of Cutting Temperatures," by E. Herbert, Proceedings of The Institution of Mechanical Engineers, vol. 1, 1926, pp. 289–329.

2 "Über die Bestimmung des Temperaturfeldes beim Spanablauf," by F. Schwerd, *Zeit. VDI*, vol. 77, 1933, pp. 211–216.

3 "Cutting Temperatures Developed by Single-Point Turning Tools," by O. Boston and W. Gilbert, Trans. ASM, vol. 23, 1935, pp. 703–726.

4 "Thermophysical Aspects of Metal Cutting," by B. T. Chao, K. J. Trigger, and L. B. Zylstra, Trans. ASME, vol. 74, 1952, p. 1039.

5 "Progress Report No. 1 on Tool-Chip Interface Temperatures," by K. J. Trigger, Trans. ASME, vol. 70, 1948, pp. 91–98.

6 "Progress Report No. 2 on Tool-Chip Interface Temperatures," by K. J. Trigger, Trans. ASME, vol. 71, 1949, pp. 163–174.

7 "An Analytical Evaluation of Metal-Cutting Temperatures," by K. J. Trigger and B. T. Chao, Trans. ASME, vol. 73, 1951, pp. 57–68.

8 "Cutting Temperatures and Metal-Cutting Phenomena," by B. T. Chao and K. J. Trigger, Trans. ASME, vol. 73, 1951, pp. 777–793.

9 "The Significance of the Thermal Number in Metal Machining," by B. T. Chao and K. J. Trigger, Trans. ASME, vol. 75, 1953, pp. 109–120.

10 "Some Factors Affecting Wear on Cemented Carbide Tools," by E. M. Trent, Proceedings of The Institution of Mechanical Engineers, vol. 166, 1952, pp. 64–74.

11 "Analytic Determination of Amount of Heat Evolved in a Chip Being Machined," *Stanki ie Instrument* (Russian), vol. 22, February, 1951, pp. 27–28.

12 "On the Temperature Developed at the Shear Plane in the Metal Cutting Process," by R. Hahn, Proceedings of the First U. S. National Congress of Applied Mechanics, June, 1951. Published by ASME, January, 1953.

13 "The Theory of Moving Sources of Heat and Its Application to Metal Treatments," by D. Rosenthal, Trans. ASME, vol. 68, 1946, pp. 848–866.

14 "Mechanics of the Metal Cutting Process, I, II," by M. Merchant, *Journal of Applied Physics*, vol. 16, 1945, pp. 267–275, 318–324.

15 "Theoretical Study of Temperature Rise at Surfaces of Actual Contact Under Oiliness Lubricating Conditions," by H. Blok, Proceedings of the General Discussion on Lubrication and Lubricants, The Institution of Mechanical Engineers, vol. 152, 1938, pp. 222–235.

Discussion

H. BLOK.[4] The author mentions the term "thermal number" previously introduced by others. The term "thermal Reynolds number" also has been proposed.[5]

It may have escaped the attention of the various authors that in the theory of heat transfer by flowing fluids the term "Péclet number" has been adopted generally for a quite similar characteristic number. Because there is no fundamental difference between the convection of heat by a moving ("flowing") solid and that by a flowing fluid, it is suggested, in order to acheive uniformity of nomenclature, henceforth to adopt the term Péclet number in the problem concerned. In so far as the author's theory is concerned, the writer may point out that he developed a similar approach to the problem in hand soon after he applied the principle of "partition"[6] to problems of frictional heat sources. On closer consideration, however, he decided to abandon this approach, which in essence is also used by E. G. Loewen and M. C. Shaw.[7] In order to save space the writer refrains from stating the reasons underlying his decision; the reader may be referred to the writer's discussion on the last-mentioned paper.

R. S. HAHN.[8] The author is to be complimented on his theory of the partitioning of energy between the chip and workpiece. It is to be hoped that the author's curve, shown in Fig. 7, will receive experimental verification.

The writer has discussed a recent paper by Loewen and Shaw[7] covering shear-plane energy, and that discussion would apply equally well to the author's paper.

M. C. SHAW[9] AND E. G. LOEWEN.[10] Although the author has not compared his solution of the shear-plane temperature problem

[4] Professor of Mechanical Engineering, Technological University, Delft, Holland.

[5] "The Life of Carbide-Tipped Turning Tools," by F. F. P. and G. H. Bisacre, Proceedings of the Institution of Mechanical Engineers, War Emergency Issue No. 35, London, England, vol. 157, 1947, pp. 452–461.

[6] Author's bibliography (15).

[7] "On the Analysis of Cutting Tool Temperatures," by E. G. Loewen and M. C. Shaw, Paper No. 53—S-15, presented at the Spring Meeting, Columbus, Ohio, April 28–30, 1953, of THE AMERICAN SOCIETY OF MECHANICAL ENGINEERS.

[8] Research Engineer, The Heald Machine Company, Worcester, Mass. Mem. ASME.

[9] Professor of Mechanical Engineering, Machine Tool Division, Massachusetts Institute of Technology, Cambridge, Mass. Mem. ASME.

[10] Assistant Professor of Mechanical Engineering, Machine Tool Division, Massachusetts Institute of Technology. Jun. ASME.

with that presented at the Toronto meeting of the Society in 1952,[11] there is remarkable similarity between these two solutions and the results they predict. Both solutions utilize the technique of solving for the shear-plane temperature in two ways, once as a point in the chip and once as a point in the workpiece, and then equating the two temperatures to obtain the distribution of thermal energy between chip and workpiece. Both solutions also assume a uniform distribution of shear work along the shear plane.

In addition to the similarities there are important differences in the two methods. The present author ignores the inclination of the shear plane and assumes a horizontal slider moving with velocity V_c when applying the moving heat source equations. In the references mentioned, however, the inclination of the shear plane is retained and the important velocity is taken to be the velocity along the shear plane between chip and work in accordance with the Piispanen card model of chip formation. The author equates the temperatures at the mid-point of the slider to obtain the energy distribution between chip and workpiece, whereas the mean shear-plane temperatures were equated in the afore-mentioned references. It is of interest to note that Blok[6] did not use either of these techniques but rather equated the maximum temperatures reached in the two cases in his treatment of the plane slider. It cannot be said which method is to be preferred, although it would appear that use of either the mean or center temperature might lead to results closer to the truth. Another difference in the author's treatment and that mentioned lies in the fact that he uses Blok's solution for a square moving heat source, while in the previous case Jaeger's finite area-moving heat source solution was used.

Despite these differences the end results obtained are essentially the same. A representative example was found to yield values of the two end results that were identical within less than 1 per cent.

K. J. Trigger[12] and B. T. Chao.[13] The author's analysis sheds further light on the complex problem of temperatures in metal cutting. The writers are particularly gratified to note the trend in Fig. 7 of the paper. They have contended that the proportion of total energy which shows up in the workpiece decreases with increase in speed and/or feed. This decrease has been expressed as a function of the thermal number. (Possible confusion can be avoided by indicating the units in the first column of Table 1 of the paper, as inches per second.)

With reference to the proportion of energy of deformation which is present as latent energy in the chip, the writers in their analytical study (1950) used the then accepted best figures of Taylor and Quinney. Recent studies and some now in progress may indicate the need for revisions.

At the time the paper was presented the writers stated that "further refinements undoubtedly are possible, particularly with reference to the proportion of heat left in the workpiece in turning, and to the latent energy left in the chip due to deformation." This paper contributes significantly to those refinements.

Author's Closure

The author appreciates Professor Blok's desire for uniformity of nomenclature. Fortunately, people in the metal-cutting field have been careful to define the factors that enter the characteristic number concerned so that clarity has been maintained. However, comparisons with work in other fields would make it advantageous to use a common name, such as "Péclet number."

In Professor Blok's discussion of the paper by E. G. Loewen and M. C. Shaw,[7] the writer concludes that the principle of partition is not applicable to the shear-zone heat in metal cutting. It should be noted that the main objection to the use of this principle is that it yields inaccurate "side-leakage" values. For high velocities, side leakage is not considered of large enough magnitude to be important. The author agrees that solution of the model of Fig. 16 in that discussion would be desirable.

The author is grateful for Dr. Hahn's interest and, of course, shares his hope that the curve of Fig. 7 will receive experimental verification.

Professors Loewen and Shaw have pointed out the similarities and differences in their solution and that of the author. Since presentation of these papers the author has compared values of shear-zone heat going into the workpiece by the two solutions for most of the data in the writers' paper. The end results are indeed almost identical.

The author wishes to thank Professors Trigger and Chao for their comments.

[11] "Surface Temperatures in Grinding," by J. O. Outwater and M. C. Shaw, Trans. ASME, vol. 74, 1952, p. 73; see also "On the Analysis of Cutting Tool Temperatures," by E. G. Loewen and M. C. Shaw, Paper No. 53—S-15, presented at the Spring Meeting, Columbus, Ohio, April 28–30, 1953, of The American Society of Mechanical Engineers.

[12] Professor of Mechanical Engineering, University of Illinois, Urbana, Ill. Mem. ASME.

[13] Assistant Professor of Mechanical Engineering, University of Illinois.

Transient Thermal Stresses in Circular Disks and Cylinders

By G. HORVAY,[1] SCHENECTADY, N. Y.

The effect of a suddenly applied peripheral temperature

$$\vartheta(R, \varphi, z, t) = T \cos n\varphi \, \mathbf{1}(t)$$

upon circular disks and cylinders is considered. The most interesting results are (*a*) for thermal shock (*t* = very small) the stresses in an unrestrained cylinder are

$$\widehat{\varphi\varphi} \sim \widehat{zz} \sim -\frac{E\alpha T}{1-\mu} (r/R)^{R/\sqrt{\pi d}} \cos n\varphi$$

and all other stresses vanish; (*b*) in the steady state (*t* = ∞) the temperature distribution is

$$\vartheta(r, \varphi) = T(r/R)^n \cos n\varphi$$

and all stresses vanish.

Nomenclature

The following nomenclature is used in the paper:

R = disk radius
x, y, z = rectangular co-ordinates
r, φ, z = cylindrical co-ordinates
ρ = r/R
t = time
u, v, w = radial, tangential, and axial displacements
$\epsilon_r, \epsilon_{r\varphi}, \epsilon_\varphi, \epsilon_z$ = radial, shear, hoop, and axial strains
$\widehat{rr}, \widehat{r\varphi}, \widehat{\varphi\varphi}, \widehat{zz}$ = radial, shear, hoop, and axial stresses
μ, E = elastic constants
F = Airy's function
α = coefficient of thermal expansion
T = maximum temperature at rim of disk or cylinder
ϑ = temperature at point r, φ, z at time t
κ = diffusivity
τ = dimensionless time = $\kappa t/R^2$
S = $E\alpha T$
l = $R\alpha T$
$A_m, a_{nk}, \gamma_m, \delta_{nk}$ = coefficients and phase constants in various expansions
a, b, etc. = coefficients in certain expressions
Δ = expression in [4*a*]
p, λ = summation or integration variables
$\mathcal{R}es$ = residue
ν_j = root of $J_n(\nu) = 0$
$\mathbf{1}(t)$ = Heaviside's unit function = $\begin{cases} 0 \text{ for } t < 0 \\ 1 \text{ for } t \geqslant 0 \end{cases}$

Subscripts

d, c, f = disk, cylinder constrained at ends, cylinder free at ends

1 Introduction

Two distinct, but closely related, problems are treated in this paper: (*a*) The stresses and deformations of a disk due to a steady-state temperature distribution

$$\vartheta(r, \varphi) = T(r/R)^k \cos n\varphi$$

are determined. This problem is of significance for a tube sheet when the flow which passes through it is of nonuniform temperature both in the radial and in the azimuthal direction.[2] (*b*) The stresses and deformations are determined which occur in a disk or cylinder which is heated on one side, cooled on the other side, according to the law

$$\vartheta = T \cos \varphi$$

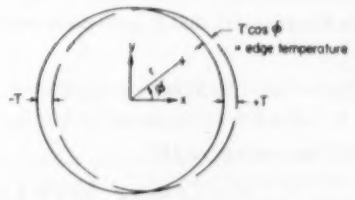

Fig. 1 Disk Subject to Sinusoidal Edge Temperature

as indicated in Fig. 1, or according to the somewhat more general law

$$\vartheta = T\Sigma A_m \cos(m\varphi + \gamma_m)$$

when this edge temperature is applied at time $t = 0$ to an originally unheated disk or cylinder [$\vartheta(r, \varphi, z, t) = 0$ for $t < 0$]. It is found that the resultant temperature distribution is of the form

$$\vartheta(r, \varphi, z, t) = T \sum_{n,k} a_{nk}(t)(r/R)^k \cos(n\varphi + \delta_{nk})$$

and, therefore, solution of problem (*a*) and the slight changes needed in the disk formula to make them applicable to a cylinder, permits resolution also of problem (*b*).

2 Stresses in Solid Circular Disk Due to an $r^k \cos n\varphi$ Temperature Distribution[4]

It is shown by R. D. Mindlin and M. G. Salvadori (2) that an

---

[1] Development Engineer, Knolls Atomic Power Laboratory. Mem. ASME. The Knolls Atomic Power Laboratory is operated by the General Electric Company for the Atomic Energy Commission. The work reported here was carried out under Contract No. W-31-109 Eng-52.

Contributed by the Heat Transfer Division and presented at a joint meeting with the Heat Transfer and Fluid Mechanics Institute at the Semi-Annual Meeting, Los Angeles, Calif., June 28–July 2, 1953, of The American Society of Mechanical Engineers.

Note: Statements and opinions advanced in papers are to be understood as individual expressions of their authors and not those of the Society. Manuscript received at ASME Headquarters, June 11, 1951. Paper No. 53—SA-51.

[2] It is shown elsewhere (1)[3] that the tube-sheet problem can be reduced in many cases to that of a solid disk.

[3] Numbers in parentheses refer to the Bibliography at the end of the paper.

[4] In his original draft the author, unaware of Equations [2*a*, *b*], determined the stresses by solving simultaneously two equilibrium and one compatibility equation. Some time later, in a lecture on thermal stresses to members of the "Advanced Engineering Program" of the General Electric Company, one of his students, R. Culbertson, derived Equations [2*a*, *b*]. The equations subsequently were located also in reference (2). Once Equations [2*a*, *b*] are available the problem of solving for three stresses can be replaced by the simpler problem of solving for one stress function.

unrestrained disk of radius R, subject to the temperature distribution $\vartheta(r, \varphi)$ incurs stresses

$$\left.\begin{aligned}\widehat{rr} &= F_{\varphi\varphi}/r^2 + F_r/r \\ \widehat{\varphi\varphi} &= F_{rr} \\ \widehat{r\varphi} &= -(F_\varphi/r)_r\end{aligned}\right\} \quad \ldots\ldots [1]$$

where F is solution of the equation

$$\nabla^4 F = (\partial^2/\partial r^2 + \partial/r\partial r + \partial^2/r^2\partial\varphi^2)^2 F = -E\alpha\nabla^2\vartheta \quad \ldots [2a]$$

subject to the boundary conditions

$$\widehat{rr}(R) = \widehat{r\varphi}(R) = 0 \quad \ldots\ldots [2b]$$

For the assumed temperature distribution

$$\vartheta = T\rho^k \cos n\varphi \quad \ldots\ldots [3]$$

the particular solution of Equation [2a] can be written as

$$F_p = -S(R^2/\Delta)\rho^{k+2} \cos n\varphi, \quad k + 2 \neq n \quad \ldots\ldots [4a]$$

$$\Delta = (k + 2)^2 - n^2$$

$$F_p = -S(R^2/2n)\rho^n \ln \rho \cos n\varphi, \quad k + 2 = n \quad \ldots\ldots [4b]$$

where

$$S = E\alpha T \quad \ldots\ldots [5]$$

One finds, by Equations [1], that F_p gives rise to certain boundary stresses

$$\left.\begin{aligned}\widehat{rr}_p(R) &= S[(n^2 - k - 2)/\Delta] \cos n\varphi, \ \widehat{r\varphi}_p(R) \\ &= -S[n(k + 1)/\Delta] \sin n\varphi \text{ for } k + 2 \neq n \\ \widehat{rr}_p(R) &= -(S/2n) \cos n\varphi, \ \widehat{r\varphi}_p(R) \\ &= -\frac{1}{2} S \sin n\varphi \quad \text{for } k + 2 = n\end{aligned}\right\} \quad \ldots [6]$$

which should not be present. Therefore we next solve the homogeneous equation

$$\nabla^4 F_h = 0 \quad \ldots\ldots [7a]$$

subject to the boundary conditions

$$[F_{h,\varphi\varphi}/r^2 + F_{h,r}/r]_{r=R} = -\widehat{rr}_p(R), \ [(F_{h,\varphi}/r)_r]_{r=R} = \widehat{r\varphi}_p(R) \quad \ldots [7b]$$

and find that

$$\left.\begin{aligned}F_h &= -\frac{SR^2}{2(k + 2 + n)} \rho^n \left[1 - \frac{2}{k + 2 - n} - \rho^2\right] \\ &\quad \times \cos n\varphi \quad \text{for } k + 2 \neq n \\ F_h &= -\frac{SR^2}{4n} \rho^n [1 - \rho^2] \cos n\varphi \quad \text{for } k + 2 = n\end{aligned}\right\} \quad \ldots [8]$$

is the appropriate biharmonic function. We add this to solution [4] to constitute the complete solution of Equation [2]

$$F = F_p + F_h \quad \ldots\ldots [9]$$

From this the stresses are obtained by differentiation, as indicated in Equations [1]. The stresses induced by the temperature distribution Equation [3] therefore are as follows:

Case $k \neq n - 2$

$$\left.\begin{aligned}\widehat{rr} &= (a\rho^k + b\rho^{n-2} + c\rho^n)S \cos n\varphi \\ \widehat{\varphi\varphi} &= (A\rho^k + B\rho^{n-2} + C\rho^n)S \cos n\varphi \\ \widehat{r\varphi} &= (\alpha\rho^k + \beta\rho^{n-2} + \gamma\rho^n)S \sin n\varphi\end{aligned}\right\} \quad \ldots [10a]$$

Case $k = n - 2$

$$\left.\begin{aligned}\widehat{rr} &= (a'\rho^{n-2} + b'\rho^{n-2} \ln \rho + c\rho^n)S \cos n\varphi \\ \widehat{\varphi\varphi} &= (A'\rho^{n-2} + B'\rho^{n-2} \ln \rho + C\rho^n)S \cos n\varphi \\ \widehat{r\varphi} &= (\alpha'\rho^{n-2} + \beta'\rho^{n-2} \ln \rho + \gamma\rho^n)S \sin n\varphi\end{aligned}\right\} \quad \ldots [10b]$$

where[5]

$$\left.\begin{aligned}a &= (n^2 - k - 2)/\Delta, \ A = -(k + 1)(k + 2)/\Delta, \ \alpha \\ &\quad = -n(k + 1)/\Delta \\ b &= -B = -\beta = -n(n - 1)(n - k)/2\Delta \\ c &= -(n + 1)(n - 2)/2(k + 2 + n) \\ C &= (n + 1)(n + 2)/2(k + 2 + n) \\ \gamma &= (n + 1)n/2(k + 2 + n) \\ a' &= (n + 1)(n - 2)/4n, \ A' = (-n^2 - 3n + 2)/4n \\ \alpha' &= -(n + 1)/4 \\ b' &= -B' = -\beta' = (n - 1)/2\end{aligned}\right\} \quad . [10c]$$

The stresses $\widehat{rr}$, $\widehat{\varphi\varphi}$, $\widehat{r\varphi}$ are plotted in Figs. 2(*a*, *b*, *c*), 3(*a*, *b*, *c*), and 4(*a*,[6] *b*, *c*) for $n = 1, 2, 3$. The case $n = 0$ is treated in reference (3).

We note in particular that when ϑ is a harmonic function

$$\vartheta = \rho^n \cos n\varphi \quad \ldots\ldots [11a]$$

i.e., when steady-state temperature distribution is maintained, and there are no heat sources or sinks within the disk then

$$\widehat{rr} = \widehat{\varphi\varphi} = \widehat{r\varphi} = 0 \quad \ldots\ldots [11b]$$

is the correct solution of Equations [1], [2]: i.e., the unrestrained disk is stressless. This is a particular case of Biot's theorem.[7]

3 Displacements

The displacements u, v are obtained from the stress-strain relations

$$E\epsilon_r = \widehat{rr} - \mu\widehat{\varphi\varphi} + E\alpha\vartheta \quad \ldots\ldots [12a]$$

$$E\epsilon_\varphi = \widehat{\varphi\varphi} - \mu\widehat{rr} + E\alpha\vartheta \quad \ldots\ldots [12b]$$

$$E\epsilon_{r\varphi} = 2(1 + \mu)\widehat{r\varphi} \quad \ldots\ldots [12c]$$

by integration, as follows

$$\left.\begin{aligned}\text{Radial displacement} &= u = \int_0^\rho R\epsilon_r \, d\rho \\ \text{Tangential displacement} &= v = \int_0^\varphi (R\rho\epsilon_\varphi - u) \, d\varphi\end{aligned}\right\} \quad \ldots [13]$$

The following formulas result:

Case $k \neq n - 2$

$$\left.\begin{aligned}u/l \cos n\varphi &= [(1 + \mu)/\Delta][(k + 2)\rho^{k+1} - \frac{1}{2} n(n - k)\rho^{n-1}] \\ &\quad + [1 - \mu - (1 + \mu)n/2]\rho^{n+1}/(k + 2 + n) \\ v/l \sin n\varphi &= [(1 + \mu)/\Delta][-n\rho^{k+1} + \frac{1}{2} n(n - k)\rho^{n-1}] \\ &\quad + [1 - u + (1 + \mu)(1 + n/2)]\rho^{n+1}/(k + 2 + n)\end{aligned}\right\} \quad \ldots\ldots [14a]$$

[5] In Equations [10] α denotes the coefficient of ρ^k in $\widehat{r\varphi}$. Elsewhere it denotes, as usual, the coefficient of thermal expansion.

[6] Fig. 4(*a*) is same as Fig. 2(*a*) when referred to in text.

[7] Reference (2), p. 773.

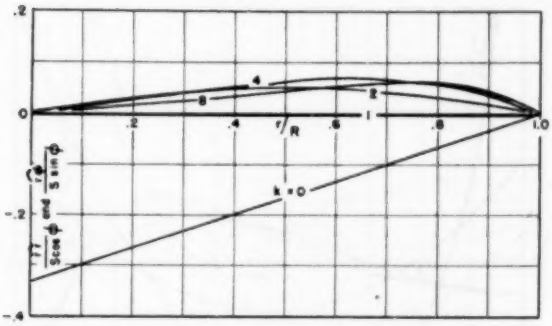

(*a*)

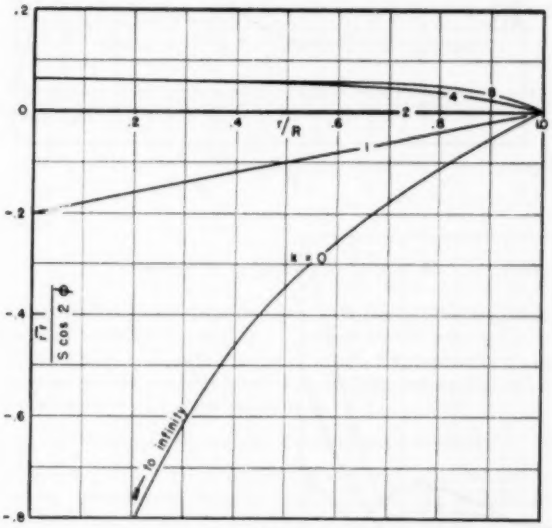

(*b*)

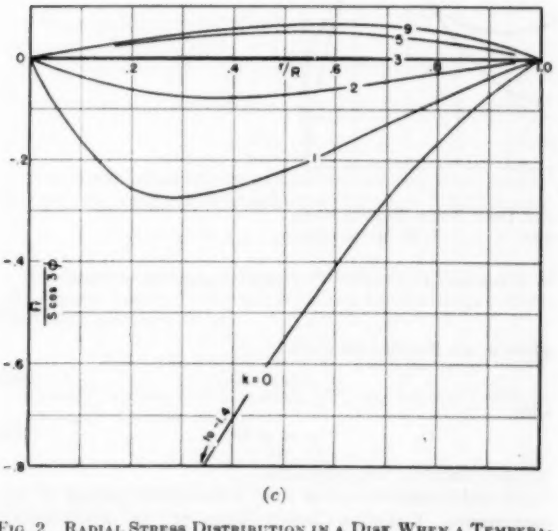

(*c*)

FIG. 2 RADIAL STRESS DISTRIBUTION IN A DISK WHEN A TEMPERATURE DISTRIBUTION $\vartheta = T(r/R)^k \cos n\varphi$ ($n = 1, 2, 3$) IS MAINTAINED
[Fig. 2(*a*) is identical with Fig. 4(*a*) as referred to in text.]

Case $k = n - 2$

$$\left.\begin{aligned} u/l \cos n\varphi &= (1+\mu)\left[\left(\frac{1}{4}+\frac{1}{2}n\right)\rho^{n-1} + \frac{1}{2}\rho^{n-1}\ln\rho\right] \\ &\quad + [1-\mu-(1+\mu)n/2]\rho^{n+1}/2n \\ v/l \sin n\varphi &= (1+\mu)\left[-\frac{1}{4}\rho^{n-1} - \frac{1}{2}\rho^{n-1}\ln\rho\right] \\ &\quad + [1-\mu+(1+\mu)(1+n/2)]\rho^{n+1}/2n \end{aligned}\right\} \quad \ldots\ldots\ldots\ldots [14b]$$

where

$$l = R\alpha T \ldots\ldots\ldots\ldots\ldots\ldots [14c]$$

One readily verifies that the foregoing u, v are consistent with Equation [12c]. At the disk periphery, $\rho = 1$, the Displacements [14] reduce to the simple expressions

$$u/\cos n\varphi = v/\sin n\varphi = 2l/(k+2+n) \quad \text{at} \quad \rho = 1 \ldots [15]$$

and are independent of μ. The displacements u, v are plotted in Figs. 5(*a*, *b*, *c*), and Figs. 6(*a*, *b*, *c*) for $n = 1, 2, 3$, when $\mu = 0.3$ and $\mu = 0.3/0.7 = 0.43$,[8] respectively.

4 TEMPERATURE DISTRIBUTION IN DISK DUE TO NONUNIFORM EDGE-HEATING

We assume that up to the time $t = 0$ the temperature of the disk is 0

$$\vartheta(r, \varphi, t) = 0 \quad \text{for} \quad t < 0 \ldots\ldots\ldots\ldots [16a]$$

At time $t = 0$ we impose an edge temperature

$$\vartheta(R, \varphi, t) = T \cos n\varphi (1 - e^{-t/t_0}) \quad \text{for } t \geqslant 0 \ldots [16b]$$

which rapidly reaches the final value $T \cos n\varphi$. (The time-dependent part of Equation [16*b*] may be replaced by some other suitable function which is 0 at $t = 0$ and ~ 1 at t not much greater than t_0.) We assume the time constant t_0 small enough so that the final edge temperature be reached before noticeable amount of heat is conducted from rim to the core of the disk—in this sense we may replace Equations [16*b*] by

$$\vartheta(R, \varphi, t) = T \cos n\varphi \, 1(t) \ldots\ldots\ldots\ldots [16c]$$

and speak, somewhat loosely, of imposing a "thermal shock" on the disk; at the same time we assume t_0 large enough so that the time required for a sound wave to travel from one end of the disk to the other be many times smaller than t_0.[9] Many practical problems adhere rather well to these two restrictions.

The temperature change which the disk experiences upon application of Equation [16*c*] is governed by the equation

$$\partial\vartheta/\partial t = \kappa(\partial^2/\partial r^2 + \partial/r\partial r + \partial^2/r^2\partial\varphi^2)\vartheta \; (t \geqslant 0) \ldots [16d]$$

where $\kappa = k/\rho c$ (ft²/hr) is the diffusivity of the disk material.

To determine the temperature distribution in the disk at time t we follow (4) precisely.[10] We take the Laplace transform

$$\overline{[\,]} = \int_0^\infty [\,]\, e^{-pt}\, dt$$

[8] Through the middle terms in u and v, Equations [14*a*] include, for the case $n = 1$, a rigid-body displacement of the disk of magnitude $\frac{1}{2}(k-1)(1+\mu)l/(k+3)(k+1)$ in the $\varphi = 0$ direction. Retention of this "stressless" displacement expression is, naturally, somewhat arbitrary, but is of convenience in preserving symmetry of the formulas.

[9] The author is indebted to Prof. W. H. Hoppmann, 2nd, at Johns Hopkins University for pointing out that if such restriction is not made then the problem becomes a dynamic one in which thermal, inertia, and stress effects all have to be treated simultaneously.

[10] Reference (4), p. 272.

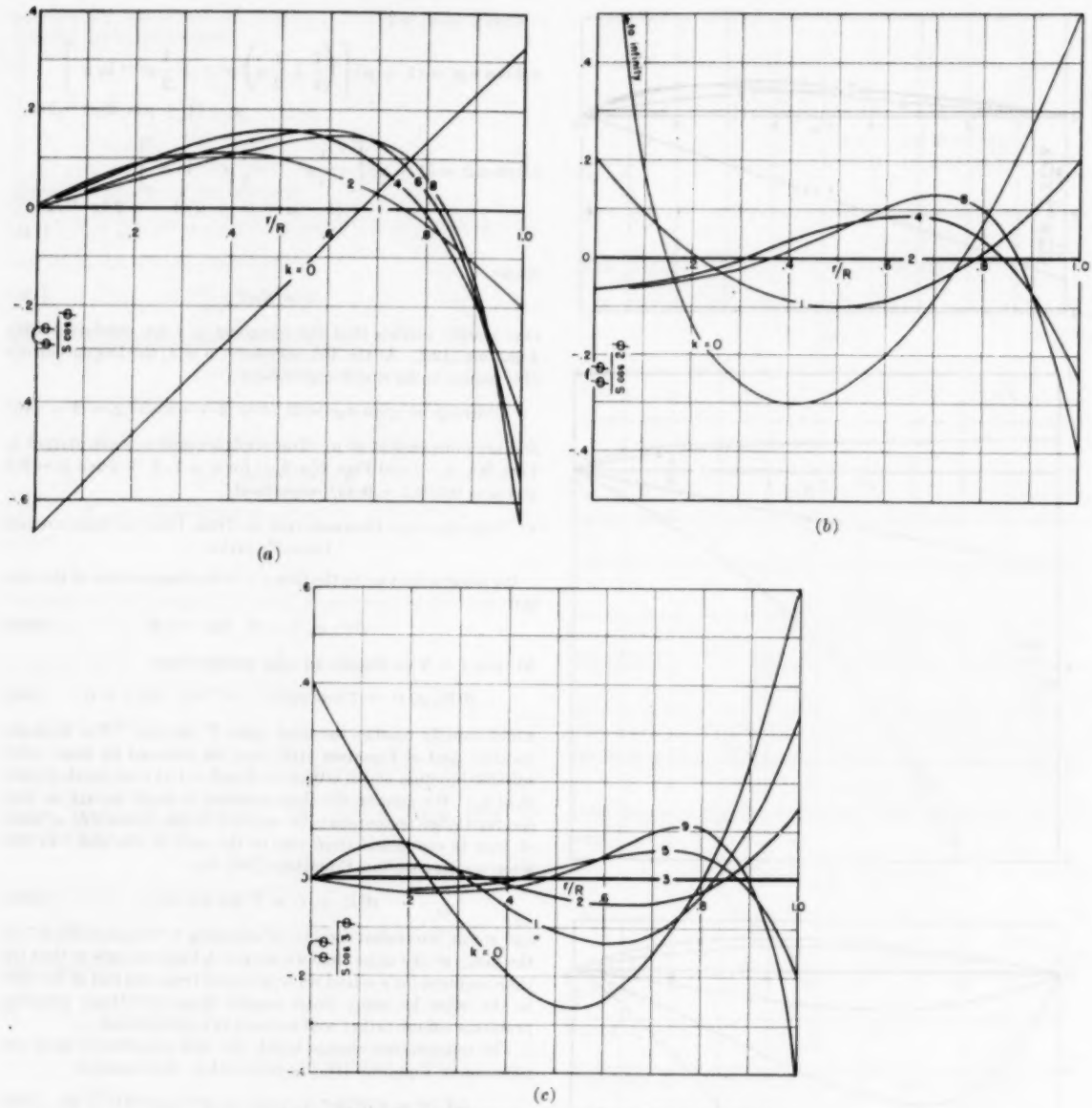

FIG. 3 HOOP-STRESS DISTRIBUTION IN DISK WHEN TEMPERATURE DISTRIBUTION $\vartheta = T(r/R)^k \cos n\varphi$ ($n = 1, 2, 3$) IS MAINTAINED

of Equations [16c], [16d]. Solution of the resultant differential equation for $\bar{\vartheta}$

$$[\partial^2/\partial r^2 + \partial/r\partial r + \partial^2/r^2\partial\varphi^2 - p/\kappa]\ \bar{\vartheta}(r, \varphi) = 0 \quad [17a]$$

subject to the boundary conditions

$$\bar{\vartheta}(R, \varphi) = \frac{1}{p}\ T \cos n\varphi,\ \bar{\vartheta}(0, \varphi) = \text{finite} \quad [17b]$$

yields

$$\bar{\vartheta}(p) = T \cos n\varphi\ I_n\left(\sqrt{p/\kappa}\ r\right)/pI_n\left(\sqrt{p/\kappa}\ R\right) \quad [18]$$

By the Fourier-Mellin inversion theorem one then obtains

$$\vartheta(r, \varphi, t) = T \cos n\varphi \sum \mathcal{R}es\left[e^{\lambda t} I_n\left(\sqrt{\lambda/\kappa}\ r\right)/\lambda I_n\left(\sqrt{\lambda/\kappa}\ R\right)\right] \quad [19a]$$

$$= T \cos n\varphi \left\{\rho^n + 4\sum_j e^{-\nu_j^2\tau} J_n(\nu_j\rho)/\nu_j[J_{n-1}(\nu_j) - J_{n+1}(\nu_j)]\right\} \quad [19b]$$

where ν_j are the positive roots of

$$J_n(\nu) = 0 \quad [20a]$$

and

$$\tau = \kappa t'/R^2 \quad [20b]$$

is a dimensionless time parameter.

For small times the Series [19b] is unsuitable because of slow convergence. Following Carslaw-Jaeger, (4), use of the asymptotic expansion of Equation [18] leads to the asymptotic expansion of ϑ

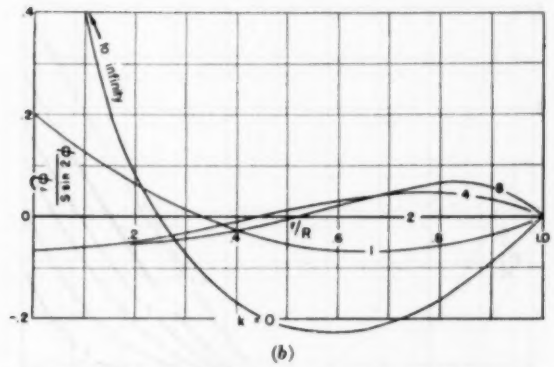

(b)

FIG. 4 SHEAR-STRESS DISTRIBUTION IN DISK WHEN TEMPERATURE DISTRIBUTION $\vartheta = T(r/R)^n \cos n\varphi$ $(n = 2, 3)$ IS MAINTAINED
[Case $n = 1$, Fig. 4(a), is identical with Fig. 2(a).]

$$\frac{\vartheta(r, \varphi, t)}{T \cos n\varphi} = \frac{1}{\sqrt{\rho}} \operatorname{erfc} \frac{1-\rho}{2\sqrt{\tau}} + \frac{(4n^2-1)(1-\rho)}{8\rho\sqrt{\rho}} \times \left[(1-\rho) \operatorname{erfc} \frac{1-\rho}{2\sqrt{\tau}} - 2\sqrt{\frac{\tau}{\pi}}\, e^{-(1-\rho)^2/4\tau} \right] + \ldots . [21a]$$

where

$$\operatorname{erfc}(x) = 1 - \left(2/\sqrt{\pi}\right) \int_0^x e^{-\lambda^2}\, d\lambda \ldots\ldots [21b]$$

is the complementary error function. The Series [21a] is suitable for small t and not too small ρ.

Figs. 7(a, b, c) illustrate the temperature distribution in a disk or cylinder when the edge is raised to the temperature $\vartheta(R, \varphi) = T \cos n\varphi$ $(n = 1, 2, 3)$ at time $t = 0$.

5 THERMAL SHOCK AND STEADY-STATE STRESSES

From Fig. 7 (a, b, c) it is apparent that directly after the instant the edge temperature, Equation [16c], is applied, the temperature $\vartheta(r, \varphi)$ within the disk can be represented by the curve[11]

$$\vartheta(r, \varphi) \simeq T\rho^n \cos n\varphi, \quad \left(k = 1/\sqrt{\pi\tau} \gg n\right) \ldots\ldots [23]$$

For this case Equations [10] reduce to

$$\widehat{rr} \sim \widehat{r\varphi} \sim 0, \quad \widehat{\varphi\varphi} \sim -S\rho^n \cos n\varphi \ldots\ldots [24a]$$

The corresponding displacements u, v, Equations [14], are zero

$$u \sim 0, v \sim 0 \ldots\ldots [24b]$$

After the transient has taken place and a steady state has been reached, the temperature distribution, Equation [19b] becomes

$$\vartheta(r, \varphi) = T\rho^n \cos n\varphi, \quad (\tau = \infty) \ldots\ldots [25]$$

We have seen earlier, in Equation [11b], that for this case all the stresses vanish. The corresponding displacements, Equations [14], are found to be

$$u/\cos n\varphi = v/\sin n\varphi = \rho^{n+1}\, l/(n+1) \ldots\ldots [26]$$

One readily verifies that Equations [26] are consistent with the condition of stressless strain

$$\epsilon_r = \epsilon_\varphi = \alpha\vartheta, \quad \epsilon_{r\varphi} = 0 \ldots\ldots [27]$$

[11] Using the convergent expansion of the error function, Equation [21] can be written as

$$\vartheta/T \cos n\varphi = \rho^{-1/2}[1 - (1-\rho)(\pi\tau)^{-1/2} + \ldots] \ldots\ldots [22]$$

Its slope at $\rho = 1$ is $(\pi\tau)^{-1/2}$; and so is the slope of ρ^k for $k = (\pi\tau)^{-1/2}$.

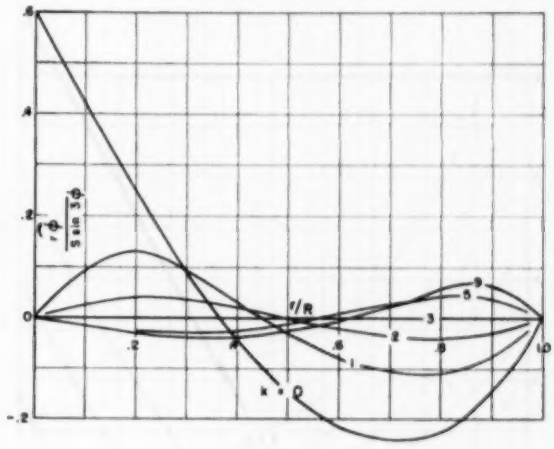

(c)

Stresses at intermediate times can be analyzed by expanding the Bessel functions $J_n(\nu_j\rho)$ of Equation [19b] into power series. This brings the temperature function to the form

$$\vartheta(r, \varphi, t) = T\rho^n \cos n\varphi \left[1 + \sum_1^\infty a_{2\lambda}\rho^{2\lambda}\right], \left(\sum_1^\infty a_{2\lambda}(t) = 0\right) \ldots [28]$$

and permits each $\rho^k \cos n\varphi$ term to be treated individually. This procedure involves no novel steps, hence is omitted here. A similar procedure applies when the edge temperature has the somewhat more general form

$$\vartheta(R, \varphi) = T\sum_m A_m \cos(m\varphi + \gamma_m) \ldots\ldots [29]$$

However, a preferable method, reference (5), is available for treatment of these cases. (In reference 5 the Bessel function expansion is utilized directly.)

6 ADAPTATION OF FOREGOING ANALYSIS TO CYLINDERS

The temperature results of Section 4 apply unchanged to a cylinder. So do the stress and deformation formulas derived in earlier sections, only the substitutions

$$E \to E/(1-\mu^2), \qquad \alpha \to (1+\mu)\alpha, \qquad \mu \to \mu/(1-\mu) \ldots [30]$$

must be made.[12] Thus the stress graphs, Figs. 2 to 5, can be used also for cylinders if we remember that

$$\widehat{rr}_c = \widehat{rr}_d/(1-\mu), \quad \widehat{r\varphi}_c = \widehat{r\varphi}_d/(1-\mu), \quad \widehat{\varphi\varphi}_c = \widehat{\varphi\varphi}_d/(1-\mu) \ldots\ldots [31]$$

In addition there arises, for the temperature Distribution [3], an axial stress

$$\widehat{zz}_c = \mu(\widehat{rr}_c + \widehat{\varphi\varphi}_c) - E\alpha\vartheta = \left[-\frac{\rho^k}{1-\mu} + \frac{\mu}{1-\mu}\frac{2(n+1)\rho^n}{k+n+2} \right] S \cos n\varphi \ldots [32]$$

The displacement graphs must be recalculated for $\mu \to \mu/(1-\mu)$. This was done for $\mu = 0.3$; the resultant curves, $\mu = 0.43$, are shown in Figs. 5 and 6 by dashed lines. They can be barely distinguished from the curves $\mu = 0.3$. The graphs can now be used in the form

[12] We follow closely reference (3), p. 408. Subscript d stands for disk, c stands for cylinder constrained at ends (against axial strain), f stands for cylinder free at ends.

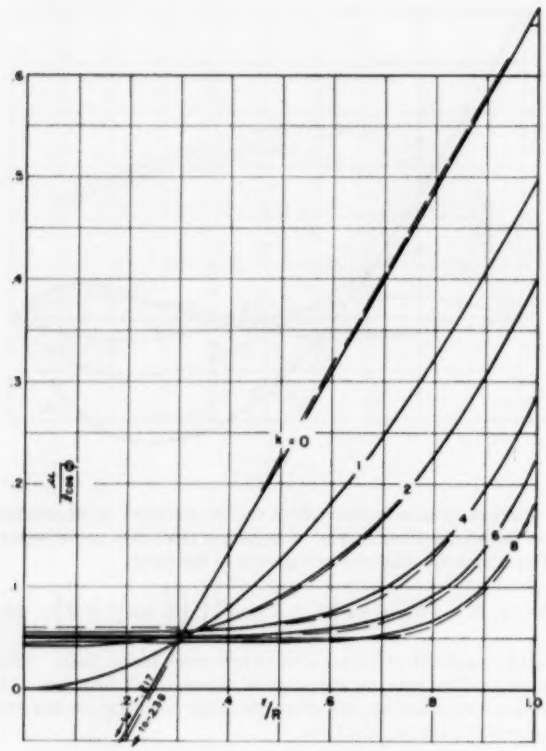

(*a*)

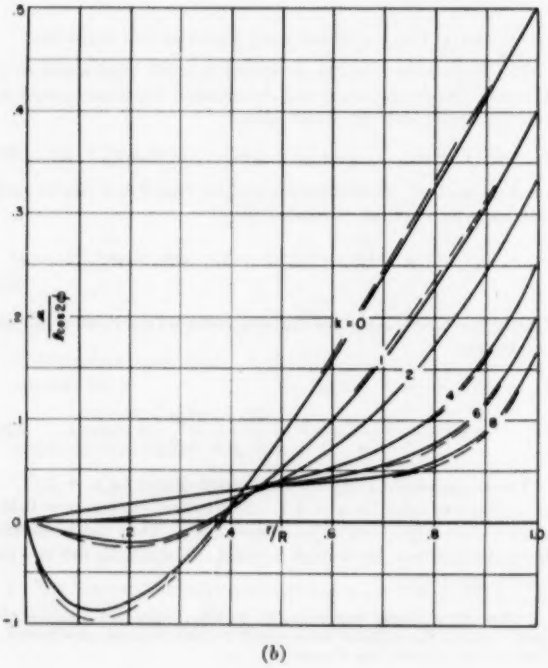

(*b*)

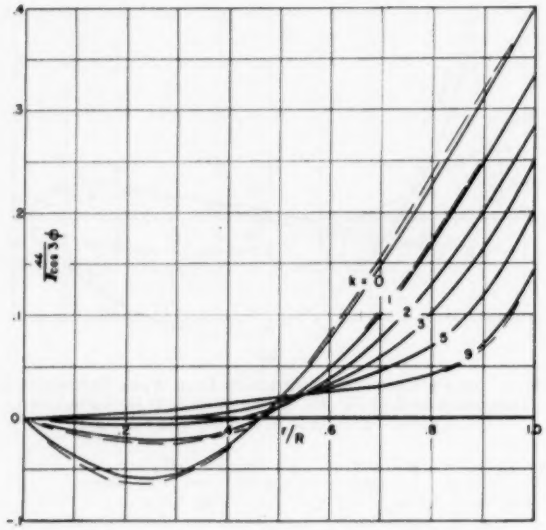

(*c*)

FIG. 5 (*left and above*) RADIAL DISPLACEMENT DISTRIBUTION IN DISK WHEN TEMPERATURE DISTRIBUTION $\vartheta = T(r/R)^k \cos n\varphi$ ($n = 1, 2, 3$) IS MAINTAINED
(Full lines, $\mu = 0.3$; dashed lines, $\mu = 0.43$.)

$$u_c(\mu) = (1 + \mu)u_d\left(\frac{\mu}{1 - \mu}\right),\ v_c(\mu) = (1 + \mu)v_d\left(\frac{\mu}{1 - \mu}\right),$$
$$w_c = 0 \quad \ldots\ldots [33]$$

The foregoing modifications apply when the cylinder is constrained at the ends so that axial strain is prevented

$$\epsilon_z = \partial w/\partial z = 0 \quad \ldots\ldots [34]$$

When the cylinder is free at the ends, then, except in the immediate neighborhood of the end faces, the foregoing results still apply for $n \geqslant 2$ (for then $\widehat{zz_c}$ produces no resultant force or moment). Furthermore, the expressions of $\widehat{rr_c}$, $\widehat{r\varphi_z}$, $\widehat{\varphi\varphi_c}$ remain unchanged also for $n = 0, 1$. Thus

$$\left.\begin{aligned} &\widehat{rr_f} = \widehat{rr_c},\ \widehat{r\varphi_f} = \widehat{r\varphi_c},\ \widehat{\varphi\varphi_f} = \widehat{\varphi\varphi_c} \quad \text{for} \quad n = 0, 1, 2, \ldots \\ &\widehat{zz_f} = \widehat{zz_c} \qquad\qquad\qquad\quad \text{for} \quad n = \quad 2, 3, \ldots \end{aligned}\right\} \quad \ldots\ldots [35]$$

The other results, however, must be modified as follows: When $n = 0$ then

$$\widehat{zz_f} = \widehat{zz_c} - \overline{zz_c} = \left(\frac{2}{k + 2} - \rho^k\right)\frac{S}{1 - \mu} \quad \ldots\ldots [36a]$$

where $\widehat{zz_f}$ is the axial stress of the free cylinder, $\widehat{zz_c}$ is the Expression [32] of the constrained cylinder, and

$$\overline{zz_c} = (2/R^2)\int_0^R \widehat{zz_c}\, r dr = \text{average of } \widehat{zz_c} = -2S/(k + 2)$$
$$\ldots\ldots [36b]$$

The displacements of the cylinder are obtained by adding the displacements produced by the uniform tensile force

$$N = 2R^2\pi S/(k + 2) \quad \ldots\ldots [37]$$

to the displacement Values [33].

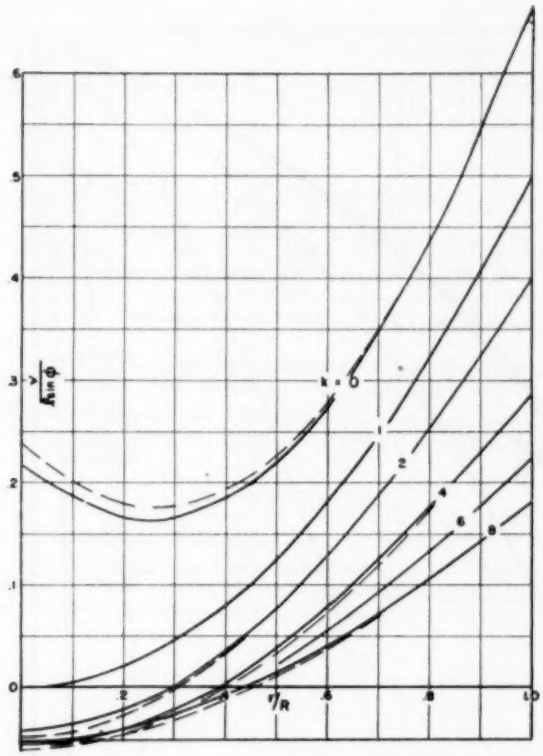

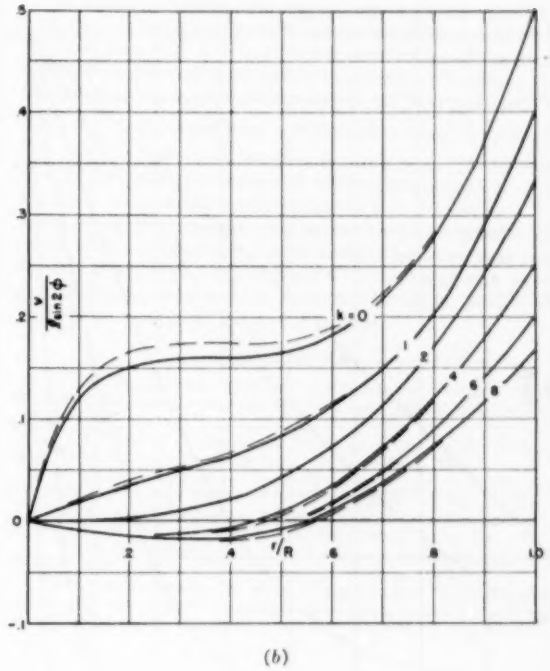

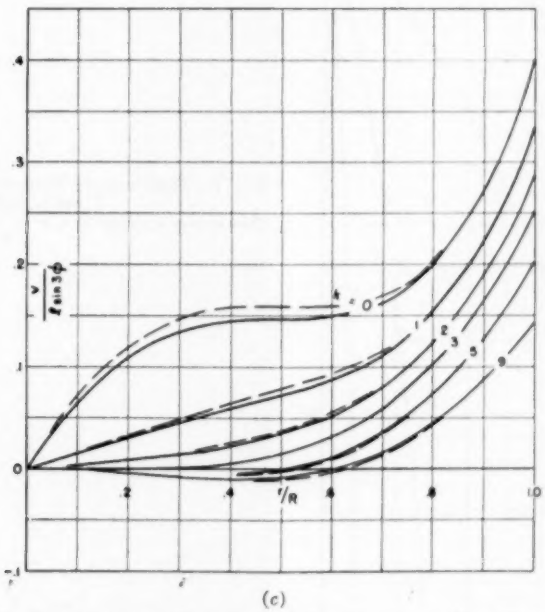

FIG. 6 TANGENTIAL DISPLACEMENT DISTRIBUTION IN DISK WHEN TEMPERATURE DISTRIBUTION $\vartheta = T(r/R)^k \cos n\varphi$ ($n = 1, 2, 3$) IS MAINTAINED

(Full lines, $\mu = 0.3$; dashed lines, $\mu = 0.43$.)

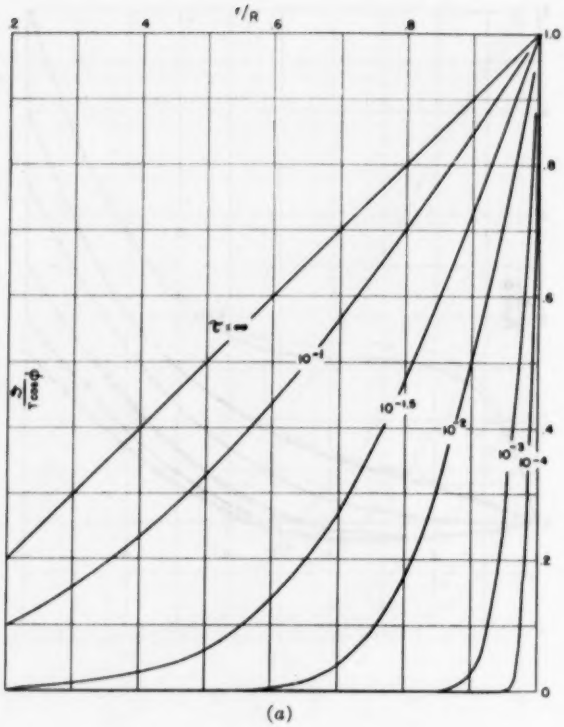

(a)

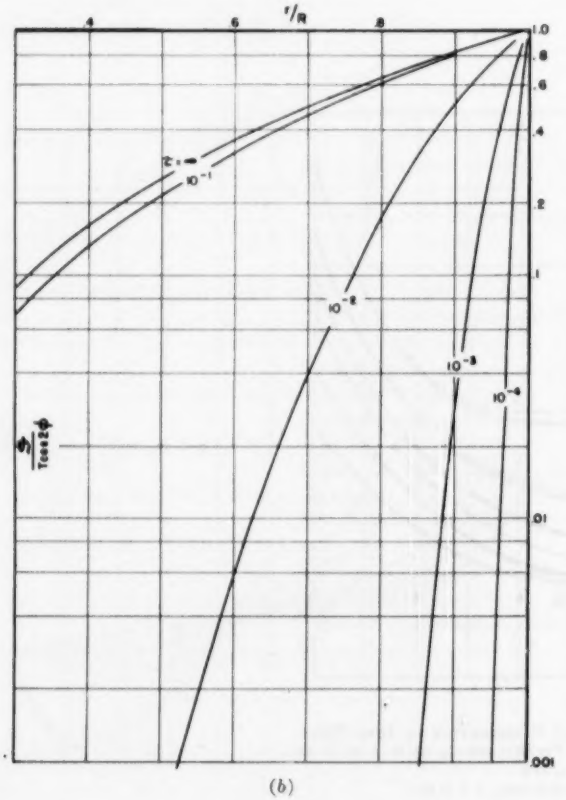

(b)

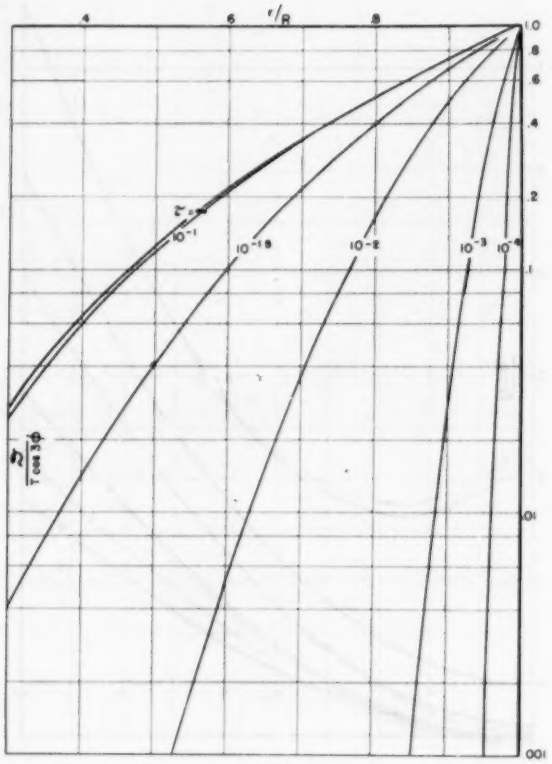

(c)

FIG. 7 TEMPERATURE DISTRIBUTION IN DISK DUE TO $\vartheta(R, \varphi) = T \cos n\varphi \, 1(t)$ EDGE-HEATING

(Linear plot is shown for $n = 1$; logarithmic plots are shown for $n = 2$ $n = 3$.)

When $n = 1$, then

$$\widehat{zz}_f = \widehat{zz}_s - \left[\overline{zz_s r\cos\varphi}\Big/\overline{Sx(r/R)\cos\varphi}\right] S(r/R)\cos\varphi$$

$$= [-\rho^k + 4\rho/(k+3)]\frac{S}{1-\mu}\cos\varphi \ldots\ldots [38a]$$

Here

$$\left.\begin{aligned}\overline{zz_s r\cos\varphi} &= (1/R^2\pi)\int_{-\pi}^{+\pi}\int_0^R \widehat{zz_s} r^2\cos\varphi dr d\varphi \\ &= \text{average moment of } \widehat{zz_s} = -RS/(k+3) \\ \overline{Sx(r/R)\cos\varphi} &= (1/R^2\pi)\int_{-\pi}^{+\pi}\int_0^R S(r^3/R)\cos^2\varphi dr d\varphi \\ &= \text{average moment of stress } Sx/R = RS/4\end{aligned}\right\} .[38b]$$

The subtrahend in the first expression of $\widehat{zz}_f$ denotes the uniform bending stress which produces the same integrated moment as the nonuniform $\widehat{zz}_s$ does. The displacements of the cylinder are obtained by adding the effect of the uniform bending moment about the y-axis

$$M = R^3\pi S/(k+33) \ldots\ldots [39]$$

to the displacement Values [33].

For the special cases $k = n$ (steady state), $k = \infty$ (thermal shock) the "free" cylinder expressions reduce to the results quoted in the Abstract at the beginning of this paper.

The foregoing stresses and displacements obtain throughout most of the cylinder, except in the immediate neighborhood of the end faces (say, $z = 0$, $z = L$) where short-range effects of self-equilibrating stress systems modify the solution. To obtain these modifications we must superimpose—on all that preceded—the effect of a (self-equilibrating) stress system $-\widehat{zz}_f(0)$ applied to face $z = 0$ and of $-\widehat{zz}_f(L)$ applied to face $z = L$. (The application of these tractions removes all residual stresses acting on the end faces; hence we now arrive at a truly free cylinder.)

The effect of self-equilibrating end tractions on a cylinder is an open problem in elasticity. Some initial steps have been taken toward its solution [see reference 6 for an approach to the case of symmetric ($n = 0$) loading], but the major work in this phase of the theory still remains to be done.

BIBLIOGRAPHY

1 "The Plane-Stress Problem of Perforated Plates," by G. Horvay, *Journal of Applied Mechanics*, Trans. ASME, vol. 74, 1952, pp. 355–360.

2 "Handbook of Experimental Stress Analysis," by M. Hetenyi, John Wiley & Sons, Inc., New York, N. Y., 1951, p. 761.

3 "Theory of Elasticity," by S. Timoshenko and J. N. Goodier, McGraw-Hill Book Company, Inc., New York, N. Y., 1951, p. 410.

4 "Conduction of Heat in Solids," by H. S. Carslaw and J. C. Jaeger, Oxford University Press, New York, N. Y., 1950.

5 "On the Integration of the Thermo-Elastic Equations," by J. N. Goodier, *Philosophical Magazine*, vol. 23, 1937, p. 1017.

6 Discussion of paper, "Stresses in Pipe Bundles," by H. Poritsky and G. Horvay, *Journal of Applied Mechanics*, Trans. ASME, vol. 74, 1952, p. 229.

News of Important Publications

MANUAL ON CUTTING OF METALS WITH SINGLE-POINT TOOLS

This book contains shop-tested data on the machining of high-nickel alloys, stainless steels, copper and brass alloys, magnesium, cast irons, and plastics. It offers valuable information on the structure of the metals to be machined, the correct tool material, size and shape of cut, and the proper cutting fluid. It shows how to predetermine the power requirements and best operating speed for all jobs. It helps time-study men to set standards of practice and cost of production, and it provides 322 tables of cutting speeds and horsepower for various feeds and depths of cut when turning commonly used steels and cast iron. $10.00

SMALL-PLANT MANAGEMENT

This is a well rounded management aid which will help you in setting up an internal organization that will function smoothly, in choosing the production process, in machine and equipment planning, and creating a good distribution system. Pertinent topics discussed are financing and banking, how to organize the plant, principles of scientific management, rating products, choosing the legal form of the organization, getting the best workers and labor relations, technical research, obtaining the best facilities and materials, and about everything else that would be likely to interest an individual or a group planning to start a small manufacturing business. $6.50

TEN YEARS' PROGRESS IN MANAGEMENT, 1942–1952

Prepared in collaboration with fifteen nationally recognized authorities, this Report reviews and appraises the significant achievements made in such areas as statistical quality control; production planning and control; work simplification; wage incentive; industrial-plant operation; purchasing, marketing, and distribution; personnel; public and labor relations; cost accounting; federal administrative management; and international co-operation. $1.50

GLOSSARY OF TERMS IN NUCLEAR SCIENCE AND TECHNOLOGY

This standard authority places at your fingertips nearly 2000 nuclear terms and affords you an opportunity to become acquainted with the newly-coined terms used in and outside your own sphere of activity.

Covering the fields of Physics, Reactor Theory, Reactor Engineering, Chemistry, Chemical Engineering, Biophysics and Radiobiology, Instrumentation, Isotope Separation, and Metallurgy, the Glossary lists and defines the terms peculiar to each of these fields, terms used in them in a different sense or with different emphasis from what is commonly understood in other connections, and those used elsewhere in the same way but so infrequently as to be unfamiliar. An index to all the terms shown at a glance the section in which each term and its definition will be found.

Seventeen scientific and technical societies, ten national government agencies, and four divisions of the National Research Council participated in the compilation of this work. Spiral Bound $7.00

Just Published

Metals Engineering—Design

This first of the four-volume ASME Handbook is the design engineer's own guidebook of vital data on the properties, testing, inspection, and selection of metals. Comprising 48 sections and written by 43 well-known authorities, it provides:

- Criteria for facing the overall problems of selection of materials.
- Facts on potential weaknesses of various metals and ways of making the metals strong.
- Details of the specific problems of corrosion and the mechanical factors which influence corrosion.
- Present knowledge of testing by nondestructive methods.
- Special requirements of design and surface finish set up by mass production.
- Modern basic information on the design theory, design practice, experimental design, and the special requirements of aluminum and magnesium.

Here, too, are important design data—equations for determining such factors as stress, creep, impact strength; results of such methods as the use of residual stresses to improve fatigue resistance, the use of flame hardening to increase resistance to fatigue failure; methods for making your structure or machine part stronger, such as shot peening, cold working, and case carburizing.

All in all, Metals Engineering—Design is an invaluable source of reference on materials and design practice. With its help the design engineer can make a better engineering selection of materials . . . meet new requirements with the new design principles and the improved materials that are so clearly detailed in the book . . . find the best method to use in determining how his design will work in practice . . . correct failures by new design procedures or by treatment of materials in corrective ways.

400 Pages 560 Illustrations $10.00

50% Discount to ASME Members

THE AMERICAN SOCIETY OF MECHANICAL ENGINEERS
29 West 39th Street, New York 18, N. Y.